**University of South-Eastern Norway**
Faculty of Technology, Natural Sciences and Maritime Studies
—
Doctoral dissertation no. 26
**2019**

Udara S. P. R. Arachchige

# Carbon Dioxide Capture by Chemical Absorption: Energy Optimization and Analysis of Dynamic Viscosity of Solvents

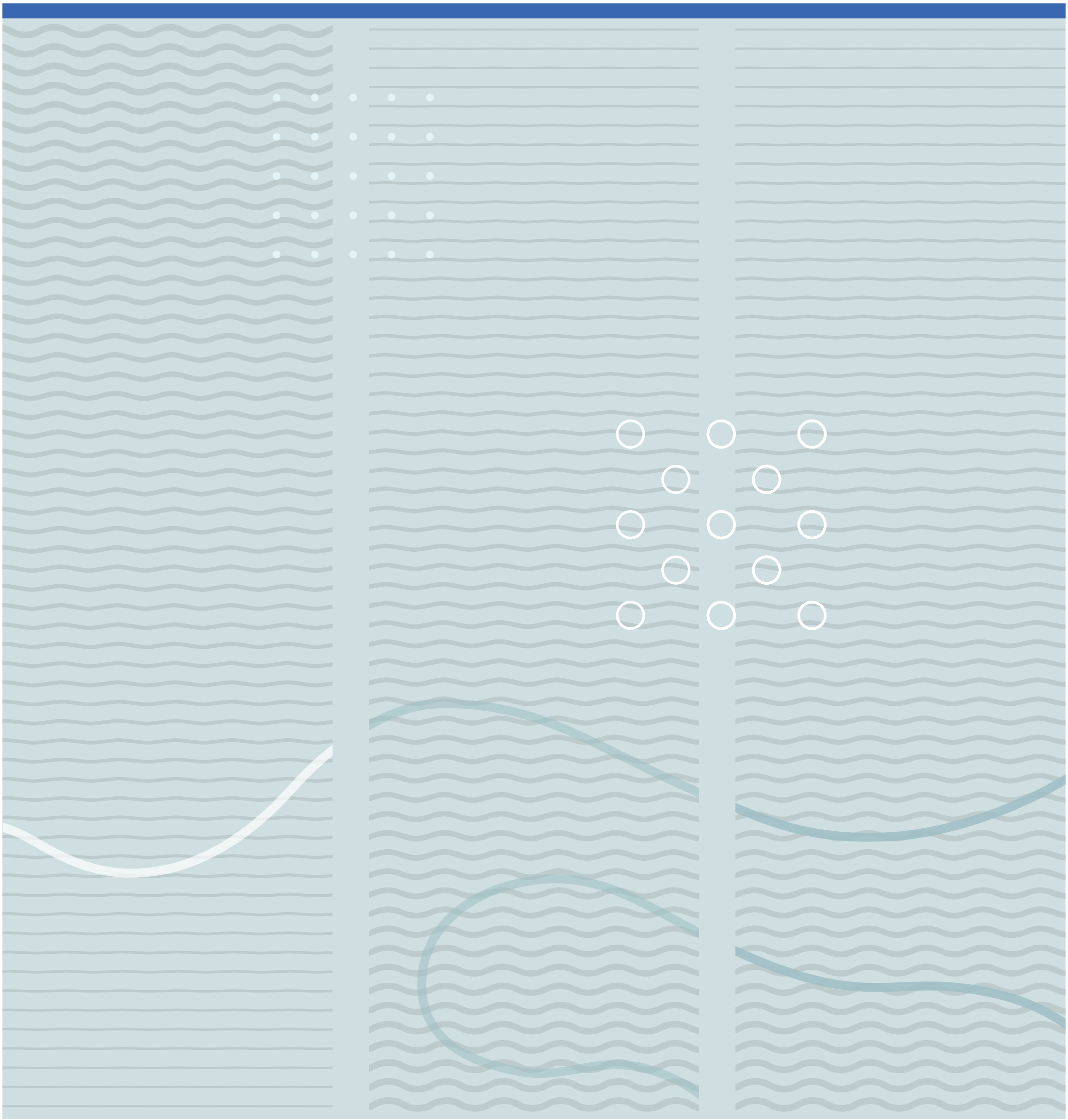

Udara S. P. R. Arachchige

# Carbon Dioxide Capture by Chemical Absorption: Energy Optimization and Analysis of Dynamic Viscosity of Solvents

A PhD dissertation in

**Process, Energy and Automation Engineering**

Faculty of Technology, Natural Sciences and Maritime Studies
University of South-Eastern Norway
Porsgrunn, 2019

**Doctoral dissertations at the University of South-Eastern Norway no.26**

ISSN: 2535-5244 (print)
ISSN: 2535-5252 (online)

ISBN: 978-82-7206-515-6 (print)
ISBN: 978-82-7206-516-3 (online)

Print: University of South-Eastern Norway

*Dedicated to my Professor Morten Christian Melaaen*

# Preface

This dissertation is submitted to the University of South-Eastern Norway (Telemark University College) as a partial fulfillment of the requirements for the degree of Philosophiae doctor (PhD). The thesis consists of the research work performed during the academic period of relevance.

I would like to take this opportunity to sincerely acknowledge those people who helped me to complete the journey.

At this moment of accomplishment, first of all I would like to express my sincere gratitude to my advisor Professor Morten C. Melaaen for the continuous support of my Ph.D study and research, for his patience, motivation, enthusiasm, and immense knowledge. I could not have imagined having a better advisor for my Ph.D study. Under his guidance I successfully overcame many difficulties and learned a lot related to new areas of study. Prof. Morten has also been very generous in providing opportunities to expand my experience outside of research being attending the several international conferences and seminars.

I would also like to give my regards to Professor Dag A. Eimer who supported and guided me as my co-supervisor throughout the period. I appreciate your time taken and valuable discussion which helped me to complete the work by overcoming difficulties.

I am grateful to the academic staff of the master's degree course of Energy and Environmental Technology at TUC for giving the knowledge, courage, as well as making an international level Process Engineer who can work under any pressure. I take this opportunity to sincerely acknowledge the Professor Lars-André Tokheim for his kind support, motivational speech and advices while working with several research papers.

The road to my Ph.D started ten years ago when I came to the beautiful country, Norway. I met many remarkable people around me during last ten years in Norway. Eldrid Eilertsen is one of them who helped me lot, care me lot while I was having health problems. I will never forget the things you have done during this period.

I would also like to mention several fellow students who gave me support, courage and make the time enjoyable and unforgettable. I can't name all of you here, but I must remind few of you, Mishan Rai, Suroj Maharjan, Shyam Thapa, Rajan Kumar Thapa, Amrit Adhikari, Hiromi Ariyaratne, Sanoja Jayarathna, Chameera Jayarathna, Nora Cecilie Furuvik and Gamunu Samarakoon for the nice talking, gossiping we had during the period.

Most of the results described in this thesis would not have been obtained without a close collaboration with few friends. I owe a great deal of appreciation and gratitude to Neelakantha Aryal, Mohsin Muhammad, Chandra Prakash Paneru, Kishan Prajapati and Bhupendra Singh.

I also like to extend my huge, warm thanks to my family members for their support courage and love. I am of course indebted to my parents, Mom (Kusum Perera) and Dad

(Sumanadasa), who have always put their utmost faith in me and my ability to achieve my highest potential.

Last but not least, I would like to pay high regards to my two brothers, Dinesh Kawan and Ravin Kawan for their sincere encouragement and inspiration, love and caring throughout my research work and lifting me uphill in most beautiful part of life. I never feel that I was away from home only because of you. I owe everything to them.

One of the happiness of completion is to look over the journey and remember the wonderful moments!

Thank you.

# Abstract

Global warming resulted from the emissions of greenhouse gases; especially carbon dioxide has received widespread attention. The concentration of $CO_2$ in the atmosphere reaches 400 ppmv and that is a considerably high value for emission's regulations. Efficient $CO_2$ mitigation techniques will become increasingly demanding due to environmental issues. There are many sources that release $CO_2$ and combustion of fossil fuel plays the major role. Coal fired power plants are the most prominent $CO_2$ emitting source today. Though with various carbon mitigation technologies available, there are still challenges remain unsolved. One of the most promising technologies for carbon mitigation is the chemical absorption process based on post combustion. The operation of the chemical absorption process is deeply reviewed for the present study.

The $CO_2$ capture model was developed in Aspen Plus process simulation software. The available parameters in the Aspen Plus databank and the data available in the literatures are used for the development of the model. There are four different types of case studies which are taken into consideration, they are flue gases from coal fired power plant, gas fired power plant, cement industry and aluminium industry as $CO_2$ emitting manmade sources.

The main drawback of the chemical absorption process is a high amount of re-generation energy requirement in stripper. Therefore, main attention was focused on re-boiler energy minimization with several optimization steps. The major concerns of this technology, including removal efficiency optimization and re-boiler energy minimization, are addressed by implementing solvent condition, solvent flow rate, parameter optimization, and selection of packing material. More effective and less energy consuming solvent and the parameter values of selected solvents are identified for model implementation.

The simulations of the absorption process are presented for sensitivity analyses of important parameters on the removal efficiency: lean loading, solvent concentration, flue gas temperature, the solvent temperature, packing height, packing diameter and absorber pressure. Moreover, the sensitivity analysis was performed for single parameter effect, as well as, multiple parameters effect on the desired output. Both the main effect and interaction effect of the parameters have been studied. The data collected from simulation are analyzed using Principal Component Analysis (PCA), Principal Component Regression (PCR) and Partial Least Square-regression (PLS-R) to develop the linear relationship between parameters and output. The most important parameters (highest influence parameters on re-boiler duty) are lean $CO_2$ loading, absorber diameter and absorber height. Similarly, the correlation between variables were studied for $CO_2$ removal efficiency, which indicates that inlet solvent flow rate, absorber packing height and diameter, absorber pressure and temperature of the solvent stream are positively correlated with $CO_2$ removal efficiency whereas the lean loading and temperature of flue gas are negatively correlated with efficiency.

The required re-boiler energy demand was calculated for four different cases with optimized parameter values for every section in the process. The lean solvent loading and solvent concentration, were found to have a major effect on the solvent circulation and then on the re-generation energy in stripping section, which has been identified as the main problem for

implementing carbon capture plant in real industry. Even though, increasing the amine concentration will cause corrosion effects that can be minimized by adding a small amount of inhibitors. Use of blended amines to replace the single amines also gives a significant impact on re-generation energy.

The implemented model is designed for the flue gases from coal fired power plant, gas fired power plant, cement plant as well as the aluminium industry. The required re-boiler duty was calculated for every situation. The temperature profiles, as well as $CO_2$ loading profiles, were analyzed to check the process behavior.

Moreover, physical properties of the solvents are also important to model the carbon capture process. However, lack of data availability for the physical properties of amines was motivated to perform the experimental studies, as well. The dynamic viscosity of the amine solutions was identified as one of the main physical properties which are needed for implementing the process design. Different amines such as, monoethanolamine (MEA), diethanolamine (DEA), N-methyldiethanolamine (MDEA) were mainly considered for the laboratory experiments. Viscosity experiments were performed for single amines as well as blended amines (blend of two amines). Amine concentration was varied from (10-100) % mass basis with the temperature variation from (293.15- 423.15) K. The amine solutions were analyzed for the $CO_2$ loaded as well as unloaded solutions. Amine viscosities with $CO_2$ loading are rare can be found in literatures and it was only available for low temperature values. Eventually, measured viscosity data were analyzed with the values available in the literature to validate the experimental results. Moreover, available linear regression models were used to fit the data into the correlations. The measured viscosities are in good agreement with the literature data.

# List of Papers

The following journal and conference papers are generated during the period of study and given in the part II of the thesis.

## Journal papers

1. Arachchige U.S.P.R., Melaaen M.C. **Aspen Plus Simulation of $CO_2$ Removal from Coal and Gas Fired Power Plants**. Energy Procedia, 2012, 23: 391–399. (***Paper A***)

2. Arachchige U.S.P.R., Melaaen M.C. **Alternative solvents for post combustion carbon capture.** International Journal of Energy and Environment, 2013, 4, No. 3: 441-448. (***Paper C***)

3. Arachchige U.S.P.R., Muhammed M., Melaaen M.C. **Optimization of post combustion carbon capture process-solvent selection**. International Journal of Energy and Environment, 2012, 3, No. 6: 861-870. (***Paper D***)

4. Arachchige U.S.P.R., Melaaen M.C. **Selection of Packing Material for Gas Absorption**. European Journal of Scientific Research, 2012, 87, No. 1: 117-126. (***Paper F***)

5. Arachchige U.S.P.R., Nair J.U., Muhammed M., Halstensen M., Melaaen M.C. **Multivariate Data Analysis for Identification of Important Parameters on Re-Boiler Duty in a Post-Combustion Chemical Absorption Process**. European Journal of Scientific Research, 2013, 95, No. 2: 289-302. (***Paper H***)

6. Arachchige U.S.P.R., Aryal N., Ghimire P., Halstensen M., Melaaen M.C. **Multivariate data analysis for parameters effect on $CO_2$ removal efficiency**. Energy Procedia, 2013, Volume 37: 2011-2020. (***Paper I***)

7. Arachchige U.S.P.R., Muhammed M., Melaaen M.C. **Optimized $CO_2$ flue gas separation model for a coal fired power plant**. International Journal of Energy and Environment, 2013, 4, No. 1: 39-48. (***Paper J***)

8. Arachchige U.S.P.R., Muhammed M., Melaaen M.C. **Optimized Carbon Dioxide Removal Model for Gas Fired Power Plant**. European Journal of Scientific Research, 2012, 86, No. 3: 348-359. (***Paper K***)

9. Arachchige U.S.P.R., Kawan D., Tokheim L.A., Melaaen M.C. **Model Development for $CO_2$ Capture in the Cement Industry**. International Journal of Modeling and Optimization, 2013, 3, No. 6: 535-540. (***Paper L***)

10. Arachchige U.S.P.R., Kawan D., Tokheim L.A., Melaaen M.C. **Impact of kiln thermal energy demand and false air on cement kiln flue gas $CO_2$ capture.** International Journal of Energy and Environment, 2013, 5, No. 1: 45-52. (***Paper M***)

11. Arachchige U.S.P.R., Kawan D., Tokheim L.A., Melaaen M.C. **Waste heat utilization for $CO_2$ capture in the cement industry**. International Journal of Modeling and Optimization, 2014, 4, No. 6: 438-442. (***Paper N***)

12. Arachchige U.S.P.R., Kawan D., Melaaen M.C. **Simulation of carbon dioxide capture for aluminium production process.** International Journal of Modeling and Optimization, 2014, 4, No. 1: 43-50. (***Paper O***)

13. Arachchige U.S.P.R., Aryal N., Eimer D.A., Melaaen M.C. **Viscosities of pure and aqueous solutions of monoethanolamine (MEA), Diethanolamine (DEA) and N-Methyldiethanolamine (MDEA)**. Annual Transactions - The Nordic Rheology Society 2012, 2012, Volume 21: (***Paper P***)

14. Arachchige U.S.P.R., Singh B., Prajapati K., Melaaen M.C. **Viscosities of Aqueous Solutions of Monoethanolamine (MEA), Diethanolamine (DEA) and N-Methyldiethanolamine (MDEA) at T = (90-150) °C.** Annual Transactions - The Nordic Rheology Society 2014, 2014, Volume 22: (***Paper Q***)

15. Arachchige U.S.P.R., Singh B., Prajapati K., Melaaen M.C. **Viscosity of Aqueous Solutions of N-Methyldiethanolamine + Monoethanolamine (MDEA+MEA).** Submitted to the International Journal of Thermo physics. (***Paper R***)

16. Arachchige U.S.P.R., Singh B., Prajapati K., Melaaen M.C. **Dynamic Viscosity of Partially Carbonated Aqueous Monoethanolamine (MEA) from (20 to 150) °C.** Applied Chemical Engineering (2018) Volume 1: 1-9 (***Paper S***)

## Conference papers

1. Arachchige U.S.P.R., Jayarathna S.A., Melaaen M.C. **Comparison of temperature profiles in $CO_2$ removal process with Aspen Plus and MATLAB**. The 36th Clear water clean coal conference, Florida, USA, 2011, 3-7 June. (***Paper B***).
2. Arachchige U.S.P.R., Melaaen M.C. **Blended Amines' Effect on Post Combustion $CO_2$ Capture Process.** Proceedings of the 2nd International Conference on Environmental Pollution and Remediation, Montreal, Quebec, Canada, 2012, 28-30 August. (***Paper E***).
3. Arachchige U.S.P.R., Aryal N., Melaaen M.C. **Case study for flue gas separation of a coal fired power plant and parameters' effect on removal efficiency.** APCRE'11 chemical engineering symposium, Beijing, China, 2011, 18-21 September. (***Paper G***).

# Contents

# List of Figures

# Nomenclature

## Latin Symbols

| Symbol | Description | Unit |
|---|---|---|
| r | Mass ratio | - |
| T | Temperature | K |
| P | Pressure | bar |
| $H_{CO2-S}$ | Henry's constant | - |
| $C_i^H$ | Henry's components | - |
| R | Universal gas constant | J/mol. K |
| $V_m$ | Molar volume | $m^3$/mol |
| $T_{C_i}$ | Critical temperature of species i | K |
| $P_{C_i}$ | Critical pressure of species i | bar |
| $A_j, B_j, C_j, D_j$ | Constant values | - |
| $k_j$ | Rate coefficient | - |
| $r_j$ | Rate of reaction | mol $m^{-2}$ $s^{-1}$ |
| $n_j$ | Parameter values in kinetic equation | - |
| $E_j$ | Activation energy | J/mol |
| $T_0$ | Absolute temperature | K |

## Greek Symbols

| Symbol | Description | Unit |
|---|---|---|
| $\alpha$ | $CO_2$ loading | mol $CO_2$/mol amine |

## Abbreviations

| Abbreviation | Meaning |
|---|---|
| ppmv | Parts per million (volume basis) |
| IEA | International Energy Agency |
| CCS | Carbon capture and storage |
| $CO_2$ | Carbon Dioxide |
| MEA | Monoethanolamine |

| | |
|---|---|
| DEA | Diethanolamine |
| DGA | Diglycolamine |
| TEA | Triethanolamine |
| MDEA | Methyldiethanolamine |
| AMP | 2-Amino-2-methyl-1-propanol |
| DIPA | di-2-propanolamine |
| PCA | Principal component analysis |
| PCR | Principal component regression |
| PLS-R | Partial least squares regression |
| EOR | Enhanced oil recovery |
| CO | Carbon monoxide |
| $NO_X$ | Nitrogen compounds |
| $SO_X$ | Sulphur compounds |
| ELECNRTL | Electrolyte non random two liquid |
| $NH_2$- | Amino groups |
| -OH- | Hydroxyl groups |
| $H_2$ | Hydrogen |
| $H_2O$ | Water |

# Part I

# Overview

# Chapter 1

# Introduction

This chapter describes the background of the study, objectives and main contribution of the thesis work.

## 1.1. Background

Recent emphasis on the release of carbon dioxide and the resulting potential for global warming and climate change has gained the important consideration due to political and environmental issues. The atmospheric level of carbon dioxide ($CO_2$) has increased tremendously during last few decades.

$CO_2$ is the main anthropogenic contributor for greenhouse gas effect as a result of a major contribution to the global temperature rising. This will continue for future if there is no serious action taken into consideration. Approximately one third of the manmade $CO_2$ emissions come from generating electricity. $CO_2$ is produced in a large amount by many industries like coal and gas fired power plants, steel production, cement production, chemical and petrochemical production, etc. [1].

Global greenhouse gas emissions are increasing rapidly and in 2013 carbon-dioxide ($CO_2$) composition in the atmosphere reached the 400 parts per million (ppmv) [2]. International energy agency (IEA) reports that the growth in energy demand will result in increase of 57 percent of $CO_2$ emissions in year 2030 [3].

$CO_2$ release to the atmosphere must be reduced. There are various options that have been suggested by scientist, including switching to green energy sources (wind power), improving process efficiency of the power plants, and capturing $CO_2$ emissions. However, many trends indicate that fossil fuel consumption will continue as it is for several decades. Therefore, carbon capture and storage will be one of the remaining solutions for maintaining a green environment.

The emissions of different greenhouse gases have been studied and measured all around the world. Carbon dioxide ($CO_2$) is considered as the most significant greenhouse gas (GHG) and annual percentage emission from different sectors are seen in Figure 1.1 [4]. Fossil fuel (especially coal) still plays the most important role in the energy sector. Therefore, carbon dioxide capture and storage (CCS) technologies are important if we are continue fossil fuel fired power plants.

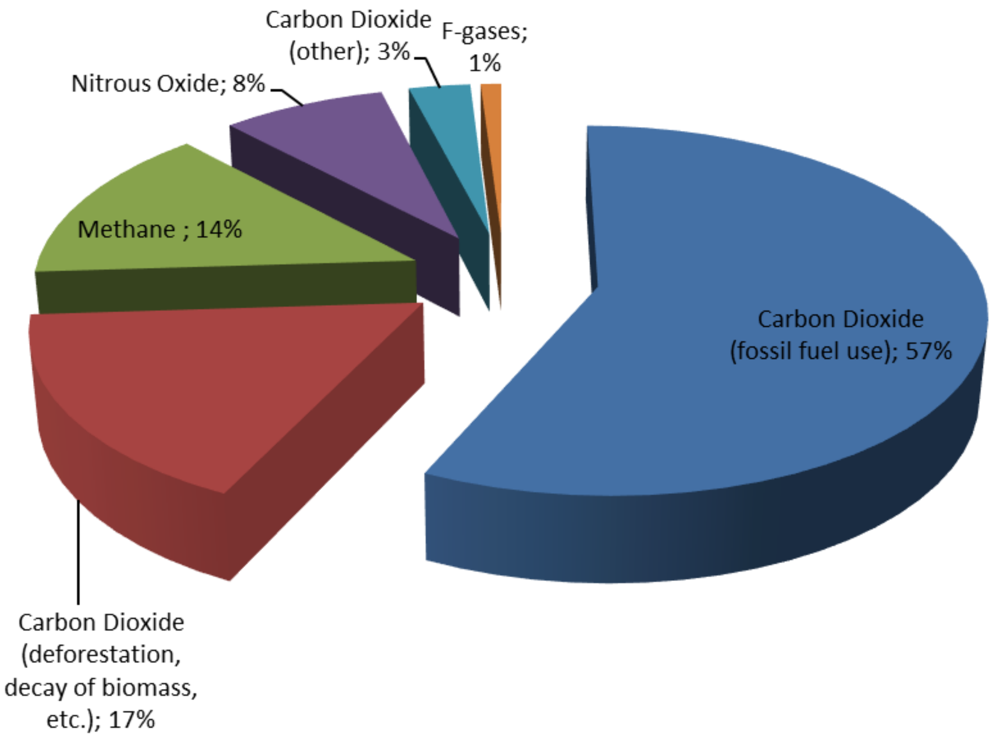

Figure 1.1: Percentage of $CO_2$ [GHG] emissions from different sources [4].

CCS is still having many challenges in large scale, and CCS will significantly reduce the overall efficiency of a power plant. The reduction of the main energy requirements in the $CO_2$ capture process is related to the re-boiler duty in stripper section is important. An energy requirement for $CO_2$ capture is one of the key issues for considering gas treating processes. The main idea of this study is to reduce the energy requirement in re-boiler duty in the carbon capture process. The possibilities have been considered during the period of the study with several case studies. The dynamic viscosities of the solvent that is important in CCS modeling is estimated by laboratory experiments. Possibilities of optimizing parameters of the capture plant have also been considered.

There are several actions that can be activated to reduce the emissions. Increase of renewable energy sources is one of the possible discussions all around the world. However, it will take considerable period for renewable energy to penetrate the energy market which has already obtained with fossil fuels.

## 1.2. Objectives

Carbon dioxide capture and storage (CCS) are considered as one of the main practical option for mitigation of greenhouse gas emissions from fossil fuel based power plants [5].

Carbon capture technologies are not a new technique which can be introduced for flue gas treatment. It has been started several decades ago. However, the CCS technologies used in the emission reduction from power plants is not currently applied as mitigation technology due to high energy requirement in the solvent regeneration process. The post combustion chemical absorption process is the most prominent technique to use for carbon capture. The acid gas mainly $CO_2$ can be chemically captured with amine solvents. Once $CO_2$ has been captured with amine solvent, it can be regenerated to collect purified $CO_2$. However, with the current situation, post combustion chemical absorption process inflicts an energy penalty of about 30% to 60% for coal fired power plants [6]. Therefore, reduction of energy requirement in carbon capture process is necessary to be implemented in the industries and power plants. The purpose of conducting this research is to optimize the carbon capture process with low re-generation. Aspen Plus process simulation software is used to model the carbon capture process. The reduction of the energy requirement is analyzed with several possible ways by optimizing all the possible parameters, inlet streams, solvents or by changing the operating conditions.

The development of the process model will require a number of equations and physical properties to perform the calculations. However, the availability of the physical properties in literatures are limited. Therefore, measurements of the physical properties, as an example dynamic viscosity, have also been considered.

The main objectives of the present study can be summarized as:

- Optimization of the properties of the equipment's and inlet streams, and the selecting of the appropriate operating conditions to achieve the minimum re-boiler energy requirement.
- Estimation of the dynamic viscosity of the solvents with and without $CO_2$ loading.

## 1.3. Main Contribution

The $CO_2$ capture model development and optimization are studied and presented in this study. The brief explanation of every part of the contribution areas can be summarized as follow:

- The base case carbon capture model was implemented in Aspen Plus for flue gas from coal and gas fired power plants. Monoethanolamine (MEA) was used as a solvent with $25\, {}^{w}\!/_{w}\%$ concentration and 0.25[mol $CO_2$/mol MEA] lean loading. The parameters and operating conditions were selected from literatures for starting position. The variation of removal efficiency with different parameters was considered to understand the effect of the parameters on the removal system. The results from the simulations were presented in the paper **A**. The effect of the parameters were understood for future analysis. The developed base case model was used for other optimizations. Moreover, the developed model by Aspen plus was also validated with a developed model in MATLAB software and results present in paper **B**.

- There are several solvents available and selections of best solvent and properties of the solvent stream are important to optimize. The developed base case model was used to check the solvent effect on $CO_2$ removal process. The solvent concentration and $CO_2$ lean loading for $CO_2$ capture process was considered. Both coal and gas-fired power plant flue gases are considered to develop the capture plant with different efficiencies. The optimized solvent concentration and lean $CO_2$ loading values were found for both coal and gas fired capture model and present in paper **D**. Two solvents that can be used for post combustion $CO_2$ capture with lower energy requirement were studies. As an example MEA and DEA were considered for comparison and the results published in paper **C**. The blended amine effect on $CO_2$ removal process was also studied and present in paper **E**. The comparison with single amine model with the same 85% efficiency is performed to understand the benefits of blended amines.

- The absorption process can be performed with either tray or packed column. However, use of a packed column is considered as the preferred option for $CO_2$ capture. Packing material that is used in the gas absorption process can be selected as either random packing or structured packing. The effect of different packing types on gas absorption processes were considered. The selected coal and gas-fired flue gas data and optimized packing dimensions as well as solvent conditions were used for the model implementation. The results that were obtained by this study are present in paper **F**.

- The developed base case model was used for further studies. The impact of all the possible parameters on $CO_2$ removal efficiency and re-boiler duty was considered. The sensitivity analyses are performed to check the variation of $CO_2$ removal efficiency and variation of re-boiler energy requirement with different parameters. By varying several parameters randomly, the effects on re-boiler duty and on removal efficiency were found and tabulated. The collected data from simulation, were analyzed using principal component analysis (PCA), and partial least squares regression (PLS-R) models. The results obtained from this study were reported and presented in papers **G**, **H** and **I**.

- The optimized parameters, solvent conditions, as well as operating conditions, were used to implement the carbon capture model in four different case studies. The flue gases from gas fired power plant, coal fired power plant, and cement industry and aluminium production industry were considered. The required re-boiler energy duty were calculated for every situation. The results obtained from the simulation studies are present in papers **J**, **K**, **L**, **M**, **N** and **O**.

- A data set with dynamic viscosity of pure and aqueous unloaded and $CO_2$ loaded MEA, DEA, MDEA and blended amines are generated. The unloaded viscosities of MEA, DEA and MDEA pure and aqueous solutions with amine mass ratio, $r \in [0.1, 1.0]$ at temperatures, $T \in [293.15, 423.15]$ K were estimated. The unloaded viscosities of MDEA+MEA and MDEA+DEA blends are measured at various combinations of mass fractions with total mass ratio, $r \in [0.2, 0.4]$ at temperatures, $T \in [293.15, 423.15]$ K. The $CO_2$ loaded amine viscosities of single amines of MEA, DEA and MDEA are produced from the solutions with mass ratio, $r \in [0.1, 0.5]$ and $CO_2$

loading, $\alpha \in [0, 0.5]$ at temperatures, $T \in [293.15, 423.15]$ K and the $CO_2$ loaded MDEA+MEA and MDEA+DEA blends are measured for the various combinations of mass fractions with total mass ratio, $r \in [0.2, 0.4]$ and $CO_2$ loading, $\alpha \in [0, 0.5]$ at temperatures, $T \in [293.15, 423.15]$ K. All the measurements with temperatures up to 353.15 K are produced under the pressure, $P = 1$ bar and higher temperature values are generated with pressure, $P = 5$ bar. Data which is produced during this work are analyzed, correlated and presented in Papers **P**, **Q, R** and **S.**

- The results obtained from this study is used to produce 16 journal papers and 3 conference papers.

## 1.4. Outline of the Thesis

The thesis is divided into two parts: Part I – Overview and Part II - Published and submitted papers. The part I consist of six chapters. In chapter 1, entitled "Introduction", back ground, objectives and most contribution areas of the thesis are presented. Chapter 2, called "Literature Overview," give general description of the $CO_2$ mitigation technologies, relevant chemical reactions, thermodynamics and kinetic behavior of the process. Chapter 3, called "Base Case Model Development" presents the most important steps of model development in the present study. This chapter will also explain the important information related to the Aspen plus process simulation software. Chapter 4, entitled "Model Implementation", presents all the necessary works performed during the study to implement the $CO_2$ capture model. The main body of the thesis is described under this section. An overview of the dynamic viscosity measurements performed during the study is presented in Chapter 5 which is entitled as "Dynamic viscosity measurements." The overall picture of the study is provided in Chapter 6, entitled as "Conclusions and Recommendation".

# Chapter 2

# Literature Overview

The emissions of acid gases, mainly $CO_2$ will results in global warming which refers to an unequivocal and rapid continuing rise in the average global temperature. One of the main contributors for the increment of the $CO_2$ level in the atmosphere is well identified as human activities.

## 2.1. Carbon dioxide capture and storage

According to a report published by International Energy Agency (IEA) 2007 [7], it has been asserted that energy demand will increase by more than 60% value in 1990 to 2035. Therefore, mitigation technologies have to be considered mainly for the energy sector. Some of the potential mitigation technologies are listed below.

- Switching to low carbon content fuels
- Increase the use of renewable energy
- Using nuclear energy
- Increase the efficiency of the fuel conversion
- Carbon dioxide capture and storage

Even though, there are several carbon reduction methods available, some of them are not economically friendly. When considering the low carbon content fuel, it can be a good option if it is widely available for use. However, it will not be a practical solution for current energy requirement in the world. Switching to renewable energy sources (solar energy) or increase the use of nuclear energy is highly cost consumption methods. The capital cost and plant operating cost is highly significant amount compared to the fossil fuel. Nuclear energy is already in the global energy market with a considerable amount. However, increase of the amount of usage is problematic due to safety issues, waste management, political and public issues and capital cost. Therefore, those options may have limited attractiveness while considering as mitigation technologies. However, tradeoff between capital and operating cost and environmental impact have to be implemented in near future.

Increase of the efficiency of the existing plants will have an economic impact due to installation and modification cost. Therefore, that may also not be a good option for carbon mitigation. Hence, fossil will remain as the main energy source for several decades from now. It is, therefore, important to find a possible solution that will account for less environmental impact with fossil fuel consumption. Therefore, considering all the possible options, one of the most promising method of $CO_2$ mitigation technology is carbon dioxide capture and storage considering the escalating energy demand. The different energy sources contributing for global energy demand from past to the projected future is shown in the Figure 2.1 [8].

The overwhelming percentage of carbon emissions from fossil fuel combustion has gained prime importance of carbon capture and mitigation. Coal and gas-fired power plants are the most impact man made factor for $CO_2$ emissions. Even though renewable energy sources come to a significant level, use of fossil fuel is still the comprised majority of the power generation around the world. It is apparent that fossil fuel will continue the trend even for several decades from now. The efficiency and the cost are the main considerable factors while selecting the energy source. However, the fossil fuel has a huge impact on global climate change, but shows tremendous economically advantages compared to the renewable sources. The approximate amount of carbon production percentages from different sources are given in the Table 2.1.

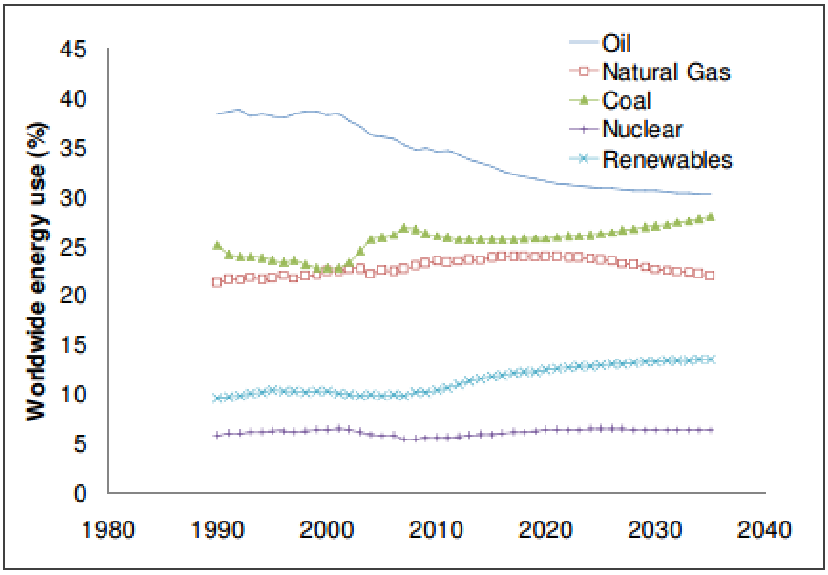

Figure 2.1: Global energy demand from past to the projected future [8].

Table 2.1: Amount of $CO_2$ percentages in flue gas from different sources.

| Source | Coal plant [9] | Gas plant [10] | Cement plant [11] | Aluminium plant [12] |
|---|---|---|---|---|
| $CO_2$ content in the flue gas [vol%] | 14% | 4% | 14-33% | 1% |

Carbon dioxide capture requires separating $CO_2$ from industrial and energy related emission sources into relatively pure streams and pressurizing it and transport it for further storage facility. However, large amount of emission sources, such as fossil fuel based power plants, steel industry, cement manufacturing and fertilizer industries are mainly considered for the mitigation process. These sources have high impact on global $CO_2$ emissions, which are forecasted to increase gradually absent of mitigation.

There are three main types of carbon capture technologies available: pre-combustion, post-combustion and oxy-fuel combustion. As an example, carbon dioxide generation from coal fired power plant can be considered. In the pre-combustion $CO_2$ capture, carbon is removed from the fuel prior to combustion as shown in Figure 2.2. On the other hand, the coal can be combusted with oxygen instead of air (Figure 2.3) with $CO_2$ enriched environment in the oxy-fuel combustion. Finally, post combustion capture, where fossil fuel is combusted with air to produce energy, and in the end, $CO_2$ is removed from the flue gas. Figure 2.4 shows the post combustion method of $CO_2$ removal.

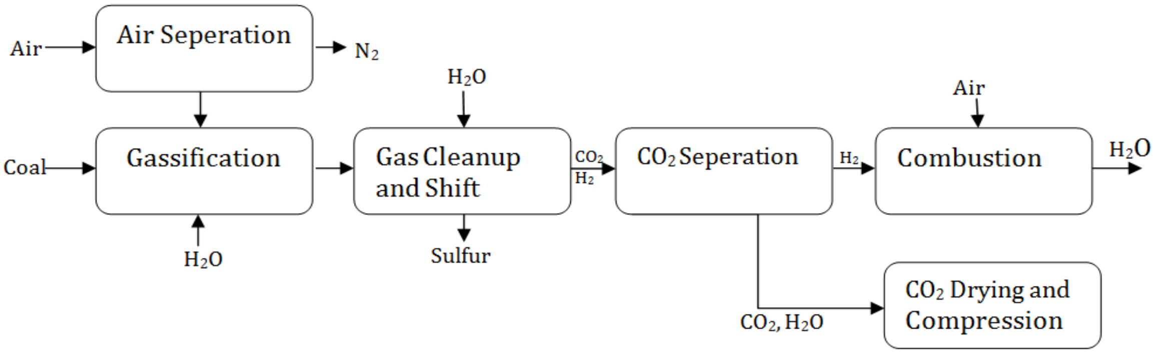

Figure 2.2: Pre-combustion $CO_2$ capture.

First, for the pre-combustion process fuel bound carbon can be converted to another form which is easy to capture through reacting coal with steam and oxygen. The process itself is called the coal gasification and mainly it produces carbon monoxide (CO) and hydrogen ($H_2$). The output of the gasification process has to be sent through further processing to convert CO to $CO_2$ which is able to capture. That process is called Gas cleanup and shift reactor. The $CO_2$ is separated from $H_2$-$CO_2$ mixture by membrane separation and dried and compressed before transportation while $H_2$ is used for combustion process. The final product $H_2$ is carbon free fuel and will not generate harmful pollutant during the combustion process.

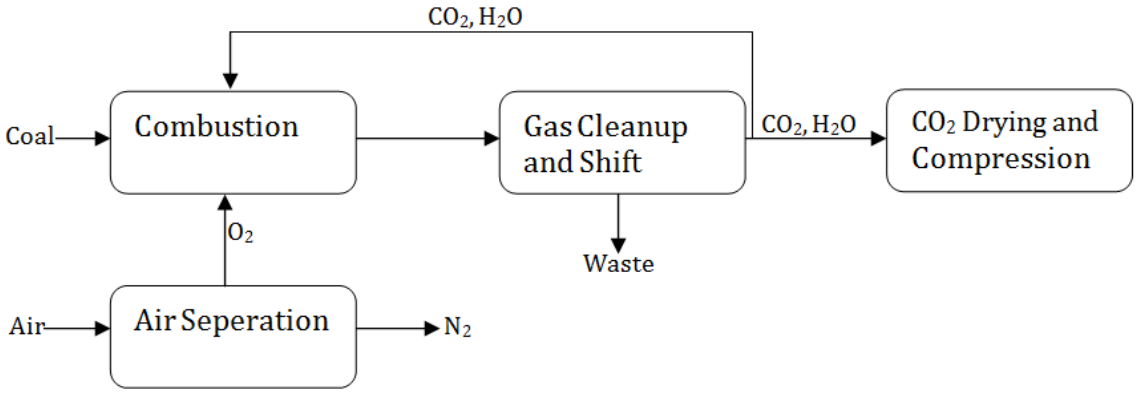

Figure 2.3: Oxy-fuel combustion $CO_2$ capture.

In the oxy-fuel combustion system, fossil fuel is reacted with re-circulated mixture of flue gases and oxygen. The flue gas which is rich with $CO_2$ is re-circulated back to the boiler and that will maintain the temperature of the boiler during the process of combustion. The remaining $CO_2$ and $H_2O$ in the flue gas stream is sent through further process. During that process, $CO_2$ will separate as dry $CO_2$ and compressed for transportation to the storage site. The main drawback of the process is huge cost of production of oxygen during the process.

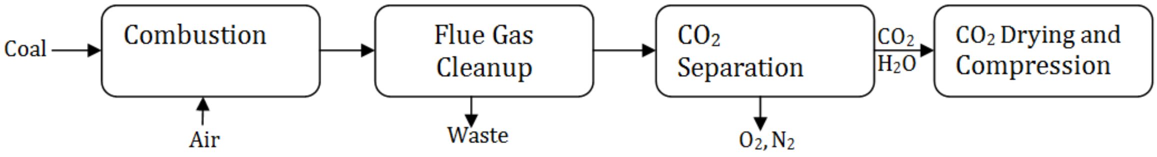

Figure 2.4: Post combustion $CO_2$ capture.

Greenhouse gas mitigation technologies are important to reduce the climate change effect in the power generation sector. The most viable option of $CO_2$ capture is post combustion carbon capture process. However, prior cleaning process is required before the $CO_2$ capture in order to remove the NOx and SOx compounds as well as particulate matter which will cause corrosion and fouling from the flue gas stream. $CO_2$ capture and storage can be a best solution to reduce the $CO_2$ emissions from power plants and other industries [9].

There are several options for post combustion carbon capture from flue gas [13].

- Chemical absorption
- Physical absorption
- Membrane separation
- Cryogenic separation
- Adsorption

In chemical absorption, $CO_2$ is separated from the flue gas by a continuous scrubbing system. The reversible chemical reactions of $CO_2$ and amine solvent are taking place in the absorber. In the stripping section, chemically bound $CO_2$ is separated by high temperature steam and pure $CO_2$ stream is collected for compression section. On the other hand, in the physical absorption process, solid absorbent is in contact with the gas stream, and $CO_2$ is attached by surface forces. However, the efficiency of the process is low compared to the chemical absorption [13]. High purity flue gas streams are required for the membrane separation. Therefore, it is difficult to apply in power plants' flue gas separation due to the high amount of particulate matter in the flue gas. Cryogenic separation of the $CO_2$ removal will produce liquid $CO_2$ with high pressure. Even so, it is not economical viable due to high refrigeration cost. This technology is only applicable to high $CO_2$ concentration stream. Adsorption technology has a lower capability to remove $CO_2$ because of poor selectivity. Therefore, adsorption is not an economically efficient technique for $CO_2$ removal process in power plants [1]. Out of the above mentioned methods, chemical absorption is selected as best post combustion $CO_2$ removal technology for the power plant flue gas separation process. Figure 2.5 shows the previous discussed post combustion methods with simple process flow diagram [14].

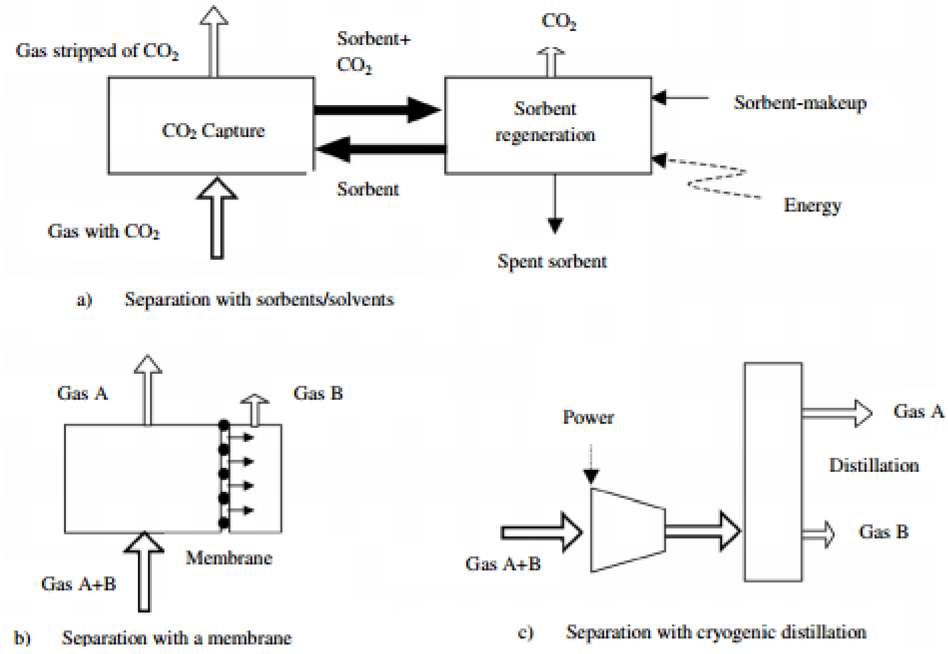

Figure 2.5: Post combustion $CO_2$ capture-possible alternative ways [14].

The capturing $CO_2$ is  arising with two main ideas: green house gas mitigation and enhanced oil recovery (EOR). $CO_2$ is injected into the oil reservoirs to increase the mobility of the oil and, thus the productivity of the reservoir will increase. The main problem related to the amine base $CO_2$ capture process is the large energy requirements for the regeneration process and the size of the capture plant. $CO_2$ absorption with aqueous amine has been used since the early 1930's [15].

The post combustion chemical absorption process is mainly considered for the present study. All the simulation works are based on the post combustion chemical absorption process. The basic operating principals of post combustion chemical absorption process are briefly described below. The flue gas stream after temperature reduction is sent to the absorption column. Flue gas is entering in the bottom of the column while the solvent is entering at the top. The flue gas flow counter currently through the absorber with solvent. There are different solvents available: amine base solvents, ammonia, etc. The pleasant reactant temperature of absorber is 40°C and operating pressure are around 1.1 bar. Non reacted gases (purge-gas) is leaving the absorber column at the top while the rich solvent is leaving the bottom of the column. The rich solvent which consists of chemically bound $CO_2$ is pumped to the top of the stripper column after heated up to the (110-120) °C using lean/rich cross heat exchanger. The operating temperature and the pressure of a stripper column are around 112°C and 1.9 bar.

Low pressure steam is used to supply the heat to the re-boiler for the regeneration process. The regenerated $CO_2$ is captured at the top of the stripper with around 98% purity. At the same time, water is condensed and send back to the stripper. Bottom of the stripper is taking lean MEA after regenerating process. The stripper bottom stream is passing through the lean/rich heat exchanger to exchange the available heat and reduce the temperature of the recycle stream to the temperature suitable for absorber column. However, some amount of solvent degradates during the process. Therefore, makeup stream has to be added to the recirculated stream before sending it back to the absorber. A simplified process flow diagram of the post combustion chemical absorption is given below (Figure 2.6).

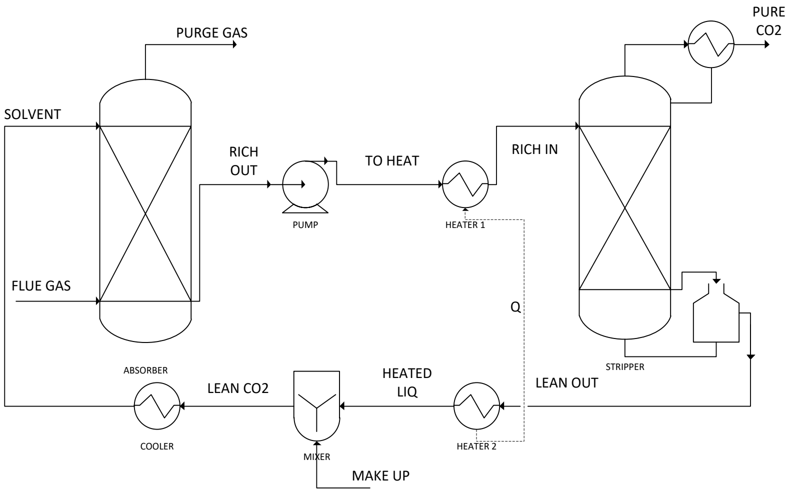

Figure 2.6: Post combustion $CO_2$ capture model developed in Aspen Plus.

## 2.2. Solvents for Chemical absorption

The partial pressure of $CO_2$ in the flue gas stream is low. Therefore, technologies driven by high partial pressures are not efficient for post combustion $CO_2$ capture. The most suitable method is the chemical absorption process with amine based solvents.

### 2.2.1. Available solvents

There are different types of amines available and some of them are categorized as primary amines (MEA, DGA), secondary amines (DEA), tertiary amines (MDEA, TEA), hindered amines (AMP) and cyclic amines (Piperazine). Primary amines are formed when one of three hydrogen atoms in ammonia is replaced by alkyl group. Secondary amines are formed when two hydrogen atoms are substituted by two alkyl group and tertiary amines are formed with three alkyl groups combines with nitrogen. Cyclic amines are formed with 3-member ring called aziridine or 6-member ring piperidine. Hindered amines are arising with amine functional group surrounded by a crowded steric environment. Alkanolamines consists of both hydroxyl groups (-OH-) and amino groups (-NH2). The hydroxyl part helps to reduce vapor pressure and increase solubility of water while the amino group provides the required alkalinity in a solution to perform reactions with acid gases [16]. The amines are categorized as primary, secondary and tertiary according to the number of organic groups attached to the alkaline nitrogen atom [17]. Typically primary and secondary amines form carbamate species ($RNH^+CO^-$) while reacting with $CO_2$.

The basic information related to some of the amines, Monoethanolamine (MEA), Diethanolamine (DEA), Diglycolamine (DGA) and Methyldiethanolamine (MDEA) are given in Table 2.2.

Table 2.2: Basic information about different kind of amines [16].

| | MEA | DEA | DGA | MDEA |
|---|---|---|---|---|
| Chemical formula | $C_2H_7NO$ | $C_4H_{11}NO_2$ | $C_4H_{11}NO_2$ | $C_5H_{13}NO_2$ |
| Amines category | Primary | Secondary | Primary | Tertiary |
| Molecular weight [g/mol] | 61.08 | 105.14 | 105.14 | 119.163 |
| Density [g/cm$^3$] | 1.012 | 1.090 | 1.06 | 1.043 |
| Boiling point[°C] | 170 | 217 | 223 | 247 |

Important factors when considering the selection of solvent for $CO_2$ capture are summarized below.

- Absorption capacity - high absorption capacity require less amount of solvent circulation and reduced equipment size.
- Absorption rate - high absorption rate reduces the size of the column and then the cost of the column.
- Solvent heat of absorption - low heat of absorption will reduce the amount of energy required in stripping process.
- Solvent stability and volatility - solvent should be resistant to degradation and vapor pressure of the solvent should be low to avoid the losses.
- Solvent price - it should be low cost to maintain economically friendly.
- Toxicity - due to environmental issues, solvent should be less toxic and environmental friendly.

By considering above factors, solvent should be selected for the $CO_2$ capture process. MEA is considered more attractive and reasonable by analyzing related factors. However, blended amines also seems to be economically friendly and is considered for further analysis.

### 2.2.2. Solvent degradation

Solvent degradation is one of the major drawbacks of the chemical absorption process. There are three main types of degradation in the gas absorption process, carbamate polymerization, oxidative degradation and thermal degradation. The carbamate polymerization is the most common method of amine degradation. It occurs with the presence of $CO_2$ and high operating temperature in the system [18]. Carbamate polymerization starts by the formation of the higher molecular weight chemical compound called oxazolidone that is a product of the reaction between alcohol and carbamate. The rate of degradation highly depends on the concentration of the solvent and temperature of the reacting system [19].

Presence of the high level of oxygen in the flue gases leads to oxidative degradation in the $CO_2$ capture process. This degradation can be controlled by adding a small amount of inhibitors. Thermal degradation is a result of high temperature in the operating process. However, it will not happen very often due to the requirement of high temperature is not often achieve in the $CO_2$ absorption process.

## 2.3. Chemistry of the amine + $CO_2$ reacting system

In the amine system, $CO_2$ is solubilized in the liquid phase either as carbamate, carbonate or bicarbonate form. The following chemical reactions are a common style given in equation 1-4 [17]. Here R and R2 indicate an alkyl group in primary or secondary amines, respectively. Equation 1 and 2 represent for primary amines whereas 3 and 4 are used for secondary amines.

$$CO_2 + RNH_2 \leftrightarrow RNH_2^+COO^- \tag{1}$$

$$RNH_2^+COO^- + RNH_2 \leftrightarrow RNH_2COO^- + RNH_2^+ \tag{2}$$

$$CO_2 + R_2NH \leftrightarrow R_2NH^+COO^- \tag{3}$$

$$R_2NH^+COO^- + R_2NH \leftrightarrow R_2NCOO^- + R_2NH_2^+ \tag{4}$$

However, tertiary amines are not able to form carbamate species due to lack of hydrogen attached to a nitrogen atom. The reaction pattern and results between tertiary amines and $CO_2$ is given as,

$$CO_2 + R_3N + H_2O \leftrightarrow HCO_3^- + R_3NH^+ \tag{5}$$

One of the most important reactions is carbamate formation. There have been two mechanisms proposed for the formation of the carbamate that are the zwitterion mechanism and the termolecular mechanism. Zwitterion mechanism explains the reaction of $CO_2$ with primary and secondary alkanolamines and form zwitterion intermediate, rather than one-step carbamate formation. The basic reactions are explained in equation 6 and 7.

$$CO_2 + R_1R_2NH \leftrightarrow R_1R_2N^+HCOO^- \tag{6}$$

$$R_1R_2N^+HCOO^- + B \leftrightarrow BH^+ + R_1R_2NCOO^- \tag{7}$$

The intermediate zwitterion reacts with base B, where B corresponds to any species in the solution that can act as a base to abstract a proton from the zwitterion and produced the carbamate as given in equation 7. The base can be any solution, amine itself, OH- or $H_2O$, as well.

On the other hand, termolecular mechanism is proposed by Crooks and Donnellan, 1989 [20] by questioning the validity of the zwitterion mechanism. The termolecular mechanism assumes that the reaction takes place in one step, where the initial product is a loosely bound encounter complex rather than zwitterion. The complex breaks up and form reactant molecules, while a small fraction reacts with a second part of the molecule of amine or water to give ionic products (equations 8-11).

$$R_1R_2NH + H_2O \leftrightarrow (R_1R_2NH)(H_2O) \tag{8}$$

$$R_1R_2NH + R_1R_2NH \leftrightarrow (R_1R_2NH)(R_1R_2NH) \tag{9}$$

$$CO_2 + (R_1R_2NH)(H_2O) \leftrightarrow (H_3O^+)(R_1R_2NCOO^-) \tag{10}$$

$$CO_2 + (R_1R_2NH)(R_1R_2NH) \leftrightarrow (R_1R_2NH_2^+)(R_1R_2NCOO^-) \tag{11}$$

## 2.4. Aspen Plus process simulation

The base case process flow diagram is developed in the Aspen Plus process simulation tool (rate based process simulation). There are several possible property methods available in the Aspen Plus. A collection of property calculation procedures available in Aspen Plus is called property method. Each unit operation model requires property method to carry out the calculations related to that model [21]. There are four main types of property methods available in Aspen Plus for $CO_2$ and amine processes:

ELECNRTL - handle both very low and high concentrations of aqueous and mixed solvent systems.
ENTRL-HF- similar to the ELECNRTL property method except that it uses the HF equation of state for vapor phase calculation model.
ENTRL-HG - similar to the ELECNRTL property method except it uses the Helgeson model for standard property calculations.
AMINES - this property method uses Kent-Eisenberg correlation for K-values and enthalpy calculation.

The ELECNRTL property method is selected for the simulations related to $CO_2$ capture. The ELECNRTL is the most versatile electrolyte property method as it can handle both very low and high concentrations of aqueous and mixed solvent systems. Henry's law is used for modeling of solubility of gases while the Redlich - Kwong equation of state is used for the calculation of vapor phase properties. As an example, the MEA + $CO_2$ system is described. Henry's law is used to calculate the solubility of gases in electrolyte NRTL model. Therefore, Henry's constants have a direct effect on the $CO_2$ removal process. The Henry's constants used in this simulation are summarized in Table 2.3. In this model, Henry's constants of $CO_2$ in both $H_2O$ and MEA solvents are required and are calculated as (eq: 12);

$$\ln H_{CO2-S} = C_1^H + C_2^H / T + C_3^H \ln T + C_4^H T \tag{12}$$

Table 2.3: Henry's components [22, 23].

| | $C_1^H$ | $C_2^H$ | $C_3^H$ | $C_4^H$ |
|---|---|---|---|---|
| $CO_2$-$H_2O$ | 170.7126 | -8477.711 | -21.95743 | 0.005780748 |
| $CO_2$-$MEA$ | 556.182121 | -19877.6314 | -81.667091 | 0 |

The Redlich-Kwong equation of state is used to model the vapor phase of the $CO_2$ capture process. The brief explanation of the equation of state is given below (eq: 13) [13, 24].

$$P = \frac{RT}{V_m - b} - \frac{a}{V_m(V_m - b)} \tag{13}$$

Where:

Vm is the molar volume

R is universal gas constant

T is temperature in K

$$a = 0.42748 \frac{R^2 T_C^2}{p_C} \left[ 1 + \left(0.480 + 1.574\omega - 0.176\omega^2\right) \cdot \left( 1 - \sqrt{\frac{T}{T_C}} \right) \right]^2 \tag{14}$$

$$b = 0.08664 \frac{RT_c}{P_c} \tag{15}$$

The parameters giving in the equation (eq: 14) are,

Tc is the critical temperature of species i

Pc is the critical pressure of species i ω is the acentric factor, and ω were found by fitting experimental data on a variety of compounds to the equation.

The required operating conditions for MEA and DEA in Electrolyte NRTL property method are presented in Table 2.4 [22]. Aspen Plus simulation tool has certain limitations as indicated in the table. The limitations of MEA and DEA mass fractions are 50 and 30 wt%, respectively.

Table 2.4: Range of applicability of amine models [22].

| Range of applicability | MEA | DEA |
|---|---|---|
| Temperature [K] | <393.15 | <413.15 |
| Concentration [w/w%] | <50 | <30 |

Due to the limitations of solvent applicability in Aspen Plus, solvent concentration is maintain below that point.

## 2.5. Gas absorption by packed column

Packed columns are being widely adopted for gas absorption processes due to several advantages. The pressure drop, which leads for maximizing mass transfer rate, of the packed towers are considerably less compared to the tray towers. Mainly there are two types of packing, random and structured packing.

There are different packing types available in the Aspen Plus process simulation tool. Packing material is available for both random and structured packing. Packing section in the absorption process plays a vital role supplying required surface area for the gas and liquid phases to contact each other. For the simulation in the present study random packing (Pall ring, IMTP, Raschig rings) and structured packing (Flexipac, Mellapak, Gempak, BX) are selected. The overall mass transfer coefficient is high in structured packing compared to the random packing [25]. This is due to large contacting area by structured packing for flow distribution in gas-liquid flow.

The most important factors for packing material selection can be categorized as follows:

- Maximize the specific surface area - This maximizes vapour-liquid contact area, and, therefore, efficiency.
- Spread the surface area uniformly - This improves vapour-liquid contact, and, therefore, efficiency.
- Maximize the void space per unit column volume - Enhancing packing capacity.
- Minimize friction - This helps an open shape that has good aerodynamic characteristics
- Minimize cost.

The selection of packing material for $CO_2$ capture is performed for coal and gas fired flue gases. The packing types are considered for the evaluation and the required re-boiler duty is calculated according to the packing material.

Mass transfer coefficients in the gas absorption process are calculated using Onda et al. [26] for random packing while the Bravo et al. [27] correlation is used to calculate mass transfer coefficients and interfacial area for structured packing. Moreover, the Billet and Schultes [28] correlation calculates mass transfer coefficients and interfacial area for any packing. Stichlmair correlation [29] is used for pressure drop calculations in both types of packing.

# Chapter 3

# Base Case Model Development

In order to apply the $CO_2$ capture plant in real industrial applications, reduction of cost by improving the process is in priority. Therefore, the following factors are taken into consideration during the study.

- Solvent selection which gives minimum regeneration energy and optimum efficiency.
- Absorber and stripper column parameters.
- Packing selection.
- Single amines vs. blended amines.
- Multivariate data analysis to understand the most important parameters for efficiency and re-boiler duty.
- Measurements of physical properties to understand the process.

## 3.1. Equations

The base case process flow diagram is developed in the Aspen Plus process simulation tool (Figure 2.6). Solvent concentration and lean $CO_2$ loading are selected as 30 % and 0.25 mol $CO_2$/mol MEA respectively with MEA as a solvent for base case process. The main chemical reactions involve with $CO_2$+MEA process is given in equation 16-20.

Hydrolysis reaction:

$$MEACOO^{-} + H_2O \leftrightarrow MEA + HCO_3^{-} \tag{16}$$

Dissociation of dissolved carbon dioxide:

$$CO_2 + 2H_2O \leftrightarrow HCO_3^{-} + H_3O^{+} \tag{17}$$

Dissociation of bicarbonate:

$$HCO_3^{-} + H_2O \leftrightarrow H_3O^{+} + CO_3^{2-} \tag{18}$$

Dissociation of protonated MEA:

$$MEAH^{+} + H_2O \leftrightarrow MEA + H_3O^{+} \tag{19}$$

Ionization of water:

$$2H_2O \leftrightarrow OH^{-} + H_2O^{+} \tag{20}$$

The mole fraction of each component in both liquid and vapor phase is calculated using above equations. The equilibrium constant is calculated for every single step using equation (21),

$$\ln K_j = A_j + \frac{B_j}{T} + C_j \ln T + D_j T \tag{21}$$

According to the literatures [23], constants in equation (21) which are corresponding to equations (16) to (20) are given in Table 3.1.

Table 3.1: Constant values of equilibrium constant equation (21).

| Parameter | Reaction 16 | Reaction 17 | Reaction 18 | Reaction 19 | Reaction 20 |
|---|---|---|---|---|---|
| $A_j$ | -0.52 | 231.46 | 216.05 | -3.038 | 132.89 |
| $B_j$ | -2545.53 | -12092.1 | -12431.7 | -7008.3 | -13445.9 |
| $C_j$ | 0 | -36.78 | -35.48 | 0 | -22.47 |
| $D_j$ | 0 | 0 | 0 | -0.00313 | 0 |

## 3.2. Kinetic

Calculation of kinetic behavior of the reactions is important to understand the process. The rate model replaces the equation (16) and (17) with kinetic equations (22) and (23) and reverse reactions (24) and (25).

$$MEA + CO_2 + H_2O \rightarrow MEACOO^- + H_3O^+ \tag{22}$$

$$CO_2 + OH^- \rightarrow HCO_3^- \tag{23}$$

$$MEACOO^- + H_3O^+ \rightarrow MEA + CO_2 + H_2O \tag{24}$$

$$HCO_3^- \rightarrow CO_2 + OH^- \tag{25}$$

Table 3.2 is representing the parameter values required for kinetic equation (26) to perform the calculation.

$$r_j = k_j \left( \frac{T}{T_0} \right)^{n_j} \exp\left[ -\frac{E_j}{R} \left( \frac{1}{T} - \frac{1}{T_0} \right) \right] \tag{26}$$

Table 3.2: Rate constant values.

| Parameter | Reaction 22 | Reaction 23 | Reaction 24 | Reaction 25 |
|---|---|---|---|---|
| $k_j$ | 9.77e+10 | 4.32e+13 | 2.7963e+20 | 2.38e+17 |
| $n_j$ | 0 | 0 | 0 | 0 |
| $E_j$(cal/mol) | 9855.809 | 13249 | 17229.79 | 29450.89 |
| $T_O$ (K) | 298 | 298 | 298 | 298 |

Most of the specifications that are used in the base case simulations are recommended specifications for rate based model of the $CO_2$ capture process by Aspen Tech [13], and some of them are taken from literature [29]. The packing type is randomly selected which has been mostly discussed in many of the previous works. However, selection of the packing material is discussed later in chapter 4. The height and diameter of the packing of absorber and stripper are selected according to the $CO_2$ removal efficiency obtained. The base case specifications of the process model is given in Table 3.3.

Table 3.3: Aspen Plus model specifications of absorber and stripper column.

| Specification | Coal fired flue gas | |
|---|---|---|
| | Absorber | Stripper |
| Number of stages | 15 | 15 |
| Operating pressure | 1 bar | 2 bar |
| Re-boiler | None | Kettle |
| Condenser | None | Partial-vapour |
| Packing type | Mellapak, Sulzer, Standard, 250Y | Flexipac, Koch, metal,1Y |
| Packing height | 20m | 18m |
| Packing diameter | 15m | 12m |
| Mass transfer coefficient method [27] | Bravo et al. (1985) | Bravo et al. (1985) |
| Interfacial area method [27] | Bravo et al. (1985) | Bravo et al. (1985) |
| Interfacial area factor | 1.5 | 2 |
| Heat transfer coefficient method | Chilton and Colburn | Chilton and Colburn |
| Holdup correlation [28] | Billet and Schultes (1993) | Billet and Schultes (1993) |
| Film resistance | Discrxn for liquid film and Film for vapour film | Discrxn for liquid film and Film for vapour film |
| Flow model | Mixed | Mixed |

The flue gas condition used for the base case simulation is related to the coal fired power plant flue gas composition. Table 3.4 is indicating the flue gas composition which is used for the simulation.

Table 3.4: Flue gas composition and parameters [9].

| Parameter | Coal Fired |
|---|---|
| Flow rate [kg/s] | 673.4 |
| Temperature [K] | 313 |
| Pressure [bar] | 1.1 |
| Major Composition | Mol% |
| $H_2O$ | 8.18 |
| $N_2$ | 72.86 |
| $CO_2$ | 13.58 |
| $O_2$ | 3.54 |
| $H_2S$ | 0.05 |

The re-boiler duty is calculated for base case simulation. The base case re-boiler duty is 4100 kJ/kg $CO_2$ for coal fired power plant. However optimization of parameters, solvent condition and selection of solvent have been considered in upcoming sections.

## Chapter 4

# Model Implementation

The main idea of this chapter is to point out the main reason behind every paper and the brief description of the contribution. All the published papers related to this section are attached in part II.

## 4.1. Modeling and Simulation

The main idea behind this study was to develop and implement the $CO_2$ capture model and optimize the process. There are several possibilities considered for the implementation.

The main problem of post combustion chemical absorption is the high installation cost and a large amount of energy requirement in the re-generating sector. Therefore, the reduction of capital and operating cost are important to implement for the removal process in power plant flue gas treating. The model is developed and implemented in Aspen Plus to optimize the removal process. The Electrolyte NRTL (ELECNRTL) property method is used to handle the chemical reacting system in Aspen Plus. The flow diagram is modeled to capture the 85% of $CO_2$ from coal and gas fired power plant flue gas and the efficiency is achieved with the variation of distillate rate in the stripper.

Inlet flue gas and solvent stream are supplied at 40ºC and absorber is operating at 1bar absolute pressure. Temperature profiles, as well as $CO_2$ loading profiles, are analyzed to understand the process. The required re-boiler energy demand is calculated for every simulation. Some of the parameters' effect on $CO_2$ removal efficiency is initially investigated to understand the impact of different parameters. A detailed description of this study is described in the paper **A**. Moreover, the developed model for the $CO_2$ removal process is validated with a model developed with MATLAB and given in the paper **B**.

The main drawbacks of $CO_2$ capture process are high energy requirements in the regeneration section, cost of the solvent circulation, operating and maintenance cost and capital cost for building the plant. Therefore, in order to apply the $CO_2$ capture plant in real industrial scale, several implementations have to be done.

The ability of solvents to capture the $CO_2$ is strongly depending on its equilibrium conditions, mass transfer condition and chemical kinetic behavior. There are several types of alkanolamines available according to the number of groups containing carbon which are attached with the nitrogen atom. As an example, primary amines, secondary amines, tertiary amines, chemically hindered amines can be used.

## 4.2. Solvent type selection

In this study, the effect of MEA and DEA on $CO_2$ removal process is considered. The coal and gas fired flue gas data are used to develop a process model for both solvents. The model is developed for 85%, 90% and 95% removal efficiencies. Detailed information related to the study is given in the paper **C**. Base on the study mentioned in the article **C**, re-boiler duties are compared for both solvents. Table 4.1 presents the re-boiler duty variation with respect to solvent type and efficiency of $CO_2$ removal.

Table 4.1: Re-boiler duty variation with alternative solvents.

| Specification | 85% Removal Efficiency | | 90% Removal Efficiency | | 95% Removal Efficiency | |
|---|---|---|---|---|---|---|
| Coal fired power plant $CO_2$ capture | | | | | | |
| | MEA | DEA | MEA | DEA | MEA | DEA |
| Re-boiler duty [kJ/kg $CO_2$] | 3507 | 3371 | 3581 | 3462 | 3914 | 3747 |
| Solvent flow rate [tonne/hr] | 7845 | 8698 | 8480 | 9620 | 8400 | 10825 |
| Gas fired power plant $CO_2$ capture | | | | | | |
| Re-boiler duty [kJ/kg $CO_2$] | 3641 | 3381 | 3982 | 3471 | 4100 | 3756 |
| Solvent flow rate [tonne/hr] | 3624 | 4053 | 3168 | 4421 | 3890 | 6000 |

As it can be seen from the Table 4.1, DEA solvent processes have lower re-boiler energy demand for all the cases. The main reason behind that is, that DEA has lower heat of reaction compared to MEA process. The overall re-boiler energy requirement is mainly based on three major parts. The energy needed to liberate the $CO_2$ from amines, amount of heat required to increase the solvent temperature and energy required for the water evaporation process. It is not just the amount of re-boiler duty that is less for DEA but as well the corrosiveness is also less in DEA compared to MEA solvent. The final conclusion based on this study was that MEA can be replaced the DEA solvent with several advantages.

Moreover, mole fraction of different components are plotted to understand the reactivity of the solvent. Figure 4.1 and 4.2 explains the mole fraction variation in the liquid phase with $CO_2$ loading in the absorber bottom outlet stream.

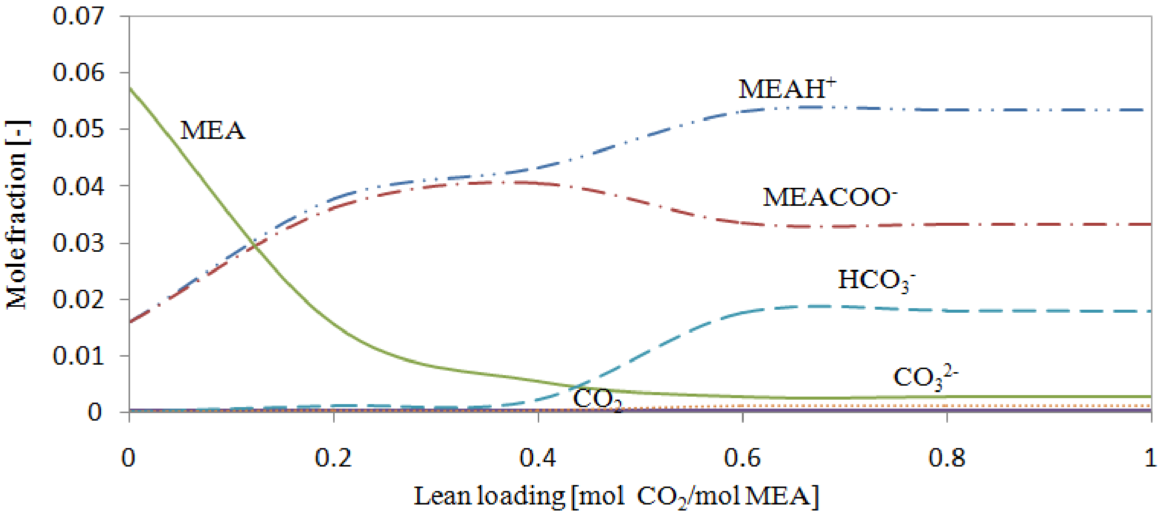

Figure 4.1: Liquid phase composition of a 25 wt% MEA solution loaded with $CO_2$ at 40°C.

Figure 4.1 shows stable liquid phase concentrations after 0.6 loading. Up to loading level almost 0.6, MEA protonation level (MEAH+) increases and MEA level decreases. Figure 4.2 explains the mole fraction variation in liquid phase for DEA solvent in the absorber bottom outlet stream. It is almost similar pattern to MEA plot (Figure 4.1).

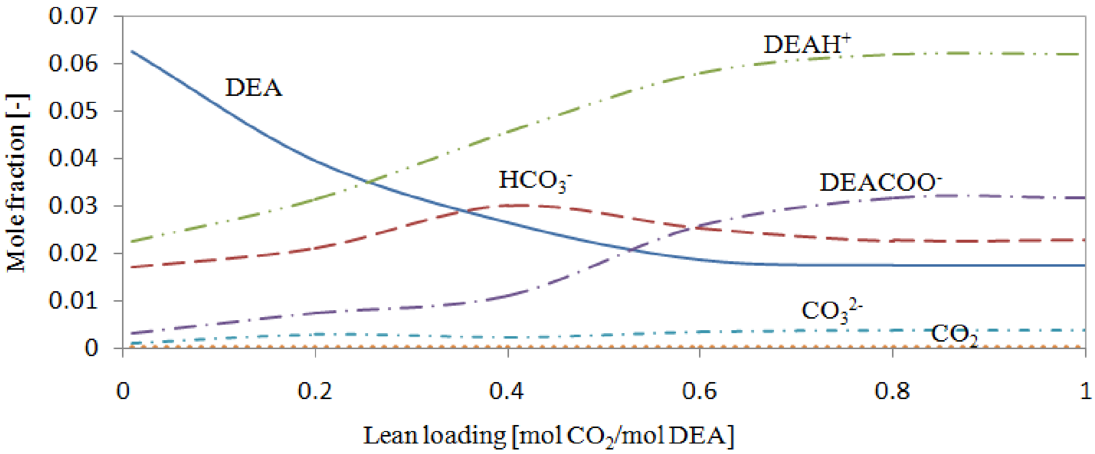

Figure 4.2: Liquid phase composition of a 40 wt% DEA solution loaded with $CO_2$ at 40°C.

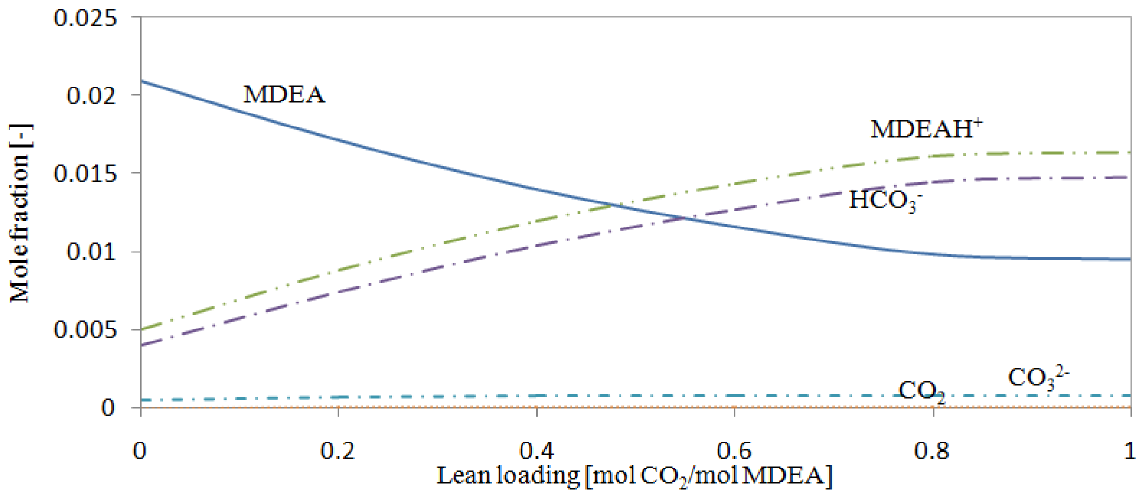

Figure 4.3: Liquid phase composition of a 15 $^w\!/_w$ % MDEA solution loaded with $CO_2$ at 40°C

Moreover, mole fraction variation of MDEA solvent is given in Figure 4.3 for liquid phase. MDEA has a low heat of regeneration, and high loading capacity as well as it is less corrosive than MEA. The drawback of pure MDEA, on the other hand, is having low reaction capability directly with $CO_2$ due to lack of N-H bond, which required forming carbamate ion with $CO_2$ [30].

Chakravarty et al. [31] indicated that adding a small amount of primary or secondary amines, such as MEA or DEA, to the aqueous MDEA can enhance the absorption rate of $CO_2$. The use of blended amines for absorption of $CO_2$ from flue gas streams has received considerable attention because of the potential for low energy requirements for regeneration, good chemical stability, high $CO_2$ absorption capacity, and acceptable rate of $CO_2$ absorption.

According to the studies that we have performed, it is clear that the energy need is the most important factor. Moreover, the following disadvantages are found to be existing with the $CO_2$ capture plant for the fossil fuel based power plants.

- High energy requirement
- Significant efficiency reduction
- Large size of the capture plant and equipment cost
- Difficult to install for full scale power plant
- Huge amount of operating cost for solvents

However, above mentioned disadvantages forced us to continue the research to overcome disadvantages for the $CO_2$ capture plant. After selection of the solvent parameters, energy requirement is analyzed for capture plant. But, regeneration energy penalty is still high with the optimum solvent conditions. In the literatures, it is claimed that use of blended amines will give significant reduction of capital and operating cost [32].

## 4.3. Blended amines vs. single amine

The use of another amine together with primary or secondary amine will reduce the amount of solvent requirement as well as energy consumption. The primary amine, MEA, can be loaded up to 50% [mol $CO_2$/mol MEA] and tertiary amines, MDEA, can be loaded up to 1 mol $CO_2$/ mol MDEA. Therefore, mixing of these two amine will cause high $CO_2$ loading as well as less solvent requirement. Therefore, blended amine solvents effect on $CO_2$ capture is considered. The effect of blended amine on $CO_2$ capture is investigated and given in the paper **E**. The model is developed in Aspen Plus and the same coal fired power plant flue gas condition is used (Table 3.4). The primary or secondary amines are usually added to the tertiary system (MDEA) in the amount of 5-10 wt% of the total amine present in the mixture [33]. The blended amine is produced by mixing MDEA/MEA with 4:1 mixing ratio in weight basis (Table 4.2).

Table. 4.2: Inlet solvent stream compositions in single and blended amine system.

| Parameter | Single amine (MEA) | Blended amine (MEA/MDEA) |
|---|---|---|
| MEA (wt%) | 25 | 10 |
| MDEA (wt%) | - | 40 |
| $H_2O$ (wt%) | 75 | 50 |
| $CO_2$ lean loading (mol $CO_2$/mol amines) | 0.25 | 0.15 |

Efficiency of the model is maintained at 85% of $CO_2$ removal efficiency to calculate the re-boiler energy requirement for both cases. By maintaining other parameters constant, solvent amount is varied to get the exact removal efficiency. The re-boiler duty is calculated as 3809 kJ/kg $CO_2$ and 2937 kJ/kg $CO_2$ for conventional solvent method (single amine) and blended amine system respectively. Present study of blended amines produce lower re-boiler duty and it is confirmed with literatures [34]. The 22.9% of re-boiler energy reduction is achieved with blended amine. Therefore, it can be concluded that use of blended amine has a huge impact on re-boiler energy penalty. The primary problems concerning the use of amine base alkanolamines can be described as an amount of energy needed for regeneration of the solvents, corrosion of the equipments, amine losses and degradation, emission of amines into the atmosphere as purge gas in the absorber unit.

## 4.4. Solvent concentration and $CO_2$ loading effect

The most important thing for solvent selection is concentration of the solvent and $CO_2$ loading which gives minimum re-boiler duty with a highest efficiency. There are several researchers who have studied and evaluated the different solvent capabilities by changing concentration and $CO_2$ loading. In this study amine concentration is varied from 25 to 40 ($^{w}/_{w}$ %) and $CO_2$ lean loading was varied from 0.15 to 0.30 (mol $CO_2$/mol MEA) for 70-95 (mol %) $CO_2$ removal efficiencies. At the same time, other operating conditions were maintained at constant value (absorber and stripper packing dimensions, operating pressure and temperature, etc.) to give exact variation of solvent condition. The required removal efficiency was achieved by varying the solvent flow rate.

The results of the analysis are given in the paper **D**. The simulation studies are performed for both coal and gas fired flue gas system. Coal fired power plant flue gas data were taken from the Table 3.4. The flue gas data related to the gas fired power plant is given in the Table 4.3 [10].

Table 4.3: Flue gas stream conditions [10].

| Parameter | Gas fired flue gas |
|---|---|
| Flow rate [kg/s] | 793.9 |
| Temperature [K] | 313 |
| Pressure [bar] | 1.1 |
| Major Composition | mol% |
| $H_2O$ | 8.00 |
| $N_2$ | 76.00 |
| $CO_2$ | 4.00 |
| $O_2$ | 12.00 |

Finally, simulation results are analyzed to understand the solvent properties such as solvent concentration, lean amine loading, and solvent flow rate on re-boiler duty. Figure 4.4 indicates re-boiler duty variation with $CO_2$ lean loading for coal fired system when MEA concentration is fixed at 25, 30, 35 and 40, (wt%) respectively.

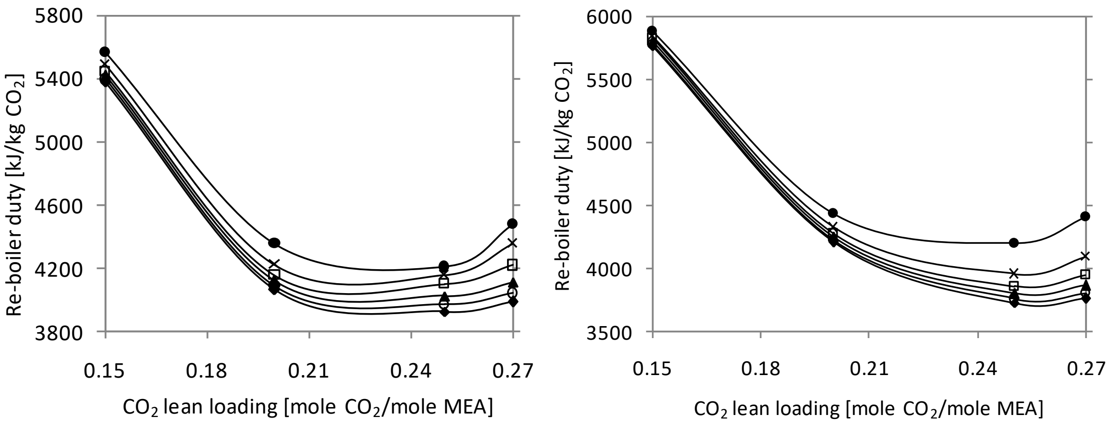

(a) (b)

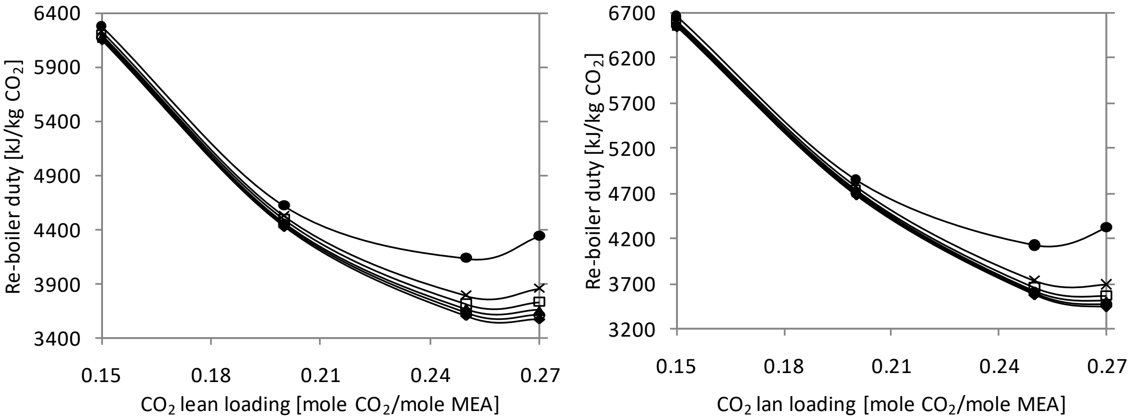

(c) (d)

Figure 4.4: Re-boiler duty variation with $CO_2$ lean loading with different MEA concentrations, (a) 25 $^{w}/_{w}$% (b) 30 $^{w}/_{w}$% (c) 35 $^{w}/_{w}$% (d) 40 $^{w}/_{w}$%, in coal fired flue gas, symbols refer to efficiencies: ♦, 70%; o, 75%; ▲, 80%; □, 85%; ×, 90%; ●, 95%.

From Figure 4.4, it is clear that the re-boiler energy requirement decreases with the increase of lean solvent loading until the minimum is obtained. However, after a certain limit of the lean loading value, re-boiler duty again starts to increase. The point which gives lowest re-boiler energy is defined as the optimum lean solvent loading. It is not just re-boiler duty requirement, but also solvent flow rate minimization which is important to optimize. The overall re-boiler energy requirement consists of three major parts, which are the energy needed for liberating attached $CO_2$ from amines, the heat required to increase the solvent temperature, and energy use for water evaporation process.

When the removal efficiency is gradually increased, the required solvent flow rate is increasing. For all removal efficiency models, the lowest solvent flow rate requirement is given for 40% MEA concentration. However, increasing the amine concentration is believed to have corrosive effects in all sections, in the capture plant. This can be minimized by adding a small amount of corrosive inhibitors to the inlet solvent stream. The presence of these inhibitors is supposed to have a negligible effect on the $CO_2$ removal process.

## 4.5. Selection of packing material

The absorption process can be either tray or packed column. With reference to tray towers, lower residence time and the lower bottom temperature provide an advantage for separation of heat sensitive mixtures in packed columns [35]. The purpose of this study is to assess the characteristics of packing types on the absorption process for $CO_2$ capture. The 85% removal process model is developed for simulations with monoethanolamine (MEA) as a solvent. Flue gas compositions are taken for coal (Table 3.4) and gas fired power plants (Table 4.3).

The Pall-16, Pall-25, Pall-38, IMTP-25 and Raschig rings are selected for the random packing category and Flexipac-1Y, Flexipac-250Y, Mellapak-250Y and 350Y, BX and Gempak are selected for the structured packing. The re-boiler duty requirement is calculated for every single case. A detailed description of the results obtained is given in the paper **F** in appendix.

## 4.6. Parameters optimization

The operating conditions in the $CO_2$ capture process model was optimized. The most important input parameters for the simulations are inlet gas stream flow rate, composition, pressure, temperature, packing material data, inlet solvent properties and stream conditions. Parameter effects on the implemented model for $CO_2$ removal efficiency is analyzed with the same base case model. By changing the parameters, the effect on $CO_2$ removal efficiency and re-boiler duty is investigated. In order to study the effect of one parameter on energy consumption in the re-boiler or removal efficiency, other parameters of the model are kept constant. The most important parameters are identified and given in the paper **G**, **H** and **I**.

Moreover, by changing several parameters at once, the most important parameters on re-boiler heat duty and removal efficiency and the corresponding effect are also investigated. Finally, tabulated results are subject to multivariate analysis in order to find the effects of the parameters on re-boiler duty as well as on removal efficiency. The data collected from simulation were analyzed using principal component analysis (PCA), and partial least squares regression (PLS-R) models. Eventually, the results from the PLS-R are used to develop the model for re-boiler duty and removal efficiency.

## 4.7. Case studies

Four major industries (coal fired power plant, gas fired power plant, cement industry and aluminium industry) which contribute for greenhouse gas emissions were considered for simulation studies. The flue gas data used for the simulation, are given in the Table 4.4.

Table 4.4: Flue gas data used for simulation studies.

| Parameter | Coal fired power plant | Gas fired power plant | Cement industry | Aluminium industry | | | |
|---|---|---|---|---|---|---|---|
| | | | | Case 1 | Case 2 | Case 3 | Case 4 |
| Flow rate [kg/s] | 673.4 | 793.9 | 84.7 | 112.1 | 84.5 | 49.1 | 34.9 |
| Temperature [K] | 313 | 313 | 433 | 225 | 265 | 329 | 365 |
| Pressure [bar] | 1.1 | 1.1 | 1.1 | 1.1 | | | |
| | | Major Composition [%] | | | | | |
| $N_2$ | 72.86 | 76.00 | 68.10 | 75.30 | 75.10 | 73.00 | 70.90 |
| $H_2O$ | 8.18 | 8.00 | 7.20 | 1.00 | 0.90 | 0.60 | 0.30 |
| $CO_2$ | 13.58 | 4.00 | 22.40 | 3.00 | 4.00 | 7.00 | 10.00 |
| $O_2$ | 3.54 | 12.00 | 2.30 | 20.70 | 20.00 | 19.40 | 18.80 |

The basic idea behind this study is to develop and implement the $CO_2$ capture model for flue gas from different industrial plant. Moreover, required re-boiler duty is calculated for every case. The optimized $CO_2$ capture model is developed for different removal efficiencies. The $CO_2$ removal model is developed and implemented for cement industry flue gas and that is used for further evaluations to check the parameter effect on that industry. The specific thermal energy demand, as well as the false air factor of the kiln system, were varied in order to determine the effect on $CO_2$ capture plant performance, such as the solvent regeneration energy demand. The utilization of waste heat in a cement kiln flue gas in an amine-based $CO_2$ absorption process is considered. The high temperature flue gas from the cement kiln is used to generate steam in a waste heat boiler. The required surface area of the heat exchange, the cost of installing this area and the payback time of the installation is calculated.

The detailed description of the case studies is given in the paper **J**, **K**, **L**, **M**, **N** and **O.**

# Chapter 5

# Dynamic Viscosity Measurements

Alkanolamine aqueous solutions are mainly used for acid gas removal. Most significant alkanolamines for industrial application are monoethanolamine (MEA), diethanolamine (DEA), di-2-propanolamine (DIPA) and N-methyldiethanolamine (MDEA) [36]. However, the available physical properties of those alkalanomines are limited. Therefore, physical property estimation of alkalanomines solvents are important. It is worth to study the behavior of physical properties of the solvent which are used in the $CO_2$ capture process. Viscosity variations of different kinds of amines are mainly considered for this study. Knowledge of the pure amine viscosity as well as aqueous amine viscosity is important to understand for the acid gas treating process. The experiments were performed to check the viscosities of monoethanolamine (MEA), diethanolamine (DEA) and methyldiethanolamine (MDEA). Pure and aqueous amine viscosities of single amines (MEA, DEA, MDEA) as well as blended amines (MEA+MDEA, DEA+MDEA) with $CO_2$ loading and without $CO_2$ loading are experimentally analyzed. When possible available literature data are used for the verification of the research.

The measured amine viscosity values are compared with those available from the literature. The pure viscosity data of MEA, DEA, and MDEA solutions are compared with data from Li and Lie [36], DiGuilio et al [37] and Mandal et al [38]. The data given by Amundsen et al. [39], Rinker et al [40] and Li and Lie [36] are used to compare the aqueous viscosity data measured for MEA, DEA and MDEA solutions.

The viscosity data of blended amines have been reported in several literatures such as ($MEA+MDEA+H_2O$) [41, 36, 42] and ($DEA+MDEA+H_2O$) [40, 43, 44, 45]. Most of the reported data in the above literatures are available for the viscosities of blended amines over the temperature range (303.15 to 353.15)K. Bishnu et.al. 2003 [46] have performed the density and viscosity measurements for temperature range (293.15 to 323.15)K to complete the gap with previous works. Hence, in this work the viscosity measurements of blended amines are done in the temperature range, (293.15 to 413.15)K to complete the range with high temperature.

The lack of data available at high temperature ranges mostly motivated us for performing the experimental studies. Viscosities are measured by MCR 101 Anton Paar double-gap rheometer. All the measured viscosity data are given in the papers **P**, **Q**, **R, S**. The viscosities of pure and aqueous solutions of alkanolamines are experimentally calculated for different temperature ranges. The main objective of this section is to calculate the viscosities of different aqueous amines at different temperatures that are needed for the acid gas absorption process. Physical properties of amines are important to estimate over the different temperature range to perform mathematical calculations. The results that are obtained from the experiments were used to generate the correlations for amine viscosity at different temperatures.

## 5.1. Experimental Section

Dynamic viscosity was experimentally analyzed using MCR 101 Anton Paar double-gap rheometer. First of all, the viscometer was calibrated against the petroleum distillate and mineral oil calibration fluid. The calibration factor was calculated according to the given temperature for the calibration liquid and experimentally achieved viscosity during the calibration. The Anton Paar double gap rheometer is shown in Figure 5.1. Two different pressure values are used for the measuring process in order to avoid the water vaporization at high temperatures. First part of the process (293.15 – 353.15) K was completed with pressure 1.01 bar and the second part of the process (363.15 – 423.15) K is completed with 4.5 bar pressure.

Figure 5.1: MCR 101 Anton Paar double-gap rheometer.

## 5.2. Amine concentration and temperature range

The pure and aqueous amine viscosities are measured for temperature range (293.15 - 423.15) K for different concentrations. Concentration of the aqueous amines are varied from (10 - 90) wt%. The MEA, DEA, and MDEA amines are considered for single amine viscosity measurements. Moreover, blended amines viscosities are also investigated. The measured data for the different amines are compared with those available from the literature. The results that are obtained from the experiments were used to produce correlations for viscosity at different temperatures. Table 5.1 shows the complete set of information regarding experimental section. The viscosities of single amines, as well as blended amines with and without $CO_2$ loading, was measured.

Table 5.1: Amine information related to the experiments.

| Parameter | Single amine | | | | | | Blended amine | | | |
|---|---|---|---|---|---|---|---|---|---|---|
| | Unloaded | | | $CO_2$ loaded | | | Unloaded | | $CO_2$ loaded | |
| | MEA | DEA | MDEA | MEA | DEA | MDEA | MEA/MDEA | DEA/MDEA | MEA/MDEA | DEA/MDEA |
| Concentration range (W/W%) | 10-100 | | | 10-50 | | | 20, 30, 40 | | | |
| $CO_2$ loading (molCO2/mol amine) | - | | | 0.1 - 0.5 | | | - | | 0.1-0.5 | |
| Temperature range (K) | 293.15 - 423.15 | | | | | | | | | |

## 5.3. Sample generation

Aqueous solutions of amines were prepared using degassed, purified water and amines. Sample concentration is maintained by adding required portion of amine and water with the help of analytical balance that has an accuracy of $\pm 1 \cdot 10^{-7}$.The high $CO_2$ loaded samples, $\alpha$ = (>0.5), prepared by bubbling $CO_2$ gas through an unloaded solution at required mass flow rate of $CO_2$ for appropriate period (Figure 5.2). The required $CO_2$ loaded samples were prepared by diluting of high $CO_2$ loading with an unloaded solution in the appropriate ratio to get required loading values, $\alpha$ = (0 to 0.5).

The high loaded amine solutions were analyzed using titration method to check the exact $CO_2$ loading value and the amine concentration. The 1 $mol \cdot L^{-1}$ HCl solution is used to perform the titration to check the mass concentration of the amine solution. The sample is prepared by adding 2 g of each prepared amine solution with de-ionized water until each sample became 100 $cm^3$ in total. The amount of amine present in the sample is calculated by using the amount of HCl used for the titration. The sample preparation for the loading analysis was carried out by mixing about (0.5 to 1.0) g of the loaded amine solution with 50 $cm^3$ each from 0.3 $mol \cdot L^{-1}$ $BaCl_2$ and 0.1 $mol \cdot L^{-1}$ NaOH. Those samples were heated around 5 min to let $CO_2$ in the samples to react with $BaCl_2$ and make precipitate as $BaCO_3$, then cooled down in a water bath. Moreover, the precipitate is collected and added to the 100 $cm^3$ of de-ionized water and then titrated with 0.1 $mol \cdot L^{-1}$ HCl solution until the mixture reached the equilibrium point. To remove all of the dissolved $CO_2$, the mixture was heated. Then, the same mixture was used for back titration with 0.1 mol·L$^{-1}$ NaOH solution to check the amount of excess HCl. At last, the moles of HCl reacted with $BaCO_3$ precipitate was used to find the amount of $CO_2$ in the corresponding partially carbonated aqueous amine sample and subsequently the $CO_2$ loading value of the sample. The sample analysis using titration method is given in the Figure 5.3.

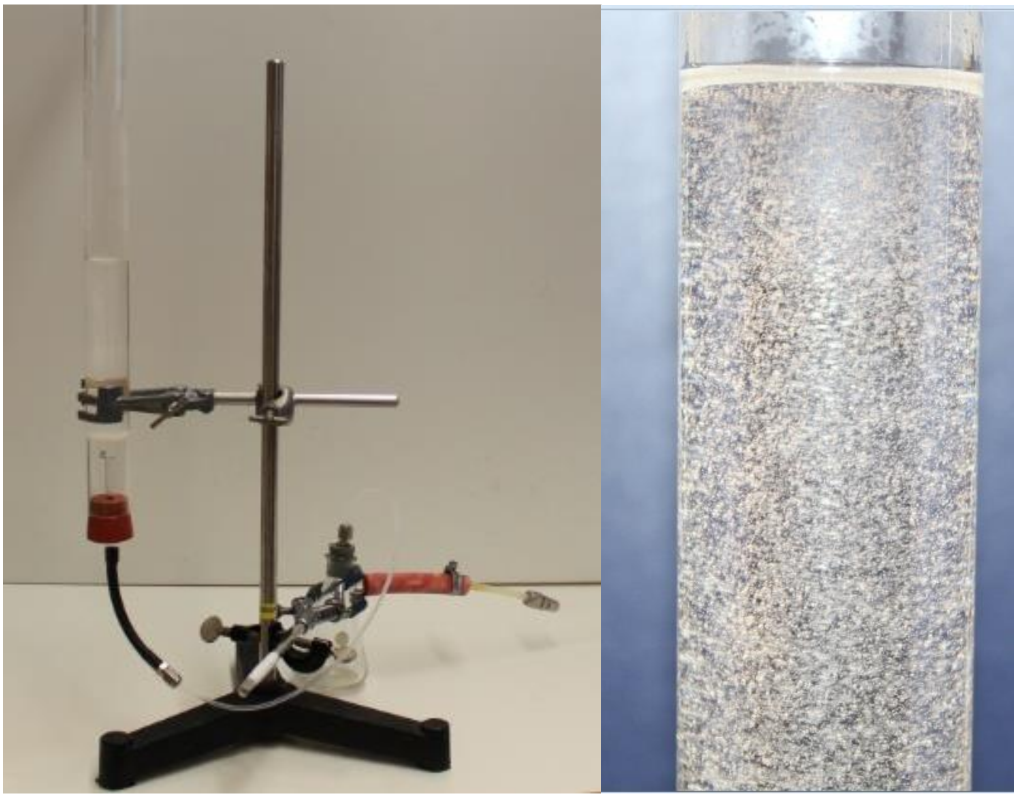

Figure 5.2: $CO_2$ bubbling to prepare loaded samples.

Figure 5.3: Sample analysis using titration method.

## Chapter 6

# Conclusions and Recommendations

This study has focused on process modeling and simulation of $CO_2$ capture with the post combustion chemical absorption process. The carbon capture model is developed and implemented in the Aspen Plus process simulation tool. The experimental studies are also performed to evaluate the dynamic viscosity of the amine base solvents which is important for chemical absorption process modeling. The main idea of this chapter is to point out the main reason behind every paper and the brief description of the contribution as well as the conclusion which is obtained from every publication. All the published papers are attached in part II.

## 6.1. Conclusions

This study has been performed under the two different sub categories such as modeling and simulation and experimental studies.

### 6.1.1. Modeling and Simulations

- (**Paper A**) The main problem of the post combustion chemical absorption technology is the high installation cost and large amount of energy requirement in the re-generating sector. Therefore, the reduction of capital and operating cost are important to achieve for the removal process in power plant flue gas treating. The model is developed and implemented in Aspen Plus to optimize the removal process. The Electrolyte NRTL (ELECNRTL) property method is used to handle the chemical reacting system in Aspen Plus. The makeup stream is added to maintain the component losses during the process. The required re-boiler energy demand is calculated for both coal and gas fired power plants. The required re-boiler duty was calculated as 4540 kJ/kg $CO_2$ for the gas fired flue gas system and 4100 kJ/kg $CO_2$ for the coal fired flue gas system. Some of the parameters effect on $CO_2$ removal efficiency as well as on re-boiler duty are initially investigated to understand the impact of different parameters. Temperature profiles, as well as $CO_2$ loading profiles, are analyzed to understand the process. Both temperature profiles in liquid and vapor phase follow similar patterns and temperature bulges are shown close to the top of the column. The coal fired temperature profile reach higher temperatures than gas fired system.

- (Paper **B**) Moreover, the developed model for the $CO_2$ removal process is validated with a model developed with MATLAB. Hence, two models are developed and implemented in Aspen Plus and MATLAB with the same physical properties to represent the absorber given in the Texas pilot plant study. The rate based Electrolyte NRTL model is used in the Aspen Plus model and the Kent-Eisenberg (K-E) model is selected for the development of the rate based MATLAB model. Simulations are performed by forcing the $CO_2$ removal efficiencies to be the same as in the pilot plant study. The simulation results from the Aspen Plus and MATLAB models are compared using the temperature profiles. Both models follow similar patterns for the temperature profiles and those are approximately equal with the Texas plant data. Therefore, the developed base case model is validated as a suitable model for the post combustion carbon capture process.

- (**Paper C, D, E**) The main purpose of this study is to understand the solvent's effect on $CO_2$ removal efficiency for power plant flue gas treating. The aqueous Monoethanolamine (MEA) for removal of $CO_2$ from flue gases is the most common solvent. The possibility of using other solvents has to be analyzed in order to enhance $CO_2$ capturing. The solvent strength and lean loading are considered as most relevant factors for analyzing. With the variation of these factors, efficiency of $CO_2$ removal from power plant flue gas is examined for different solvents. Both coal and gas-fired power plant flue gases are considered to develop the capture plant with different efficiencies. A number of simulations were performed in Aspen Plus with different solvent conditions to check the lowest re-boiler duty and lowest solvent inlet flow rate. The lowest re-boiler duty with lowest solvent flow rate will decide the optimal energy requirement and lowest operating cost. The lowest re-boiler duties are achieved as 3634, 3736, and 4185 kJ/kg $CO_2$ for the 85, 90, and 95% $CO_2$ removal process for coal fired power plant and 3781, 4050, and 4240 kJ/kg $CO_2$ for 85%, 90%, and 95% for gas fired power plant.
  Moreover, MEA and DEA solvents are selected to optimize the $CO_2$ capture process. The same simulation conditions are used to develop the model for $CO_2$ capture process with both solvent. Finally, re-generation energy demand is calculated and compared to evaluate the alternative solvents for carbon capture. Re-boiler energy requirement is significantly lower for DEA than MEA. Since DEA is less corrosion than MEA, DEA can be recommended as a better solvent for carbon capture plants. At present time, amine blends are widely studied to overcome drawbacks with single amines. The model is developed for MDEA/MEA blended solvent with 4:1 mixing ratio in weight basis. Finally, the model is implemented with optimized parameters to get 85% removal efficiency with a closed system. The temperature profiles in absorber, as well as $CO_2$ loading profiles, are studied. The comparison with the single amine model with the same 85% efficiency is performed to understand the benefits of blended amines. The blended amine system requires 2937 kJ/kg $CO_2$ for the coal fired plant flue gas capture process according to the present study. This is a significant lower value compared with single amine re-boiler duties.

- (**Paper F**) The main two types of absorption towers consist of either tray column or packed column. By comparing with tray column, packed columns are more beneficial for the gas absorption process. Packing material use in the gas absorption process can be categorized as random packing and structured packing. For the simulation studies, both random and structured packing are considered. The purpose of this study is to assess the characteristics of packing types on the absorption process. There are five different types of random packing and six different types of structured packing which are used to compare the packing material for the gas absorption process. Structured packing is given the lowest re-boiler duty, and that can be summarized as BX, Flexipac-1Y followed by Mellapak-350Y. The most important two factors for selecting packing material are identified as surface area and void fraction. The higher surface area gives the lower solvent requirement and will lead to lower re-boiler duty. Therefore, BX, Flexipac-1Y or Mellapak-350Y can be recommended for coal and gas fired power plant flue gas treating.

- (**Paper G, H, I)** The most important input parameters for the simulations are inlet gas stream flow rate, composition, pressure, temperature, packing material data, inlet solvent properties and stream conditions. The parameters' effects on $CO_2$ removal efficiency, as well as effect on re-boiler duty, are examined. The simulations of the absorption process are presented for sensitivity analyses of important parameters on the removal efficiency: lean loading, solvent concentration, flue gas temperature, the solvent temperature, packing height, packing diameter and absorber pressure. The rate based Electrolyte NRTL model was used to implement the model in Aspen Plus. The sensitivity analysis results show that the $CO_2$ removal efficiency increases with the solvent temperature, solvent concentration, packing height, packing diameter and absorber pressure.

  Moreover, the sensitivity analysis was performed for single parameter effect, as well as, multiple parameters effect on the desired output. Both the main effect and interaction effect of the parameters have been studied. The data collected from the simulation are analyzed using Principal Component Analysis (PCA), Principal Component Regression (PCR) and Partial Least Square-regression (PLS-R) to develop the linear relationship between parameters and output. From the PLS-R analysis solvent flow rate, temperature of the solvent, stripper packing height, stripper pressure, stripper packing diameter are positively correlated while solvent concentration, lean $CO_2$ loading, flue gas temperature, absorber pressure, absorber packing height and diameter are negatively correlated to re-boiler duty. The most important parameters (highest influence parameters on re-boiler duty) are lean $CO_2$ loading, absorber diameter and height. Similarly, the correlation between variables were studied for $CO_2$ removal efficiency, which indicate that inlet solvent flow rate, absorber packing height and diameter, absorber pressure and temperature of the solvent stream are positively correlated with $CO_2$ removal efficiency whereas the lean loading and temperature of flue gas are negatively correlated with efficiency.

- (**Paper J, K, L, M, N, O**) The base case model developed at the beginning of the project was implemented with optimized parameters, packing conditions and stream values to get better performance. The implemented model designed for the flue gases is used for coal fired power plant, gas fired power plant, cement plant as well as the aluminium industry. The required re-boiler duty was calculated for every situation. The temperature profiles, as well as $CO_2$ loading profiles, were analyzed to check the process behavior. The optimized $CO_2$ capture model is developed for different removal efficiencies.

The implemented model is properly working and converging for both coal and gas fired flue gas system. Three different models were developed with 85-95% removal efficiency. The calculated re-boiler duties are 3634, 3736, 4185 kJ/kg $CO_2$ for the 85, 90 and 95% $CO_2$ removal process respectively. The energy requirement in the re-generation process (re-boiler duty) are 3781, 4050, and 4240 kJ/kg $CO_2$ for 85%, 90%, and 95% capture models respectively for gas fired power plant.

Moreover, required re-boiler duties for the cement industry are also calculated for different efficiencies. The required re-boiler duties are calculated as 3229, 3306, and 3365 kJ/kg $CO_2$ for 85%, 90% and 95% removal efficiencies, respectively. The $CO_2$ removal model developed and implemented for cement industry flue gas is used for further evaluations of parameter effect on that industry. The specific thermal energy demand, as well as the false air factor of the kiln system, were varied in order to determine the effect on $CO_2$ capture plant performance, such as the solvent regeneration energy demand. In general, an increase in the mentioned kiln system factors increases the regeneration energy demand. The simulations showed that a variation in specific thermal energy demand of the kiln process within a relatively wide range, applicable to real cement kiln systems, does not give a substantial impact on the operation of the $CO_2$ capture plant. However, increasing the false air ingress in the kiln system pre-heater from 25 to 70 % results in a 4 % increase in the re-boiler duty. This indicates that false air ingress, which is a well-known phenomenon in the cement industry, should be kept low in order to reduce the energy consumption of the $CO_2$ capture plant.

The amount of energy available in the cement kiln exhaust gas is calculated as around 18MW. This will cover 18% of the total energy requirement in the stripper regeneration process. The equivalent amount of steam generated by installing a waste heat boiler in the cement kiln system is 28862 kg/hr. The required heat exchange area is calculated as 3115m$^2$. The total cost of the waste heat boiler installation is calculated as 3.9 million dollars. The installation cost for the waste heat boiler is paid back through a reduction in consumption of externally generated steam. The payback time is calculated approximately as 1 year. Therefore, heat integration with the cement kiln system by installing a waste heat boiler may be economically very attractive when implementing an amine-based carbon capture process in the cement industry.

Four different $CO_2$ concentrations, 3, 4, 7 and 10 vol%, in the flue gas from the aluminium production are considered for the simulation study. The re-generation energy in the stripping process is in the range of 3.0 - 3.5 MJ/kg $CO_2$ for 85% removal efficiency and 3.2 - 3.5 MJ/kg $CO_2$ for 90% removal efficiency and 3.4 - 3.6 MJ/kg $CO_2$ for 95% removal efficiency. It is shown that, (58-65)%, (67-75)%, (61-67)% and (52-60)% of energy requirement of case I, II, III and IV (3%, 4%, 7% and 10% of $CO_2$ in the flue gas) can be replaced by available heat on the re-generation process. According to the present study, it can be stated that 4% $CO_2$ content in the flue gas is given the maximum available heat to replace the maximum amount of energy requirements in the re-generation process.

### 6.1.2. Experimental Studies

- (**Paper P, Q**) The experiments were performed to check the viscosities of monoethanolamine (MEA), diethanolamine (DEA) and methyldiethanolamine (MDEA). The viscosity of the amines are reported in the literatures. However, high concentration amine viscosities as well as viscosities at high temperatures are not found. Therefore, viscosities of the above mentioned amines are measured. The concentration of the amine is varied from (10-100) wt% and the temperature also varied from (293.15-423.15) K. The measured data for the different kind of amines are compared with those available from the literature. Eventually, the obtained results were used to produce correlations for amine viscosity at different temperatures.

- (**Paper R**) The viscosities of MDEA+MEA+$H_2O$ mixtures for different concentrations have been analyzed for temperature range from 293.15 to 413.15 K. The total amine strength in the solution is maintained at 0.2, 0.3 and 0.4 mass basis. Temperature range 293.15 to 303.15 K is performed with cooling system to achieve the lower stable temperatures during the experiment. Operating pressure is maintained at 1 bar for temperature range 293.15 to 353.15 K and 4.5 bar for higher temperatures. A decrease in the viscosity with increasing temperature was observed. Measured viscosities were compared with the available literature values as well as with viscosities calculated by Grunberg and Nissan equation. The experimental data is in good agreement with literature data as well as with the calculated data.

- (**Paper S**) The dynamic viscosity of partially carbonated MEA solution was measured for the temperature range (20 to 150)°C for mass fraction (10 to 50)% and $CO_2$ loading (0.1 to 0.5) mol $CO_2$/mol MEA. The agreement with the literature data for temperature range (25 to 80)°C is satisfactory for mass fraction (20 to 40)%. The comparison between Weiland's proposed model and measurement data is in good agreement. However, regression model is valid only for mass fraction of MEA up to 40% and temperature up to 125°C. Therefore, measurement data were compared for only for valid operating conditions. The AAD between this work and equation regression data are 0.02, 0.09, 0.36, 0.19 mPa·s, respectively, for mass fraction of amine, r = (0.1, 0.2, 0.3, 0.4). However, Weiland's regression model can be used for estimation of viscosity inside the limitations.

## 6.2. Recommendations

- The model developed in this study can be used for other possible amines, as well. As an example the effect of TEA, PZ, DGA can also be analyzed for the carbon capture process. On the other hand, possibilities of other blended amines can also be evaluated.

- The main problem of the Aspen Plus process simulation is the limitation of operating concentration of amines. The data availability for amine base reactions are limited. Therefore, experimental studies of physical properties at high concentration necessary.

- Different configurations of the $CO_2$ capture process can be evaluated by simulations to reduce the re-generation energy requirement.

- The model developed in Aspen Plus can be validated with experimental results if there is pilot plant data available. That will be interesting to understand the operating procedure of the carbon capture process.

- The viscosities of the single and blended amines are evaluated in this study. However, the dynamic viscosity of other amines, as an example, TEA and DGA can also be examined. The blended amines viscosities are only evaluated for MEA+MDEA and DEA+MDEA. However, experiments can be extended to check the viscosities of other blends as well.

# Chapter 7

# Bibliography

[1] Sholeh M. Selection and Cheracterization of New Absorbents for Carbon Dioxide Capture. Ph.D Thesis, NTNU, Norway, 2005.

[2] International Energy Agency. *Redrawing the Energy Climate Map*. International Energy Agency Publications, 2013.

[3] International energy Agency (IEA). *world energy outlook 2007*- china and India insight. IEA publications, 2007.

[4] Intergovernmental Panel on Climate Change (IPCC). *Climate Change 2007: Synthesis Report*. IPCC, Geneva, Switzerland, 2007.

[5] Anderson S., Newell R. Prospects for carbon capture and storage technologies. discussion paper, *Resources for the future*, January 2003.

[6] Jeremy D., Herzog H.J. The cost of carbon capture. *Proc. of the* 5*th International Conference on green house gas control technologies,* Cairns, Australia, 13-16 August 2000.

[7] International Energy Agency. *Technology roadmap- Carbon capture and storage*. IEA/OECD, Paris, 2010.

[8] Victor D. $CO_2$ capture using aqueous ammonia. Ph.D thesis, DTU Chemical Engineering, Denmark, 2011.

[9] Alie C.F. $CO_2$ Capture with MEA: Integrating the Absorption Process and Steam Cycle of an Existing Coal-Fired Power Plant. Master Thesis, University of Waterloo, Canada, 2004.

[10] Fluor for IEA GHG Program. *Improvement in Power Generation with Post-Combustion Capture of* $CO_2$. Final Report, 2004.

[11] Adina B., Ondrej M., John E.O. $CO_2$ capture technologies for cement industry. *Energy procedia*, 2009, 1: 133-140.

[12] Björk H., Aronsson J. Process Integration and Performance of Chilled Ammonia $CO_2$ Capture Technology. M.Sc Thesis, Department of Energy and Environment, Chalmers University of Technology, Sweden, 2011.

[13] Kothandaraman A. Carbon dioxide capture by Chemical Absorption: A Solvent Comparison Study. PhD Thesis, Massachusetts Institute of Technology, USA, 2010.

[14] Faramarzi L. Post-Combustion Capture of $CO_2$ from fossil fueled power plants. Ph.D thesis, Technical University of Denmark, 2010.

[15] Kohl A.L., Nielsen R.B. *Gas Purification.* 5th edition. Gulf Publishing Company, Huston, Texas, 1997.

[16] Polasek J., Bullin J.A. Process Considerations in Selecting Amine. *Energy Progress*, September 1984: 146-150.

[17] Freguia S. Modeling of $CO_2$ removal from Flue Gas with Mono-ethanolamine. Master Thesis, University of Texas, Austin, USA, 2002.

[18] Goff G.S., Rochelle G.T. Oxidation inhibitors for copper and iron catalyzed degradation of monoethanolamine in $CO_2$ capture processes. *Industrial & Engineering Chemistry Research*, 2006, 45(8): 2513-2521.

[19] Chakma A., Meisen A. Degradation of Aqueous DEA Solutions in a Heat- Transfer Tube. *Canadian Journal of Chemical Engineering*, 1987, 65(2): 264-273.

[20] Crooks J.E., Donnellan J.P. Kinetics and Mechanism of the Reaction between Carbon-Dioxide and Amines in Aqueous-Solution. *Journal of the Chemical Society-Perkin Transactions* 2, 1989(4): 331-333.

[21] Aspen Plus. *Rate Based model of the $CO_2$ capture process by MEA using Aspen Plus*. Aspen Technology Inc, Cambridge, MA, USA, 2008.

[22] Aspen Plus. *Aspen Plus 2006 Documentation, Aspen Physical Property Methods, Aspen Technology Inc* , MA, USA, 2006.

[23] Liu Y., Zhang L., Watanasiri S. Representing Vapor-Liquid Equilibrium for an Aqueous MEA-$CO_2$ System Using the Electrolyte Nonrandom-Two-Liquid Model. *Ind. Eng. Chem. Res*. 1999, 38: 2080-2090.

[24] Giorgio S. Equilibrium constants from a modified Redlich-Kwong equation of state. *Chemical Engineering Science*. 2012, 27 (6): 1197-1203.

[25] Montigny D., Tontiwachwuthikul P., Chakma A. Parametric Studies of carbon Dioxide Absorption into Highly Concentrated Monoethanolamine Solutions. *The Canadian journal of chemical engineering*, 2001, 79: 137-142.

[26] Onda K., Takeuchi H., Okumoto Y. Mass Transfer Coefficients Between Gas and Liquid Phases in Packed Columns. *J. Chem. Eng. Jap*, 1968, 1-1: 56-62.

[27] Bravo J.L., Rocha J.A., Fair J.R. Mass Transfer in Gauze Packing. *Hydrocarbon Processing*, January, 1985, 91–95.

[28] Billet R., Schultes M. Predicting Mass Transfer in Packed Columns. *Chem. Eng. Technology*, 1993, 16: 1-9.

[29] Stichlmair J., Bravo J.L., Fair J.R. General model for prediction of pressure drop and capacity of countercurrent gas/liquid packed columns. *Gas separation and purification*, 1989, 3: 19-28.

[30] Edali M., Aboundheir A., Idem R. Kinetics of carbon dioxide absorption into mixed aqueous solutions of MDEA and MEA using laminar jet apparatus and numerically solved absorption rate/kinetic model. Proceedings of the COMSOL Conference 2007, Boston.

[31]Chakravarty T., Phukan U.K., Weiland R.H. Reaction of acid gases with Mixtures of amines. *Chem. Eng. Prog*, 1985, 81: 32-36.

[32] Shao R., Stangeland A. *Amines used in $CO_2$ capture- Health and Environmental Impacts*, Bellona Report, The Bellona Foundation, Norway, 2009.

[33] Bullin J.A., Polasek J.C., Donnelly S.T. The use of MDEA and mixtures of amines for bulk $CO_2$ removal. Proceedings, 69th Gas processors association Convention, 1984, Lousiana.

[34] Aroonwilas A., Veawab A. Integration of $CO_2$ capture unit using single and blended amines into supercritical coal-fired power plants: implications for emission and energy management. *Int. J. Greenhouse Control*, 2007, 1: 143-150.

[35] Billet R., Schultes M. Advantage in correlating packed column performance. *IChemE. Symp*, 1992, Ser. No. 128: B129.

[36] Li M.H., Lie Y.C. Densities and Viscosities of Solutions of Monoethanolamine + N-methyldiethanolamine + Water and Monoethanolamine + 2-Amino-2-methyl-1-propanol + Water. *J. Chem. Eng. Data*, 1994, 39: 444-447.

[37] DiGuilio R.M., Lee R.J., Schaeffer S.T., Brasher L.L., Teja A.S. Densities and viscosities of the ethanolamines. *J. Chem. Eng. Data, 1992*, 37: 239-242.

[38] Mandal B.P., Kundu M., Bandyopadhyay S.S. Density and Viscosity of Aqueous Solutions of (N-Methyldiethanolamine + Monoethanolamine), (N-Methyldiethanolamine + Diethanolamine), (2-Amino-2-methyl-1-propanol + Monoethanolamine), and (2-Amino-2-methyl-1-propanol + Diethanolamine). *J. Chem. Eng. Data,2003,* 48: 703-707.

[39] Amundsen T.G., Øi L.E., Eimer D.A. Density and Viscosity of Monoethanolamine + Water + Carbon Dioxide from (25 to 80) °C. *J. Chem. Eng. Data,2009,* 54: 3096-3100.

[40] Rinker E.B., Oelschlager D.W., Colussi A.T., Henry K.R., Sandall O.C. Viscosity, Density, and Surface Tension of Binary Mixtures of Water and N-Methyldiethanolamine and Water and Diethanolamine and Tertiary Mixtures of These Amines with Water over the Temperature Range 20-100.degree.C. *J. Chem. Eng. Data*, 1994, 39: 392-395.

[41] Li M.H., Shen K.P. Densities and solubilities of solutions of carbon dioxide in water + monoethanolamine + N-methyldiethanolamine. *J. Chem. Eng. Data*, 1992, 37- 3: 288-290.

[42] Hagewiesche D.P., Ashour S.S., Sandall O.C. Solubility and Diffusivity of Nitrous Oxide in Ternary Mixture of Water, Monoethanolamine, and N-Methyldiethanolamine and Solution Densities and Viscosities. *J. Chem. Eng. Data*, 1995, 40: 627-629.

[43] Teng T.T., Maham Y.J., Hepler L.G., Mather A.E. Viscosity of aqueous solutions of N-Methyldiethanolamine and of Diethanolamine. *J. Chem. Eng. Data*, 1994, 39: 290-293.

[44] Hsu C.H., Li M.H. Densities of Aqueous Blended Amines. *J. Chem. Eng. Data*, 1997, 42: 502-507.

[45] Hsu C.H., Li M.H. Viscosities of aqueous blended amines. *J. Chem. Eng. Data*, 1997, 42: 714-720.

[46] Mandal B.P., Kundu M., Bandyopadhyay S.S. Density and viscosity of aqueous solutions of (MDEA+MEA), (MDEA+DEA), (AMP+MEA), and (AMP+DEA). *J. Chem. Eng. Data*, 2003, 48: 703-707.

# Part II

# Published and Submitted Papers

# Paper A

## Aspen Plus Simulation of $CO_2$ Removal from Coal and Gas Fired Power Plants

This paper was presented in Trondheim CCS Conference (TCCS-6) at Trondheim, Norway on June 2011. The paper was also published in Energy Procedia 23 (doi: 10.1016/j.egypro.2012.06.060, Elsevier Ltd., pp 391–399, 2012).

Available online at www.sciencedirect.com

SciVerse ScienceDirect

Energy Procedia 23 (2012) 391 – 399

Energy Procedia

Trondheim CCS Conference (TCCS-6)

# Aspen plus simulation of $CO_2$ removal from coal and gas fired power plants

Udara Sampath P.R.Arachchige[a], Morten Christian Melaaen[a,b,*]

[a]*Telemark University College, Porsgrunn, 3901, Norway*

[b]*Tel-Tek, Porsgrunn, 3901, Norway*

---

**Abstract**

This paper presents a description of the $CO_2$ removal process of 500MW coal and gas fired power plants. The parameters and other operating conditions for Aspen Plus rate based model were selected to achieve 85% of $CO_2$ removal. The effects of absorber pressure and packing height on re-boiler duty are studied. Re-boiler duty is decreasing with the increase of packing height and absorber pressure. The effect of solvent properties on $CO_2$ removal efficiency is also analyzed. The removal efficiency increases as the increase of MEA concentration and temperature. When the lean loading of MEA solvent is increased, efficiency of the removal process is decreasing. The liquid and vapour phase temperature profiles and $CO_2$ loading in the absorber are analyzed to understand the model behaviour.

*Keywords*: Carbon capture; Absorption; Aspen Plus; Sensitivity analysis; Re-boiler duty; Removal efficiency

---

## 1. Introduction

Carbon capture and storage (CCS) is considered as an important option for stabilization of atmospheric green house gases and minimizing global warming effects. Carbon dioxide ($CO_2$) is considered as the major green house gas, and fossil fuel fired power plants are the main emitting sources [1]. Therefore, the capture of $CO_2$ is important to maintain the emission levels according to the standards. There are three main options available for carbon capture in fossil fuel fired power plants: pre combustion $CO_2$ capture, where carbon is removed from the fuel prior to combustion; oxy-fuel combustion, where coal is combusted with oxygen instead of air with $CO_2$ enriched environment; and post combustion capture, where fossil fuel is combusted to produced energy and $CO_2$ is removed from the flue gas after combustion

---

* Corresponding author. Tel.: +47-355-75-286; fax: +47-355-75-001.
*E-mail address*: Morten.C.Melaaen@hit.no.

doi:10.1016/j.egypro.2012.06.060

[2]. Out of these options, post combustion $CO_2$ capture by absorption and stripping process is currently considered as the most feasible option for $CO_2$ removal from fossil fuel fired power plants [3].

## 2. Model Development

The main problem of post combustion chemical absorption technology is the high installation cost and large amount of energy requirements in the re-generating sector. Therefore, the reduction of capital and operating cost are important to implement for the removal process in power plant flue gas treating. The model is developed and implemented in Aspen Plus to optimize the removal process. The Electrolyte NRTL (ELECNRTL) property method is used to handle the chemical reacting system in Aspen Plus. The flue gas streams data for 500 MW coal and gas fired power plant are extracted from the literature [1, 4]. The implemented process flow diagram is given in the Fig. 1.

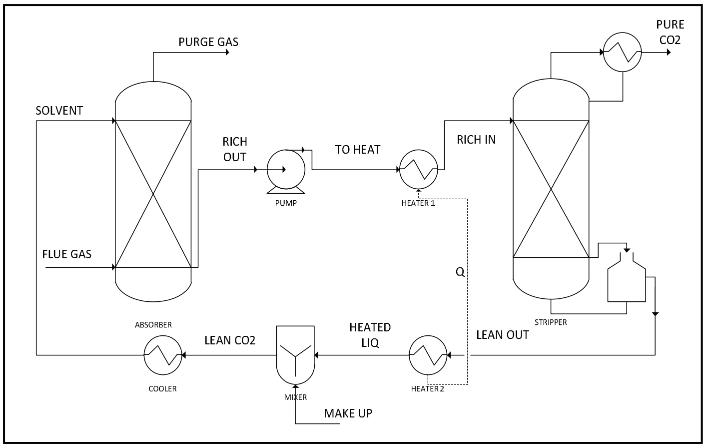

Fig. 1. Process Flow Diagram

In the chemical absorption, flue gas (FLUE GAS) enters the absorber at the bottom while the solvent (SOLVENT) enters at the top. The reactions start between MEA and $CO_2$ while flowing through the column (packing bed). An un-reacted gas leaves the column at the top (PURGE GAS), while the $CO_2$ rich solvent discharges the column at the bottom (RICH OUT). The rich solvent goes through the heat exchanger to increase the temperature before sending it to the stripper section. The heated rich MEA stream (RICH IN) then goes to the stripper at the top. In the stripper, steam is used for the regeneration process. Finally, separated acid gases leave the stripper at the top (PURE CO2). The lean MEA then leaves the system at the bottom of the stripper (LEAN OUT) and go through the heat exchanger. The MEA and water are added to the lean MEA stream (MAKE UP) to balance the component before recycled back to the absorber unit.

The flow diagram is modelled to capture the 85% of $CO_2$ from coal and gas fired power plants' flue gas with the variation of distillate rate in the stripper. Inlet flue gas and solvent stream are supplied at 40ºC and absorber is operating at 1bar absolute pressure. The rich solvent stream is heated up to 115ºC before sending it to the stripper section for maximum performance and the stripper is operating at 2 bars absolute pressure. The inlet flue gas stream data are given in the Table 1.

Table 1. Flue gas composition and parameters at inlet [1, 4]

| Parameter | Coal Fired | Gas Fired |
|---|---|---|
| Flow rate [tones/hr] | 2424 | 2861 |
| Temperature [°C] | 40 | 40 |
| Pressure [bar] | 1.1 | 1.1 |
| Composition | Mol% | Mol% |
| $H_2O$ | 8.18 | 8.00 |
| $N_2$ | 72.86 | 76.00 |
| $CO_2$ | 13.58 | 4.00 |
| $O_2$ | 3.54 | 12.00 |
| $H_2S$ | 0.05 | 0.00 |

### 2.1. Chemical Reactions

The main chemical reactions taking place in a MEA+$CO_2$ system are described in this section. The absorption/stripping section required rigorous thermodynamic model [5] to find the equilibrium compositions in the system. Following chemical reactions (Equations 1-7) are taking place when $CO_2$ is absorbed into an aqueous solution [6].

Hydrolysis reaction:

$$MEACOO^- + H_2O \leftrightarrow MEA + HCO_3^- \tag{1}$$

Dissociation of dissolved carbon dioxide:

$$CO_2 + 2H_2O \leftrightarrow HCO_3^- + H_3O^+ \tag{2}$$

Dissociation of bicarbonate:

$$HCO_3^- + H_2O \leftrightarrow H_3O^+ + CO_3^{2-} \tag{3}$$

Dissociation of protonated MEA:

$$MEAH^+ + H_2O \leftrightarrow MEA + H_3O^+ \tag{4}$$

Ionization of water:

$$2H_2O \leftrightarrow OH^- + H_3O^+ \tag{5}$$

In addition to these main reactions, following two reactions are taking place when a sulphur compound exists in the flue gas system (coal fired flue gas).

Hydrogen sulfide:

$$H_2O + H_2S \leftrightarrow HS^- + H_3O^+ \tag{6}$$

Hydrogen bisulfide:

$$H_2O + HS^- \leftrightarrow S^{2-} + H_3O^+ \tag{7}$$

### *2.2. Equilibrium data*

The mole fractions of every single component in the liquid and vapour phase are calculated by solving above equations. The equilibrium constant is calculated using following rate equation (equation 8).

$$ln\,K_j = A_j + \frac{B_j}{T} + C_j\,ln\,T + D_jT \tag{8}$$

The equilibrium constant data which is imported from Freguia [7] is considered for mathematical model development and tabulated in Table 2.

Table 2. Constant values of equilibrium constant equations [7]

| *Parameter* | *Reaction 1* | *Reaction 2* | *Reaction 3* | *Reaction 4* | *Reaction 5* | *Reaction 6* | *Reaction7* |
|---|---|---|---|---|---|---|---|
| $A_j$ | -0.52 | 231.46 | 216.05 | -3.038 | 132.89 | 214.58 | -9.74 |
| $B_j$ | -2545.53 | -12092.1 | -12431.7 | -7008.3 | -13445.9 | -12995.4 | -8585.47 |
| $C_j$ | 0 | -36.78 | -35.48 | 0 | -22.47 | -33.55 | 0 |
| $D_j$ | 0 | 0 | 0 | -0.00313 | 0 | 0 | 0 |

### *2.3. Rate kinetic data*

Rate kinetic data are important to understand for reacting system. The equilibrium reactions 1 and 2 are replaced by rate model equations 9 and 10 and reverse reactions 11 and 12.

$$CO_2 + OH^- \rightarrow HCO_3^- \tag{9}$$

$$MEA + CO_2 + H_2O \rightarrow MEACOO^- + H_3O^+ \tag{10}$$

$$HCO_3^- \rightarrow CO_2 + OH^- \tag{11}$$

$$MEACOO^- + H_3O^+ \rightarrow MEA + CO_2 + H_2O \tag{12}$$

The kinetic equation used for mathematical calculations is defined in Aspen Plus and given in Equation (13) with constant values in Table 3.

$$r_j = k_j \left(\frac{T}{T_O}\right)^{n_j} \exp\left[-\frac{E_j}{R}\left(\frac{1}{T} - \frac{1}{T_O}\right)\right] \quad (13)$$

Table 3: Rate constant values

| *Parameter* | *Reaction 9* | *Reaction 10* | *Reaction 11* | *Reaction 12* |
|---|---|---|---|---|
| $k_j$ | 4.32e+13 | 9.77e+10 | 2.38e+17 | 2.7963e+20 |
| $n_j$ | 0 | 0 | 0 | 0 |
| $E_j$ (cal/mol) | 13249 | 9855.80 | 29450.89 | 17229.79 |
| $T_O$ (K) | 298 | 298 | 298 | 298 |

## 3. Simulations

The main idea of this paper is to develop the model that will help to optimize the process with sensitivity analysis. Initially, the open loop process flow diagram is developed to optimize the parameters and finally, the process flow diagram is modified with optimized parameters for closed loop system. Open loop model should be used for parameter optimization. Once the process flow diagram is closed, model is not able to use for parameter optimization due to recirculation stream. The process model is closed with individual material balance. Therefore, change of one parameter causes to change the material balance in the process.

### *3.1. Solvent properties effect on removal efficiency*

The sensitivity analysis is performed to check the solvent properties' behaviour for removal efficiency in capture plant. As the most important factors, solvent strength, lean loading and solvent temperature are considered for analyzing. According to the variation of these factors, removal efficiency is studied and given in Fig. 2-4, respectively.

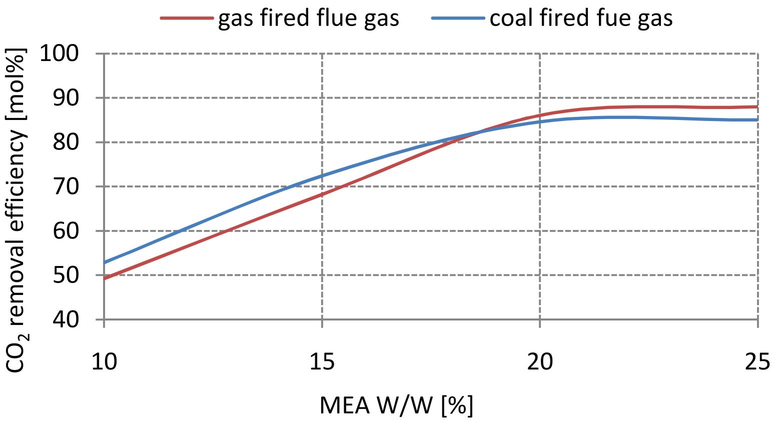

Fig. 2. $CO_2$ removal efficiency variation with MEA concentration

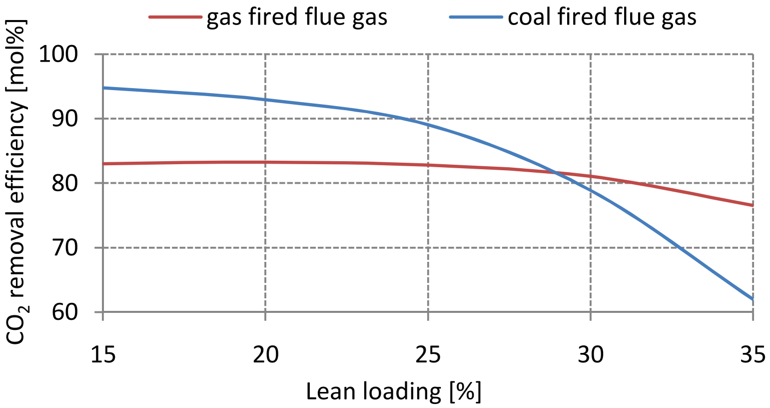

Fig. 3. $CO_2$ removal efficiency variation with lean loading

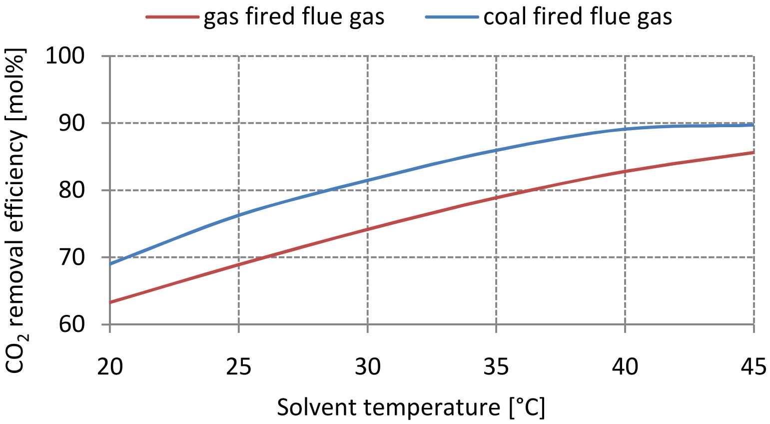

Fig. 4. $CO_2$ removal efficiency variation with solvent temperature

As it can be seen from Fig. 2 and 4, the efficiency of the $CO_2$ removal is increased as the MEA strength and solvent temperature are increased. The maximum efficiency is achieved when MEA concentration at 22-25% and temperature is around 40-45°C. When the lean loading of MEA solvent is increased, efficiency of the removal process is decreasing (Fig. 3). Both gas and coal fired flue gas system follow the similar pattern in all three cases. However, the values of coal fired flue gas model are slightly higher than the gas fired model.

### 3.2. Parameters effect on re-boiler duty

The main problem with the post combustion capture is the high energy requirement in the regeneration sector, i.e. re-boiler duty in stripper column. Therefore, parameters' effect on the re-boiler duty is important to optimize. The effect of absorber pressure and absorber packing height on re-boiler duty is studied to optimize the energy requirement. Fig. 5 and 6 represent the re-boiler duty variation with absorber pressure and packing height, respectively. With the increase of absorber pressure and packing height, re-boiler duty is decreased. Gas fired flue gas system has higher re-boiler duty compared to the coal fired system. Reason for that is, gas fired flue gas consist of fewer carbon dioxide amounts compared to coal fired flue gas. Therefore, to achieve the same efficiency defined in the model is required to process more flue gas compared to the coal fired system.

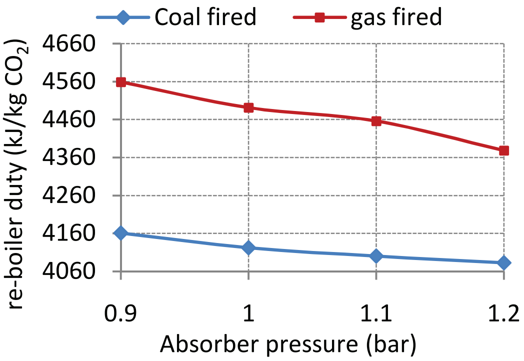

Fig. 5. Re-boiler duty variation with Absorber pressure

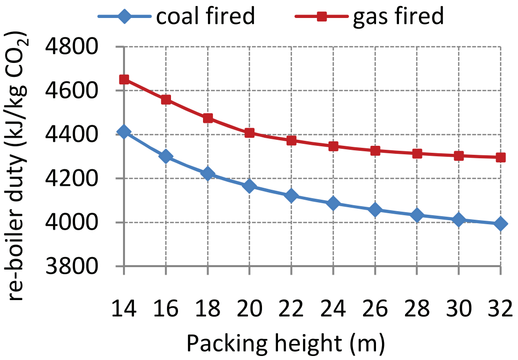

Fig. 6. Re-boiler duty variation with absorber packing height

### 3.3. Simulated profiles for closed loop capture model

The process flow diagram is implemented with the optimized parameters for closed loop system. After the simulation, temperature profiles, $CO_2$ concentration profiles and loading are analyzed for both coal and gas fired implemented model to understand the model behaviour. Fig. 7 represents the liquid and vapor phase temperature profiles in the absorber for coal and gas fired systems. According to the Fig. 7, the coal fired flue gas model has higher temperature range along the column. Coal fired flue gas consist of more $CO_2$ than gas fired system. Therefore, more reactions are taking place in the absorber column in coal fired model. Hence, liquid and vapour phase temperature of the absorber unit are increasing and maximum value is higher in gas fired system temperature profiles. The temperature profiles in both liquid and vapour phases are overlapped in gas fired system and slight deviation in coal fired process. Similarly,

Fig. 8 represents the liquid phase $CO_2$ loading in the absorber. The $CO_2$ loading is gradually increasing down the column for both cases.

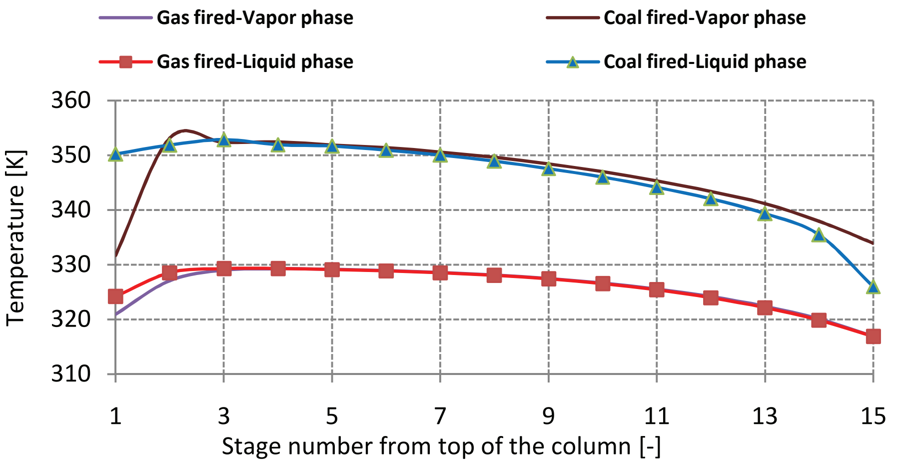

Fig. 7. Liquid and vapor phase temperature profiles in absorber

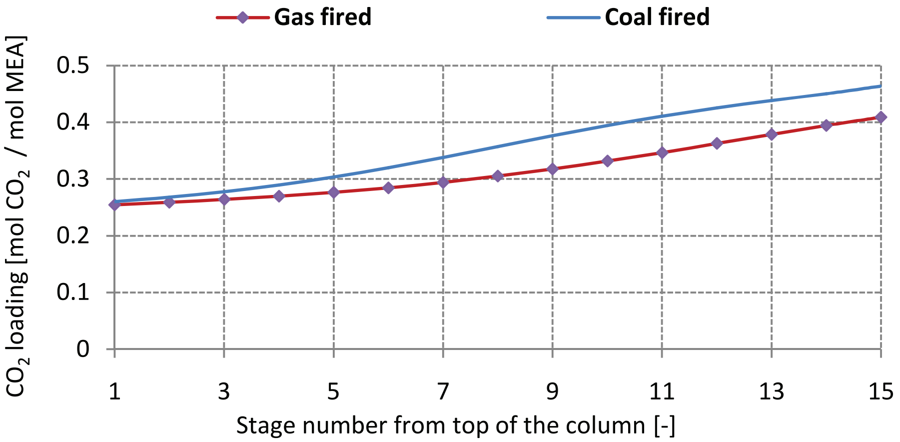

Fig. 8. $CO_2$ loading in absorber

## 4. Discussion and Conclusion

The efficiency of the removal process is strongly depending on the solvent properties like solvent concentration, lean loading and solvent temperature. The removal efficiency is proportional to the solvent concentration and temperature while lean loading is inversely effect on removal efficiency. This is because of; increasing the amine concentration will cause for the increasing capture capacity. With the increase of lean loading, the capacity of the solvent for $CO_2$ absorption decreases, hence efficiency of the $CO_2$ removal is decreasing. As the solvent temperature increases, the driving force for absorption decreases. However, the rate of reaction and diffusivity increases as the solvent temperature is increased. Therefore, efficiency of $CO_2$ removal is increased with the increase of solvent temperature.

The re-boiler duty is functions of absorber pressure and absorber packing height and when the increase of both factors, re-boiler duty is decreased. The reason for that is the attained rich loading increase with the increases in the absorber packing height. Similarly, re-boiler duty decreases with the increase of absorber pressure due to higher $CO_2$ partial pressure. The required re-boiler duty was calculated as 4540 kJ/kg $CO_2$ for the gas fired flue gas system and 4100 kJ/kg $CO_2$ for coal fired flue gas system. Both re-boiler duties are reasonable with the literature values [3].

The implemented model in Aspen Plus for gas and coal fired removal system functioned properly. The amount of $CO_2$ removal is 85% and calculated with the variation of distillate rate in the stripper. The make up stream is added to maintain the component losses during the process. The MEA and $H_2O$ requirement for the make-up stream was calculated as 362 kg/hr and 87.8 tones/hr for gas fired system and 627 kg/hr and 119 tones/hr for coal fired system, respectively.

Both temperature profiles in liquid and vapor phase follow the similar patterns and temperature bulges are shown close to top of the column. Coal fired temperature profile reach higher temperatures than gas fired system. The $CO_2$ loading profile has the similar flow pattern in both cases. The maximum value is reached to around 0.4 and higher in coal fired flue gas system. Those profiles are important to understand the column behaviour.

## References

[1] Alie CF. $CO_2$ Capture with MEA: Intergrating the Absorption Process and Steam Cycle of an Existing Coal-Fired Power Plant. Master Thesis, University of Waterloo, Canada; 2004.

[2] Vural A. Clean coal and carbon capture and storage technology roadmap of Turkey. Master Thesis, Middle East Technical University, Turkey; 2010.

[3] Kothandaraman A. Carbon dioxide capture by Chemical Absorption: A Solvent Comparison Study. PhD Thesis, Massachusetts Institute of Technology, USA; 2010.

[4] Fluor for IEA GHG Program. Improvement in Power Generation with Post-Combustion Capture of $CO_2$. Final Report. Report Number PH4/33; November 2004.

[5] Aboudheir AA. Kinetics, Modeling, and Simulation of Carbon Dioxide Absorption into Highly Concentrated and Loaded Monoethanolamine Solutions. PhD Thesis, University of Regina, Canada; 2002.

[6] Michael AD. A model of vapour-liquid equilibria for acid gas-alkanolamine-water systems. PhD Thesis, University of Texas, USA; 1989.

[7] Freguia S. Modeling of $CO_2$ removal from Flue Gas with Mono-ethanolamine. Master Thesis, University of Texas, USA; 2002.

# Paper B

## Comparison of temperature profiles in $CO_2$ removal process with Aspen Plus and MATLAB

This paper was presented in the 36th International Technical Conference on Clean Coal & Fuel System at Florida, USA on June 2011. The paper is published in conference proceedings (ISBN: 978-0-932066-36-4, Coal Technologies Associates, pp 379 - 387, 2011). Edited by: Barbara A. Sakkestad.

# Comparison of temperature profiles in $CO_2$ removal process with Aspen Plus and MATLAB

Udara S.P.R. Arachchige[1], Sanoja A. Jayarathna[1], Morten C. Melaaen[1, 2, *]

[1]*Telemark University College, Porsgrun, Norway*
[2]*Tel-Tek, Porsgrunn, Norway*

*corresponding author: **Morten.C.Melaaen@hit.no**
Tel.: +47-93406122; fax: +47-3557-5001.

---

# Abstract

The power generating sector is identified to be the main source of $CO_2$ emission. Due to the climate change effect, $CO_2$ capture technologies are being important in current scenario. Out of several gas cleaning methods, post combustion $CO_2$ removal by chemical absorption technology is the closest to commercialization. This paper presents a simulation study of the chemical absorption process with the MEA system as the solvent. Data found in literature (Texas case 32 and case 47) are compared with the simulation results. Two models are developed and implemented in Aspen Plus and MATLAB with the same physical properties to represent the absorber given in the Texas pilot plant study. The rate based Electrolyte NRTL model is used in the Aspen Plus model and the Kent-Eisenberg (K-E) model is selected for the development of the rate based MATLAB model. Model simulations are done using 32.5[w/w %] MEA solution and 0.28 [mol $CO_2$/mol MEA] lean $CO_2$ loading. Simulations are performed by forcing the $CO_2$ removal efficiencies to be the same as in the pilot plant study. The simulation results from the Aspen Plus and MATLAB models are compared using the temperature profiles. Both models follow similar patterns for the temperature profiles and those approximately equal with the Texas plant data.

Key words: $CO_2$ capture, simulation, Aspen Plus, MATLAB, Temperature profiles

---

# 1. INTRODUCTION

The global warming and climate change, believed to be caused by acid gases, has taken increasing attention in last few years. The main pollutant gases, cause for climate change are, $CO_2$, $CH_4$, $N_2O$, $SF_6$, CFC's and HFC's [1]. The global warming potential of those gases is given in the Table 1. Even though $CO_2$ has the lowest global warming potential, it has the highest climate change potential due to the largest emission compared to the other sources. Thus, reduction of $CO_2$ emission is very important for maintaining the emission levels according to the standards.

Table 1: Global Warming Potential [1].

| Source | Global Warming Potential |
|---|---|
| $CO_2$ | 1 |
| $CH_4$ | 21 |
| $N_2O$ | 310 |
| HFC's | 40-1170 |
| CFC's | 6500-9200 |
| $SF_6$ | 23900 |

Carbon capture and sequestration (CCS) technologies are required to reduce the environmental impact by $CO_2$ emissions. Present time, the most interesting and preferred method is the post combustion $CO_2$ capture via chemical absorption. This technology can be used to remove the carbon dioxide from flue gas using re-generable solvents.

The monoethanolamine (MEA) is selected as the best solvent due to several advantages on the absorption process. For an example it has the lowest molecular weight hence, it has the highest reaction capability with carbon and absorbs more $CO_2$ than other solvents. The low cost, possibility to recycle to the absorption column after regenerating, high absorbing capacity on a mass basis, reasonable thermal stability and low thermal degradation rate are some other advantages of using MEA over the other solvents [2].

In the post combustion chemical absorption process, the solvent stream is entering the absorber at the top while the flue gas is introduced from the bottom of the column. There are several chemical reactions taking place in the solvent once MEA absorbs the $CO_2$. Cleaned gas leaves the column at the top with some amount of $CO_2$ remaining. The rich solvent (with chemically bound $CO_2$) then goes through the heater to increase the temperature before entering the desorption column. The desorption process operate with steam to regenerate the solvent. The acid gas that is separated from the rich solvent leaves the column at the top and the lean solvent leaves from the bottom. The rate based modeling approach gives better prediction for $CO_2$ capture technology than the equilibrium approach.

### 1.1 Objective

$CO_2$ capture by post combustion represents an expensive solution for gas cleaning. Therefore, research works on this technology have to be carried out in order to reduce the operating cost and to improve the existing technologies to be able to capture high amount of $CO_2$.

This paper presents a simulation study of the chemical absorption process for the Texas case 32 and 47 with MEA as the solvent [3]. Two models are developed and implemented in Aspen Plus and MATLAB for the absorber of a $CO_2$ capture plant. The Aspen Plus model, which is a steady state model with advanced thermodynamics is validated against the experimental data. The model will be developed further and used for design and optimization purposes.

The MATLAB model, which is a dynamic model, is validated against the Aspen Plus model and the experimental data using its steady state predictions. The model is supposed to be using for analyzing the transient conditions of the absorber. Further, the model will be expanded to cover the whole capture plant and will be used for developing a control system.

## 2. MODEL DEVELOPMENT

Two models are developed and implemented in Aspen Plus and MATLAB for the absorber of a $CO_2$ capture plant. Both models have used the non-equilibrium rate based approach to represent the interfacial mass transfer. Same operating conditions and parameters as in the pilot plant study are used in both models.

### 2.1. MATLAB model

The MATLAB model is developed by applying the specie and energy balances on the liquid and vapor phases separately.

The physical properties and parameters used in the model are found from literature either as correlations or constant values. The main model equations and more details have been presented by Jayarathna et al [4]. The flue gas and solvent stream conditions used for the simulations are given in the section 3.1.

### 2.1.1. Reaction Kinetics and phase equilibrium

The reaction kinetics and phase equilibrium are important for representing the specie generation and interfacial mass transfer. The rate of specie generation is calculated using the overall reaction between MEA and $CO_2$ (Eq. 1). The reaction and phase equilibrium constants are introduced from the Kent-Eisenberg model [5]. The reason for using the K-E model is to maintain the simplicity of the MATLAB model. Simplicity is an advantage for a dynamic model as it permits to predict the complex transient conditions easily.

$$CO_2 + 2MEA \leftrightarrow MEA^+ + MEACOO^- \quad (1)$$

The reaction rate coefficient for the forward reaction is introduced via a correlation found from literature [6] and the backward reaction coefficient is calculated based on the equilibrium coefficient and the forward reaction rate coefficient.

### 2.1.2. Physical properties and other parameters

Important physical properties and parameters are introduced to the model as correlations or constant values taken from the literatures. Some of them are tabulated in Table 2 with their literature sources.

Table 2: Physical properties and other parameters used in the MATLAB model [4].

| Property | Source |
|---|---|
| Liquid density & Specific heat capacity | Cheng et al. [7] |
| Liquid diffusivity of $CO_2$ | Versteeg et al. [8] |
| Liquid holdup | Billet et al. [9] |
| Overall heat transfer coefficient between phases | Cussler et al. [10] |
| Heat of absorption of $CO_2$ | Khol et al. [11] |
| Heat of vaporization of $H_2O$ | Kvamsdal et al. [12] |

### 2.1.3 Model Assumptions

The most relevant model assumptions are listed below [4].

1. Continuous stirred tank (CSTs) behavior is assumed for each phase in a control volume.
2. Both gas and liquid phases are considered as ideal conditions.
3. Only $H_2O$ and $CO_2$ are considered for interfacial mass transfer process.
4. Liquid phase reactions are the most important for reacting system.
5. Behavior of the pressure drop along the column is considered as linear.
6. The specific area of the packing material is taken as the effective contact area between the gas and liquid phases.
7. Vapor and liquid flow is constant.
8. Negligible heat losses to the surrounding.

## 2.2. Aspen Plus Model

The rate based Electrolyte NRTL model is used in the Aspen Plus model with given MEA solution (section 3.1). When the species are dissociated in solutions, ions enter to the liquid phase, and it causes non-ideal behavior in that phase. To handle this situation wisely, the Aspen Plus electrolyte is recommended.

### 2.2.1. Thermodynamic Model

The $CO_2$ absorption process requires a rigorous thermodynamic model to determine the liquid phase driving forces and solution specification. In the absorption and stripping process following equilibrium reactions are used in solution chemistry.

$$MEACOO^- + H_2O \leftrightarrow MEA + HCO_3^- \quad (2)$$

$$CO_2 + 2H_2O \leftrightarrow HCO_3^- + H_3O^+ \quad (3)$$

$$HCO_3^- + H_2O \leftrightarrow H_3O^+ + CO_3^{2-} \quad (4)$$

$$MEAH^+ + H_2O \leftrightarrow MEA + H_3O^+ \quad (5)$$

$$2H_2O \leftrightarrow OH^- + H_3O^+ \quad (6)$$

The mole fractions of each component in both the liquid and vapor phases are calculated by solving the above equations at a given temperature and pressure. There is an equilibrium constant for every single reaction. The equilibrium constants are temperature dependent and given by,

$$ln\,K_j = A_j + \frac{B_j}{T} + C_j\,ln\,T + D_jT \quad (7)$$

The constant values of equation 7 for the given reactions are tabulated below. According to the literatures [13], Table 3 is generated.

Table 3: Constant values of Eq. 7.

| Rea: # | A | B | C | D |
|---|---|---|---|---|
| 2 | -0.52 | -2545.53 |  | 0 |
| 3 | 231.46 | -12092.1 | -36.78 | 0 |
| 4 | 216.05 | -12431 | -35.48 | 0 |
| 5 | -3.038 | -7008.3 | 0 | -0.0031 |
| 6 | 132.89 | -13445 | -22.47 | 0 |

### 2.2.2. Rate Model

The rate model used in the system is consistent with the ELECNRTL thermodynamic model and the equilibrium model. Following reactions are the most important for the rate model [14].

$$CO_2 + OH^- \rightarrow HCO_3^- \tag{8}$$

$$MEA + CO_2 + H_2O \rightarrow MEACOO^- + H_3O^+ \tag{9}$$

$$HCO_3^- \rightarrow CO_2 + OH^- \tag{10}$$

$$MEACOO^- + H_3O^+ \rightarrow MEA + CO_2 + H_2O \tag{11}$$

The temperature dependent kinetic expression defined in Aspen Plus is given below with the constant values.

$$r_j = k_j \left(\frac{T}{T_O}\right)^{n_j} \ exp \left[-\frac{E_j}{R}\left(\frac{1}{T} - \frac{1}{T_O}\right)\right] \tag{12}$$

The parameter values for kinetic expression is selected from the MEA rate based example given in Aspen Plus and tabulated in Table 4.

Table 4: Rate constant values.

| Rea: # | $k_j$ | $n_j$ | $E_j$ (cal / mol) | $T_O$ (K) |
|---|---|---|---|---|
| 8 | 4.32e+13 | 0 | 13249 | 298 |
| 9 | 9.77e+10 | 0 | 9855.809 | 298 |
| 10 | 2.38e+17 | 0 | 29450.89 | 298 |
| 11 | 2.796e+20 | 0 | 17229.79 | 298 |

### 2.3 Experimental Model

The model simulations are validated using the data taken from Texas case 32 and case 47. The absorber diameter and the packing height are given as 0.427m and 6.1m in the pilot plant study. The packed bed is filled with IMTP-40 packing type.

There are several experimental cases done by the Texas research group. Out of those, only the cases 32 and 47 are selected for this work. Reason for that is the relatively high and low liquid to gas (L/G) ratios respectively in those two cases. When the liquid flow rate is relatively high, almost all the $CO_2$ is absorbed at the bottom of the column and very little amount of $CO_2$ is reacting at the top. Then the temperature bulge is happening near the bottom of the column [15]. With the low liquid rate the temperature bulge appears close to the top of the tower.

Flow rates and other operating conditions are given in Table 5. Due to high L/G ratio, $CO_2$ capture efficiency is high in case 32 compared to case 47.

# 3. SIMULATIONS

The simulation results from the Aspen Plus, and MATLAB models and the pilot plant experimental results are compared using the temperature profiles. Two cases from the pilot plant study (cases 32 and 47) are selected as started earlier for the steady state result comparison. The packing height in Aspen Plus and MATLAB simulations and the gas flow rate in the MATLAB simulations are adjusted to achieve the same removal efficiencies as obtained in the pilot plant. The packing height is divided into 50 equal sized control volumes both in Aspen Plus and MATLAB simulations.

The simulated temperature profiles and the pilot plant data results and the pilot plant data for the gas and liquid phases along the tower are presented in Figures 1 – 4 for the cases 32 and 47, respectively. The experimental data gives only common temperature values for the column though (doesn't have different measurements for the vapor and liquid phases).

### 3.1. Inlet Stream conditions

Experimental conditions from the Texas case 32 and case 47 is considered for the simulations. The flue gas composition used is given in the Table 5 and flow rates and other operating conditions are given in Table 6.

Table 5: Flue gas composition [3].

| Component | Flue gas composition (mol %) |
|---|---|
| $H_2O$ | 1.60 |
| $N_2$ | 75.28 |
| $CO_2$ | 18.41 |
| $O_2$ | 4.71 |

Table 6: Inlet stream parameters and packing details [3].

| Case no: | Inlet liquid temperature [K] | Inlet gas temperature [K] | Inlet liquid rate [$m^3/s$] | Inlet gas rate [mol/s] | | Packing height[m] | |
|---|---|---|---|---|---|---|---|
| | | | | Measured | Adjusted | Experimental | Adjusted |
| 32 | 314 | 320 | $6.8 \cdot 10^{-4}$ | 3.52 | 3.70 | 6.1 | 4.1[a] |
| 47 | 313 | 332 | $5.0 \cdot 10^{-4}$ | 5.05 | 3.95[a] | 6.1 | 7.1 |

a- Adjusted only in MATLAB model

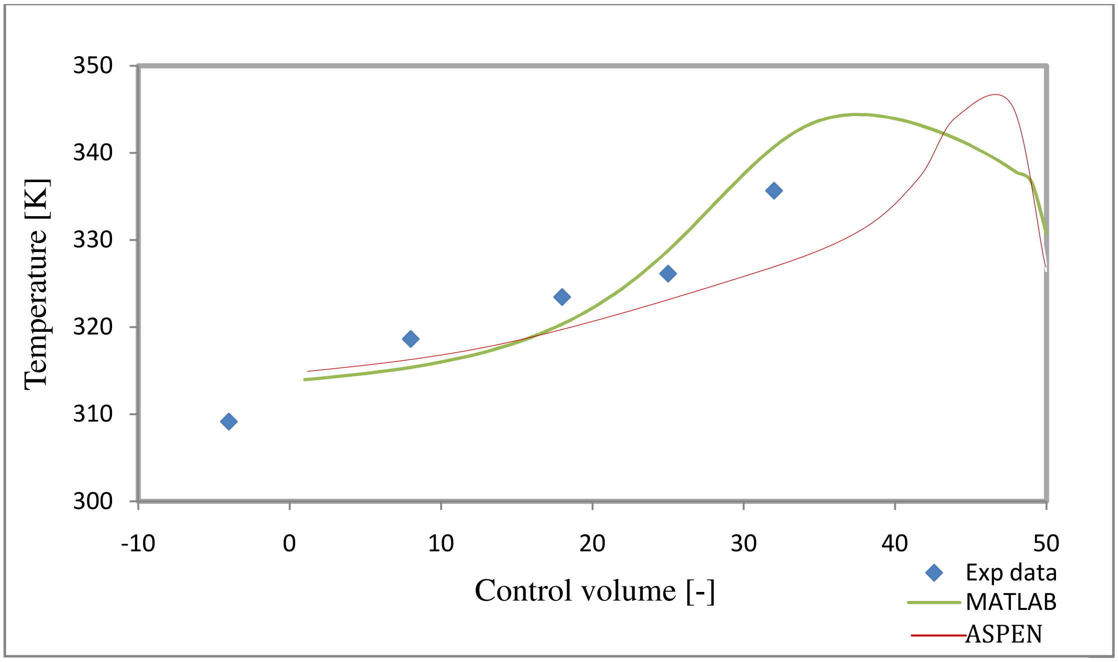

Figure 1: Liquid phase temperature profiles along the tower for case 32 (from top to bottom)

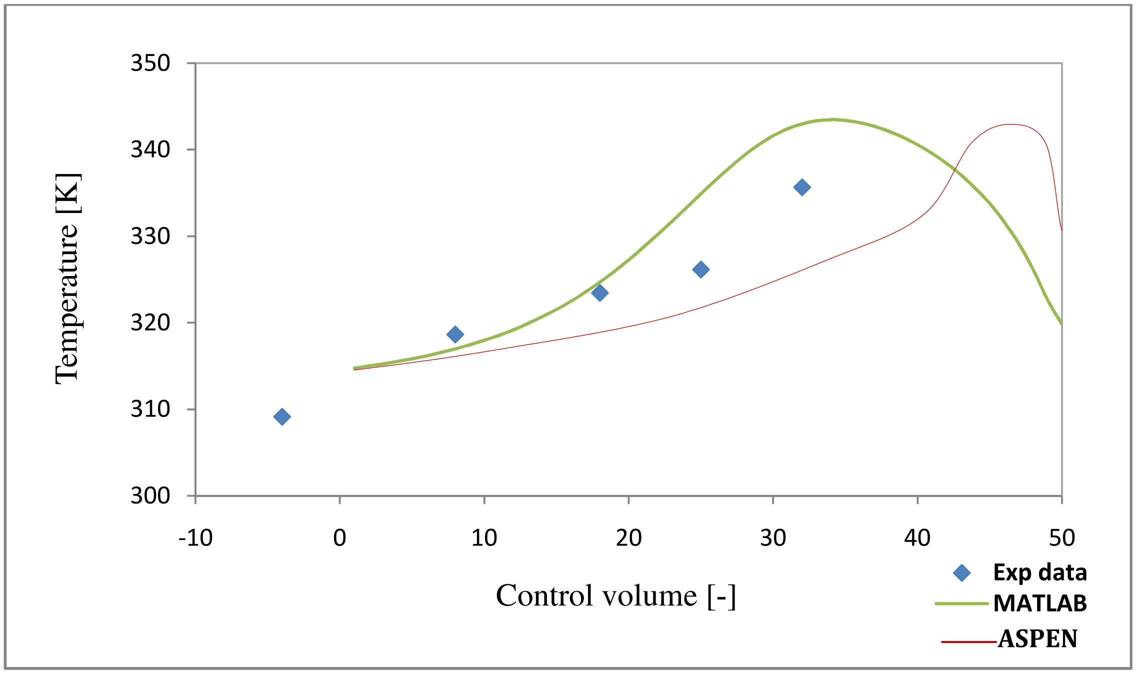

Figure 2: Vapor phase temperature profiles along the tower for case 32 (from top to bottom)

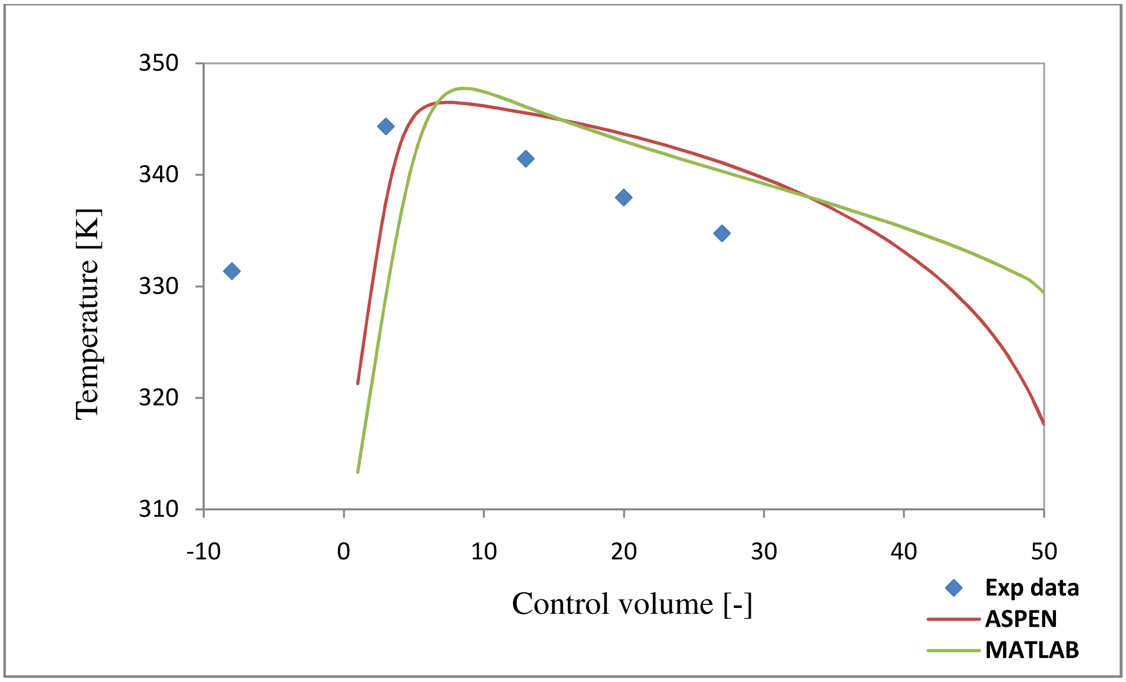

Figure 3: Liquid phase temperature profiles along the tower for case 47 (from top to bottom)

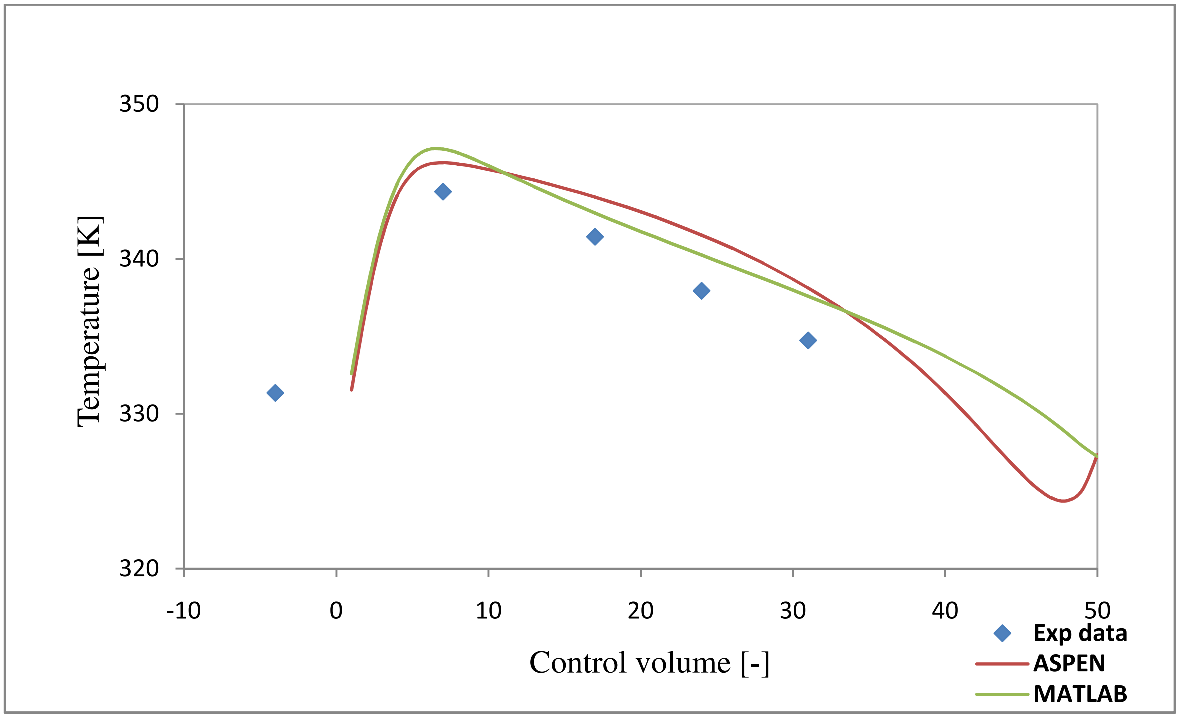

Figure 4: Vapor phase temperature profiles along the tower for case 47 (from top to bottom)

The representation of the experimental data points by the simulated temperature profiles looks promising. Pilot plant data have been normalized to 50 control volumes along the absorber for the consistency with the simulated data. The temperature profiles are given along the tower from the top to the bottom of the packing bed.

# 4. DISCUSSION

Since all the kinetic and solubility data and the equations are dependent on the temperature, the temperature profiles provide important information for analysis.

The model predictions shows the temperature bulge at the top of the absorber for the case 47 and the reverse is shown for the case 32 (Figure 1-4). The temperature bulge is due to the heat that is produced by the exothermic reactions and phase transitions. It can be concluded that the shape of the temperature profiles is similarly predicted by both models. The simulated temperature profiles with MATLAB and Aspen Plus models for the case 32 and 47 follows the trend of the experimental data points satisfactorily. The magnitude of the temperature bulge in the absorber is around 70°C and higher for the case 47 than case 32.

There can be several reasons for the deviations. Some errors in the measurements of the pilot plant and differences in the parameter values entered for the Aspen Plus and MATLAB models can be the reasons for deviations. The heat loss to the surroundings from the tower is neglected in both the Aspen Plus and MATLAB simulations.

Lack of the chemical kinetics and reactions data could have caused some deviation for the MATLAB predictions. Most of the important reactions are considered in Aspen Plus model and only the main reaction in the MATLAB model.

# 5. CONCLUSION

The temperature profiles can be used to check the model behavior. However, quantitatively there are minor deviations between the MATLAB, Aspen Plus and experimental results.

Studying the variation of the temperature within the absorber is an important analysis. The rate of reactions and solubility are strong functions of the temperature. The following principal conclusions could be drawn from the present study. Model validations should be based on the temperature profiles along the column, not just the top and the bottom of the column. The present study demonstrates that the rate based Aspen Plus and MATLAB process models can reasonably predict the key process of the chemical absorption of $CO_2$ into MEA. However, a validation with pilot plant experimental data is required before applying into real industrial processes.

# 6. FUTURE WORKS

In MATLAB model, other chemical reactions should be inserted to optimize the process. If there are any missing parameters, then parameter optimization can be used. The MATLAB and Aspen Plus models should be implemented with the stripper to get the complete $CO_2$ removal process. The models have to be validated further against pilot plant data and check the usability of the models with the different kind of amines.

In this paper, only the temperature profiles in both the liquid and gas phases are considered. Future works can be performed with the concentration profiles as well as $CO_2$ loading to validate the models further.

# 7. REFERENCES

[1] Alie C F. $CO_2$ Capture with MEA: Intergrating the Absorption Process and Steam Cycle of an Existing Coal-Fired Power Plant. Master Thesis, University of Waterloo, Canada, 2004.

[2] Lawal A, Wang M, Stephenson P, Yeung H. Dynamic modeling of $CO_2$ absorption for post combustion capture in coal-fired power plants, Cranfield University, UK, 2008.

[3] Dugas R E. Pilot plant study of carbon dioxide capture by aqueous monoethanolamine. Revision of MSE thesis. University of Texas at Austin, 2006.

[4] Jayarathna S A, Lie B, Melaaen M C. NEQ Rate Based Modeling of an Absorption Column for Post Combustion $CO_2$ Capturing. Telemark University College. Norway, 2010.

[5] Kent R L, Eisenberg B. Better Data for Amine Treating. Hydrocarbon Processing. 1976; 87-90.

[6] Jamal A, Meisen A, Lim C J. Kinetics of carbon dioxide absorption and desorption in aqueous akanolamine solutions using a novel hemispherical contactor-11: Experimental results and parameter estimation. Chem. Eng Sci. 2006; 61: 6590-603.

[7] Cheng S, Meisen A, Chakma A. Predict amine solution properties accurately. Hydrocarbon Processing. 1996; 81-4.

[8] Versteeg G F, Van Swaaij W P M. Solubility and diffusivity of acid gases ($CO_2$, $N_2O$) in aqueous alkanolamine solutions. J Chem Eng. 1988; 33: 29-34.

[9] Billet R, Schultes M. Prediction of mass transfer columns with dumped and arranged packings: updated summary of the calculation

method of billet and schultes. Trans IChemE. 1999; 77(A): 498-504.

[10] Cussler E L. Diffusion: Mass transfer in fluid systems. 3rd ed. UK: Cambridge University Press; 2009.

[11] Kohl A, Nielsen R. Gas purification. 5rd ed. Houston, Texas: Gulf professional publishing; 1997.

[12] Kvamsdal H M, Jakobsen J P, Hoff K A. Dynamic modeling and simulation of a $CO_2$ absorber column for post-combustion CO2 capture. Chem Eng and Processing. 2009; 48: 135-44.

[13] Freguia S. Modeling of $CO_2$ removal from Flue Gas with Mono-ethanolamine. Master Thesis, University of Texas, Austin, 2002.

[14] Fashami S Z. $CO_2$ removal with 7M monoethanolamine (MEA) – Aspen Plus model for base case, University of Texas, Austin, 2007.

[15] Chen C C. A rate based process modeling study of $CO_2$ capture with aqueous amine solutions using aspen ONE process engineering, aspen tech, 2008.

3. Solvent Selection

## Paper C

# Alternative solvents for post combustion carbon capture

This paper is published in the International Journal of Energy and Environment, 4, No. 3: 441-448, 2013.

INTERNATIONAL JOURNAL OF
ENERGY AND ENVIRONMENT

*Volume 4, Issue 3, 2013 pp. 441-448*

*Journal homepage: www.IJEE.IEEFoundation.org*

# Alternative solvents for post combustion carbon capture

**Udara S. P. R. Arachchige[1], Morten C. Melaaen[1,2]**

[1] Telemark University College, Porsgrunn, Norway.
[2] Tel-Tek, Porsgrunn, Norway.

**Abstract**
The process model of post combustion chemical absorption is developed in Aspen Plus for both coal and gas fired power plant flue gas treating. The re-boiler energy requirement is considered as the most important factor to be optimized. Two types of solvents, mono-ethylamine (MEA) and di-ethylamine (DEA), are used to implement the model for three different efficiencies. The re-boiler energy requirement for regeneration process is calculated. Temperature and concentration profiles in absorption column are analyzed to understand the model behavior. Re-boiler energy requirement is considerably lower for DEA than MEA as well as impact of corrosion also less in DEA. Therefore, DEA can be recommended as a better solvent for post combustion process for carbon capture plants in fossil fuel fired power industries.

**Keywords:** carbon dioxide capture; flue gas; MEA; DEA; re-boiler duty.

## 1. Introduction

Global climate change has rapidly become the most prominent environmental issue in the present day. It is a well-known fact that the main contributor for the issue is the fossil fuel based energy generation. It can be solved either by shifting to renewable energy sources (clean energy sources) or eliminating the emission of available plants with emission reduction technologies. However, green house gas emission free technologies will not be practical solution in near future. Therefore, most possible alternative is carbon capture and sequestration as it can be applied in existing power plants and industries without major modifications. The most well-established method for carbon dioxide ($CO_2$) capture is post combustion chemical absorption method with alkanolamine solvents. Weak base amines are reacted with $CO_2$ and other acid gases to form weak chemical bonds. Alkanolamine can be mainly categorized as, primary (monoethanolamine-MEA, diglycolamine-DGA), secondary (diethanolamine-DEA) and tertiary (methyldiethanolamine-MDEA, triethanolamine-TEA) amines. However, the most applicable amine among them is MEA, due to the low partial pressure of $CO_2$ in the flue gas of fossil fuel fired power plant [1]. The most important parameter when designing a carbon capture plant is operating cost, which is related to the energy requirement in regeneration process. Even though MEA is widely use amine for $CO_2$ capture, regeneration energy requirement is high for that process. Therefore, alternative solvents should be analyzed to perform the post combustion capture process with fewer energy requirements.

Both MEA and DEA are considered as highly reactive amines for gas absorption process [2]. However, secondary amines are less corrosive as well as required less heat of regeneration, due to an additional ethanol group [3]. The objective of this research was to compare the possible solvents that can be used for post combustion $CO_2$ capture with lower energy requirement. In this study, MEA and DEA solvents are selected to optimize the $CO_2$ capture process. Operating conditions are selected to avoid the main drawback of alkanolamine, which is large energy requirement. The physical properties of both amines are summarized in Table 1 [4].

Table 1. Basic information about MEA and DEA

| Specification | MEA | DEA |
|---|---|---|
| Chemical formula | $C_2H_7NO$ | $C_4H_{11}NO_2$ |
| Amines category | Primary | Secondary |
| Molecular weight [g/mol] | 61.08 | 105.14 |
| Density [g/cm$^3$] | 1.012 | 1.090 |
| Boiling point[°C] | 170 | 217 |

## 2. Model development

For the analysis of the solvent for carbon capture process, the Aspen Plus flow sheet modeling tool is used. The $CO_2$ removal model for both coal and gas fired flue gases is developed. According to the solvent type, parameters and operating conditions have to be selected. The most versatile property method in Aspen Plus, that is Electrolyte Non Random Two Liquid (NRTL) method, is used to implement the process optimization. The model is developed for 85%, 90% and 95% removal efficiencies. The flue gas compositions for both coal and gas fired systems are given in Table 2.

Table 2. Inlet flue gas composition and parameters used for the simulations [5], [6]

| Parameter | Coal Fired | Gas Fired |
|---|---|---|
| Flow rate [kg/s] | 673.4 | 793.9 |
| Temperature [K] | 313 | 313 |
| Pressure [bar] | 1.1 | 1.1 |
| Major Composition | Mol% | Mol% |
| $H_2O$ | 8.18 | 8.00 |
| $N_2$ | 72.86 | 76.00 |
| $CO_2$ | 13.58 | 4.00 |
| $O_2$ | 3.54 | 12.00 |
| $H_2S$ | 0.05 | 0.00 |

The reactions used for the $CO_2$ capture model with MEA and DEA are tabulated in Table 3 [7]. The equilibrium and kinetic data are taken from the literatures and the Aspen Plus databanks for the calculations and given in the same table [8, 9]. The reactions 4 and 5 are only valid for coal fired flue gas reacting system.

Table 3. Chemical reactions of MEA and DEA process

| Reactions | Reaction number | **Thermodynamic behavior** | | | |
|---|---|---|---|---|---|
| | | $A_j$ | $B_j$ | $C_j$ | $D_j$ |
| **MEA+CO₂+H₂O system** | | | | | |
| $2H_2O \leftrightarrow OH^- + H_3O^+$ | (1) | 132.89 | -13445.9 | -22.47 | 0 |
| $CO_2 + 2H_2O \leftrightarrow HCO_3^- + H_3O^+$ | (2) | 231.46 | -12092.1 | -36.78 | 0 |
| $HCO_3^- + H_2O \leftrightarrow H_3O^+ + CO_3^{2-}$ | (3) | 216.05 | -12431.7 | -35.48 | 0 |
| $H_2O + H_2S \leftrightarrow HS^- + H_3O^+$ | (4) | 214.58 | -12995.4 | -33.55 | 0 |
| $H_2O + HS^- \leftrightarrow S^{2-} + H_3O^+$ | (5) | -9.74 | -8585.47 | 0 | 0 |
| $MEAH^+ + H_2O \leftrightarrow MEA + H_3O^+$ | (6) | -3.038 | -7008.3 | 0 | -0.00313 |
| $MEACOO^- + H_2O \leftrightarrow MEA + HCO_3^-$ | (7) | -0.52 | -2545.53 | 0 | 0 |
| **DEA+CO₂+H₂O system (In addition to reactions 1-5)** | | | | | |
| $DEAH^+ + H_2O \leftrightarrow DEA + H_3O^+$ | (8) | -13.3373 | -4218.70 | 0 | 0.00987 |
| $DEACOO^- + H_2O \leftrightarrow DEA + HCO_3^-$ | (9) | 16.5026 | -4068.76 | -1.502 | 0 |
| $ln\, K_j = A_j + \frac{B_j}{T} + C_j\, ln T + D_j T$ | (10) Equation for equilibrium constants | | | | |
| | | **Kinetic behavior** | | | |
| | | $k_j$ | $n_j$ | $E_j$ | $T_o$ |
| **MEA+CO₂+H₂O system** | | | | | |
| $CO_2 + OH^- \rightarrow HCO_3^-$ | (11) | 4.32e+13 | 0 | 13249 | 298 |
| $HCO_3^- \rightarrow CO_2 + OH^-$ | (12) | 2.38e+17 | 0 | 29451 | 298 |
| $MEA + CO_2 + H_2O \rightarrow MEACOO^- + H_3O^+$ | (13) | 9.77e+10 | 0 | 9855 | 298 |
| $MEACOO^- + H_3O^+ \rightarrow MEA + CO_2 + H_2O$ | (14) | 2.7963e+20 | 0 | 17229 | 298 |
| **DEA+CO₂+H₂O system (In addition to reactions 11-12)** | | | | | |
| $DEA + CO_2 + H_2O \rightarrow DEACOO^- + H_3O^+$ | (15) | 6480000 | 0 | 5072 | 298 |
| $DEACOO^- + H_3O^+ \rightarrow DEA + CO_2 + H_2O$ | (16) | 1.34e+17 | 0 | 11497 | 298 |
| $r_j = k_j \left(\frac{T}{T_0}\right)^{n_j} exp\left[-\frac{E_j}{R}\left(\frac{1}{T} - \frac{1}{T_0}\right)\right]$ | (17) Equation for rate constants | | | | |

The required operating conditions for MEA and DEA in Electrolyte NRTL property method are present in Table 4 [10]. Aspen Plus simulation tool has certain limitations and indicate below. The limitations of MEA and DEA mass fractions are 50 and 30 [w/w%] respectively.

Table 4. Range of applicability of amine models [10]

| Range of applicability | MEA | DEA |
|---|---|---|
| Temperature [K] | <393.15 | <413.15 |
| Concentration [w/w%] | <50 | <30 |

The optimal specifications for the coal and gas processes such as amine concentration, lean loading, and solvent flow rate are summarized in Table 5 for different efficiency values. Optimum specifications are selected after the number of simulations which has been performed in previous studies [11].

The concentration of DEA has to be maintained less compared to MEA concentration. Even though in previous studies, it has shown that higher concentration will lead to lower re-boiler energy requirement, it is not accurate to perform simulation for higher concentrations due to limitations in Aspen Plus simulation tool (Table 4).

Table 5: Optimum solvent conditions for both coal and gas fired power plant flue gas capture process

| Specification | 85% Removal Efficiency | | 90% Removal Efficiency | | 95% Removal Efficiency | |
|---|---|---|---|---|---|---|
| Coal fired power plant $CO_2$ capture | | | | | | |
| | MEA | DEA | MEA | DEA | MEA | DEA |
| Amine concentration [w/w%] | 40 | 30 | 40 | 30 | 40 | 30 |
| $CO_2$ lean loading [mole $CO_2$/mole amine ] | 0.27 | 0.05 | 0.27 | 0.05 | 0.25 | 0.05 |
| Solvent flow rate [tonne/hr] | 7845 | 8698 | 8480 | 9620 | 8400 | 10825 |
| Gas fired power plant $CO_2$ capture | | | | | | |
| Amine concentration [w/w%] | 40 | 30 | 35 | 30 | 30 | 30 |
| $CO_2$ lean loading [mole $CO_2$/mole amine ] | 0.30 | 0.10 | 0.25 | 0.10 | 0.25 | 0.10 |
| Solvent flow rate [tonne/hr] | 3624 | 4053 | 3168 | 4421 | 3890 | 6000 |

The basic process flow scheme for post combustion process is shown in Figure 1. The description of the process is given in the previous publications [12].

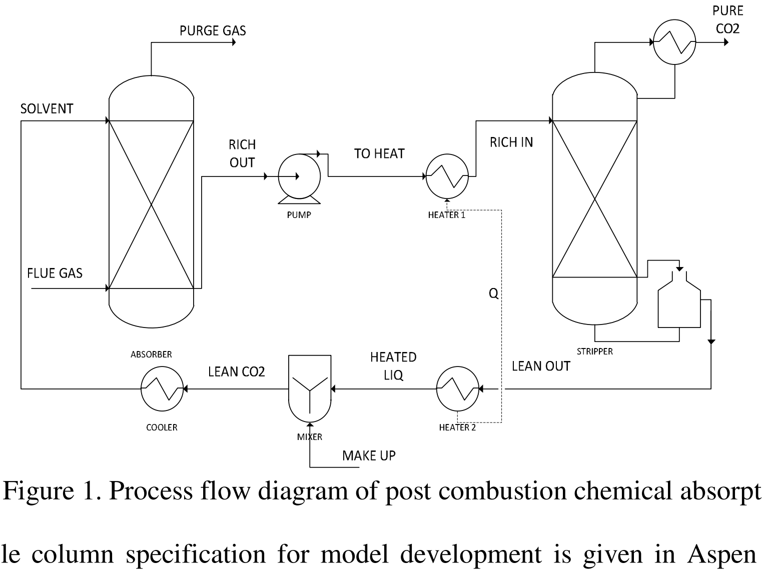

Figure 1. Process flow diagram of post combustion chemical absorption

The most suitable column specification for model development is given in Aspen Plus, 2008 [9] and Mohammad, 2009 [13].

## 3. Simulations

The $CO_2$ capture model is developed for three different efficiencies as 85%, 90% and 95% for both coal and gas fired power plant flue gases. The selected solvent conditions are used for the model implementation with recommended column parameters. Temperature profiles and $CO_2$ loading profiles are analyzed for both cases. Figure 2-5 represent the liquid and vapour phase temperature profiles in absorber column for coal and gas fired capture model.

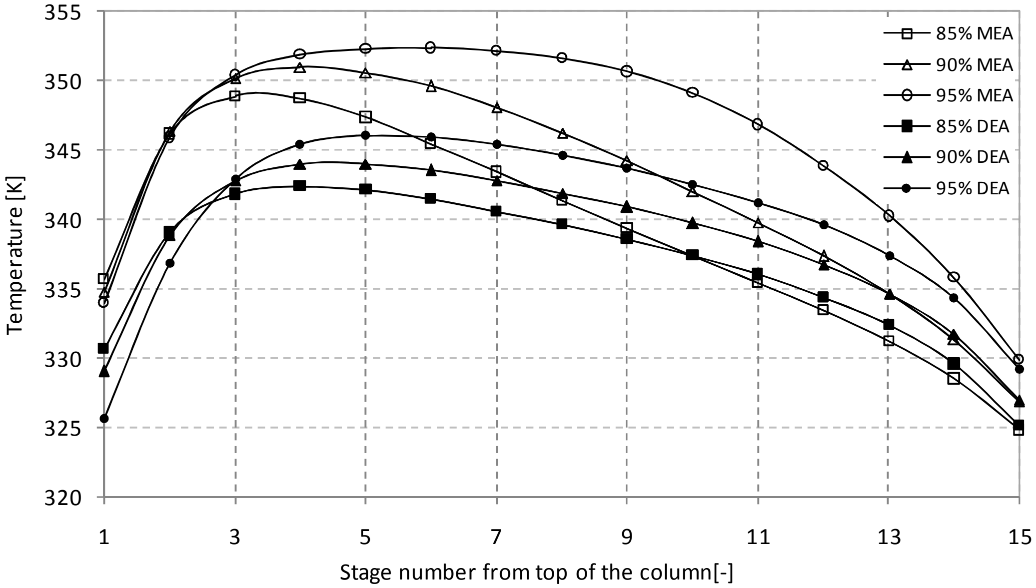

Figure 2. Liquid phase temperature profiles in absorption column for coal fired flue gas

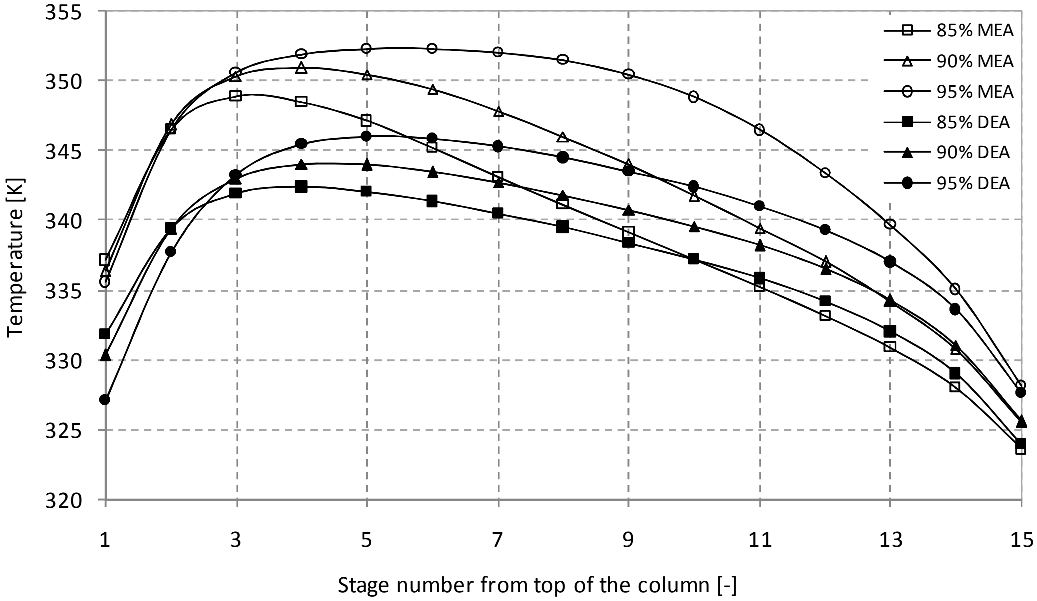

Figure 3. Vapor phase temperature profiles in absorption column for coal fired flue gas

According to the Figure 2 and 3, maximum temperature for coal fired flue gas capture process with MEA as solvent is in the range of 347 - 352 K. However, for DEA solvent process the maximum temperature reach slightly lower values, and it is around 342 - 346 K. When efficiency is higher, temperature profiles also show higher values for both MEA and DEA. Liquid and vapor phases have almost similar patterns for both solvent cases. The absorber tends to exhibit a temperature bulge at the top of the column for both liquid and vapor phase. Temperature bulge is due to highly exothermic reactions at the top of the column.

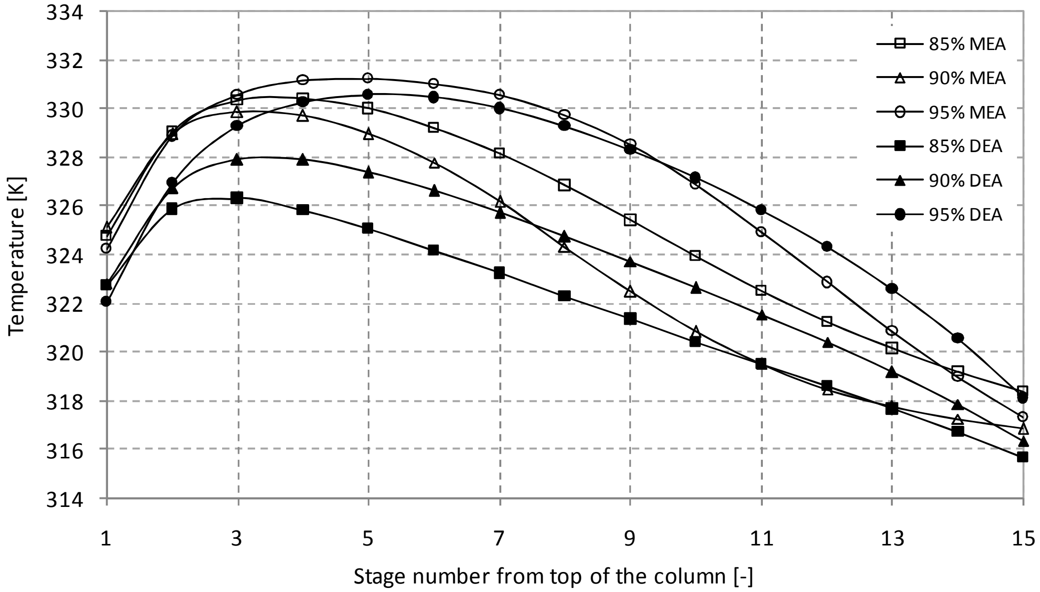

Figure 4. Liquid phase temperature profile in absorption column for gas fired flue gas

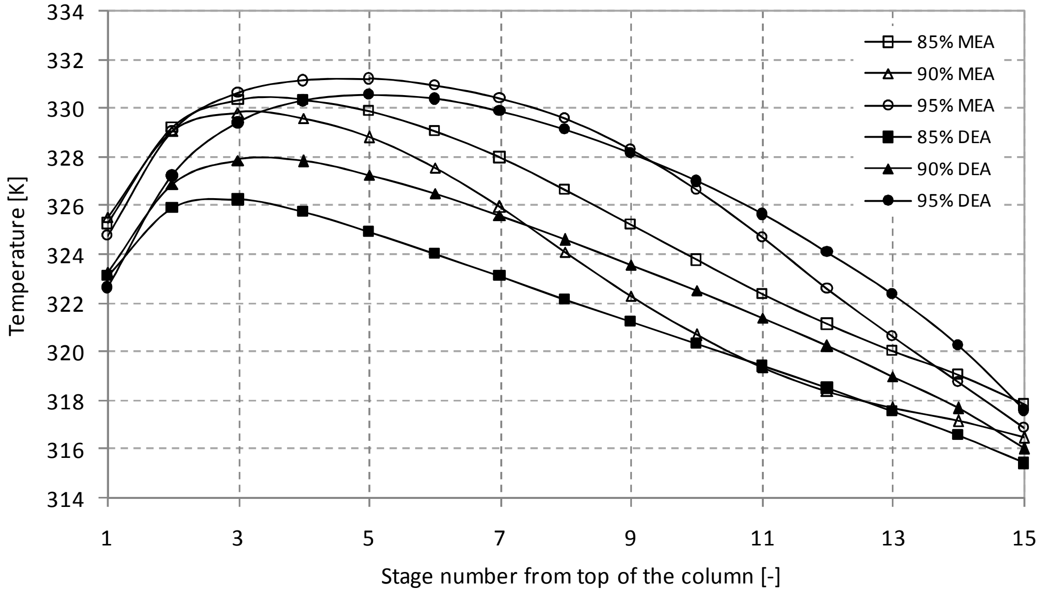

Figure 5. Vapor phase temperature profile in absorption column for gas fired flue gas

Gas fired process show lower temperature profiles compared to coal fired system. Maximum temperature is around 330-331 K and 326-330 K for MEA and DEA solvent systems, respectively. However, maximum temperature is varying with removal efficiencies. Higher removal efficiencies have higher temperature profiles along the absorption tower. The shape of the temperature profiles has the similar patterns mentioned in the literatures even though the maximum temperature value is different [14].
Figure 6 is representing the $CO_2$ loading profiles in absorption column for coal fired flue gas treating system for both MEA and DEA solvents. The $CO_2$ loading profiles for MEA are having higher values compared to DEA. Lower efficiency process models are showing higher $CO_2$ loading profiles. However, rich loading values are closer for all efficiencies and slightly higher for 85% removal model. Figure 7, which is showing $CO_2$ loading profiles for gas fired flue gas systems, have similar patterns.

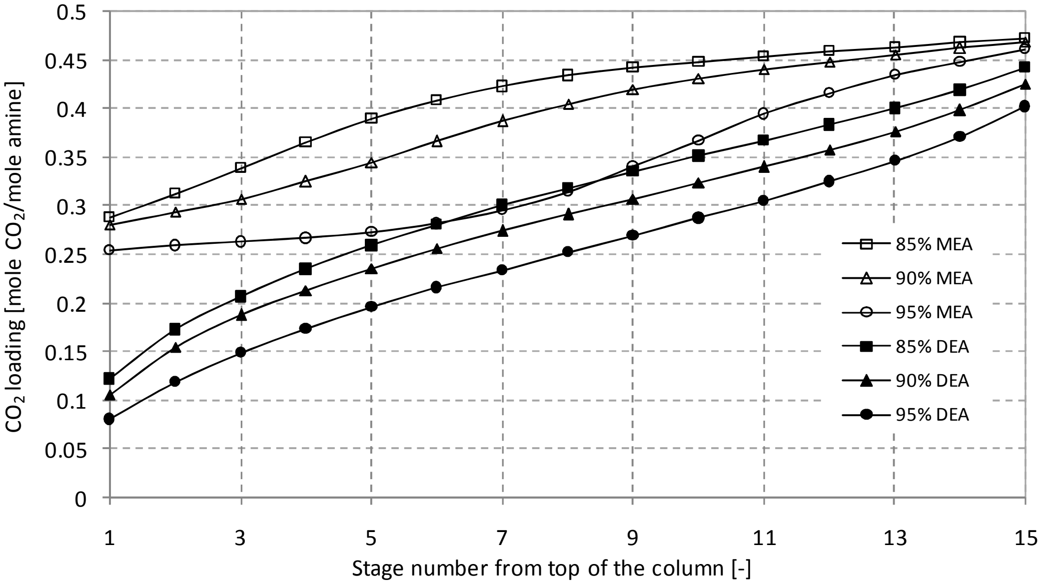

Figure 6. $CO_2$ loading profiles in absorption column for coal fired flue gas

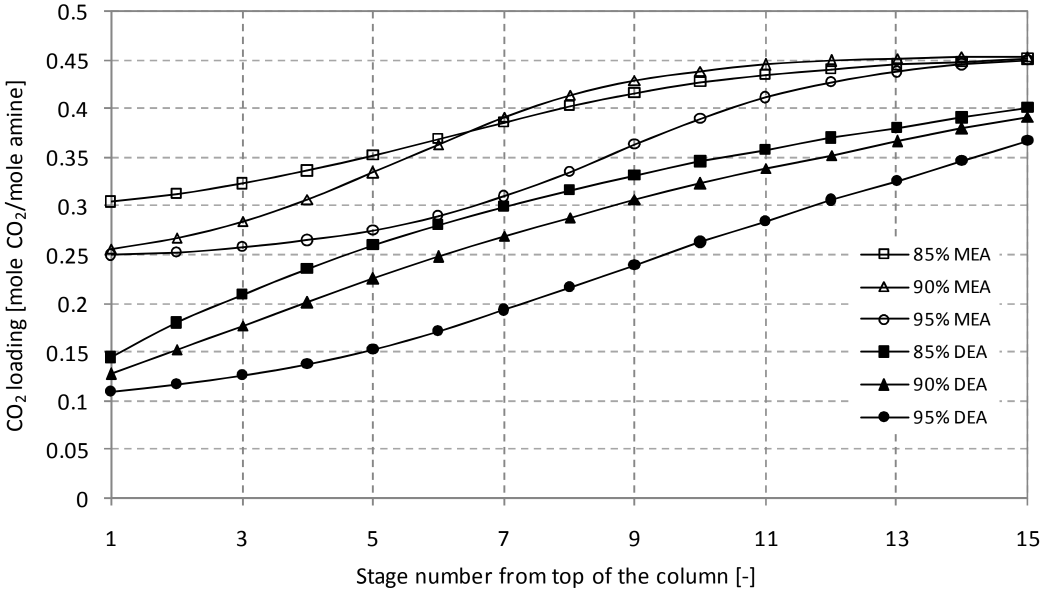

Figure 7. $CO_2$ loading profiles in absorption column for gas fired flue gas

The rich loading values for different models (six models for MEA and six models for DEA for coal and gas fired systems) are given in Table 6. The required re-boiler energy duties are tabulated in the same table for all the cases with necessary solvent circulation rates.

Table 6. Re-boiler energy requirement, rich loading and solvent circulation flow rate for coal and gas fired processes

| Specification | 85% Removal Efficiency | | 90% Removal Efficiency | | 95% Removal Efficiency | |
|---|---|---|---|---|---|---|
| Coal fired power plant $CO_2$ capture | | | | | | |
| | MEA | DEA | MEA | DEA | MEA | DEA |
| Re-boiler duty[kJ/kg $CO_2$] | 3507 | 3371 | 3581 | 3462 | 3914 | 3747 |
| $CO_2$ rich loading [mole $CO_2$/mole amine ] | 0.473 | 0.442 | 0.469 | 0.425 | 0.461 | 0.402 |
| Solvent flow rate [tonne/hr] | 7845 | 8698 | 8480 | 9620 | 8400 | 10825 |
| Gas fired power plant $CO_2$ capture | | | | | | |
| Re-boiler duty[kJ/kg $CO_2$] | 3641 | 3381 | 3982 | 3471 | 4100 | 3756 |
| $CO_2$ rich loading [mole $CO_2$/mole amine ] | 0.451 | 0.400 | 0.454 | 0.392 | 0.449 | 0.367 |
| Solvent flow rate [tonne/hr] | 3624 | 4053 | 3168 | 4421 | 3890 | 6000 |

As it can be seen from the Table 6, DEA processes have lower re-boiler energy demand for all the cases. Gas fired processes have a slightly higher re-boiler energy requirement than coal fired system. Reason for that is, gas fired flue gas consist of less amount of $CO_2$. Therefore, a large amount of liquid flow has to be purified in the stripper. Therefore, energy requirement to heat the solvent is high for gas fired process. When removal efficiency is increasing, re-boiler energy requirement also increases. Reason for that is, to capture a higher amount of $CO_2$, it has to process higher solvent in the stripper. DEA process shows lower re-boiler duties for all the models. The 85% removal model of DEA process has 3371 kJ/kg $CO_2$ for coal fired system and 3381 kJ/kg $CO_2$ for gas fired system. This is lower value compared to 3507 kJ/kg $CO_2$ and 3641 kJ/kg $CO_2$ for coal and gas fired MEA solvent systems, respectively. Similar to that, all the efficiency models show lower re-boiler duties for DEA processes. This is an agreement with the literatures, that Veawab et al. 2003 [15] reported that solvent regeneration energy is decreasing in the order MEA>DEA>MDEA. Reason behind that is, DEA has lower heat of reaction compared to MEA process. The overall re-boiler energy requirement mainly consists of three major parts. The energy needed to liberate the $CO_2$ from amines, heat required to increase the solvent temperature and energy uses for water evaporation process. DEA has lower $CO_2$ loading efficiency than MEA solvent, and that will cause for a higher amount of solvent circulation rate. Even though DEA solvent circulation rate is higher compared to MEA process, DEA has less heat of reaction. Therefore, heat of reaction or heat required to liberate the attached $CO_2$ will dominate to have less re-boiler duty for all these cases.

When we consider about corrosions, Veawab, 2003 [16] noted that corrosion takes place in almost every section of the capture plant. The impact of corrosion depends mainly on few factors, including $CO_2$ loading, amine type and concentration, temperature and degradation products [17]. The corrosivity of amines decrease in the order of MEA>AMP>DEA>MDEA [18]. Therefore, DEA is better compared to the MEA in the sense of that.

## 4. Conclusion

Using DEA will reduce the corrosive effect and required less amount of energy in the regeneration process. The 85% removal model of DEA process has 3371 kJ/kg $CO_2$ for coal fired system and 3381 kJ/kg $CO_2$ for gas fired system. This is lower value compared to 3507 kJ/kg $CO_2$ and 3641 kJ $CO_2$ for coal and gas fired MEA solvent systems, respectively. Similar to that, all the efficiency models show lower re-boiler duties for DEA processes. However, circulation rate is high in DEA model compared to MEA process because of low reactivity. That will cause for increasing operational cost. Typical temperature profiles for liquid and vapour phase in the absorber model is analyzed together with $CO_2$ loading profiles. Temperature profiles are important to understand since it shows the reaction behavior. The shape, value and the point of maximum temperature bulge depend upon where in the column the bulk of the acid gas is absorbed into lean solvent as well as heat of reactions, evaporation and amount of vapour and liquid flow rate. Finally, DEA can be recommended for coal and gas fired flue gas capture for removal efficiencies.

## Nomenclature

K : equilibrium constant for thermodynamic model
A, B, C, D : constants
T : temperature [K]
E : activation energy [J/mol]
R : gas constant [J/mol K]
k : reaction rate coefficient
j : component name
r : reaction rate

## References

[1] Gabrielsen J., Svendsen H.F., Michelsen M.L., Stenby E.H., Kontogeorgis G.M. Experimental validation of a rate-based model for $CO_2$ capture using an AMP solution. Chemical Engineering Science, 2007, Vol. 62, 2397-2413.

[2] Bae H.K., Kim S.Y., Lee B. Simulation of $CO_2$ removal in a split-flow gas sweetening process. Korean J.Chem.Eng, 2011, Vol. 28 (3), 643-648.

[3] Wang R., Li D.F., Liang D.T. Modeling of $CO_2$ capture by three typical amine solutions in hollow fiber membrane contactors. Chemical Engineering and Processing, 2004, Vol. 43, 849-856.

[4] Arachchige U.S.P.R., Aryal N., Melaaen M.C. Various amines' effect on $CO_2$ removal efficiency. Proc. APCRE'11 chemical engineering symposium, Beijing, China, 2011.

[5] Alie C.F. $CO_2$ Capture with MEA: Intergrating the Absorption Process and Steam Cycle of an Existing Coal-Fired Power Plant. Master Thesis, University of Waterloo, Canada, 2004.

[6] Fluor for IEA GHG Program, Improvement in Power Generation with Post-Combustion Capture of $CO_2$. Final Report, Report Number PH4/33, November 2004.

[7] Pellegrini G., Strube R., Manfrida G. Comparative study of chemical absorbents in postcombustion $CO_2$ capture. *Energy*, Vol. 35 (2), 851-857.

[8] Freguia S. Modeling of $CO_2$ removal from Flue Gas with Mono-ethanolamine. Master Thesis, University of Texas, USA, 2002.

[9] Aspen Plus. Rate Based model of the $CO_2$ capture process by MEA using Aspen Plus. Aspen Technology Inc, Cambridge, MA, USA, 2008.

[10] Aspen Plus. Aspen Physical Property Methods. Aspen Technology Inc, Cambridge, MA, USA, 2006, 61-63.

[11] Arachchige U.S.P.R., Muhammad M., Melaaen M.C. Optimization of post combustion carbon capture process-solvent selection, submitted to *International Journal of Energy and Environment*, 2012.

[12] Arachchige U.S.P.R., Aryal N., Melaaen M.C. Case study for flue gas separation of a coal fired power plant and parameters' effect on removal efficiency, Proc. APCRE'11 chemical engineering symposium, Beijing, China, 2011.

[13] Mohammad A, PhD Thesis, University of Delft, Netherland, 2009.

[14] Kothandaraman A, PhD Thesis, Massachusetts Institute of Technology, USA, 2010.
[15] Veawab A., Tontiwachwuthikul P., Aroonwilas A., Chakma A, Performance and cost analysis for CO2 capture from flue gas streams: absorption and regeneration aspects. Proceedings of the sixth international conference on green house gas control technologies: GHGT -6, Kyoto, Japan, 2003.
[16] Veawab A, Corrosion in CO2 capture unit for coal/fired power plant flue gas, Proceedings of the sixth international conference on green house gas control technologies: GHGT -6, Kyoto, Japan, 2003.
[17] Davidson R.M, Post combustion carbon capture from coal fired plants-solvent scrubbing, IEA clean coal centre, United Kingdom, 2007.
[18] Veawab A., Tontiwachwuthikul P., Chakma A, *Industrial and Engineering Chemistry* Research, 1999, 38 (10), 3917.

**Udara S.P.R. Arachchige** received his B.Sc Degree (2007) in Chemical and Process Engineering from University of Moratuwa, Sri Lanka and M.Sc degree (2010) in Energy and Environmental Engineering from Telemark University College, Porsgrunn, Norway. He is presently pursuing his Ph.D in Carbon dioxide capture from power plants- modeling and simulation studies at Telemark University College. He has presented and published five papers in International Conferences and 5 papers in international journals. Mr. Udara is a member of American Chemical Society.
E-mail address: udara.s.p.arachchige@hit.no

**Morten Chr. Melaaen** is Professor in process technology at Telemark University College, Porsgrunn, Norway. He is also the Dean of Faculty of Technology, Telemark University College and has a part time position at the local research institute Tel-Tek. Earlier, he has worked as a research engineer in Division of Applied Thermodynamics, SINTEF, Norway and as an Associate professor at Norwegian University of Science and Technology (NTNU). He has worked on research projects as a Senior research scientist in Norsk Hydro Research Centre Porsgrunn, Norway. He started to work as a professor at Telemark University College in 1994 and became Head of Department, Department of Process, Energy and Environmental Technology in 2002. He received his MSc in Mechanical Engineering in 1986 and his Ph.D in 1990, both from NTNU. His research interests are $CO_2$ capture, modeling and simulation, fluid mechanics and heat and mass transfer. Professor Melaaen has more than 95 scientific papers published in the above mentioned related fields in international journals and conferences.
E-mail address: Morten.C.Melaaen@hit.no

Paper D

# Optimization of post combustion carbon capture process-solvent selection

This paper is published in the International Journal of Energy and Environment 3, No. 6: 861-870, 2012.

INTERNATIONAL JOURNAL OF
ENERGY AND ENVIRONMENT

*Volume 3, Issue 6, 2012 pp.861-870*
*Journal homepage: www.IJEE.IEEFoundation.org*

# Optimization of post combustion carbon capture process-solvent selection

**Udara S. P. R. Arachchige[1], Muhammad Mohsin[1], Morten C. Melaaen[1,2]**

[1] Telemark University College, Porsgrunn, Norway.
[2] Tel-Tek, Porsgrunn, Norway.

**Abstract**
The reduction of the main energy requirements in the $CO_2$ capture process that is re-boiler duty in stripper section is important. Present study was focused on selection of better solvent concentration and $CO_2$ lean loading for $CO_2$ capture process. Both coal and gas fired power plant flue gases were considered to develop the capture plant with different efficiencies. Solvent concentration was varied from 25 to 40 (w/w %) and $CO_2$ lean loading was varied from 0.15 to 0.30 (mol $CO_2$/mol MEA) for 70-95 (mol %) $CO_2$ removal efficiencies. The optimum specifications for coal and gas processes such as MEA concentration, $CO_2$ lean loading, and solvent inlet flow rate were obtained.

**Keywords:** Carbon dioxide capture; Coal and gas power plant; Lean loading; Solvent concentration.

## 1. Introduction

The atmospheric concentration of green house gases (GHG) has mainly increased due to human activities. The emissions of different green house gases have been studied and measured all around the world. Carbon dioxide ($CO_2$) is considered as the most important GHG and annual percentage emission from different sectors are seen in Figure 1 [1].

Fossil fuel (especially coal) still plays the most important role in the energy sector. On the other hand, that is leading the percentage of $CO_2$ emissions to the atmosphere. Therefore, carbon dioxide capture and storage (CCS) technologies are important to continue fossil fuel fired power plants. However, CCS is still having several challenges in large scale, which will significantly reduce the overall efficiency of a power plant. The reduction of the main energy requirements in the $CO_2$ capture process that is re-boiler duty in stripper section is important to implement. The overall re-boiler energy requirement consists of three major parts, which are the energy needed for liberating attached $CO_2$ from amines, the heat required to increase the solvent temperature, and energy use for water evaporation process. Post combustion chemical absorption process is considered as preferred option. Main reason behind that is, it is easy to apply in already available coal and gas power plants with small modifications. Post combustion chemical absorption processes use a solvent to chemically react with $CO_2$ from the flue gas and liberated that absorbed $CO_2$ in the stripper. There are several solvents available and selections of best solvent and properties of the solvent stream are important to optimize. Present study was focused on selection of the best solvent concentration and $CO_2$ lean loading for $CO_2$ capture process. Both coal and gas-fired power plant flue gases are considered to develop the capture plant with different efficiencies. Number of simulations was performed in Aspen Plus with different solvent conditions to check the lowest re-boiler duty and lowest solvent inlet flow rate. Finally, most suitable solvent concentration and lean loading are selected for three different $CO_2$ capture processes.

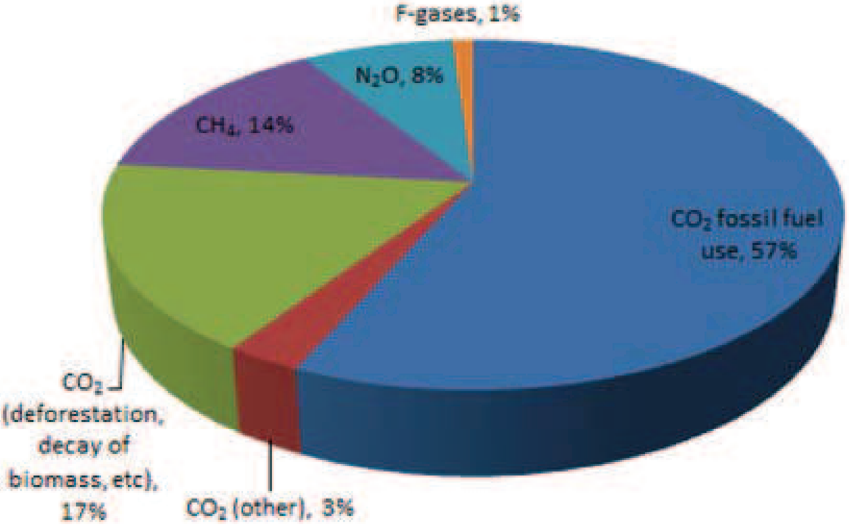

Figure 1. Percentage of $CO_2$ emissions from different sources [1]

## 2. Model development

The Electrolyte Non Random Two Liquid (NRTL) property method in Aspen Plus is used to implement the $CO_2$ capture model. The 500 MW coal and gas fired power plant flue gas data are taken from the literature [2, 3]. The composition of the flue gas inlet stream is tabulated in Table 1.

Table 1. Flue gas composition and parameters [2, 3]

| Parameter | Coal Fired | Gas Fired |
|---|---|---|
| Flow rate [kg/s] | 673.4 | 793.9 |
| Temperature [K] | 313 | 313 |
| Pressure [bar] | 1.1 | 1.1 |
| Major Composition | Mol% | Mol% |
| $H_2O$ | 8.18 | 8.00 |
| $N_2$ | 72.86 | 76.00 |
| $CO_2$ | 13.58 | 4.00 |
| $O_2$ | 3.54 | 12.00 |
| $H_2S$ | 0.05 | 0.00 |

The implemented process flow diagram for the carbon capture process is given in the Figure 2. The main chemical reactions between MEA and $CO_2$ are taken into consideration [4] with available thermodynamic and kinetic data [5].

The calculation procedure in rate based electrolyte NRTL model in Aspen Plus consists of material and energy balances, mass and heat transfer, phase equilibrium, and summation equations [6]. According to the packing type, mass transfer correlations are varied. Many of the mass transfer correlations are also provided the interfacial area value. However, interfacial area factor can be specified in the packing section in Aspen Plus model. The required area for actual mass transfer uses in Aspen Plus is the multiplication of area from the correlation with this interfacial area factor [7].Therefore, large number of input data and parameters are important to provide to achieve these complicated calculations. The input conditions and model specifications that have been used for model development in the absorber, and stripper are shown in Table 2. Most of the specifications are recommended specifications for rate based model of the $CO_2$ capture process by Aspen Tech [7], and some of them are taken from literature [8].

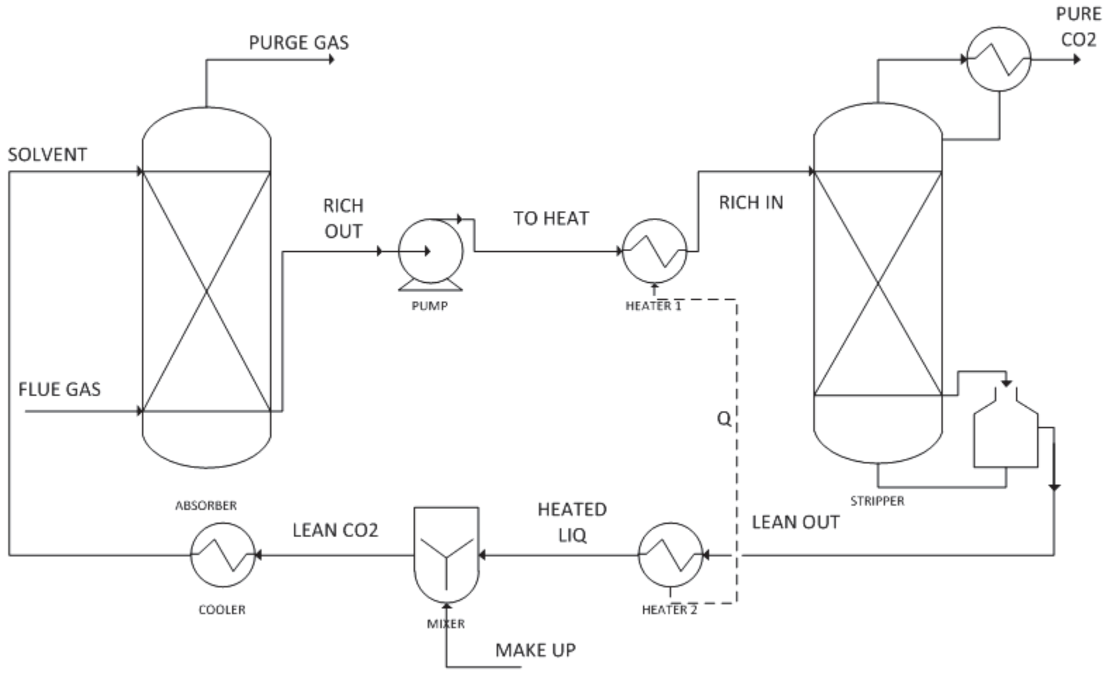

Figure 2. Process flow diagram

Table 2. Absorber and stripper column specifications

| Specification | Coal fired flue gas | | Gas fired flue gas | |
|---|---|---|---|---|
| | Absorber | Stripper | Absorber | Stripper |
| Number of stages | 15 | 15 | 15 | 15 |
| Operating pressure | 1 bar | 2 bar | 1 bar | 1.6 bar |
| Re-boiler | None | Kettle | None | Kettle |
| Condenser | None | Partial-vapour | None | Partial-vapour |
| Packing type | Mellapak,Sulzer, Standard, 250Y | Flexipac, Koch, metal,1Y | Mellapak, Sulzer, Standard, 250 Y | Flexipac, Koch, metal,1 Y |
| Packing height | 20m | 18m | 24m | 18m |
| Packing diameter | 15m | 12m | 18m | 12m |
| Mass transfer coefficient method [9] | Bravo et al. (1985) [9] | Bravo et al. (1985) [9] | Bravo et al. (1985) [9] | Bravo et al. (1985) [9] |
| Interfacial area method [9] | Bravo et al. (1985) [9] | Bravo et al. (1985) [9] | Bravo et al. (1985) [9] | Bravo et al. (1985) [9] |
| Interfacial area factor | 1.5 | 2 | 1.2 | 1.5 |
| Heat transfer coefficient method | Chilton and Colburn | Chilton and Colburn | Chilton and Colburn | Chilton and Colburn |
| Holdup correlation [10] | Billet and Schultes (1993) [10] | Billet and Schultes (1993) [10] | Billet and Schultes (1993) [10] | Billet and Schultes (1993) [10] |
| Film resistance | Discrxn for liquid film and Film for vapour film | Discrxn for liquid film and Film for vapour film | Discrxn for liquid film and Film for vapour film | Discrxn for liquid film and Film for vapour film |
| Flow model | Mixed | Mixed | Mixed | Mixed |

In both coal and gas fired capture simulation models, Mixed flow model is selected. There are four different flow models are available in the Aspen Plus rate base model. Due to the high amount of $CO_2$ composition in flue gas, Mixed flow model is recommended in literature [7].

## 3. Simulations

Solvent concentration and $CO_2$ lean loading are considered for simulations with different efficiencies. Solvent concentration is varied from 25 to 40 (w/w %) and lean loading is varied from 0.15 to 0.30 (mole $CO_2$/mole MEA) for 70-95 (mol %) $CO_2$ removal efficiency. Exactly similar simulations are performed to analyze both coal and gas fired flue gas removal processes.

### *3.1 Coal fired power plant flue gas simulations*

The simulation results for coal fired system are considered under this section. Figure 3 indicate re-boiler duty variation with $CO_2$ lean loading when MEA concentration is fixed at 25, 30, 35, and 40 (w/w %) respectively.

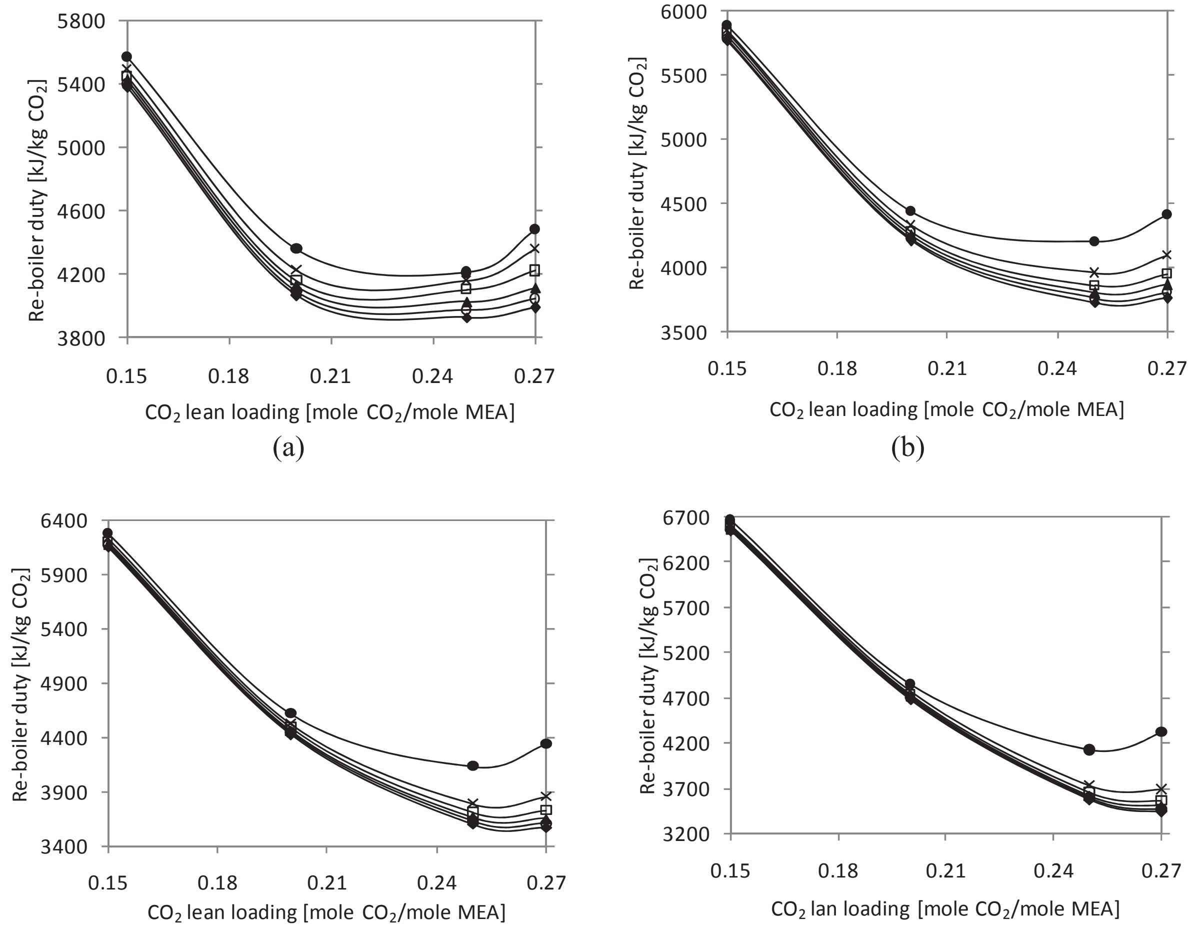

(a) (b) (c) (d)

Figure 3. Re-boiler duty variation with $CO_2$ lean loading with different MEA concentrations, (a) 25w/w%, (b) 30w/w%, (c) 35w/w% and (d) 40w/w%, in coal fired flue gas, symbols refer to efficiencies: ♦, 70%; o, 75%; ▲, 80%; □, 85%; ×, 90%; ●, 95%

From Figure 3 it is clear that the re-boiler energy requirement decreases with the increase of lean solvent loading until the minimum is obtained. However, after a certain limit of the lean loading value, re-boiler duty again started to increase. The point which gives lowest re-boiler energy is defined as the optimum lean solvent loading. At the same time, inlet solvent flow rate is changed to achieve the specified $CO_2$ removal efficiency. In all four cases (MEA concentration from 25% to 40%), lowest re-boiler duty is shown at 70% efficiency. When $CO_2$ removal efficiency is increased, re-boiler duty is increased. According to the figures, lowest re-boiler duty is shown in Figure 3(d), which has 40% MEA concentration. The required lowest energy demand in the re-boiler for most important efficiency values have been analyzed separately and given in Figure 4. The efficiencies 85%, 90% and 95% are considered as most considerable and good values for the removal process.

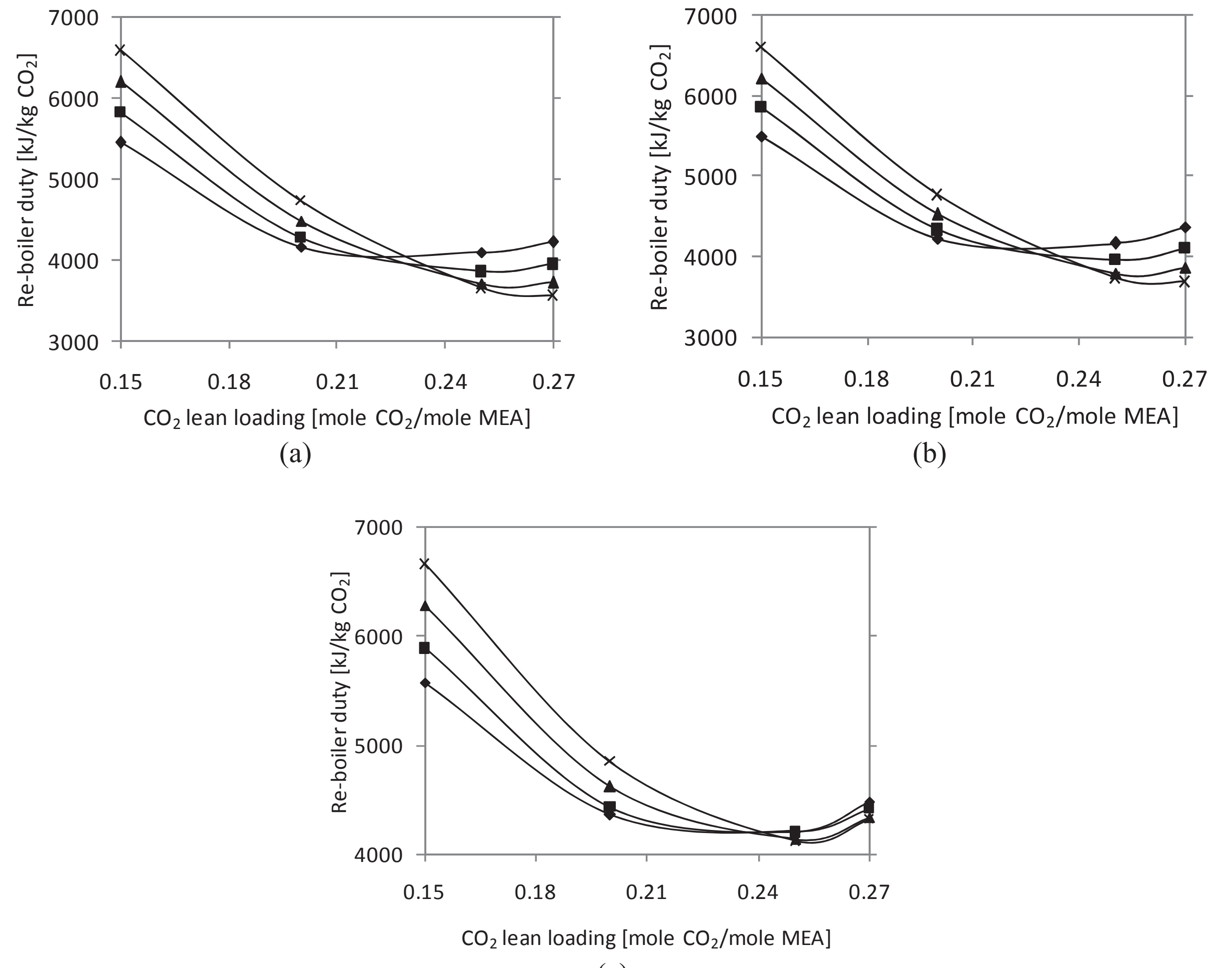

(a)

(b)

(c)

Figure 4. Re-boiler duty variation with $CO_2$ lean loading when removal efficiency is (a) 85%, (b) 90%, (c) 95% in coal fired flue gas, symbols refers to MEA concentrations: ♦, 25% MEA; ■, 30% MEA; ▲, 35% MEA; ×, 40% MEA.

For 85% $CO_2$ removal efficiency, lowest re-boiler duty is given at 40% MEA concentration and 0.27 $CO_2$ lean loading (Figure 4(a)). Similarly from Figure 4(b) and (c), it can be seen that lowest re-boiler duty is given at 40% MEA concentration and 0.27 lean loading for 90% removal efficiency process and 0.25 lean loading for 95% removal efficiency. It is not just re-boiler duty requirement, but also solvent flow rate minimization is important to optimize the process. The solvent flow rate requirement for 0.27 (mole $CO_2$/mole MEA) $CO_2$ lean loading model is given in Figure 5.

It can be seen from Figure 5, that the required solvent inlet flow rate is decreasing with the increased of MEA concentration. When the removal efficiency is gradually increased, required solvent flow rate is increasing. For all removal efficiency models, lowest solvent requirement is given for 40% MEA concentration. However, increasing the amine concentration is believed to have corrosive effects in all sections in capture plant. This can be minimized by adding a small amount of corrosive inhibitors to the inlet solvent stream. The presence of these inhibitors is supposed to have negligible effect on the $CO_2$ removal process.

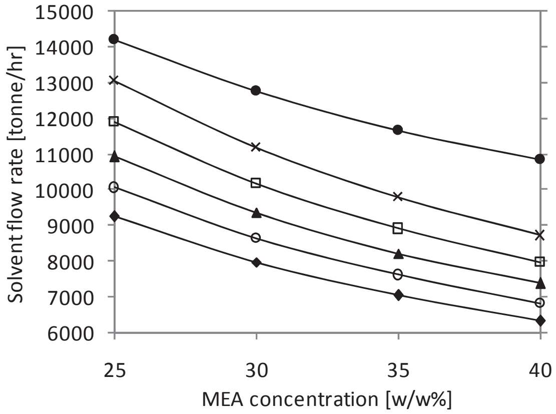

Figure 5. Solvent flow rate variation with MEA concentration when $CO_2$ lean loading 0.27(mole $CO_2$/mole MEA) in coal fired flue gas, symbols refer to efficiencies: ♦, 70%; o, 75%; ▲, 80%; □, 85%; ×, 90%; ●, 95%.

*3.2 Gas fired power plant flue gas simulations*

Figure 6 indicate re-boiler duty variation with $CO_2$ lean loading when MEA concentration is fixed at 25, 30, 35 and 40% respectively. All simulations were performed exactly similar to coal fired flue gas simulations.

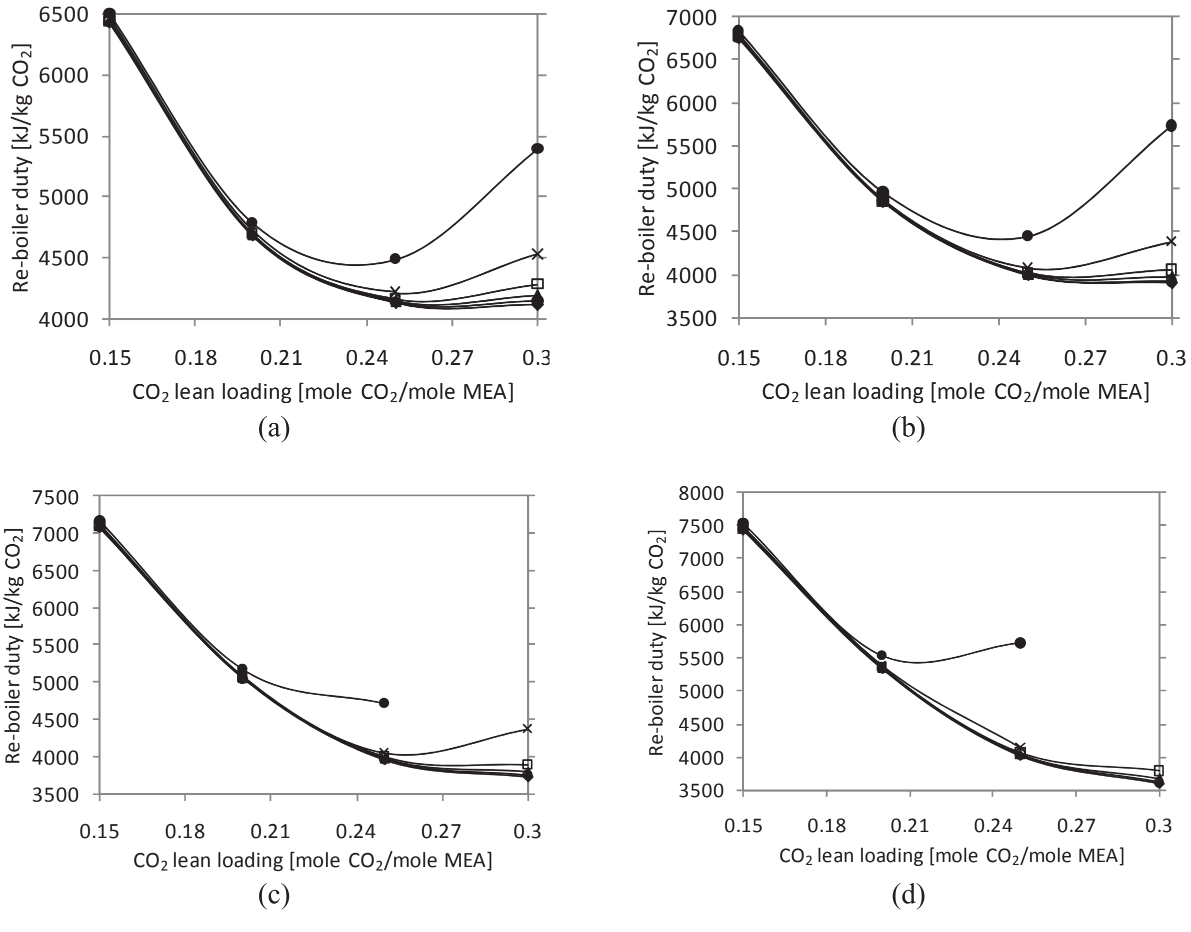

(a)

(b)

(c)

(d)

Figure 6. Re-boiler duty variation with $CO_2$ lean loading when MEA concentration, (a) 25w/w%, (b) 30w/w%, (c) 35w/w% (d) 40w/w%, in gas fired flue gas, symbols refer to efficiencies: ♦, 70%; o, 75%; ▲, 80%; □, 85%; ×, 90%; ●, 95%.

Similar to coal fired system, Figure 6, re-boiler duty is decreasing as lean loading increase. However, after a certain lean loading value, re-boiler duty again starts to increase. In all four cases (MEA concentration from 25% to 40%), lowest re-boiler duty is shown for 70% efficiency simulation plot. The trends of the figures are obtained almost similar to the coal fired cases. The required lowest energy demand in the re-boiler for efficiency values 85%, 90% and 95% have been analyzed separately and given in Figure 7.

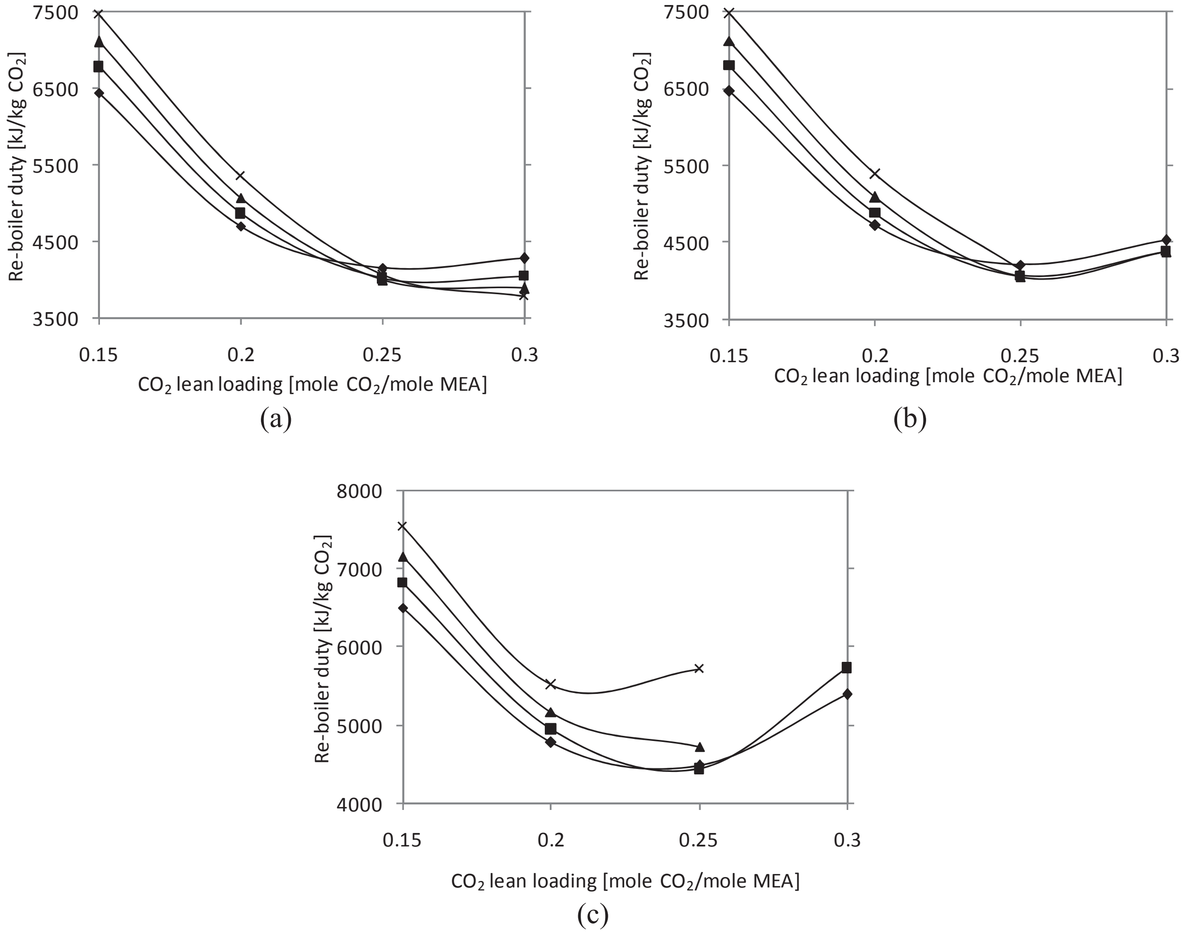

(a)

(b)

(c)

Figure 7. Re-boiler duty variations with $CO_2$ lean loading when removal efficiency is (a) 85%, (b) 90%, (c) 95% in gas fired flue gas, symbols refer to MEA concentrations: ♦, 25% MEA; ■, 30% MEA; ▲, 35% MEA; ×, 40% MEA

For 85% $CO_2$ removal efficiency, lowest re-boiler duty is given at 40% MEA concentration and 0.30 $CO_2$ lean loading (Figure 7(a)). Similar to that from Figure 7(b) and (c), it can be seen that lowest re-boiler duty is given at 35% MEA concentration and 0.25 lean loading for 90% removal efficiency, and 30% MEA concentration and 0.25 lean loading for 95% removal efficiency. Figure 8 is showing the solvent flow rate variation with MEA concentration at 0.25 and 0.30 $CO_2$ loading, respectively.

As MEA concentration is increased, required solvent flow rate is decreased. For 85% and 90% efficiency, lowest solvent flow rate is given when the lean loading is 0.25 and 40% MEA concentration and for 95% efficiency, lowest solvent flow rate gives when lean loading 0.25 and 35% MEA concentration. When the lean loading is increased to 0.30, once again lowest solvent flow rate is given for 40% MEA concentration.

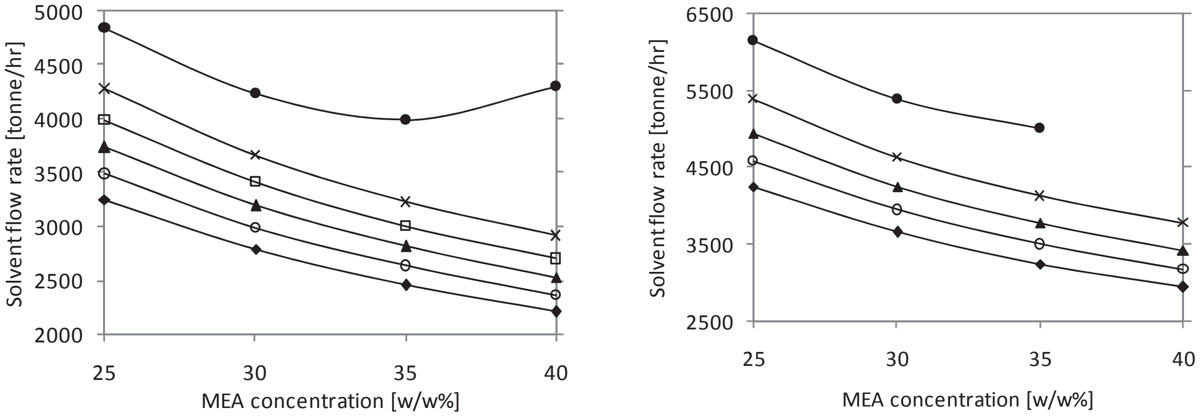

(a) (b)

Figure 8. Solvent flow rate variation with MEA concentration when $CO_2$ lean loading is (a) 0.25 and (b) 0.30 (mole $CO_2$/mole MEA) in gas fired flue gas, symbols refer to efficiencies: ♦, 70%; o, 75%; ▲, 80%; ×, 85%; ●, 90%

## 4. Conclusion

The most important factor for process optimization in the capture process is the thermal energy requirement in the regeneration process, as it is responsible for overall thermal efficiency. At the same time, inlet solvent flow rate is also considered. The lowest re-boiler duty with minimum solvent flow rate will give optimal energy requirement and lowest operating cost. The lowest re-boiler duties are calculated as 3634.2, 3736.4, and 4185.5 kJ/kg $CO_2$ for the 85, 90, and 95% $CO_2$ removal process for coal fired power plant and 3781, 4050, and 4240 kJ/kg $CO_2$ for 85%, 90%, and 95% for gas fired power plant. The optimum specifications for the coal and gas processes such as MEA concentration, $CO_2$ lean loading, and solvent inlet flow rates are summarized in Table 3 for different efficiency values. The re-boiler energy demand is decreasing with increasing amine concentration in the solvent inlet flow stream.

Table 3. Optimum solvent conditions for both coal and gas fired power plant flue gas capture process

| Specification | 85% Removal Efficiency | 90% Removal Efficiency | 95% Removal Efficiency |
|---|---|---|---|
| Coal fired power plant $CO_2$ capture | | | |
| MEA concentration [w/w%] | 40 | 40 | 40 |
| $CO_2$ lean loading [mole $CO_2$/mole MEA ] | 0.27 | 0.27 | 0.25 |
| Solvent flow rate [tonne/hr] | 7965 | 8719 | 8940 |
| Gas fired power plant $CO_2$ capture | | | |
| MEA concentration [w/w%] | 40 | 35 | 30 |
| $CO_2$ lean loading [mole $CO_2$/mole MEA ] | 0.30 | 0.25 | 0.25 |
| Solvent flow rate [tonne/hr] | 3775 | 3224 | 4240 |

## References

[1] Intergovernmental Panel on Climate Change (IPCC). Climate Change 2007: Synthesis Report. IPCC, Geneva, Switzerland, 2007, 104.

[2] Alie C.F. $CO_2$ Capture with MEA: Intergrating the Absorption Process and Steam Cycle of an Existing Coal-Fired Power Plant. Master Thesis, University of Waterloo, Canada, 2004.

[3] Fluor for IEA GHG Program. Improvement in Power Generation with Post-Combustion Capture of $CO_2$. Final Report. November 2004, Report Number PH4/33.

[4] Michael A.D. A model of vapour-liquid equilibria for acid gas-alkanolamine-water systems. Ph.D Thesis, University of Texas, USA, 1989.
[5] Freguia S. Modeling of CO2 removal from Flue Gas with Mono-ethanolamine. Master Thesis, University of Texas, USA, 2002.
[6] Aspen Plus. Aspen Physical Property Methods. Aspen Technology Inc, Cambridge, MA, USA, 2006, 61-63.
[7] Aspen Plus. Rate Based model of the $CO_2$ capture process by MEA using Aspen Plus. Aspen Technology Inc, Cambridge, MA, USA, 2008.
[8] Mohammad A. Carbon dioxide capture from flue gas. Ph.D Thesis, University of Delft, Netherland, 2009.
[9] Bravo J.L., Rocha J.A. and Fair J.R.. Mass Transfer in Gauze Packings. Hydrocarbon Processing, 1985 (January), 91–95.
[10] Billet R., Schultes M. Predicting Mass Transfer in Packed Columns. Chem. Eng. Technology, 1993,Vol. 16, 1-9.

**Udara S.P.R. Arachchige** received his B.Sc Degree (2007) in Chemical and Process Engineering from University of Moratuwa, Sri Lanka and M.Sc degree (2010) in Energy and Environmental Engineering from Telemark University College, Porsgrunn, Norway. He is presently pursuing his Ph.D in Carbon dioxide capture from power plants- modeling and simulation studies from Telemark University College, Porsgrunn, Norway. He has presented and published five paper in International Conferences. Mr. Udara is a member of American Chemical Society.
E-mail address: udara.s.p.arachchige@hit.no

**Muhammad Mohsin** received his B.Sc Degree (2011) in Electrical Engineering and Automation from Shenyang University of Chemical Technology, Shenyang, China. He is presently pursuing his Master degree in System and Control Engineering in Telemark University College, Porsgrunn, Norway. He also working as a research Assistant in Technology department in same university college. Mr. Mohsin has research interest on carbon capture, modeling and simulation, control systems in process industries.
E-mail address: mohsin.m.ansari@gmail.com

**Morten Chr. Melaaen** is Professor in process technology at Telemark University College, Porsgrunn, Norway. He is also the Dean of Faculty of Technology, Telemark University College and has a part time position at the local research institute Tel-Tek. Earlier, he has worked as a research engineer in Division of Applied Thermodynamics, SINTEF, Norway and as an Associate professor at Norwegian University of Science and Technology (NTNU). He has worked on research projects as a Senior research scientist in Norsk Hydro Research Centre Porsgrunn, Norway. He started to work as a professor at Telemark University College in 1994 and became Head of Department, Department of Process, Energy and Environmental Technology in 2002. He received his MSc in Mechanical Engineer in 1986 and his Ph.D in 1990, both from the NTNU. His research interests are $CO_2$ capture, Modeling and simulation, Fluid mechanics and Heat and Mass Transfer. Professor Morten has more than 90 scientific papers published in the above mentioned related fields in international journals and conferences.
E-mail address: Morten.C.Melaaen@hit.no

Paper E

# Blended Amines' Effect on Post Combustion CO2 Capture Process

This paper was presented in International Conference on Environmental Pollution and Remediation (ICEPR 12) at Montreal, Quebec, Canada on August 2012. The paper is published in conference proceedings (ISBN: 978-0-9867183-6-6, International ASET Inc., pp 107:1-8, 2012).

*Proceedings of the 2$^{nd}$ International Conference on Environmental Pollution and Remediation*
*Montreal, Quebec, Canada, 28-30 August 2012*
*Paper No. 107*

# Blended Amines' Effect on Post Combustion $CO_2$ Capture Process

**Udara S. P. R. Arachchige**
Telemark University College
Porsgrunn, 3901, Norway
udara.s.p.arachchige@hit.no

**Morten C. Melaaen**
Telemark University College, Tel-Tek
Porsgrunn, 3901, Norway
Morten.C.Melaaen@hit.no

***Abstract*** **-**The potential use of alkanolamine solvents for carbon capture from the flue gas from coal fired power plant, is evaluated. The key factor for determining operating cost is energy consumption for regeneration of the solvents. An alternative solvent to monoethanolamine, which have higher carbon capture potential and lower energy consumption, is necessary. The blended amines effect on carbon capture process is studied with comparison of single amines. The coal fired power plant is considered for model development. The model is implemented in the Aspen Plus with Electrolyte NRTL property method. Thermodynamic and kinetic data as well as flue gas stream data are used according to the literatures. Temperature and $CO_2$ loading profiles in absorber column and re-boiler duty requirement are considered as most important factors. The amine loading in absorber for the blended amine system is lower than the single amine process. The blended amine system requires 2937kJ/kg $CO_2$ for coal fired plant flue gas capture process according to the present study. This is reasonably lower value compared with single amine re-boiler duties 4137kJ/kg $CO_2$ and 3809kJ/kg $CO_2$ in case 1 and 2 respectively.

***Keywords*****:** Blended amines, carbon capture, Aspen Plus, simulations, Re-boiler duty

## 1. Introduction

Combustion of fossil fuel is considered as the largest $CO_2$ emitting source to the atmosphere. The atmospheric $CO_2$ level has risen 35% since the time of industrial revolution and current value is calculated as 380ppm (Faramarzi, 2010). Carbon dioxide and other green house gases are the leading sources for global climate change effect as a rise in the average terrestrial surface temperature (Andrade and Zaparoli, 2005). Therefore, $CO_2$ mitigation technologies are important to reduce the green house gas effect. Post combustion $CO_2$ capture by chemical absorption is considered as the most promising technology for power plant flue gas treating. Reason for that is, it can be applied for flue gases with low $CO_2$ concentration levels (Rao and Rubin, 2002). However, there are some drawbacks with existing solvents. The major drawbacks related to amine based processes, especially MEA, can be categorized as high amount of energy requirement for the regenerating process, size of the capture plant, corrosion effect and solvent degradation (Shao and Stangeland, 2009).

At present time, amine blends are widely studied to overcome drawbacks with single amines. Most common blends are MEA-MDEA, MEA-PZ, MDEA-PZ and blends of MDEA and triethylene tetramine (Faramarzi, 2010). MDEA has a low heat of regeneration and maximum loading capacity of 1.0 (mol $CO_2$/mol MDEA) as well as less corrosive than MEA. However, pure MDEA does not react with $CO_2$ effectively due to lack of N-H bonds (Edali et al, 2007). The N-H bond is required to generate carbamate ion with $CO_2$.

Blended amines have been studied for effectiveness of the removal process and proven to be more beneficial in acid gas absorption process (Charkravarty and Phuken, 1985). The rate of $CO_2$ absorption can be enhanced by adding small amount of primary amine (MEA) to a tertiary amine (MDEA) (Charkravarty and Phuken, 1985).

The purpose of this study is to compare the advantages of using blended amines in coal power plant flue gas treating with single amines. The model is developed in Aspen Plus and flue gas conditions are taken from the literatures. The simplified model is developed for MDEA/MEA blended solvent with 4:1 mixing ratio in weight basis (section 2.4). Finally, the model is implemented with optimized parameters to get 85% removal efficiency with closed system. The temperature profiles in absorber, as well as $CO_2$ loading profiles are studied. The comparison with single amine model with the same 85% efficiency is performed to understand the benefits of blended amines.

## 2. Process Description

Flue gas data from 500MW coal power plant are taken from the literature (Alie, 2004). The composition of the flue gas and other inlet conditions are tabulated in the Table 1. The Fig. 1 represents the simplified flow diagram for the implemented process.

Table. 1. Flue gas stream conditions for coal fired power plant (Alie, 2004)

| Parameter | Coal fired power plant flue gas | Composition | |
|---|---|---|---|
| | | Major components | Value (mol %) |
| Flow rate (kg/s) | 674 | $H_2O$ | 8.18 |
| | | $N_2$ | 72.86 |
| Pressure (bar) | 1.1 | $CO_2$ | 13.58 |
| Temperature (K) | 313 | $O_2$ | 3.54 |
| | | $H_2S$ | 0.05 |

### 2. 1. Model Development

Inlet solvent and flue gas temperatures are selected as 308K and 313K for base case model development for blended amine process. Absorber and stripper are the main two unit operation blocks in the process. Absorber is operated at 1 bar pressure while stripper is operating at 1.9 bar absolute pressure. Electrolyte NRTL rate based property method is selected for model implementation in Aspen Plus.

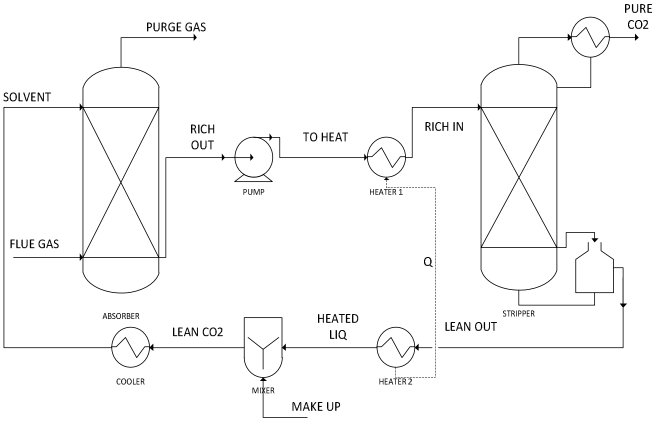

Fig. 1. Process flow diagram

The extraction process is based on the reaction between alkanolamine with $CO_2$ to produce a water soluble salt. In the absorber, $CO_2$ is chemically bonded to the amine solution. The bottom of the absorber consists of $CO_2$ rich amine while the purge gas exists from the top. In the regeneration column, $CO_2$ is liberated from the $CO_2$ rich solution by supplying steam to the regenerator. The $CO_2$ lean solution then recycles back to the absorber column after cooled down through heat exchanger.

The packing parameters of the $CO_2$ capture model in absorber and stripper are given in Table 2 for both single and blended amine systems. Single amine process model data from previous studies (Arachchige and Melaaen, 2011) is given in case 1 and new single amine model with equivalent packing condition to blended amine process is given in case 2. The inlet solvent flow rate is changed to get exact 85% removal efficiency in case 2. Inlet solvent flow rate is one of the main parameter can be used to change the removal efficiency.

Table. 2. Packing details of absorber and stripper

| Parameter | Single amine (Case 1) | Single amine (Case 2) | Blended amine |
|---|---|---|---|
| Absorber packing height (m) | 22 | 26 | 26 |
| Absorber packing diameter (m) | 16 | 20 | 20 |
| Stripper packing height (m) | 20 | 20 | 20 |
| Stripper packing diameter (m) | 15 | 15 | 15 |
| Packing type in absorber | PALL type metal | PALL type metal | PALL type metal |
| Packing type in Stripper | FLEXIPAC metal | FLEXIPAC metal | FLEXIPAC metal |
| Efficiency (mol %) | 85 | 85 | 85 |

## 2. 2. Reaction Scheme

Eqs. 1 to 11 represents the reaction scheme for the reactions of $CO_2$ and $H_2S$ with primary and tertiary amines when $CO_2$ and $H_2S$ are absorbed into blended amine system (MDEA+MEA) (Hagewiesche et al, 1995a). The symbol R refers to the $CH_2$-$CH_2$-OH in the reacting system.

Ionization of water:

$$H_2O \leftrightarrow OH^- + H^+ \tag{1}$$

Dissociation of dissolved carbon dioxide through carbonic acid:

$$CO_2 + H_2O \leftrightarrow HCO_3^- + H^+ \tag{2}$$

Dissociation of bicarbonate:

$$HCO_3^- \leftrightarrow CO_3^{2-} + H^+ \tag{3}$$

Formation of bicarbonate:

$$CO_2 + OH^- \leftrightarrow HCO_3^- \tag{4}$$

Reaction of $CO_2$ with tertiary amine:

$$CO_2 + RRCH_3N + H_2O \leftrightarrow RRCH_3NH^+ + HCO_3^- \tag{5}$$

$$RRCH_3N + H^+ \leftrightarrow RRCH_3NH^+ \tag{6}$$

Reaction of $CO_2$ with primary amine:

$$RNH_2 + CO_2 \leftrightarrow H^+ + RNHCOO^- \tag{7}$$

$$RNH_2 + H^+ \leftrightarrow +RNH_3^+ \tag{8}$$

$$RNHCOO^- + H_2O \leftrightarrow RNH_2 + HCO_3^- \tag{9}$$

Reaction with $H_2S$:

$$H_2S + RNH_2 \leftrightarrow RNH_3^+ + HS^- \tag{10}$$

$$H_2S + RRCH_3N \leftrightarrow RRCHNH^+ + HS^- \tag{11}$$

The mechanism between tertiary amines and $CO_2$ is shown in the reaction 5 and 6. Those two reactions indicate that $CO_2$ does not directly react with tertiary amines. Tertiary amines act as bases and it catalyze the $CO_2$ hydration process (Hagewiesche et al, 1995a).

### 2. 3. Thermodynamic and Kinetic Model

The eq. 12 is used to calculate equilibrium constants which are required for above reactions to calculate their vapour liquid compositions. Equilibrium constant values are imported from the literature sources (Freguia, 2002 and Aspen, 2006) as well as from Aspen Plus available databanks.

$$\ln K_j = A_j + \frac{B_j}{T} + C_j \ln T + D_j T \tag{12}$$

The power law kinetic expression (eq. 13) which is defined in Aspen Plus is used to calculate the rate constant values for MEA+ MDEA+ $CO_2$ system.

$$r_j = k_j \left(\frac{T}{T_0}\right)^{n_j} \exp\left[\frac{E_j}{R}\left(\frac{1}{T} - \frac{1}{T_0}\right)\right] \tag{13}$$

Henry's law is used to calculate the solubility of gases. The Henry's constants used in this simulation are calculated using eq. 14 given below. In this model, Henry's constants of $CO_2$ in $H_2O$, MEA and MDEA solvents are required. In this equation, $C_1^H, C_2^H, C_3^H, C_4^H$ indicated Henry's constants and solvent type is represented by S while temperature is given by T.

$$\ln H_{CO_2-S} = C_1^H + {C_2^H}/{T} + C_3^H \ln T + C_4^H T \tag{14}$$

## 2. 4. Solvent Selection

The primary or secondary amines are usually added to the tertiary system (MDEA) in the amount of 5-10 wt% of the total amine present in the mixture (Bullin et al, 1984). The solvent inlet conditions are given in the Table 3.

Table. 3. Inlet solvent stream compositions in single and blended amine system

| Parameter | Single amine (MEA) | Blended amine (MEA/MDEA) |
|---|---|---|
| MEA (wt%) | 25 | 10 |
| MDEA (wt%) | - | 40 |
| $H_2O$ (wt%) | 75 | 50 |
| $CO_2$ lean loading (mol $CO_2$/mol amines) | 0.25 | 0.15 |

## 3. Results and Discussion

The implemented model is used to analyze the temperature profiles in the absorber column. The temperature profiles for liquid and vapour phases are given in Fig. 2. The temperature profiles for both phases are given along the absorber from the top to the bottom of the packing bed. The Fig. 2 shows the temperature bulge at the top of the absorber for single amine and bottom of the absorber for blended amine. Blended amine system gives much lower temperature profiles than single amines and maximum temperature is reached to the 320K at the outlet.

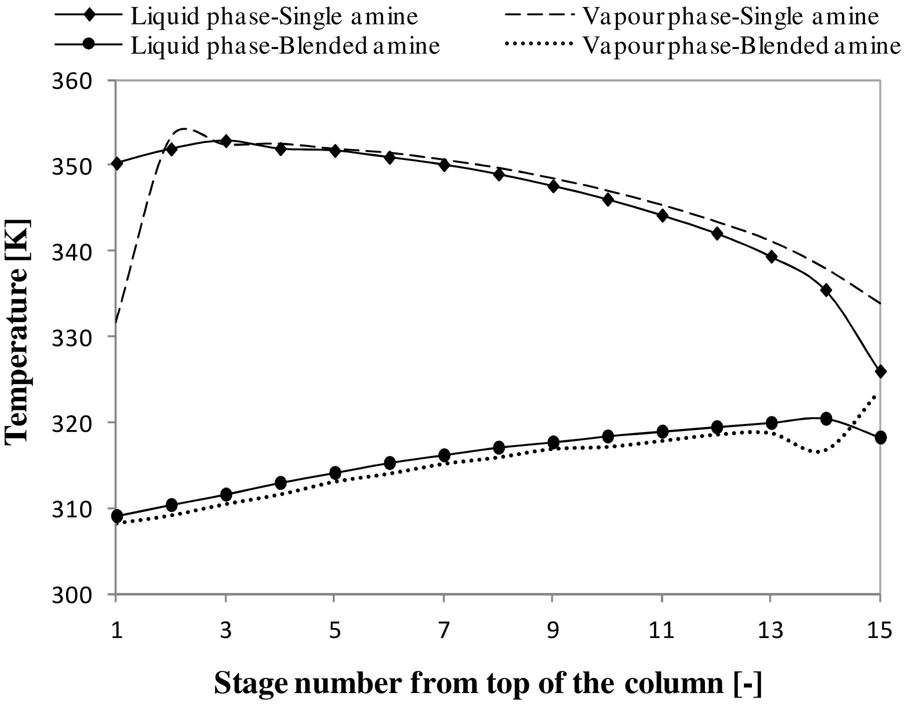

Fig. 2. Temperature profiles in absorber for single and blended amine systems

The temperature profiles in blended amines have almost similar patterns to single MDEA profiles which have been studied before (Arachchige et al, 2011). Blended amine solvent consists of more weight fraction of MDEA and it may be the reason for that.

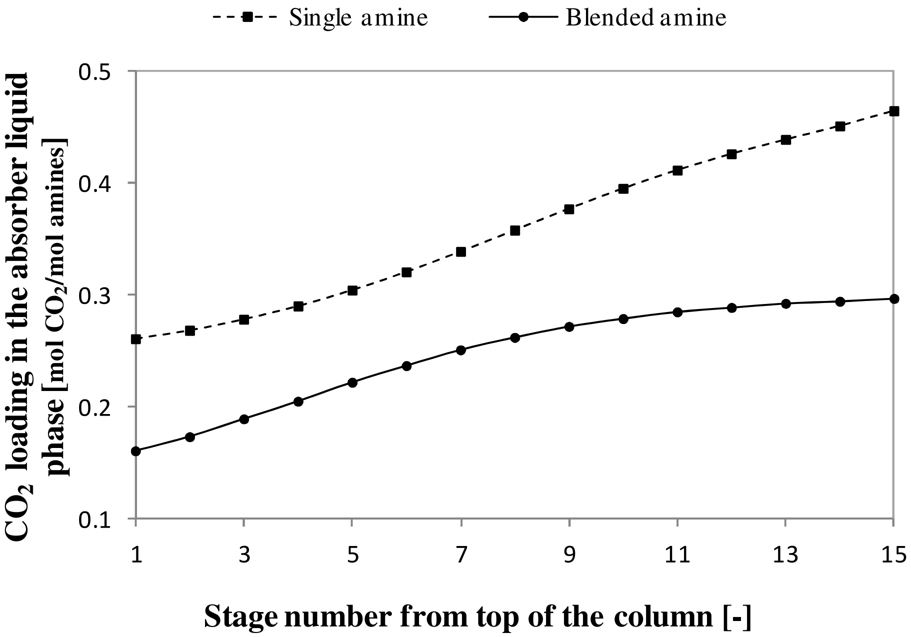

Fig. 3. $CO_2$ loading profiles in absorber for single and mixed amine systems

As shown in the Fig. 3, $CO_2$ loading for the blended amine system is lower than the single amine process. The lower $CO_2$ loading profile along the absorber means that the $CO_2$ absorption capacity is reduced in coal flue gas process with blended amine solvent. The reason behind that may be due to different solvent properties in blended amine process compared to single amine.

The re-boiler duty is the main energy penalty of the $CO_2$ capture plant. Therefore, it is important to consider about energy requirement for re-generation process. The conventional MEA (single amine) process requires approximately 4137kJ/kg $CO_2$ (case 1) and 3809kJ/kg $CO_2$ (case 2) for coal fired flue gas system for stripping section in capture plant for same 85% removal efficiency. The blended amine system requires 2937kJ/kg $CO_2$ for coal fired plant flue gas capture process according to the present study. Present study for blended amines produce lower re-boiler duty and it is confirmed with literatures (Aroonwilas and Veawab, 2007). The case 2 for single amine system is developed to check the packing effect on re-boiler duty. The case 1 can be considered as the better model for single amine process due to lower packing height and diameter which gives lower capital cost.

It should be noted that the above explanation is considered only energy aspects, not considered about capital and operating cost. Using blended amine system may require higher capital and operating cost due to higher absorption tower height. According to this study, that can be noticed by comparing height of the packing section (Table 2). The process with MEA-MDEA having slower rates of absorption causes for higher packing section (Aroonwilas and Veawab, 2004). Raphael et al. have performed experiments to investigate chemical stability of blended amines in $CO_2$ capture process. Effect of blended amines on re-boiler duty can be achieved only if chemical stability of the solvent is maintained (Idem et al, 2006).

## 4. Conclusion

Re-boiler duty is the main energy consideration in $CO_2$ capture process. Blended amine gives lower re-boiler duty comparing to the single amine system. Re-boiler duty values are 2937kJ/kg CO2 for blended amines and it is reasonable reduction comparing to the single amine process. However, it gives lower re-boiler duty, packing height and diameter of the absorber is higher compared to the single amine process (case 1). Even-though, blended amines give lower re-boiler duty, size of the column and lower energy requirement present the trade-off effect for implementing $CO_2$ capture plant with blended amines with MEA-MDEA.

## List of Symbols

| | |
|---|---|
| MEA | monoethanolamine |
| MDEA | N-methyldiethanolamine |
| PZ | piperazine |
| $K_j$ | equilibrium constant for thermodynamic model |
| A, B, C, D | constants |
| T | temperature [K] |
| $E_j$ | activation energy [cal/mol] |
| R | gas constant [J/mol K] |
| $k_j$ | rate coefficient |
| j | index |
| wt% | weight percentage |
| S | solvent |

### Acknowledgement

The support from master student Muhammad Mohsin, clarifying possible improvements to obtain better results is gratefully acknowledged.

## References

Alie C.F. (2004). $CO_2$ Capture with MEA: Intergrating the Absorption Process and Steam Cycle of an Existing Coal-Fired Power Plant. Master Thesis, University of Waterloo, Canada.

Andrade C.R., Zaparoli E.L. (2005). A survey on the carbon dioxide captures technologies from power plant flue gases. Sao Jose dos Campos, SP, Brazil.

Arachchige U.S.P.R., Melaaen M.C. (2011). Aspen plus simulation of $CO_2$ removal from coal and gas fired power plants, TCCS-6, Trondheim, Norway.

Arachchige U.S.P.R., Aryal N., Melaaen M.C. (2011). Various amines' effect on $CO_2$ removal efficiency, APCRE'11, Beijing, China.

Aroonwilas A., Veawab A. (2004). Characterization and comparison of the $CO_2$ absorption performance into single and blended alkanolamines in a packed column. Ind. Eng. Chem. Res. 43, 2228-2237.

Aroonwilas A., Veawab A. (2007). Intergration of $CO_2$ capture unit using single and blended amines into supercritical coal-fired power plants: implications for emission and energy management. Int. J. Greenhouse Control 1, 143-150.

Aspen Technology Inc. (2006). Aspen Plus 2006 Documentation, Aspen Physical Property Methods.

Bullin J.A., Polasek J.C., Donnelly S.T. (1984). The use of MDEA and mixtures of amines for bulk $CO_2$ removal. Proceedings, 69th Gas processors association Convention, Lousiana.

Charkravarty T., Phuken U.K. (1985). Reaction of acid gases with mixtures of amines. Chem. Eng. Prog, 40, 32-36.

Edali M., Aboundheir A., Idem R. (2007). Kinetics of carbon dioxide absorption into mixed aqueous solutions of MDEA and MEA using laminar jet apparatus and numerically solved absorption rate/kinetic model. Proceedings, COMSOL conference, Boston.

Faramarzi L. (2010). Post-Combustion Capture of $CO_2$ from Fossil Fueled Power Plants. Ph.D Thesis, Technical University of Denmark, Denmark.

Freguia S. (2002). Modeling of $CO_2$ removal from Flue Gas with Mono-ethanolamine. Master Thesis, University of Texas, Austin.

Hagewiesche D.P., Ashour S.S., Al-Ghawas H.A., Sandall O.C. (1995a). Absorption of Carbon dioxide into aqueous blends of monoethanolamine and N-Methyldiethanolamine. Chem. Eng. Sci, 50(7), 1071-1079.

Halim I., Srinivasan R. (2009). A simulation/Optimization Framework for Efficient $CO_2$ Capture Using Amine Absorption. National University of Singapore, Singapore.

Idem A., Wilson M., Tontiwachwuthikul P., Chakma A., Veawab A., Aroonwilas A and Gelowitz D. (2006). Pilot plant studies of the $CO_2$ capture performance of Aqueous MEA and mixed MEA-MDEA Solvents at the University of Regina $CO_2$ capture Technology Development Plant and the Boundary Dam $CO_2$ capture Demonstration Plant. Ind. Eng. Chem. Res. 45, 2414-2420.

Rao A.B., Rubin E.S. (2002). Environ. Sci. Technology, 36, 4467-4475.

Shao R., Stangeland A. (2009). Amines used in $CO_2$ capture- Health and Environmental Impacts, Bellona Report, The Bellona Foundation, Norway.

# Paper F

## Selection of Packing Material for Gas Absorption

This paper is published in the European Journal of Scientific Research, 87, No. 1: 117-126, 2012.

European Journal of Scientific Research
ISSN 1450-216X Vol. 87 No 1 September, 2012, pp.117-126

http://www.europeanjournalofscientificresearch.com

# Selection of Packing Material for Gas Absorption

**Udara S. P. R. Arachchige**
*Telemark University College, Porsgrunn, Norway*
E-mail: udara.s.p.arachchige@hit.no
Tel: +47-94284116; Fax: 0047-35575001

**Morten C. Melaaen**
*Telemark University College, Porsgrunn, Norway*
Tel-Tek, Porsgrunn, Norway
E-mail: Morten.C.Melaaen@hit.no

### Abstract

Carbon dioxide ($CO_2$) capture is the most viable option to minimize the environmental impact by $CO_2$ emissions. Amine scrubbing process is the well-known technology to achieve that. There are several packing types available for gas absorption. Both random and structured packing were considered in the simulation studies. The main idea behind this study was to select the best packing material which gives lowest re-boiler duty. Complete removal model was developed for selected packing materials. Then, Re-boiler duty requirement was calculated for every single packing. The relevant parameters of packing material were taken from the literatures. The packing types BX, Sulzer packing, Flexipac 1Y and Mellapak 350Y can be recommended for coal and gas fired power plant due to lower values of re-boiler duty.

**Keywords:** Pollution, Carbon capture, Absorption, Packed bed, Energy, Aspen Plus

## 1. Introduction

### 1.1. Carbon Dioxide Emissions and Capture

An atmospheric emission of green house gases, carbon dioxide, is the key issue of environmental pollution and global warming. Since the beginning of industrial revolution in 18th century, the average $CO_2$ concentration has increased from 280ppmv to 370ppmv while the average global temperature has increased from 0.6°C to 1°C [1]. The main carbon emitting source is fossil fuel fired power plants and will contribute to half of the emissions. Effort on limitation of $CO_2$ emission is the priority for clean environmental management. There are several $CO_2$ capture technologies available. Post combustion gas scrubbing is widely concerned technology to reduce flue gas emissions from power plants. The energy requirement to operate the carbon capture process reduces the overall efficiency of the power plant and guide to increase the electricity unit cost. An energy requirement for $CO_2$ capture is one of the key factors for considering and will continue to be high priorities in the future gas treating processes. Flue gas from fossil fuel fired power plants is considered as one of the main environmental problems to be solved. Figure 1 shows the basic process flow diagram for post combustion carbon capture process.

**Figure 1:** Process flow diagram for $CO_2$ recovery

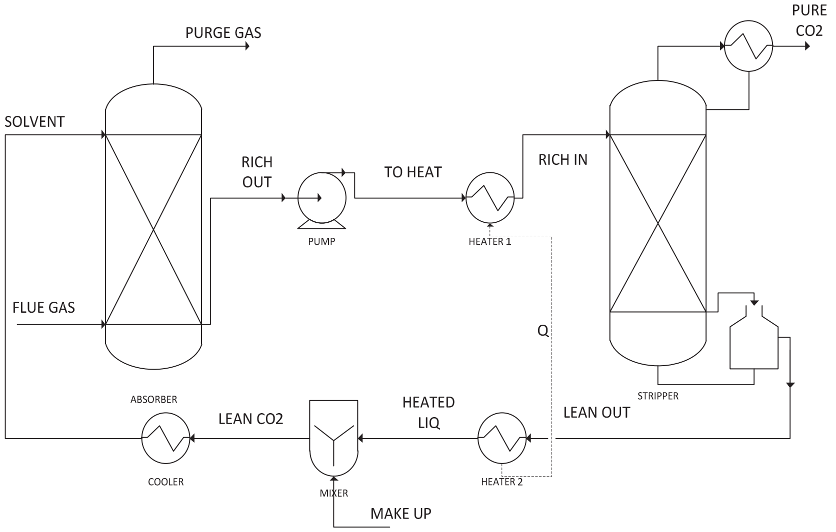

The energy requirement in stripper section is the main energy penalty in the capture process. Absorption process can be either tray or packed column. However, packed column is considered as the preferred option for $CO_2$ capture. Packed columns are being broadly used in various chemical industries and gas separation (absorption and desorption) technologies. With reference to tray towers, lower residence time and the lower bottom temperature provide an advantage for separation of heat sensitive mixtures in packed columns [2]. Packing material use in the gas absorption process can be either random packing or structured packing. There are several packing types available in the Aspen Plus process simulation tool. Both random and structured packing are considered in the simulation studies. The purpose of this study is to assess the characteristics of packing types on the absorption process for $CO_2$ capture.

## 1.2. Packing Materials

Packing section in the absorption process plays important role providing surface area for the gas and liquid phases to contact upon. Mainly, two different types of packing materials are available for gas absorption; Random packing (Pall ring, IMTP, Raschig rings) and Structured packing (Flexipac, Mellapak, Gempak, BX). The overall mass transfer coefficient is high in structured packing compared to the random packing [3]. This is due to large contacting area by structured packing for flow distribution in gas-liquid contacting. Figure 2 shows the examples for random and structured packing.

**Figure 2:** Random (left) and Structured (right) packing [4]

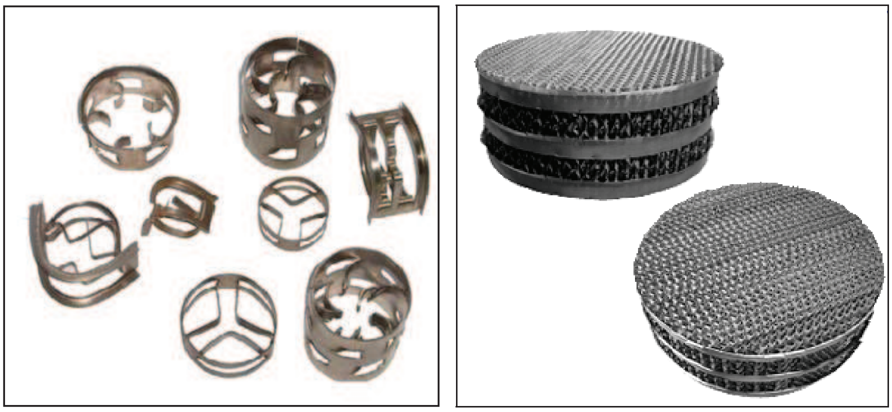

The characteristics of random and structured packing are given in table 1.

**Table 1:** Comparison of Random and Structured Packing [5]

| Random Packing | Structured Packing |
|---|---|
| Flow channels do not have a fixed shape. | It is manufactured in modular form to permit stacking in an ordered array. |
| It can have a nominal size from 1/2" to 4" and is normally dumped randomly into a column. | The height of each module can be varied from 6 to 12 inches. |
| Made of ceramic, metal or plastic. | Having higher surface area than random packing. |
| Easy transport and storage. | Provides better performance and are costly. |
| Cheaper than structured packing | Transportation is difficult without damaging the shape. |

Aspen Plus can handle a wide variety of packing types, including different sizes and materials from various vendors. Aspen Plus stores packing factors for the various sizes, materials, and vendors in databanks. The main objective of any packing is to maximize the efficiency for a given capacity, at a reasonable cost. To achieve this, packing materials are designed to get the following characteristics [6]:

- Maximize the specific surface area - This maximizes vapour-liquid contact area, and, therefore, efficiency.
- Spread the surface area uniformly - This improves vapour-liquid contact, and, therefore, efficiency.
- Maximize the void space per unit column volume - This minimizes resistance to gas up flow, thereby enhancing packing capacity.
- Minimize friction - This helps an open shape that has good aerodynamic characteristics
- Minimize cost.

The most important two factors for selecting packing material are surface area and void fraction. Aspen Plus performs liquid holdup calculations for both random and structured packing for gas absorption. However, for Raschig and Sulzer packing, it uses the vendor procedure for hold up calculation while performing the simulations. If the user does not provide these parameters, Aspen Plus will retrieve data from the built-in databank. For other packing types, Aspen Plus uses the Stichlmair correlation [7]. The Stichlmair correlation requires packing void fraction and surface area as well as three Stichlmair correlation constants to perform the calculations. The parameters in the Stichlmair correlation, $C_1$, $C_2$, $C_3$, are constants and vary with the type of packing. According to the type of packing, information is tabulated for simulations and given later. Onda et al. [8] give the correlation for mass transfer coefficients in the gas absorption process for random packing. The Bravo et al. [9] correlation, predicts mass transfer coefficients and interfacial area for structured packing. However, the Billet and Schultes [3] correlation predicts mass transfer coefficients and interfacial area for all kinds of packing. Stichlmair correlation [7] is used for pressure drop calculations in both types of packing. The comprehensive flow sheet is developed in Aspen Plus with relevant mass and heat transfer correlations as well as liquid holdup and pressure drop model.

## 2. Model Development

### 2.1. Flue Gas and Solvent Properties

Information related to the inlet flue gas and solvent condition are taken from literatures. The 85% removal process model is developed for simulations with monoethanolamine (MEA) as a solvent. Aspen Plus Electrolyte NRTL property method is used for model development. Flue gas compositions are taken from 500MW coal and gas fired power plants (table 2). The compositions of the solvent streams are given in table 3.

**Table 2:** Flue gas stream conditions [10, 11]

| Parameter | Coal fired flue gas | Gas fired flue gas |
|---|---|---|
| Flow rate [kg/s] | 673.4 | 793.9 |
| Temperature [K] | 313 | 313 |
| Pressure [bar] | 1.1 | 1.1 |
| Major Composition | Mol% | Mol% |
| $H_2O$ | 8.18 | 8.00 |
| $N_2$ | 72.86 | 76.00 |
| $CO_2$ | 13.58 | 4.00 |
| $O_2$ | 3.54 | 12.00 |
| $H_2S$ | 0.05 | 0.00 |

**Table 3:** Solvent stream conditions [12]

| Specification | Coal fired flue gas | Gas fired flue gas |
|---|---|---|
| MEA concentration [w/w%] | 40 | 40 |
| Lean $CO_2$ loading [mole $CO_2$/mole MEA ] | 0.27 | 0.30 |
| Temperature [K] | 313 | 313 |
| Pressure [bar] | 1 | 1 |

The 85% removal model is developed with selected solvent condition, which is given optimum results. The chemical reactions [13] and relevant parameters associated with those reactions are taken from the literatures [14]. Open loop removal process model is used for the simulations. The similar value of solvent and flue gas conditions are used for all the simulations. Only packing material and relevant packing factors according to the packing type is changed.

## 2.2. Packing Material Information

The relevant values for packing materials are given below (table 4). The packing information is extracted from literature, and both random and structured packing types are considered in the simulations.

**Table 4:** Packing material information used for simulations

| Packing type | Size (mm or #) | Area ($m^2/m^3$) | Voids - $\varepsilon$ (%) | $C_1$ | $C_2$ | $C_3$ | Vendor | Reference |
|---|---|---|---|---|---|---|---|---|
| **Random Packing** | | | | | | | | |
| Pall rings | 16 | 341 | 93 | 0.05 | 1 | 3 | Generic | [7] |
| Pall rings | 25 | 205 | 94 | 0.05 | 1 | 3 | Generic | [7] |
| Pall rings | 38 | 130 | 95 | 0.1 | 0.1 | 2.1 | Generic | [7] |
| IMTP | 25 | 207 | 97 | 0.815 | -0.106 | 1.499 | Koch | [6] |
| Raschig rings | 25 | 185 | 86 | 40 | 1 | 6 | Generic | [6] |
| **Structured Packing** | | | | | | | | |
| Flexipac | 1Y | 420 | 98 | -1.58 | 0.629 | 0.846 | Koch | [6] |
| Flexipac | 250Y | 250 | 99 | 0.866 | -0.088 | 0.698 | Koch | [6] |
| Mellapak | 250Y | 250 | 98 | 1 | 1 | 0.32 | Sulzer | [6] |
| Mellapak | 350Y | 350 | 98 | 1 | 1 | 0.32 | Sulzer | [6] |
| BX | - | 450 | 86 | 15 | 2 | 0.35 | Sulzer | [7] |
| Gempak | 2A | 220 | 93 | 0.83 | -0.071 | 0.681 | Koch | [15] |

# 3. Complete $CO_2$ Removal Model

The $CO_2$ capture process model is developed in Aspen Plus for different packing materials which are given in the table 4. Packing material and relevant specifications such as surface area, void fraction, and constant values are indicated for different packing types. However, packing height and diameter is maintained as a constant for all the simulations.

The simulation studies are performed to understand the effect of random and structured packing on the carbon capture process. There are five different types of random packing, and six different structured packing materials select for this study. The Pall-16, Pall-25, Pall-38, IMTP-25 and Raschig rings are selected for the random packing category and Flexipac-1Y, Flexipac-250Y, Mellapak-250Y and 350Y, BX and Gempak are chosen for the structured packing. Complete removal process model is developed in Aspen Plus to check the re-boiler energy requirement in every single case. Temperature of liquid and vapor phases and $CO_2$ loading profiles in the absorber are analyzed for all cases. However, temperature profiles and $CO_2$ loading profiles are shown only for coal fired flue gas treating because of similar observations are also obtained for gas fired systems. Figure 3 and 4 show liquid phase temperature profiles in the absorber for random and structured packing for coal fired system, respectively.

**Figure 3:** Liquid phase temperature profiles in absorber for random packing (coal fired flue gas); symbols refer to Δ, Pall-16; ♦, IMTP-25; ∗, Pall-25; ●, Raschig; ▲, Pall-38

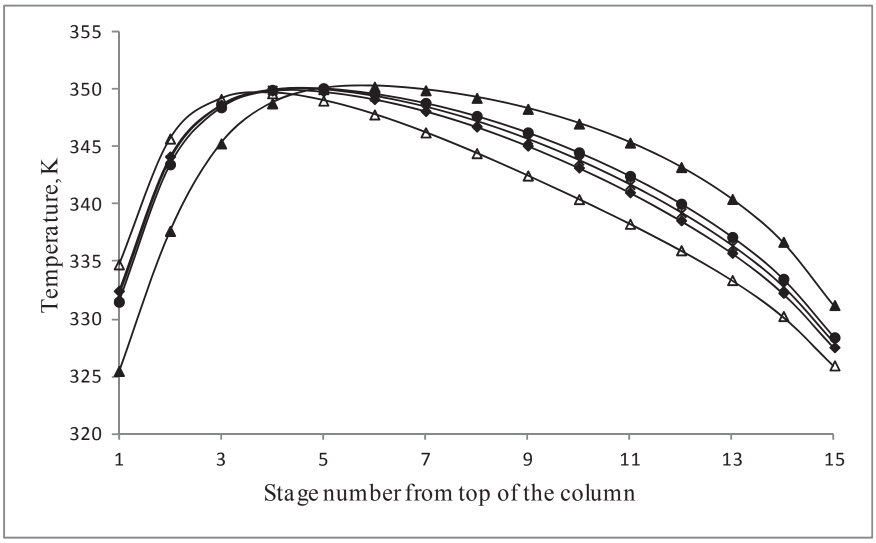

**Figure 4:** Liquid phase temperature profiles in absorber for structured packing (coal fired flue gas); symbols refer to ●, BX; Δ, Flexipac-1Y; ♦, Mellapak-350Y; ----, Mellapak-250Y; ∗, Flexipac-250Y; ▲, Gempak

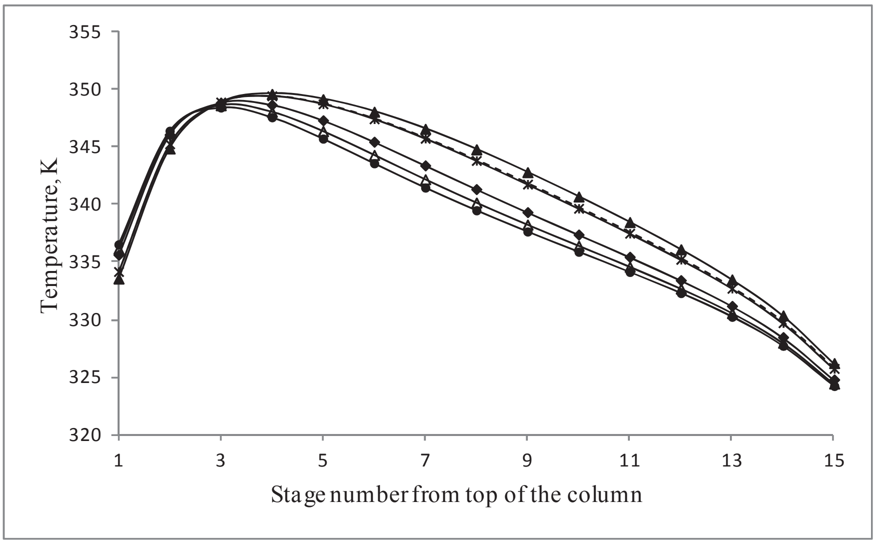

When the surface area of the packing material is decreasing, temperature profile along the column are increasing. The lowest temperature profile in random packing is given for Pall-16, which has highest surface area among all the random packing mentioned in table 4. Similar to that, lowest temperature profile for structured packing is represented by BX packing type, which has highest surface area. Reason for this is, with the higher surface area in packing section, rich $CO_2$ loading is increased and the high amount of $CO_2$ can be absorbed using fewer amount of solvent. Therefore, the total amount of solvent moving inside the absorber column is reduced and temperature inside the column is less. The maximum temperature is reached to around 350 K in liquid phase. In both cases, similar patterns are obtained in temperature profiles for all packing types.

Figure 5 and 6 show vapor phase temperature profiles in absorber for random and structured packing, respectively.

**Figure 5:** Vapor phase temperature profiles in absorber for random packing (coal fired flue gas); symbols refer to Δ, Pall-16; ♦, IMTP-25; ∗, Pall-25; ●, Raschig; ▲, Pall-38

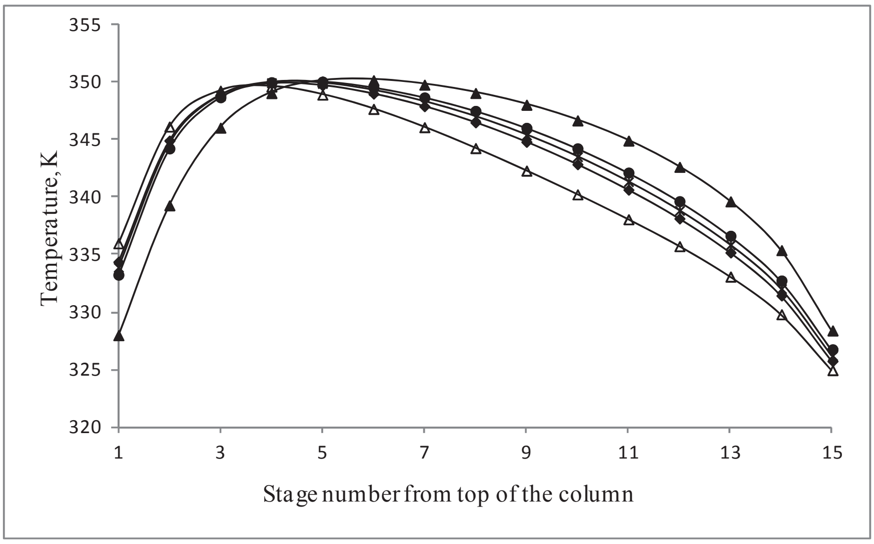

**Figure 6:** Vapor phase temperature profiles in absorber for structured packing (coal fired flue gas); symbols refer to ●, BX; Δ, Flexipac-1Y; ♦, Mellapak-350Y; ----, Mellapak-250Y; ∗, Flexipac-250Y; ▲, Gempak

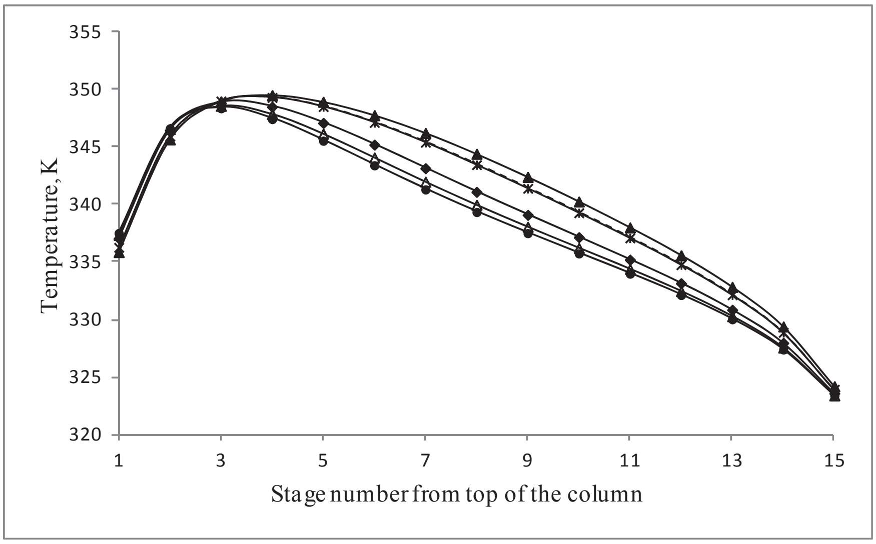

Similar observations are achieved with the temperature profiles in vapor phase. In both random and structured packing, lowest temperature profiles are given for highest surface area material. However, shapes of the profiles are almost similar and maximum temperature reach to 350K for both random and structured packing. Structured packing show the lower temperature profiles compared to random packing for both liquid and vapor phase. Reason for that is, highest surface area of structured packing materials for gas absorption process.

Figure 7 and 8 are presenting the $CO_2$ loading profiles for both random and structured packing along the absorber column.

**Figure 7:** $CO_2$ loading profiles in absorber for 85% removal efficiency for random packing (coal fired flue gas); symbols refer to ▲, Pall-38; ●, Raschig; ∗, Pall-25; ♦, IMTP-25; Δ, Pall-16

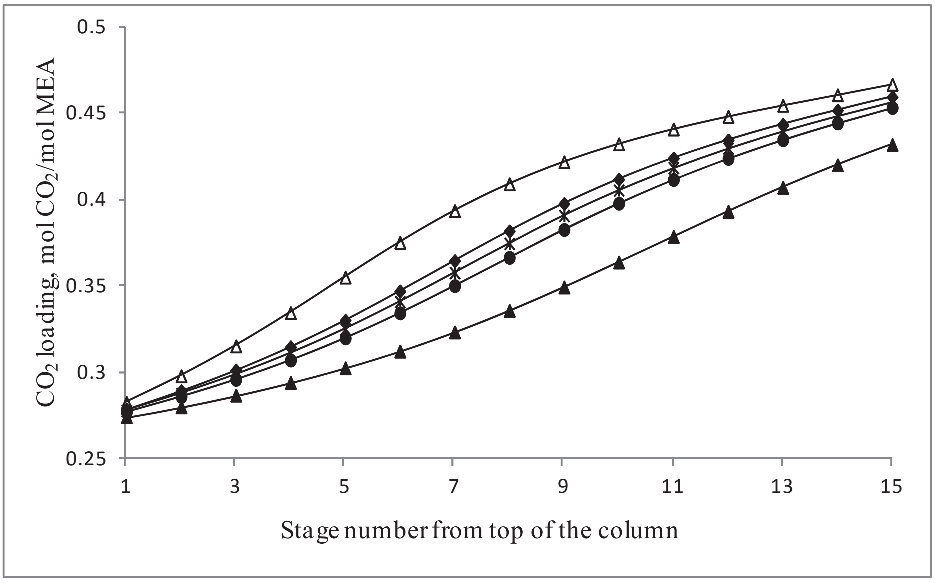

**Figure 8:** $CO_2$ loading profiles in absorber for 85% removal efficiency for structured packing (coal fired flue gas); symbols refer to ▲, Gempak; ----, Mellapak-250Y; ∗, Flexipac-250Y; ♦, Mellapak-350Y; Δ, Flexipac-1Y; ●, BX

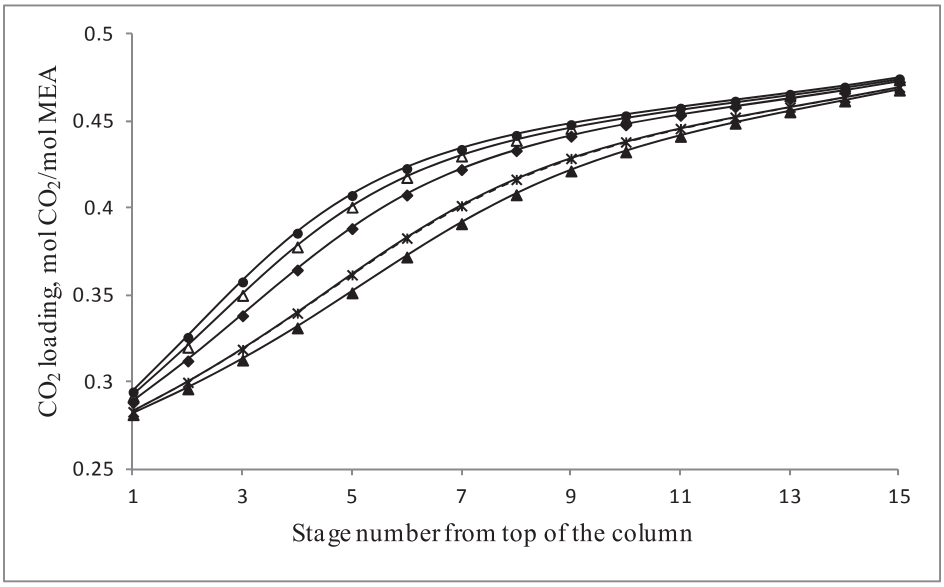

As can be seen from figure 7 and 8, highest $CO_2$ loading profiles are given by Pall-16 and BX which have highest surface area for random and structured packing, respectively. When the surface area is high, area available for reaction medium is high. Therefore, a large amount of $CO_2$ can be absorbed by the solvent stream. Hence, rich $CO_2$ loading is higher with high surface area material. Highest rich $CO_2$ loading value is reached to 0.47 and average value is around 0.45. Flexipac-250Y and Mellapak-250Y have exactly the same surface area, which is 250 ($m^2/m^3$). Because of that, liquid and vapour temperature profiles as well as $CO_2$ loading profiles are overlapped for both materials. Hence, surface area is the most important factor for temperature variation alone the absorber column and variation for $CO_2$ loading. Because of that, while selecting the packing, material with higher surface area is necessary, to improve the carbon capture process with low solvent requirement. Even though, same surface area gives exactly similar temperature and $CO_2$ loading profiles, the conclusion valid only inside one type of packing material (either both are random or both are structured packing). As an example, Pall rings 16 has an area of 341 ($m^2/m^3$) and Flexipac 250Y has an area 250 ($m^2/m^3$). However, Flexipac 250Y shows higher $CO_2$ loading compared to Pall rings 16 which has higher surface area. Main reason behind that may be better solvent distribution inside the column with structured packing. As a result, required re-boiler duty is higher in Pall 16 compared to Flexipac 250Y. Therefore, selection of structured packing is important to get better efficiency and minimum re-boiler duty.

## 4. Discussion

Temperature and $CO_2$ loading profiles follow the similar pattern in all cases and maximum temperature reached around 350K. According to rich $CO_2$ loading, BX packing proves to have a higher packing capacity than others. Rich loading is decreasing from structured packing to random packing. Furthermore, complete removal model is developed for all those packing types. The, re-boiler duty requirement is calculated for every packing type. Table 5 presents a comparison of the different packing for the required re-boiler duty achieved for coal fired flue gas simulation. When rich loading increases and the required solvent flow rate decreases, the re-boiler duty requirement is reduced. Packing height and diameter is kept constant for each simulation to understand the effect of packing type.

**Table 5:** Re-boiler duty comparison with different packing materials for coal fired flue gas capture

| Packing type | Size(mm or #) | Re-boiler duty (kJ/kg $CO_2$) | Solvent flow rate (tonne/hr) | Rich $CO_2$ loading (mole $CO_2$/mole MEA) |
|---|---|---|---|---|
| **Random Packing** | | | | |
| Pall rings | 16 | 3620 | 8103 | 0.466 |
| Pall rings | 25 | 3809 | 8535 | 0.456 |
| Pall rings | 38 | 4369 | 9850 | 0.431 |
| IMTP | 25 | 3757 | 8415 | 0.458 |
| Raschig rings | 25 | 3881 | 8700 | 0.452 |
| **Structured Packing** | | | | |
| Flexipac | 1Y | 3488 | 7800 | 0.473 |
| Flexipac | 250Y | 3561 | 7966 | 0.469 |
| Mellapak | 250Y | 3566 | 7976 | 0.469 |
| Mellapak | 350Y | 3508 | 7846 | 0.472 |
| BX | - | 3481 | 7786 | 0.474 |
| Gempak | 2A | 3592 | 8035 | 0.467 |

Lowest re-boiler duty is given by BX structured packing material as 3481 (kJ/kg $CO_2$) for 85% removal model. Followed by that, Flexipac-1Y and Mellapak-350 Y give low re-boiler duties. However, re-boiler duty values are close for all structured packing material. Reason for low re-boiler duty is high contact surface area available with structured packing. Because of that, rich $CO_2$ loading is high in absorber and required solvent circulating less. Therefore, the amount of the solvent process in stripper is reduced. Hence, the amount of energy needed to heat up the solvent is decreased. Lowest re-boiler duty in random packing is given by Pall-16, which has highest surface area for reacting system.

Similar to this, gas fired flue gas capture process was performed for similar packing materials listed in table 4. Re-boiler duty is decreased with the increased of contact area in packing material. Minimum re-boiler duty is achieved for BX structured packing material as 3598 (kJ/kg $CO_2$) for 85% removal model. Following that, Flexipac-1Y and Mellapak-350Y give low re-boiler duties for $CO_2$ removal process in the gas fired system. Random packing materials give high re-boiler duties compared to structured packing due to lower rich $CO_2$ loading. Temperature and $CO_2$ loading profiles have an almost similar trend as coal fired systems.

The selection of the packing depends on the trade-off between cost of packing and re-boiler duty energy requirement.

## 5. Conclusions

The lowest re-boiler duty is given by the structured packing, BX, Flexipac-1Y followed by Mellapak-350Y. The most important two factors for selecting packing material are surface area and void fraction. The higher surface area gives lower solvent requirement and will lead to lower re-boiler duty. Therefore, BX, Flexipac-1Y or Mellapak-350Y can be recommended for coal and gas fired power plant flue gas treating. The required both solvent and re-boiler energy demand are play the major role for operating cost. Therefore, selection of structured packing instead of random packing gives lowest re-boiler duty with minimum solvent flow rate.

## References

[1] Berger, A, 2002. "The effect of Greenhouse Gases on Climate. Proceedings of the Conference on Future Energy Systems and Technology for $CO_2$ Abatement" , Antwerp, Belgium, Nov. 18/19.

[2] Billet, R., Schultes, M, 1992. "Advantage in correlating packed column performance", IChemE. Symp, Ser. No. 128, p. B129.

[3] Montigny, D., Tontiwachwuthikul, P., Chakma, A, 2001. "Parametric Studies of Carbon Dioxide Absorption into Highly Concentrated Monoethanolamine Solutions", The Canadian journal of chemical engineering, Volume 79.

[4] Sulzer Chemtech AG, 2008. Packing types, CH-8404 Winterthur, Switzerland, http://www.sulzerchemtech.com, Accessed in 10/05/2012.

[5] Wilson, I.D, 2004. "Gas-Liquid Contact Area of Random and Structured Packing", Master Thesis, University of Texas, USA.

[6] Perry, R.H., Green, D.W, 1984. "Perry's Chemical Engineers' Handbook", 6th ed., McGraw-Hill, New York, Chapter 14.

[7] Stichlmair, J., Bravo, J.L., Fair, J.R, 1989. "General model for prediction of pressure drop and capacity of countercurrent gas/liquid packed columns", Gas separation and purification, vol 3 march.

[8] Onda, K., Takeuchi, H., Okumoto, Y, 1968. "Mass Transfer Coefficients Between Gas and Liquid Phases in Packed Columns", J. Chem. Eng. Jap, Vol. 1, No. 1, p. 56.

[9] Bravo, J.L., Rocha, J.A., Fair, J.R, 1985. "Mass Transfer in Gauze Packing", Hydrocarbon Processing January, pp. 91–95.

[10] Alie, C.F, 2004. "$CO_2$ Capture with MEA: Integrating the Absorption Process and Steam Cycle of an Existing Coal-Fired Power Plant", Master Thesis, University of Waterloo, Canada.

[11] Fluor for IEA GHG Program, 2004. Improvement in Power Generation with Post-Combustion Capture of $CO_2$, Final Report.

[12] Arachchige, U.S.P.R., Muhammad, M., Melaaen, M.C, 2012. "Optimization of post combustion carbon capture process-solvent selection", International Journal of Chemical Engineering and Applications, publish in July 23.

[13] Michael, A.D, 1989. "A model of vapor-liquid equilibria for acid gas-alkanolamine-water systems", PhD Thesis, University of Texas, USA.

[14] Freguia, S, 2002. "Modeling of $CO_2$ removal from Flue Gas with Mono-ethanolamine", Master Thesis, University of Texas, USA.

[15] Aspen Plus, 2006. "Aspen Physical Property Methods", Aspen Technology Inc., Cambridge, MA, USA, pp. 61-63.

# Paper G

## Case study for flue gas separation of a coal fired power plant and parameters' effect on removal efficiency

This paper was presented in the 6th Asia Pacific Chemical Reaction Engineering Symposium (APCRE'11) at Beijing, China on September 2011. The paper is published in conference proceedings.

**Proceedings in 6th Asia Pacific Chemical Reaction Engineering Symposium (APCRE'11)**
September 18 - 21，2011 • Beijing • China

# Case study for flue gas separation of a coal fired power plant and parameters' effect on removal efficiency

Udara S.P.R. Arachchige,[a,]* Neelakantha Aryal,[a] Morten C. Melaaen,[a,b]

[a]*Telemark University College, 3901, Porsgrunn, Norway*
[b]*Tel-Tek, Porsgrunn, Norway*
*[***udara.s.p.arachchige@hit.no***](mailto:udara.s.p.arachchige@hit.no)

## Abstract

The emissions of green house gases are expected to cause global warming and climate change effect. The carbon dioxide is the main gas, and the major emitting sources are fossil fuel fired power plants and industrial flue gas generation. Emissions can be reduced by improving efficiency of the existing technologies and shifting to carbon free energy sources. This paper presents the case study of flue gas separation in a 500MW coal power plant. The complete $CO_2$ removal process model is implemented in Aspen Plus with selected operating conditions and parameters. Monoethanolamine (MEA) is used as a solvent with 25% concentration. The possible chemical reactions are introduced in electrolyte NRTL property method. The developed model is considered as base case, and temperature, concentration as well as $CO_2$ loading profiles were examined. The $CO_2$ removal efficiency variation with different parameters such as, inlet solvent flow rate, lean loading, temperature of flue gas and solvent stream, absorber packing height and diameter, absorber pressure were analyzed. The sensitivity analysis results show that the $CO_2$ removal efficiency increases with the solvent concentration, solvent temperature, packing height, packing diameter and absorber pressure. The reverse is applicable with flue gas temperature and lean loading. When the flue gas temperature or lean loading is increased, removal efficiency decreases. It can be concluded that the above listed parameters are important when implementing the removal process in industrial flue gas purification.

**Key words:-** Aspen Plus, temperature profiles, efficiency variation, parameters, coal fired power plant

## 1. Introduction

Concentration of carbon dioxide ($CO_2$) in the atmosphere is rising daily due to the huge amount of coal power plants. Therefore, capture and sequestration of $CO_2$ from the fossil fuel-based power plants are prime importance for the prevention of global warming. $CO_2$ emission can be minimized by the number of methods, which are classified as post-combustion, pre-combustion and oxy-fuel combustion. The post combustion capture uses regenerable solvents to capture the $CO_2$ from flue gas. It can be either physical absorption or chemical absorption. However, chemical absorption is the preferred option depending on the $CO_2$ partial pressure. Even so, chemical solvents require more energy to regenerate, that is, to break the bonds between $CO_2$ and solvent ions.

In pre-combustion capture, fuel is initially reacted with air or oxygen together with steam to produce a fuel that contains CO and $H_2$. Afterwards, this fuel is reacted with the steam to produce a mixture that contains $CO_2$ and $H_2$. $CO_2$, thus generated is separated and $H_2$ is used as a fuel in gas turbine combined cycle to generate energy with high efficiency. In oxy-fuel combustion system, fossil fuel is reacted with pure oxygen instead of air. Large amount of oxygen is required, which can be obtained through the air separating sector. However, this alternative method is costly due to air separation process.

## 2. Model Development

This paper presents a case study of a 500MW coal power plant $CO_2$ removal process and simulations of parameters' effect on process efficiency. The comprehensive flow sheet is developed in Aspen Plus to implement the process model, and the base case is developed to achieve 85% removal efficiency. The flue gas stream data are cited from literature (Alie, 2004). The monoethanolamine (MEA) with 0.25[mol $CO_2$/mol MEA] lean loading and 25[w/w]% is used as a solvent. Base case process details are tabulated in Table 1.

Table 1: Main input parameters in absorber column

| Input parameter | Parameter condition (Fixed/Varied) | Base case value | Range of the parameter varied |
|---|---|---|---|
| Inlet flue gas (tones/ hour) | Fixed | 2424.4 | - |
| $CO_2$ content (mol %) | Fixed | 13.58 | - |
| Flue gas pressure (bar) | Fixed | 1.1 | - |
| Flue gas temperature (ºC) | Varied | 40 | 30-50 |
| Packing material | Fixed | PALL type metal | - |
| Height of the packing (m) | Varied | 22 | 16-36 |
| Diameter of the packing (m) | Varied | 16 | 10-22 |
| Number of stages | Fixed | 15 | - |
| Solvent temperature (ºC) | Varied | 40 | 30-44 |
| Solvent pressure (bar) | Fixed | 1 | - |
| Absorber pressure (bar) | Varied | 1 | 0.8-1.2 |
| Solvent lean loading %(mol $CO_2$/ mol MEA) | Varied | 25 | 15-35 |
| Solvent concentration (w/w)% | Varied | 25 | 10-25 |

The capture process can be broadly divided into two parts, absorber and desorber. In the absorption unit, MEA and flue gas is introduced at the top and bottom of the column, respectively. The chemical interaction takes place through the column. The cleaned gas (PURGE GAS) leaves the column at the top while the $CO_2$ loaded solvent (RICH OUT) exit at the bottom (Figure 1). Moreover, the rich MEA is transferred to the desorber section where MEA is regenerated and pure $CO_2$ being collected at the top of the column. Before rich MEA is introduced to the desorber section, temperature of the stream should be increased to get the maximum performance. Heat released by the lean solvent stream can be used to heat up the rich cold stream. Normally, a stripper (desorber) is operating at the 120ºC, hence rich solvent stream has to be heated up closer to that value. The lean solvent is recycled back to the absorber after adjustment of MEA and $H_2O$ components from make upstream.

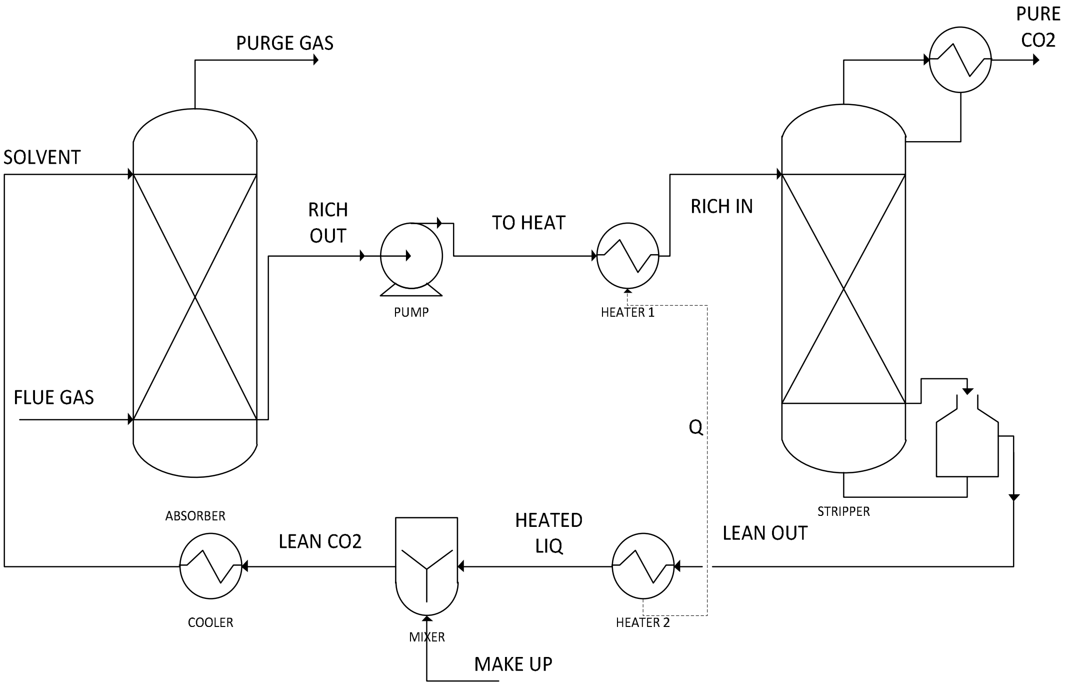

Figure 1: Process flow diagram

The parameters and chemical properties are required to calculate the mole fractions in liquid and gas phases which are involved in reacting system. The required parameters are identified before simulation and retrieved from available databanks in Aspen Plus. The molecular structure and known physical properties of the component can be used to estimate missing parameters. The parameters and property data are introduced to the model to perform the thermodynamics and kinetic process. Classification of parameters can be done as a pure component, binary interaction and electrolyte pair.

To calculate enthalpy, entropy and Gibbs free energy of ions, Aspen Plus uses standard heat of formation in water at infinite dilution (DHAQFM). Massive collection of built in binary parameters are available in Aspen Plus for the following activity coefficient models: WILSON, NRTL and UNIQUAC. Seperate databanks are available for vapor-liquid (VL) and liquid-liquid (LL) applications. The Aspen Plus physical property system contains a huge collection of Henry's law parameters.

Various types of property methods are available for $CO_2$ absorption by MEA process. To name a few, Electrolyte Non Random Two Liquid (ELECNRTL), Electrolyte HF equation of state (ENTRL-HF), Electrolyte Helgeson model (ENTRL-HG), Kent-Eisenberg property methos for amine (AMINES), are the most used ones**.** The ELECNRTL model is selected for the simulation of the $CO_2$ capture process and electrolyte wizard is used for developing simulation kinetics and reactions. Henry's law is used to calculate the solubility of superficial gases where as Redlich-Kwong equation of state is used for calculation of vapor phase properties.

The ELECNRTL property method is the most versatile calculation technique. The model is activity coefficient based, and it can be used for aqueous electrolyte systems as well as mixed solvent electrolyte systems. Activity coefficients for ionic and molecular species in both aqueous and mixed solvent electrolyte systems can be calculated for the reacting process. As the reference state for ions, the model uses the infinite dilution aqueous solution. The Born equation (Kothandaraman, 2010), is used to perform a transformation of the reference state ions from infinite dilution mixed solvent solution to the infinite dilution aqueous solution. It is necessary to introduce water as a component to calculate the transformation of the reference state of ions (Aspen, 2006).

The most important input parameters for the simulations are: inlet gas stream flow rate, composition, pressure, temperature, packing material data, inlet solvent properties and stream conditions. On the other hand, the main outputs are removal efficiency, temperature profiles in liquid and gas phases, $CO_2$ concentration profiles (Svendsen and Eimer, 2010). Therefore, simulation results of the base case are studied. Parameter effect on the implemented model for $CO_2$ removal efficiency is analyzed with the same base case model.

## 3. Chemistry of the $CO_2$ removal process

Following chemical reactions (Equation 1-5) take place during the $CO_2$ removal process with MEA solvent (Michael, 1989). The thermodynamic and kinetic data are selected according to the literatures (Freguia, 2002). Open cycle complete removal process model is developed and implemented to check the parameters' effect on removal efficiency.

Hydrolysis reaction:

$$MEACOO^- + H_2O \leftrightarrow MEA + HCO_3^- \quad (1)$$

Dissociation of dissolved carbon dioxide:

$$CO_2 + 2H_2O \leftrightarrow HCO_3^- + H_3O^+ \quad (2)$$

Dissociation of bicarbonate:

$$HCO_3^- + H_2O \leftrightarrow H_3O^+ + CO_3^{2-} \quad (3)$$

Dissociation of protonated MEA:

$$MEAH^+ + H_2O \leftrightarrow MEA + H_3O^+ \quad (4)$$

Ionization of water:

$$2H_2O \leftrightarrow OH^- + H_3O^+ \quad (5)$$

## 4. Base case simulations

The temperature variation of liquid and gas phase along the absorber is shown in Figure 2. Both temperature profiles follow the same pattern and maximum temperature value is about 353K with slightly higher vapor phase temperature. Top of the absorber shows temperature bulge in both liquid and gas phase. There is a significant amount of reaction at the top of the column. The temperature bulge is due to the heat that is produced by the exothermic reactions and phase transitions.

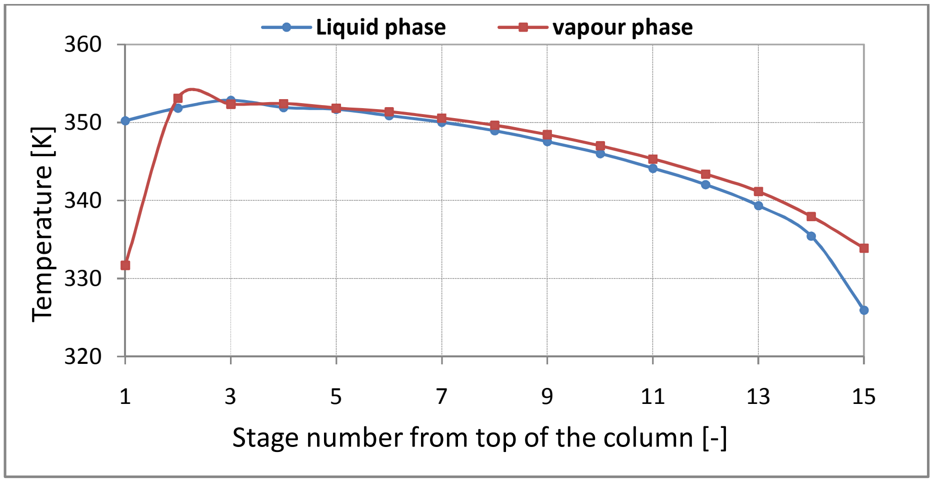

Figure 2: Liquid and vapour phase temperature profiles in absorber

$CO_2$ loading in liquid phase against the stage number is shown in Figure 3. Along the absorber column, $CO_2$ loading is increasing and maximum value reached to 0.47 [mol $CO_2$/mol MEA] at the bottom.

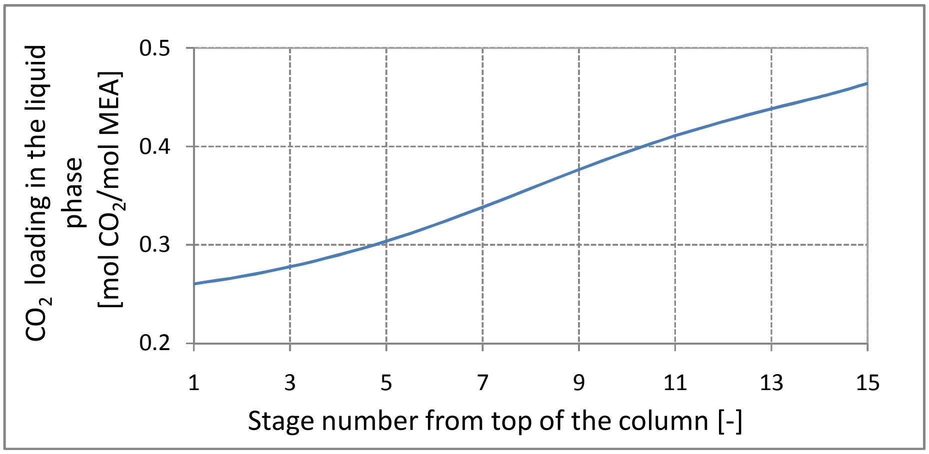

Figure 3: $CO_2$ loading in the liquid phase

## 5. Sensitivity analysis

The variation of removal efficiency with different parameters such as lean loading, solvent concentration, temperature of flue gas and solvent stream, absorber packing height and diameter, and absorber pressure is analyzed for implemented base case. Figure 4 shows how the $CO_2$ removal efficiency varies with lean loading. When the $CO_2$ loading in MEA inlet flow rate is increased, efficiency of the removal process is decreasing (Figure 4). With the increase of lean loading, the capacity of the solvent for $CO_2$ absorption decreases, hence efficiency of the $CO_2$ removal is decreasing (Kothandaraman, 2010).

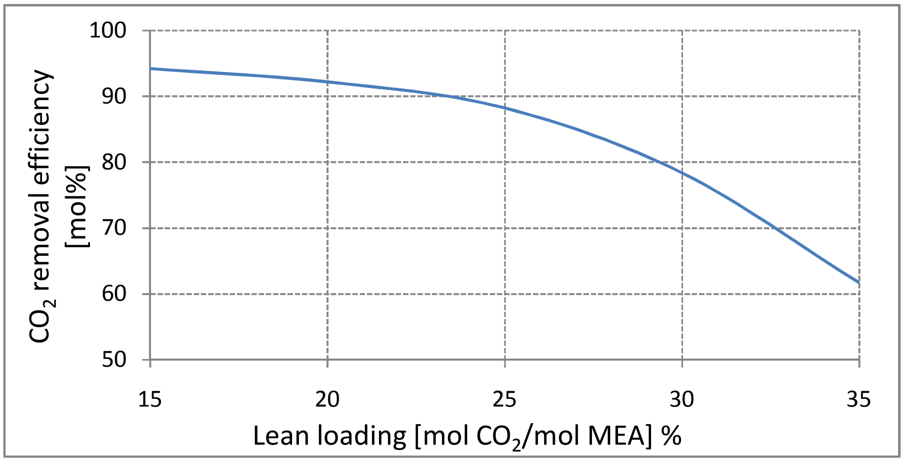

Figure 4: $CO_2$ removal efficiency variation with lean loading

Figure 5 shows how the $CO_2$ removal efficiency varies with solvent concentration. When the concentration of MEA is increased, capacity for $CO_2$ capturing increases, thus, removal efficiency increases and maximum efficiency was obtained between 20-25 $^{w}/_{w}\%$ MEA concentration (Figure 5).

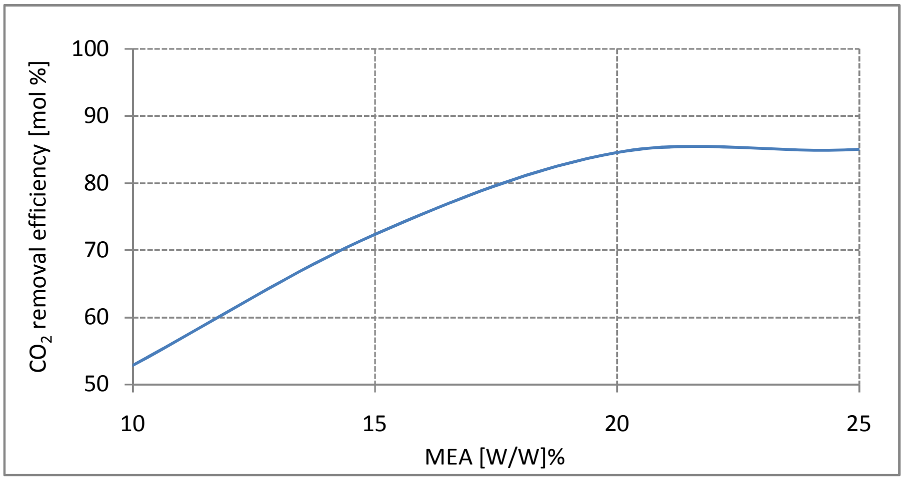

Figure 5: $CO_2$ removal efficiency variation with MEA concentration

Figure 6 shows how the $CO_2$ removal efficiency varies with flue gas temperature. The less effect on $CO_2$ removal efficiency with respect to flue gas temperature is observed.

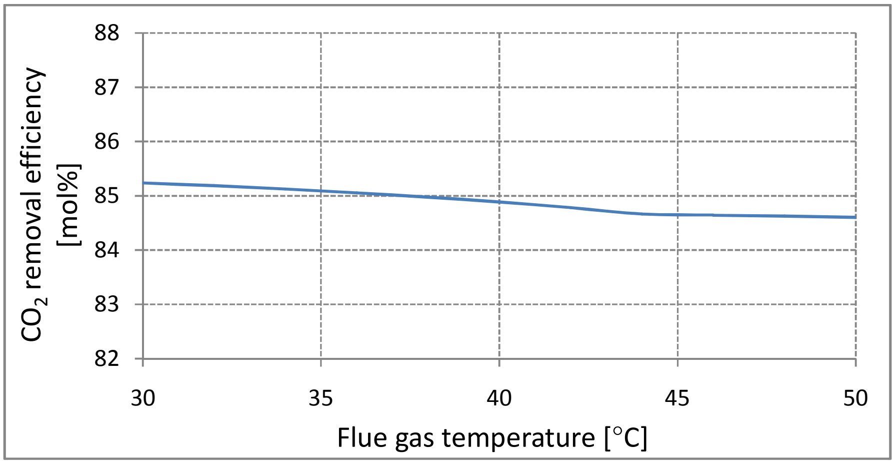

Figure 6: $CO_2$ removal efficiency variation with flue gas temperature

The $CO_2$ removal efficiency variation with solvent temperature is given in Figure 7. Simulations carried at solvent temperature range 26-45°C and maximum efficiency is obtained at the 42°C solvent temperature (Figure 7). As the solvent temperature increases, the driving force for absorption decreases. However, the rate of reaction and diffusivity increase as the solvent temperature is increased. Therefore, efficiency of $CO_2$ removal is increased with the increase of solvent temperature.

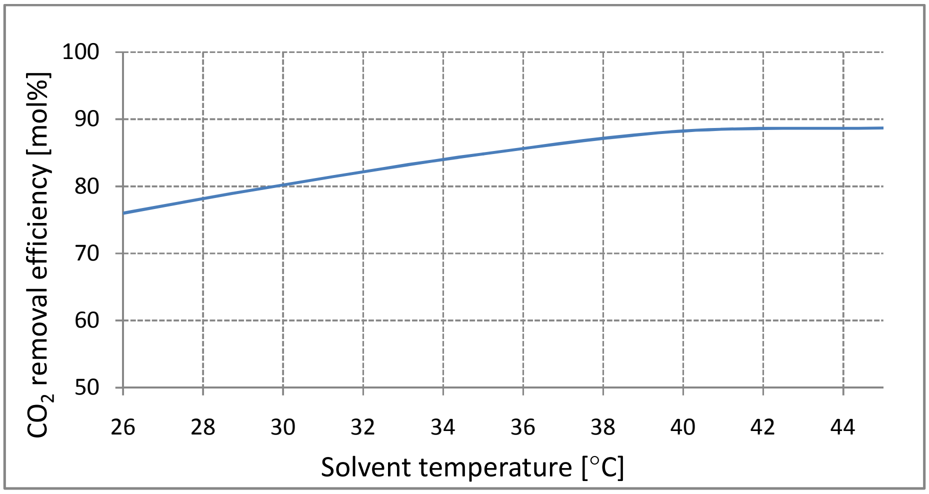

Figure 7: $CO_2$ removal efficiency variation with solvent temperature

Figure 8 presents the $CO_2$ removal efficiency variation with packing height. The packing height varied from 16 to 36m for sensitivity analyses. Similarly, Figure 9 shows how the $CO_2$ removal efficiency varies with packing diameter. Packing diameter is varied from 10 to 22m with constant packing height (22m). With increased packing height and diameter, solution contact area is increased, and also the residence time is increased resulting raised efficiency. Increasing of packing height and diameter, is resulting in higher operating cost. Therefore, packing height and diameter of the absorber has to be selected in accordance with efficiency and cost as well.

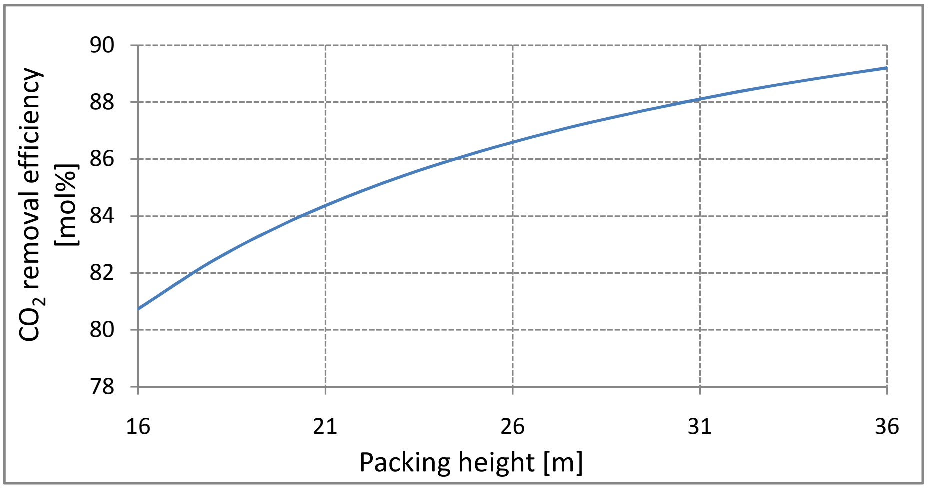

Figure 8: $CO_2$ removal efficiency variation with absorber packing height

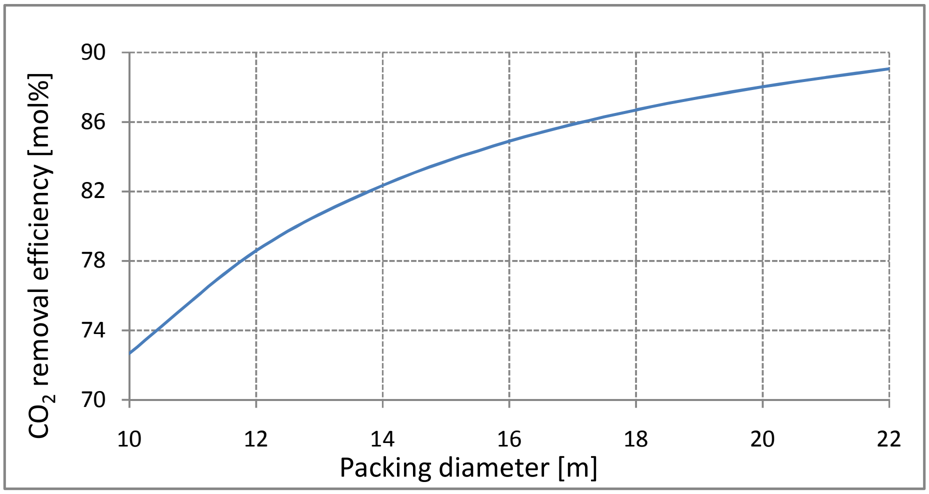

Figure 9: $CO_2$ removal efficiency variation with absorber packing diameter

Figure 10 shows how the $CO_2$ removal efficiency varies with absorber pressure. With the increase of absorber operating pressure, removal efficiency is increased.

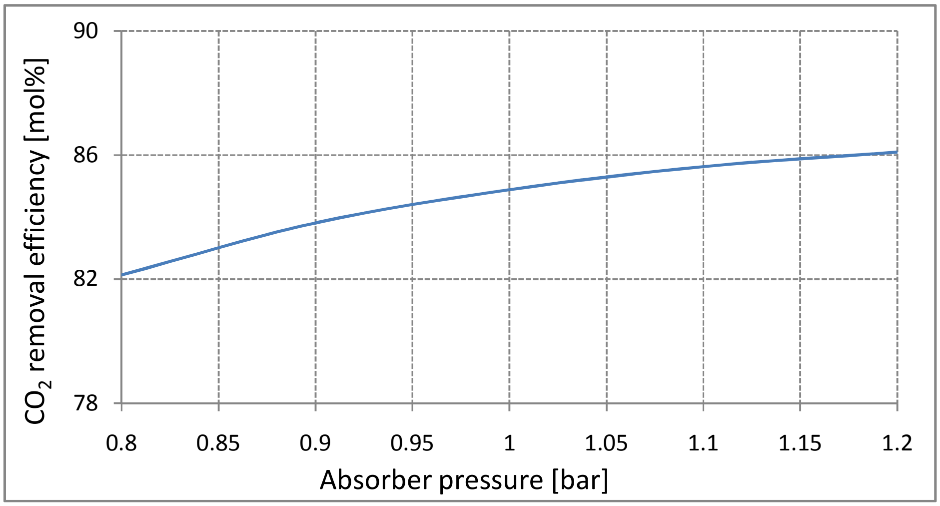

Figure 10: $CO_2$ removal efficiency variation with absorber pressure

## 6. Discussion and conclusion

This paper presents the case study of a 500MW coal power plant $CO_2$ removal process and simulations of parameters' effect on process efficiency. Base case was simulated with defined parameters and achieved 85% removal efficiency. The temperature profiles in liquid and gas phase as well as the $CO_2$ mole fraction were analyzed.

The simulations of the absorption process are presented for sensitivity analyses of important parameters on the removal efficiency: lean loading, solvent concentration, flue gas temperature, solvent temperature, packing height, packing diameter and absorber pressure. The rate based Electrolyte NRTL model was used to implement the model in Aspen Plus. The sensitivity analysis results show that the $CO_2$ removal efficiency increases with the solvent temperature, solvent concentration, packing height, packing diameter and absorber pressure. On the other hand, reduction in efficiency is observed for the parameters, such as flue gas temperature and lean loading.

It can be concluded that above listed parameters are important when implementing the removal process in industrial flue gas purification. Future works have to be carried out to check the interaction effect of multiple variables when changed simultaneously rather than changing single parameter at a time.

## Listed references:

Alie, C. F. (2004). $CO_2$ Capture with MEA: Intergrating the Absorption Process and Steam Cycle of an Existing Coal-Fired Power Plant. Master Thesis, University of Waterloo, Canada

Aspen Technology Inc. Aspen Plus. (2006). Documentation, Aspen Physical Property Methods. Aspen Technology, USA

Freguia, S. (2002). Modeling of $CO_2$ removal from Flue Gas with Mono-ethanolamine. Master Thesis, University of Texas, Austin, USA

Kothandaraman, A. (2010). Carbon dioxide capture by Chemical Absorption: A Solvent Comparison Study. PhD Thesis, Massachusetts Institute of Technology, USA

Michael, A. D. (1989). A model of vapour-liquid equilibria for acid gas-alkanolamine-water systems. PhD Thesis, University of Texas, USA.

Svendsen, J.A., Eimer, D. (2010). Case studies of $CO_2$ capture columns based on fundamental modeling. Energy Procedia 4 (2011), 1419–1426

Paper H

# Multivariate Data Analysis for Identification of Important Parameters on Re-Boiler Duty in a Post-Combustion Chemical Absorption Process

This paper is published in the European Journal of Scientific Research95, No. 2: 289-302, 2013.

European Journal of Scientific Research
ISSN: 1450-216X / 1450-202X Vol. 95 No 2 January, 2013, pp.289-302

http://www.europeanjournalofscientificresearch.com

# Multivariate Data Analysis for Identification of important Parameters on Re-Boiler Duty in a Post Combustion Chemical Absorption Process

**Udara S.P.R. Arachchige**
*Telemark University College, Porsgrunn, Norway*
E-mail: udara.s.p.arachchige@hit.no
Tel: +47-94284116; Fax: 0047-35575001

**Jishnu U. Nair**
*Telemark University College, Porsgrunn, Norway*
E-mail: jishnu.u.nair@gmail.com

**Muhammad Mohsin**
*Telemark University College, Porsgrunn, Norway*
E-mail: mohsin.m.ansari@gmail.com

**Maths Halstensen**
*Telemark University College, Porsgrunn, Norway*
E-mail: Maths.Halstensen@hit.no

**Morten C. Melaaen**
*Telemark University College, Porsgrunn, Norway*
*Tel-Tek, Porsgrunn, Norway*
E-mail: Morten.C.Melaaen@hit.no

## Abstract

The main objective behind this study is to identify the most important parameters on re-boiler heat duty and the corresponding effect on the re-boiler duty. Aspen Plus process simulation software is used to implement the $CO_2$ capture process. The 500MW coal fired power plant flue gas stream data taken from the literature is entered to develop the process model. By varying relevant process parameters, the effect on re-boiler duty were found and tabulated. The data collected from simulation were analyzed using principal component analysis (PCA), and partial least squares regression (PLS-R) models. From the PLS-R analysis solvent flow rate (SF), temperature of the solvent (ST), stripper packing height (SH), stripper pressure (SP), stripper packing diameter (SD) are positively correlated while solvent concentration (SC), lean $CO_2$ loading (LL), flue gas temperature (FT), absorber pressure (AP), absorber packing height (AH) and diameter (AD) are negatively correlated to re-boiler duty (RD). The most important parameters (highest influence parameters on re-boiler duty) are lean $CO_2$ loading, absorber diameter and height. A PLS regression model was validated and the prediction results of re-boiler duty using the developed model show a deviation between predicted and simulated re-boiler duty of ±2.5%.

**Keywords:** Parameter effect, $CO_2$ emissions, Aspen Plus, re-boiler duty, Principal component analysis, Partial Least Squares-regression

# 1. Introduction

The significant reduction of greenhouse gas emissions is recognized as a viable near-term option for environmental pollution. Carbon dioxide ($CO_2$) is considered as one of the major pollutants. There are several $CO_2$ capture technologies available and post combustion chemical absorption is the preferred and widely considerable option. However, carbon capture and sequestration (CCS) is not yet commercially viable due to several challenges. One of the most important challenges is to reduce the energy requirement in the regeneration process. The main energy requirement in the regeneration process can be considered as re-boiler duty in stripper column. The major disadvantage of the post combustion process is the large energy penalty associated with solvent regeneration.

There is several parameters effect on re-boiler duty. The re-boiler duty variation with those parameters, such as solvent flow rate (SF) , solvent concentration (SC), lean $CO_2$ loading (LL), absorber packing height (AH) and diameter (AD), absorber pressure (AP), temperature of the solvent (ST) stream and flue gas (FT), stripper packing height (SH) and diameter (SD) and stripper pressure (SP) are considered for sensitivity analysis. The main objective behind this study is to identify the most important parameters on re-boiler heat duty and the corresponding effect on the re-boiler duty. In present study, both the main effects and interaction effects of parameters on re-boiler duty were investigated.

Aspen Plus process simulation software was used to implement the $CO_2$ capture process. The 500MW coal fired power plant flue gas stream data taken from the literature [1] is entered to develop the process model. By varying several parameters randomly, the effects on re-boiler duty were found and tabulated. The data collected from simulation were analyzed using principal component analysis (PCA), and partial least squares regression (PLS-R) models.

## 1.1. Post Combustion Chemical Absorption Process

A post combustion chemical absorption process consists of several unit operation blocks. Some of them are absorber, stripper, heat exchangers and pumps and make up unit as shown in figure 1. The solvent stream (monoethanolamine-MEA in this study) is entering to the absorber column at the top while flue gas is entering at the bottom.

In the absorber, $CO_2$ is chemically combined with the amine solution. The bottom of the absorber consists of $CO_2$ rich amine and purge gas leaves at the top. In the regeneration column, $CO_2$ is released from the $CO_2$ rich solution using steam. The $CO_2$ lean solution then recycles back to the absorber column after cooled down through the heat exchanger. However, for the simulations, open loop process model is used (without recycling back to the absorber).

**Figure 1:** Process flow diagram

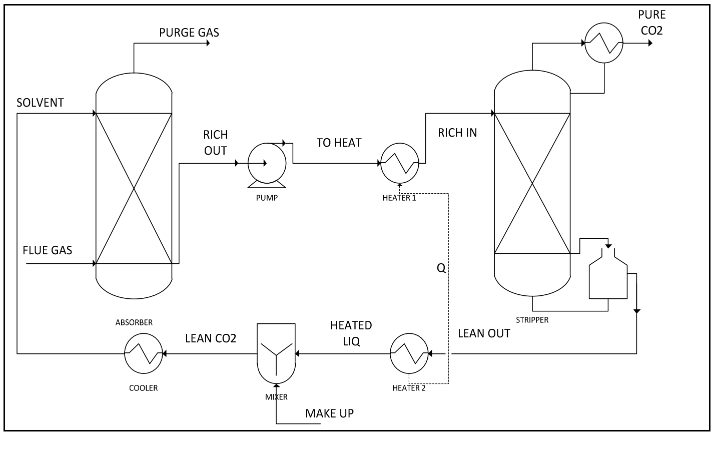

### 1.2. Aspen Plus Model Development

The flue gas data from coal fired power plant is extracted from the literature [1]. Composition of the main components and the inlet operating conditions are given in the table 1. Parameters and information about packing materials which is used in Aspen Plus model development is tabulated in table 2.

**Table 1:** Inlet flue gas stream data

| **Parameter** | |
|---|---|
| Flow rate (tones/ hour)<br>Pressure (bar)<br>Temperature (ºC) | 2424.4<br>1.1<br>40 |
| **Composition** | |
| **Major Component** | **(mol %)** |
| $H_2O$ | 8.18 |
| $N_2$ | 72.86 |
| $CO_2$ | 13.58 |
| $O_2$ | 3.54 |
| $H_2S$ | 0.05 |

**Table 2:** Aspen Plus simulation data used in model development

| |
|---|
| Property method Rate based Electrolyte NRTL |
| Absorber packing type MELLAPAK, Sulzer, Standard, 250 Y |
| Stripper packing type FLEXIPAC, KOCH, METAL,1 Y |

Monoethanolamine (MEA) is used as the solvent for carbon capture model development for base case study. The solvent inlet parameters are given in the table 3.

**Table 3:** Inlet solvent stream data

| **Parameter** | |
|---|---|
| Flow rate (tones/ hour)<br>Pressure (bar)<br>Temperature (ºC) | 9500<br>1.1<br>40 |
| **Composition** | |
| MEA Concentration | 25 W/W% |
| lean $CO_2$ loading | 0.25 (mol $CO_2$/mol MEA) |

The important chemical reactions and kinetic data are taken from the Michel (1989) and Freguia (2002) [2, 3]. Base case model is simulated to check the re-boiler duty with different parameter selections. Every single time, open loop model is used to check the re-boiler duty requirement. Simulation results are tabulated with relevant parameter values. Total of 57 samples are considered for sensitivity analysis. The selected parameters are tabulated in table 4 with corresponding range of applicability.

### 1.3. Multivariate Input Data and Pre Processing

The range of the parameter values are given in the table 4 with the base case values. The parameter values have random variation within the range given in the table and simulations were performed to calculate the re-boiler energy requirement. By varying single or several parameters, re-boiler duty is calculated and tabulated (Appendix 1). Finally, tabulated results are subject to multivariate analysis in order to find the effects of the parameters on re-boiler duty.

**Table 4:** Parameter values used in simulation studies

| No. of parameters | Input parameter | Base case value | Range of the parameter varied |
|---|---|---|---|
| 1 | Inlet solvent flow rate-SF (tones/ hour) | 9500 | 7900-11200 |
| 2 | Solvent temperature-ST (°C) | 40 | 32-45 |
| 3 | Solvent concentration-SC(w/w)% | 25 | 20-39 |
| 4 | Lean $CO_2$ loading-LL (mol $CO_2$/ mol MEA) | 0.25 | 0.18-0.30 |
| 5 | Flue gas temperature-FT (°C) | 40 | 35-43 |
| 6 | Absorber pressure-AP (bar) | 1 | 0.7-1.2 |
| 7 | Height of the packing in Absorber-AH (m) | 20 | 16-28 |
| 8 | Diameter of the packing in Absorber-AD (m) | 15 | 12-22 |
| 9 | Height of the packing in Stripper-SH (m) | 18 | 14-22 |
| 10 | Diameter of the packing in Stripper-SD (m) | 12 | 10-18 |
| 11 | Stripper pressure-SP (bar) | 1.9 | 1.6-2.1 |

The data was centered so that all the parameters have a common origin [4]. Figure 2 shows the matrix plot of the data set which can be used to check the necessity of scaling, where scaling is the method of weighting when parameters have different units and different variance. There is difference in variance for input variables, as can be seen from the matrix plot. The Solvent Flow rate (SF) has high variance than others variables. Therefore, scaling is required for the input data matrix to avoid dominating few variables on all other variables in the model.

**Figure 2:** Matrix plot for data set

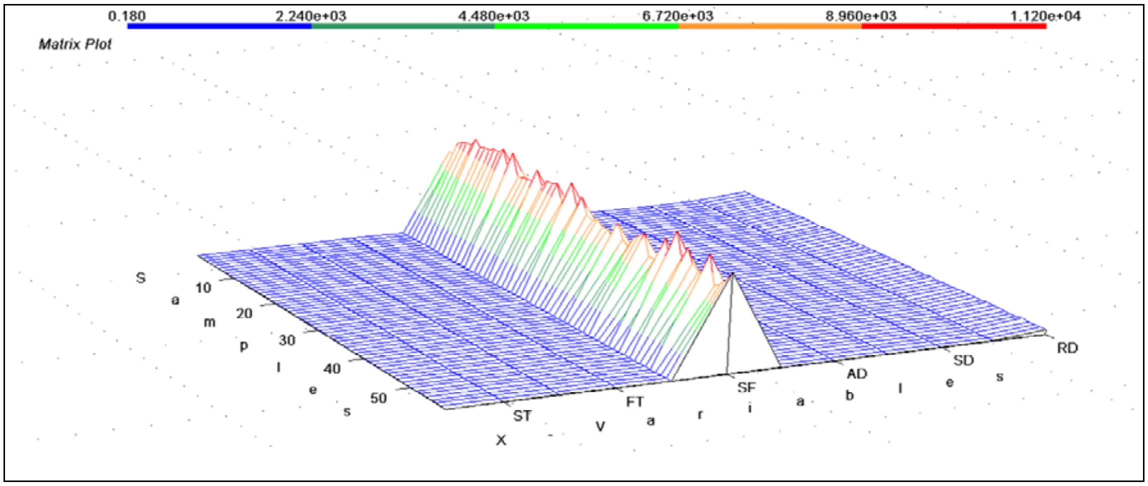

## 2. Principal Component Analysis

This section deals with raw data analysis and PCA. PCA is applied to visualize the covariance structure of the variables which allow identifying the principal directions in which the data varies. PCA is commonly used for transforming multivariate data into another coordinate system (principal component space) with lower dimension by removing non-structured noise. The final PC-space consists of a few orthogonal PCs, each lying along a maximum variance direction in decreasing order. A score plot is a pair of score vectors plotted against each other where score vectors contain the coordinates of the objects in PC-space [4]. The Score plot and loading plot of PC1 and PC2 were used in the analysis since most of the most dominant variation in the data is described by these components.

Figure 3 and 4 show score plots before and after removing the outlier respectively. Samples 4, 16 and 36 were declared as outliers and removed from the analysis.

**Figure 3:** Score plot before removing the outlier

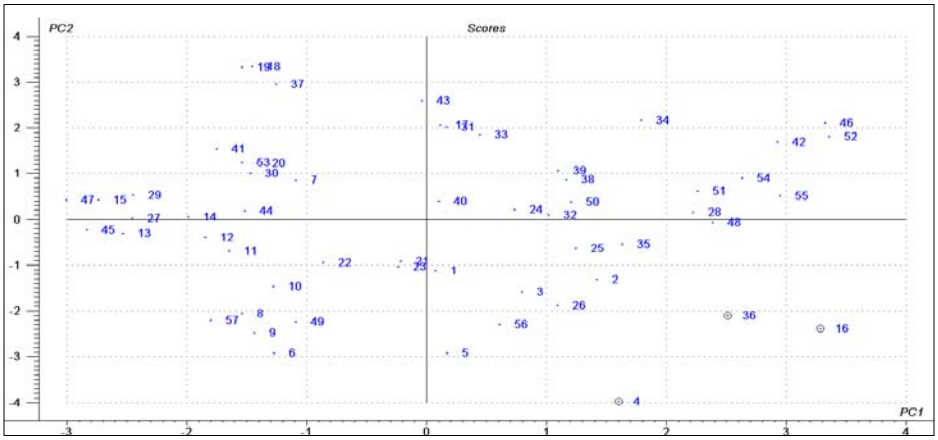

**Figure 4:** Upper left figure shows score plot after removing the outlier; upper right figure shows loading plot; lower figure shows calibration variance

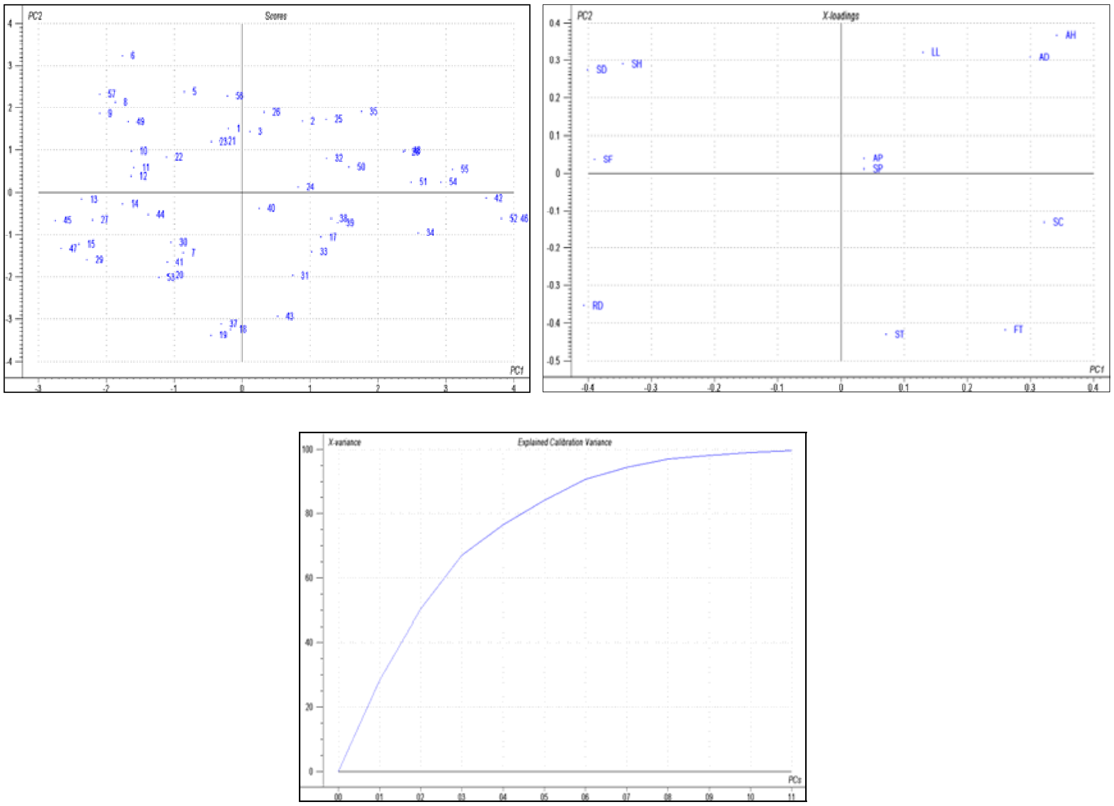

Re-boiler duty (RD) increases when moving along the PC1 (left to right) as can be seen from the score plot in Figure 5. PC1 explains 28% of the total data variance while 21% variance is explained by PC2.

Two loading vectors plotted in a scatter plot is called a loading plot. The loading plot is shown in the figure 4 upper right corner, where it provides the inter-variable relationship or variable similarities. The score and loading plots are representing the corresponding effect on the re-boiler duty. Figure 4 can be used to identify the parameters effect on re-boiler duty. As an example, increasing the values of LL, AD, AH, SC, ST and FT can tend to decrease the RD (lower and upper right corner of both figures). The variables AP and SP seem to have negligible effect on the sample distribution. If we consider about one of the samples tested in the simulation studies, sample number 55 gives one of the lowest re-boiler duties. The parameter values of LL, AD, AH, SC, ST and FT related to that sample are seemed to be very high. The upper left corner of the loading plot shows high values of SH and SD which corresponds to medium and high values of re-boiler duties. Therefore, it is clear that, analysis of score and loading plot can be used to identify the corresponding effect of parameters.

**Figure 5:** Score plot showing sample grouping

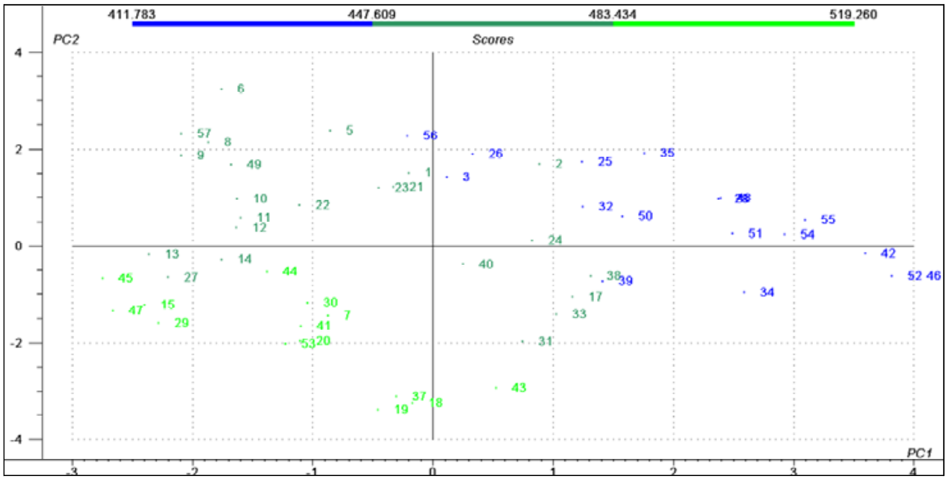

Blue colour is indicating the low re-boiler duty and green colour is shown high re-boiler duty values. After sample grouping as shown in figure 5 it can be seen that samples to the right have the low RD while those on the left side have the highest RD. However, there is no clear boundary between the low, medium and high RD groups. PC2 does not provide any information on how the data is distributed.

## 3. Partial Least Square Regression (PLS-R)

This section involves relating two sets of data X and Y by regression where X matrix contain independent variables and Y matrix consists of dependent variables. PLS is carried out to find a linear relationship between the X (input matrix) and Y (Output matrix/vector) using the equation

$$Y = XB + b_0 \tag{1}$$

Where,
B is the regression coefficients
$b_0$ is the residuals
X is the input matrix
Y is the output vector/matrix

### 3.1. Validation

Validation is a test of the prediction model based on the independent data which have not been used in the calibration stage. Validation is used to determine the correct number of PLS-components in the model [4]. There are different methods of validations available and test set validation is used in this study.

### 3.2. Test Set Validation

Test set validation is a method which has two independent data sets, one is used for calibrating the model and the other is used for testing the model. Test set validation required sufficient number of measurements for both X and Y. The training set is used for the calibration of the model. Then test set is produce from the independent sampling of the target data which will be used for the testing or validation of the model.

### 3.3. Partial Least Squares Regression

Partial Least Square-Regression (PLS-R) uses to combine the features of principal component analysis and multiple regression. X and Y loadings in the same plot shows inter-variable relationships in PLS. In PLS, the components are not principal components but PLS components, however PC components will be used for the simplicity [4].

Figure 6 shows the PLS analysis for all the data where a random selection of test samples for validation was (1, 3-4, 8-14, 19, 25, 28-29, 32, 38, 41, 49, 51, 53, 56) and the rest of the samples were used for calibration of the model. It can be seen from the score plot that PC1 explains 22% of the X-variance and 81% of the Y-variance. The optimal number of PCs to explain the Y-variance is 2 which can be seen from the Residual Validation variance plot. The SH, SD, SF and ST are positively correlated with the RD whereas LL, AH, AD, SC and FT are negatively correlated. The SP and AP have slightly positive and negative correlation respectively as shown in Figure 6.

From the Predicted Y vs. Measured Y plot in the figure 6 shows the regression line of the model and the target line. As shown in lower right corner subplot, data points are equally distributed along the plot. The values for Root Mean Square Error of Prediction (RMSEP), slope and correlation are obtained as 12.69, 0.897 and 0.899 respectively. These values can be improved by removing outliers using the T-U plot, in order to get a better RMSEP, slope and correlation. The ideal value of slope and correlation is one and that of RMSEP is zero. However, those values can be brought closer to these ideal values by removing the outliers.

**Figure 6:** PLS analysis of data set; upper left figure shows score plot; upper right figure shows loading plot; lower left figure shows residual validation variance; lower right figure represents predicted Y

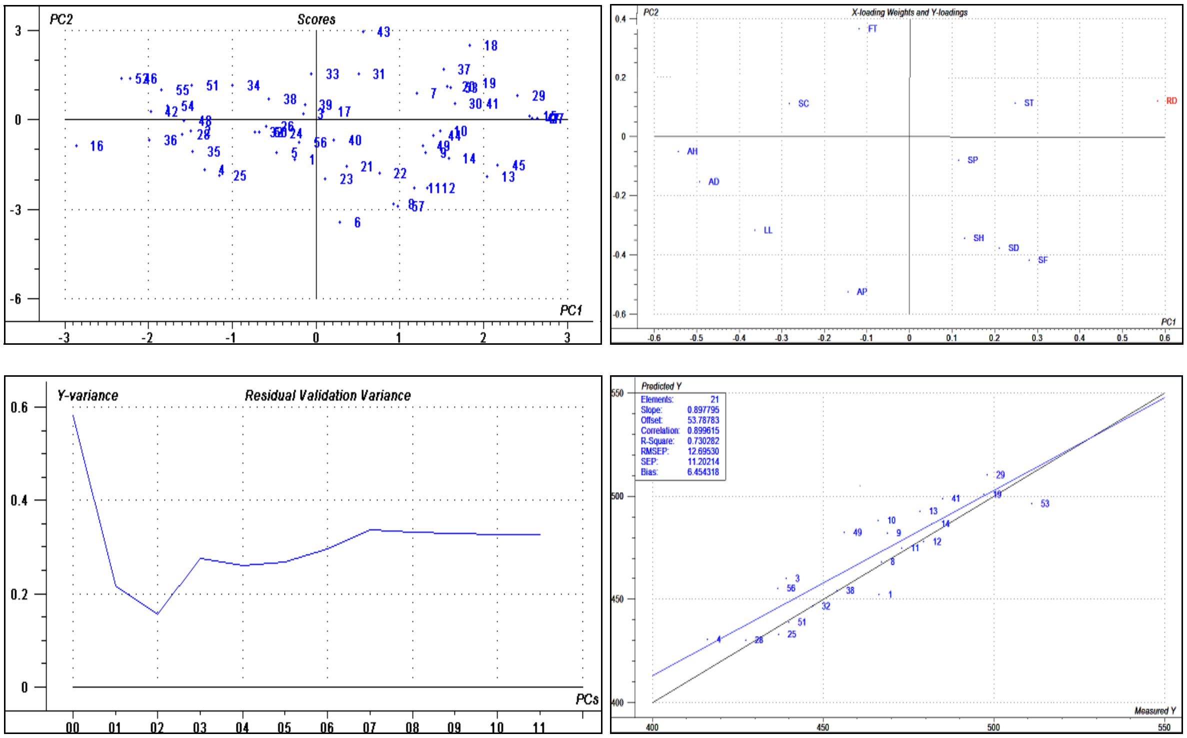

The figure 7 shows the T-U plots. From the T1-U1 plot, sample 2 seems to be outlier and for verification further T-U plots are plotted which clarify that sample 2 is outlier. At the same time we can see from the T1-U1 plot that the relationship between X and Y is linear.

**Figure 7:** T-U plots for PLS components 1-2;left figure indicating T1-U1 plot and right figure showing T2-U2 plot.

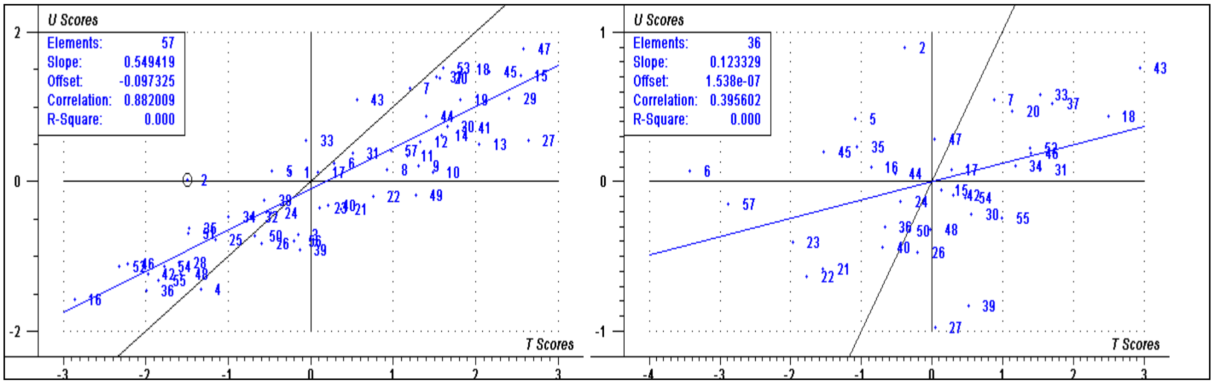

Sample 2 is removed from further analysis. It can be seen in the figure 8 that after removing the outlier the RMSEP, slope and correlation are improved.

**Figure 8:** PLS analysis after removing the outlier; upper left figure shows score plot; upper right figure shows loading plot; lower left figure shows residual validation variance; lower right figure represents predicted Y

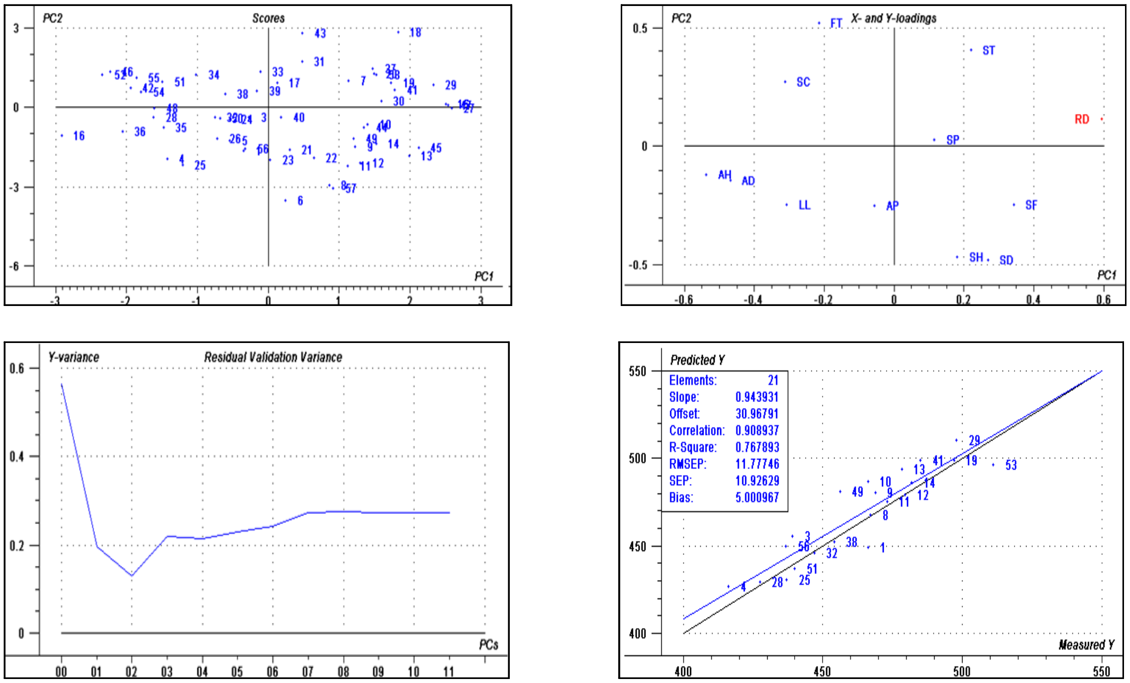

For further improving the model, Y-residual plot of Normal probability is used for detection of outliers which shows that sample number 5 and 39 are outliers as shown in the figure 9. Therefore, by removing those outliers from the analysis, it improved the RMSEP, slope and correlation as can be seen in the figure 10.

**Figure 9:** Normal probability Y-residual plot and T-U Plot

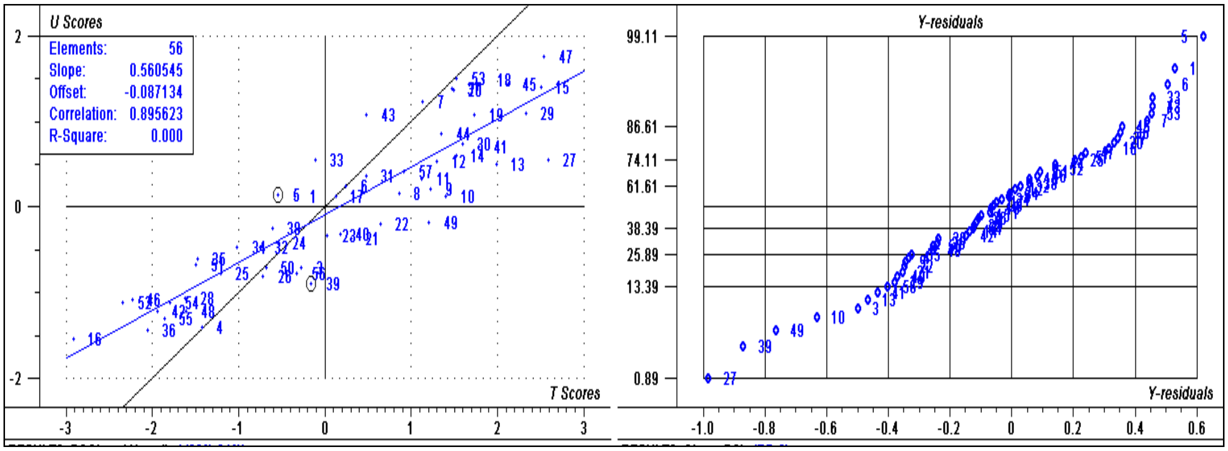

**Figure 10:** PLS model after removing the outliers; upper left figure shows score plot; upper right figure shows loading plot; lower left figure shows residual validation variance; lower right figure represents predicted Y

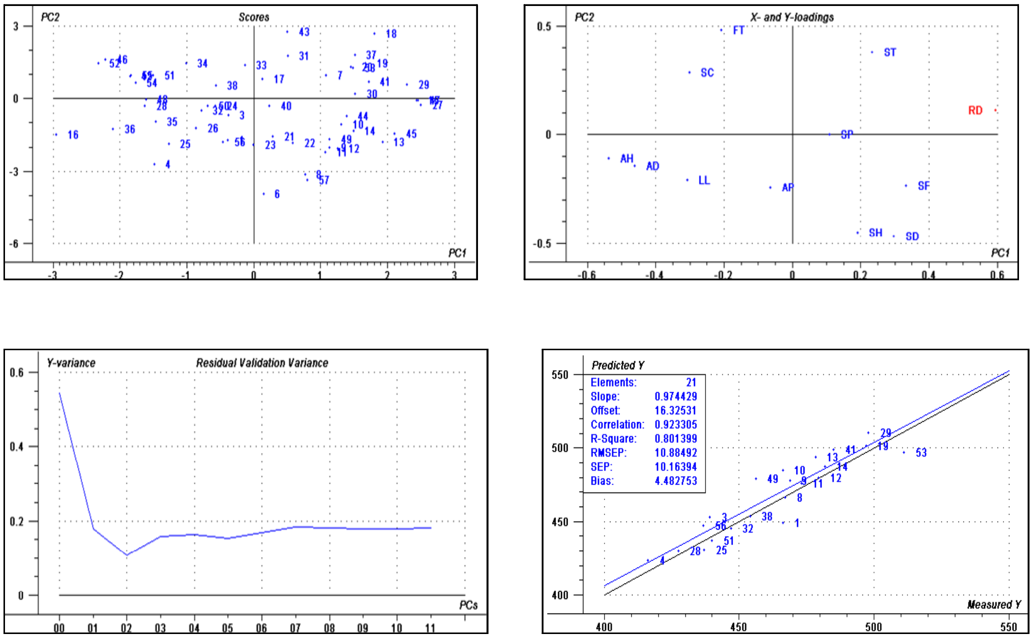

After removing all the outliers the values for Slope, correlation and RMSEP are 0.97, 0.92 and 10.88 respectively. From the Residual Validation variance plot in the above figure, the optimal number of PC is 2.

From the Regression Coefficient plot (figure 11), the AD, AH and LL are the most important X variables for reduction of re-boiler duty. These variables have very high negative correlation with the RD, which means that the increase in absorber diameter and height and lean $CO_2$ loading will result in decrease in re-boiler duty. SF and ST are positively correlated with the RD, which means that re-boiler duty will increase significantly with increase the solvent flow rate and solvent temperature. On the other hand, SC, AP is negatively correlated. The FT, SH, SD and SP have small regression coefficients and cause for negligible impact on the re-boiler duty.

**Figure 11:** Weighted regression coefficients from PLS-R

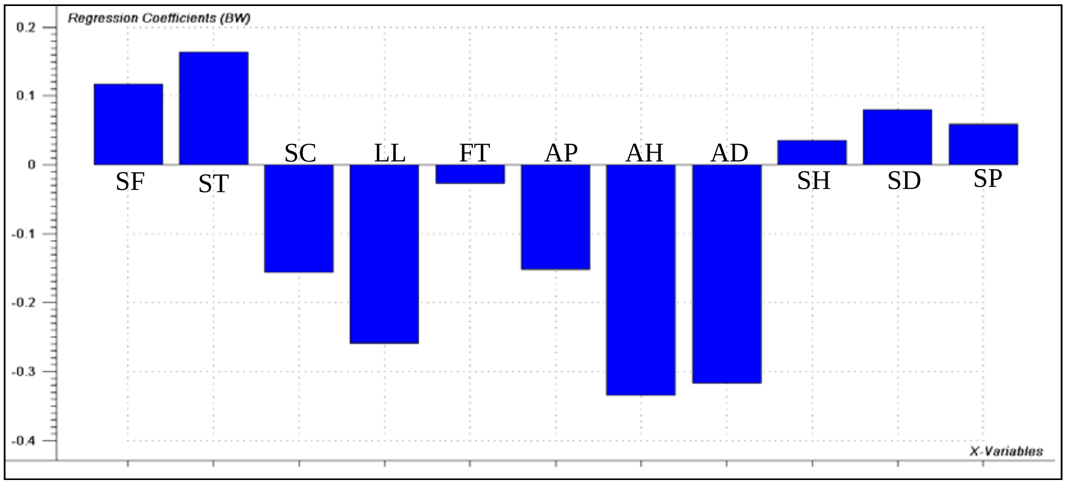

## 3.4. Model Development for Future Prediction

The results from the PLS-R are used to develop the model for re-boiler duty. It can be used to predict the re-boiler duty variation with selected parameters. However, prediction value will not be exactly similar to simulation values and will have slight deviation.

The linear relationship between X (input matrix) and Y (Output matrix/vector) can be defined as:

$$Y = XB + \hat{b}_0$$

Where,
Y is re-boiler duty,
X- Matrix
B- Un-weighted Regression coefficients
$b_0$- Offset

The related B and $b_0$ vectors are calculated from the Unscrambler software and given in the Eq-2.

$$Y = X * \begin{bmatrix} +0.003789 \\ +2.23 \\ -0.909 \\ -263.267 \\ -0.133 \\ -30.556 \\ -4.391 \\ -3.793 \\ +0.644 \\ +1.357 \\ +18.63 \end{bmatrix} + [567.39] \qquad (2)$$

Where, vector X can be replaced with the variable vector, $X^T = \begin{bmatrix} SF \\ ST \\ SC \\ LL \\ FT \\ AP \\ AH \\ AD \\ SH \\ SD \\ SP \end{bmatrix}$

The developed model (eq. 2) can be validated with few examples (few simulation data that have already used in Aspen Plus) that already used for the simulations. As an example, sample number 30, 40 and 50 will be considered. The prediction values of re-boiler duties are calculated as 493, 466, and 448 respectively and simulation values of re-boiler duties are obtained as 486, 452, and 439 respectively. The negligible deviation can be seen from every case and it is around ±2.5% of re-boiler duty. If we consider about new data set which is not performed yet, will be good example to check the behavior of the predicted model. As an example, X vector consider as [9050, 33, 27, 0.26, 40, 1, 23, 17, 18, 11, 1.9] and re-boiler duty can be calculated from the predicted model as 442.8 kJ/kg $CO_2$. The re-boiler duty from Aspen Plus can be calculated for verification. It is given as 453.6 kJ/kg $CO_2$ after the Aspen Plus simulations. The deviation is calculated as 2.4% ((Aspen Plus simulated value - Predicted value)*100%/Simulated value) of the simulated re-boiler duty. Therefore, the predicted re-boiler duty for new set of data is within the acceptable range. Therefore, if parameter values are available for the carbon capture process model, re-boiler duty easily predictable with proposed model. That will be very useful for process industries to understand the behavior of $CO_2$ capture process and required energy for regeneration system. The process simulation tool Aspen Plus is complex, costly and time consuming. With the help of proposed model, effect of parameters on re-boiler energy requirement can be easily calculated without wasting time and money on Aspen Plus.

### 3.5. The Expected Individual Parameters Effect

According to the selected parameters for the study, effect of individual parameters are expected before analyze the multivariate simulation model. According to the previous studies, the re-boiler duty should be decreased with the increase of absorber packing height, packing diameter, absorber pressure, solvent temperature, stripper packing height and diameter, stripper pressure, solvent concentration, lean loading. Re-boiler duty is expected to be increase with the solvent flow rate and flue gas temperature [5, 6]. However, stripper packing height and diameter as well as flue gas temperature should give negligible deviation on re-boiler duty. According to the PLS-R analysis, an expected result for individual parameter’s effect on re-boiler duty has been slightly deviated due to interaction effect of parameters. The effect of stripper packing height and diameter as well as stripper pressure give positive impact on re-boiler duty. However, total impact on re-boiler duty when considering all the selected parameters are agrees with the Aspen Plus simulation results. The re-boiler duty from predicted model and the simulated re-boiler duty value using Aspen Plus is compared to analyze the deviation. As can be seen from figure 12, predicted re-boiler duty values exactly follow the simulated re-boiler values with negligible deviation. Deviation is calculated as ±2.5% for re-boiler duty calculation which is acceptable range. The simulation results are also approximate values and not exactly correct. Therefore, this model can be used for future prediction in carbon capture process. When parameter values changing, then required energy for regeneration process can be easily calculated without doing further simulations in Aspen Plus as it consume more time. This will be valid for coal fired flue gas capturing model with approximately similar flue gas compositions. If the solvent is changed from MEA to another amine, model has to be re-designed or modified. The purpose of the model is not to skip Aspen Plus and use this to calculate re-boiler duty. The main idea of this model is calculate energy requirement in already available carbon capture model when there is parameter changing or modifications in parameters.

**Figure 12:** Simulated vs. Predicted re-boiler duties

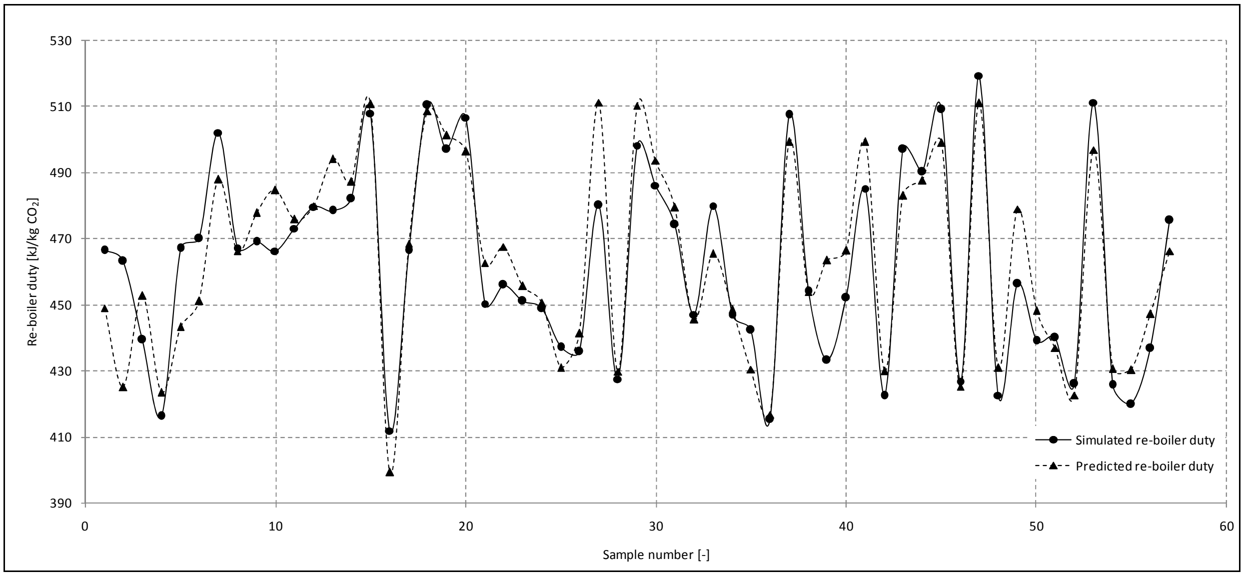

## 4. Conclusion

Experiments were performed in Aspen Plus process simulation tool to obtain the multivariate data by using random design. The selected parameter values were changed randomly within the range as given in the appendix 1 and simulations were performed to calculate the re-boiler energy requirement. From the PLS-R analysis we can see that solvent flow rate (SF), temperature of the solvent (ST), stripper packing height (SH), stripper pressure (SP), stripper packing diameter (SD) are positively correlated while solvent concentration (SC), lean $CO_2$ loading (LL), flue gas temperature (FT), absorber pressure (AP), absorber packing height (AH) and diameter (AD) are negatively correlated to the re-boiler duty (RD). Most important parameters are lean $CO_2$ loading, absorber diameter and height. According to the PLS-R analysis, an expected result for individual parameter’s effect on re-boiler duty (RD) has been slightly deviated due to interaction effect of parameters. The optimal number of PC is two for the model prediction. The relationship between the input data and output response is linear. The slope and the Root Mean Square Error of Prediction (RMSEP) of the final model for PLS is 0.97 and 10.88, respectively. Test Set validation method used in the PLS-R model where 21 samples were randomly selected from the total data set. The proposed model can be nicely used for the future prediction in carbon capture process as it gives maximum ±2.5% deviation. The proposed model (Eq. 2) is only valid for MEA solvent with all mentioned parameters within the range specified in the table 4. The new model has to be re-designed according to the solvent type and new parameter range. The Unscrambler software can be used to understand the behavior of multivariate data process in any kind of applications. The model can be improved with the increase of number of samples which were used in the simulations. By doing that, the error of the predicted model will be reduced.

## References

[1] Alie, C.F, 2004. "$CO_2$ Capture with MEA: Integrating the Absorption Process and Steam Cycle of an Existing Coal-Fired Power Plant", Master Thesis, Master Thesis, University of Waterloo, Canada.

[2] Michael, A.D, 1989. "A model of vapor-liquid equilibria for acid gas-alkanolamine-water systems", PhD Thesis, University of Texas, USA.

[3] Freguia, S, 2002. "Modeling of CO2 removal from Flue Gas with Mono-ethanolamine", Master Thesis, University of Texas, USA.

[4] Esbensen, K.H, 2001. Multivariate Data Analysis – in practice. 5.th Ed. (Oct. 2001), CAMO AS Publ. ISBN 82-993330-2-4.

[5] Arachchige, U.S.P.R., Muhammad, M., Melaaen, M.C, 2012. "Optimization of post combustion carbon capture process-solvent selection", International Journal of Energy and Environment, Vol. 3, Issue 6, pp. 861-870.

[6] Arachchige, U.S.P.R., Muhammad, M., Melaaen, M.C, 2012. "Optimized $CO_2$-flue gas separation model for a coal fired power plant", International Journal of Energy and Environment, Vol. 4, Issue 1, pp. 39-48.

# Appendix 1

**Table 5:** Parameter values with calculated re-boiler duty

| | SF | ST | SC | LL | FT | AP | AH | AD | SH | SD | SP | RD |
|---|---|---|---|---|---|---|---|---|---|---|---|---|
| 1 | 7900 | 36 | 28 | 0.3 | 38 | 1 | 22 | 16 | 20 | 15 | 1.9 | 466.34 |
| 2 | 7900 | 34 | 30 | 0.29 | 36 | 0.9 | 24 | 17 | 18 | 12 | 1.6 | 462.97 |
| 3 | 9200 | 33 | 35 | 0.28 | 38 | 0.7 | 23 | 14 | 19 | 14 | 1.7 | 439.18 |
| 4 | 9500 | 33 | 35 | 0.28 | 38 | 0.7 | 26 | 20 | 22 | 18 | 1.6 | 416.16 |
| 5 | 9700 | 35 | 36 | 0.25 | 38 | 0.7 | 26 | 18 | 22 | 18 | 1.6 | 466.89 |
| 6 | 9700 | 37 | 20 | 0.24 | 35 | 1.1 | 26 | 20 | 22 | 18 | 1.9 | 469.8 |
| 7 | 10500 | 41 | 36 | 0.28 | 41 | 0.7 | 22 | 12 | 20 | 12 | 1.9 | 502 |
| 8 | 9900 | 37 | 23 | 0.26 | 36 | 1.1 | 23 | 17 | 21 | 17 | 1.9 | 467.12 |
| 9 | 10100 | 38 | 23 | 0.26 | 36 | 0.7 | 23 | 17 | 21 | 17 | 1.7 | 468.86 |
| 10 | 10100 | 38 | 27 | 0.25 | 37 | 0.7 | 22 | 16 | 20 | 16 | 1.8 | 466.14 |
| 11 | 10400 | 40 | 29 | 0.24 | 37 | 1.2 | 22 | 16 | 20 | 16 | 1.8 | 473.01 |
| 12 | 10400 | 41 | 29 | 0.24 | 37 | 1.2 | 22 | 16 | 20 | 16 | 1.9 | 479.45 |
| 13 | 10900 | 41 | 23 | 0.23 | 39 | 1.2 | 21 | 15 | 20 | 16 | 1.7 | 478.28 |
| 14 | 9100 | 41 | 23 | 0.23 | 39 | 1.2 | 21 | 15 | 20 | 16 | 1.7 | 481.83 |
| 15 | 10900 | 43 | 26 | 0.22 | 38 | 0.8 | 21 | 15 | 19 | 15 | 1.8 | 507.79 |
| 16 | 8900 | 35 | 35 | 0.28 | 40 | 0.8 | 28 | 22 | 20 | 14 | 1.6 | 411.7829 |
| 17 | 9000 | 45 | 27 | 0.18 | 43 | 1.1 | 26 | 20 | 18 | 14 | 2 | 466.3928 |
| 18 | 9200 | 45 | 27 | 0.18 | 43 | 0.8 | 22 | 16 | 16 | 13 | 2 | 510.2663 |
| 19 | 9000 | 39 | 32 | 0.22 | 40 | 1.2 | 16 | 12 | 14 | 11 | 1.8 | 496.98 |
| 20 | 10450 | 41 | 36 | 0.28 | 42 | 0.7 | 20 | 12 | 20 | 12 | 1.9 | 506.5606 |
| 21 | 9150 | 40 | 28 | 0.3 | 38 | 1 | 22 | 16 | 20 | 15 | 1.9 | 450.18 |
| 22 | 9850 | 36 | 28 | 0.3 | 40 | 1.1 | 20 | 14 | 20 | 15 | 1.8 | 455.89 |
| 23 | 9850 | 38 | 28 | 0.3 | 40 | 1.1 | 22 | 16 | 20 | 15 | 1.8 | 451 |
| 24 | 10100 | 40 | 28 | 0.29 | 42 | 1 | 24 | 16 | 18 | 12 | 1.7 | 448.73 |
| 25 | 8600 | 37 | 30 | 0.29 | 36 | 1.2 | 24 | 17 | 18 | 12 | 1.9 | 436.99 |
| 26 | 9000 | 32 | 32 | 0.29 | 35 | 0.8 | 23 | 14 | 19 | 11 | 1.6 | 435.77 |
| 27 | 10900 | 42 | 23 | 0.22 | 38 | 0.8 | 21 | 15 | 19 | 15 | 1.8 | 480 |
| 28 | 8900 | 40 | 35 | 0.28 | 40 | 1 | 26 | 18 | 18 | 12 | 1.9 | 427.3781 |
| 29 | 10000 | 42 | 23 | 0.23 | 43 | 0.8 | 20 | 14 | 21 | 15 | 1.6 | 498 |
| 30 | 8500 | 39 | 31 | 0.2 | 37 | 1 | 20 | 14 | 18 | 14 | 1.8 | 486 |
| 31 | 8150 | 43 | 39 | 0.23 | 42 | 0.9 | 21 | 15 | 19 | 13 | 1.8 | 474.06 |
| 32 | 8600 | 40 | 28 | 0.25 | 40 | 1 | 26 | 18 | 18 | 14 | 1.9 | 446.9751 |
| 33 | 8000 | 40 | 28 | 0.25 | 42 | 0.9 | 22 | 16 | 16 | 12 | 1.8 | 479.8246 |
| 34 | 8150 | 42 | 30 | 0.25 | 42 | 1 | 24 | 18 | 16 | 10 | 1.9 | 446.9128 |
| 35 | 7400 | 40 | 30 | 0.25 | 40 | 1 | 26 | 22 | 22 | 14 | 2.1 | 442.1284 |
| 36 | 9200 | 35 | 35 | 0.28 | 40 | 0.8 | 26 | 20 | 20 | 14 | 1.6 | 415.2422 |
| 37 | 7900 | 45 | 28 | 0.24 | 40 | 1 | 18 | 14 | 16 | 12 | 1.7 | 507.3331 |
| 38 | 7400 | 41 | 38 | 0.25 | 40 | 1 | 22 | 16 | 18 | 14 | 1.6 | 454 |
| 39 | 8500 | 43 | 38 | 0.25 | 41 | 1 | 22 | 16 | 19 | 13 | 1.7 | 433 |
| 40 | 9000 | 43 | 38 | 0.25 | 41 | 1.1 | 22 | 16 | 21 | 15 | 1.7 | 452 |

**Table 5:** Parameter values with calculated re-boiler duty - continued

| | | | | | | | | | | | | |
|---|---|---|---|---|---|---|---|---|---|---|---|---|
| 41 | 9500 | 40 | 23 | 0.23 | 43 | 1 | 20 | 14 | 19 | 13 | 1.9 | 485 |
| 42 | 7500 | 45 | 38 | 0.25 | 42 | 1.1 | 26 | 20 | 18 | 12 | 1.9 | 422.4 |
| 43 | 7500 | 41 | 33 | 0.23 | 45 | 0.8 | 20 | 14 | 18 | 12 | 1.6 | 497 |
| 44 | 7000 | 43 | 33 | 0.23 | 36 | 1.1 | 20 | 14 | 22 | 16 | 1.7 | 490 |
| 45 | 10000 | 43 | 33 | 0.23 | 36 | 1.1 | 20 | 14 | 22 | 16 | 1.7 | 509 |
| 46 | 7900 | 41 | 36 | 0.26 | 42 | 1 | 26 | 18 | 14 | 10 | 1.8 | 426.7189 |
| 47 | 11200 | 43 | 26 | 0.22 | 38 | 0.8 | 21 | 15 | 20 | 14 | 1.8 | 519.26 |
| 48 | 8900 | 40 | 35 | 0.28 | 40 | 0.9 | 26 | 18 | 18 | 12 | 1.8 | 422.4676 |
| 49 | 10100 | 39 | 27 | 0.25 | 36 | 0.7 | 23 | 17 | 21 | 17 | 1.7 | 456.11 |
| 50 | 8900 | 42 | 30 | 0.25 | 38 | 1 | 24 | 20 | 18 | 12 | 1.9 | 439.0266 |
| 51 | 8400 | 42 | 30 | 0.25 | 40 | 0.8 | 26 | 20 | 18 | 10 | 1.7 | 439.8983 |
| 52 | 8200 | 41 | 36 | 0.26 | 42 | 1 | 26 | 18 | 14 | 10 | 1.6 | 425.9172 |
| 53 | 10600 | 41 | 36 | 0.28 | 42 | 0.7 | 20 | 12 | 20 | 12 | 1.9 | 511.1188 |
| 54 | 7900 | 41 | 36 | 0.26 | 42 | 1 | 26 | 18 | 18 | 12 | 1.8 | 425.5189 |
| 55 | 8250 | 41 | 36 | 0.26 | 42 | 0.8 | 26 | 20 | 18 | 12 | 1.8 | 419.7019 |
| 56 | 9000 | 32 | 32 | 0.29 | 35 | 0.8 | 23 | 14 | 19 | 14 | 1.7 | 436.73 |
| 57 | 9900 | 37 | 20 | 0.24 | 35 | 1.1 | 24 | 18 | 21 | 17 | 1.9 | 475.36 |

## Paper I

# Multivariate data analysis for parameters effect on CO2 removal efficiency

This paper was presented in 11th International Conference on Greenhouse Gas Technologies (GHGT 11) at Kyoto, Japan on November 2012. The paper was also published in Energy Procedia 37 (doi: 10.1016/j.egypro.2013.06.081, Elsevier Ltd., pp 2011–2020, 2013). Edited by: Tim Dixon and Kenji Yamaji.

Available online at www.sciencedirect.com

SciVerse ScienceDirect

Energy Procedia 37 (2013) 2011 – 2020

Energy Procedia

GHGT-11

# Multivariate data analysis for parameters effect on $CO_2$ removal efficiency

Udara Sampath P.R.Arachchige[a,*], Neelakantha Aryal[a], Pramod Ghimire[a], Maths Halstensen[a], Morten Christian Melaaen[a,b]

[a]*Telemark University College, Porsgrunn, 3901, Norway*
[b]*Tel-Tek, Porsgrunn, 3901, Norway*

## Abstract

In this paper, both the main effects and interaction effects of parameters on $CO_2$ removal efficiency were investigated. Flue gas stream data from a 500MW coal power plant has been used for the model development. The complete removal process is implemented in Aspen Plus with selected operating conditions and parameters using Monoethanolamine as solvent. The base case model is developed in Aspen Plus with specific parameter values to achieve 85% removal efficiency. The $CO_2$ removal efficiency variation with different parameters; such as number of stages, inlet solvent flow rate, lean loading, temperature of the flue gas and solvent stream, absorber packing height and diameter and absorber pressure are considered as the most important parameters for sensitivity analyses. The data collected from simulations were analysed using Principal Component Analysis, Principal Component Regression and Partial Least Square-regression. The correlation between variables were studied, which indicate that inlet solvent flow rate, absorber packing height and diameter, absorber pressure and temperature of the solvent stream are positively correlated with $CO_2$ removal efficiency whereas the lean loading and temperature of flue gas are negatively correlated with efficiency.

*Keywords*: Power generation; $CO_2$ emissions; Aspen Plus; Removal efficiency; Principal component analysis; Partial Least Square-regression

## 1. Introduction

Global warming and climate change effect, believed to be caused by the increased green house effect, has gained increasing attention in the last few years. Carbon released from large scale fossil fuel combustion

---

* Corresponding author. Tel.: +47-9428-41-16; fax: +47-355-75-001.
E-mail address: udara.s.p.arachchige@hit.no.

1876-6102
doi:10.1016/j.egypro.2013.06.081

is defined as the major emitting source today. Research studies on reducing green house gas emissions using $CO_2$ capture and sequestration has been implemented in recent years. The post combustion $CO_2$ capture via chemical absorption is still considered as a promising technology to achieve this goal. In order to make this process more economical, it is important to minimize the energy used in the regeneration section (re-boiler duty). The overall objective of this research study is to develop and implement a $CO_2$ removal model to find the most important parameters, and the corresponding effect on the removal efficiency.

The single parameter effect on removal efficiency has previously been studied [1]. Both the main effects (the effect of each individual parameter) and the interaction effects (interaction between two or several parameters) are discussed [2]. The objective in this study is to compare single parameter effects and multiple parameters effects on the $CO_2$ removal efficiency. The basic information related to the implemented model is described in the next section (Section 2).

The $CO_2$ removal base case model is developed for 500MW coal fired power plant flue gas. There is several parameters effect on $CO_2$ removal efficiency. The sensitivity analyses are performed to check the $CO_2$ removal efficiency variation with different parameters such as number of stages, inlet solvent flow rate, lean loading, temperature of the flue gas and solvent stream, absorber packing height and diameter and absorber pressure. By changing those parameters, $CO_2$ removal efficiency is calculated in Aspen Plus model. A total of 80 simulations are performed with different set of parameter values.

The data collected from simulation are analysed using Principal Component Analysis (PCA), Principal Component Regression (PCR) and Partial Least Square-regression (PLS-R). PCA can be defined as an orthogonal linear transformation that transforms the data to a new coordinate system. The transformation is defined according to the variance by any projection of the data and greatest variance is called first principal component, the second greatest variance is called the second coordinate, and so on [3]. PCR is considered as a powerful method for analysis of collinear data, which include both PCA and Multiple Linear Regression (MLR) [2].

## 2. Model Development

The flue gas stream data for 500 MW coal power plant is taken from Alie (2004), and implemented for removal process [4]. The composition of the flue gas is given in Table 1.

Table 1. Flue gas composition and parameters at inlet [ 4]

| Parameter | Coal Fired |
|---|---|
| Flow rate [tones/hr] | 2424 |
| Temperature [°C] | 40 |
| Pressure [bar] | 1.1 |
| Major Component | Mol% |
| $H_2O$ | 8.18 |
| $N_2$ | 72.86 |
| $CO_2$ | 13.58 |
| $O_2$ | 3.54 |
| $H_2S$ | 0.05 |

The base case model is developed in Aspen Plus with specific parameter values to achieve 85% removal efficiency. Fig. 1 represents the flow diagram of the $CO_2$ removal process.

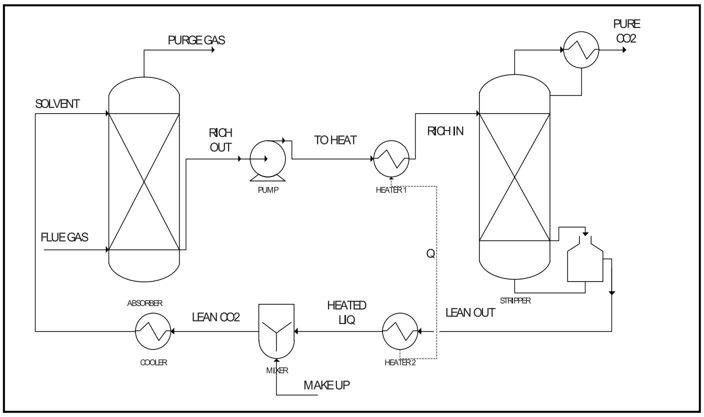

Fig. 1. Process Flow Diagram

The flue gas stream and solvent stream supply to the bottom and top of the column, respectively. Monoethanolamine (MEA) is used as the solvent for $CO_2$ capture. Chemical reactions take place in the packing material in the absorber column. A small portion of non-reacted $CO_2$ and other components leave from purge stream (PURGE-GA) deciding on overall capture efficiency. Rich out (RICH-OUT) is $CO_2$ abundant stream which is sent to other column for further processing. The main chemical reactions take place during the $CO_2$ removal process with MEA solvent [5].

The thermodynamic and kinetic data are selected according to the literature [6]. An open cycle complete removal process model is used and implemented to check the parameters' effect on $CO_2$ removal efficiency. The parameter values and operating range are tabulated in Table 2. A total of 80 samples were taken into consideration for parameter analyses.

The efficiency of the removal process is calculated using Equation 1.

$$\text{Efficiency} = \frac{\text{Total CO}_2\text{ inflow} - \text{Purge gas CO}_2\text{ outflow}}{\text{Total CO}_2\text{ inflow}} * 100\% \qquad (1)$$

The interaction effects on the removal efficiency were found by varying several parameters according to a full factorial design scheme [2]. The data collected from simulation were analysed using PCA, PCR and PLS-R. The PCR and PLS models were validated using a so-called test set of independent data. A total of 80 samples were taken from the simulation out of which 30 were only used for validation of the PCR and PLS-R models. For the principal component analysis all 80 data samples were used. The commercial software The unscrambler were used for multivariate data analysis [7].

Table 1. Input parameter values in absorber column

| Input parameter | Parameter condition (Fixed/Varied) | Base case value | Range of the parameter varied |
|---|---|---|---|
| Inlet flue gas (tones/ hour) | Fixed | 2424.4 | - |
| $CO_2$ content (mol %) | Fixed | 13.58 | - |
| Flue gas pressure (bar) | Fixed | 1.1 | - |
| Flue gas temperature-FT (ºC) | Varied | 40 | 20-48 |
| Packing material | Fixed | PALL type metal | - |
| Height of the packing-PH (m) | Varied | 22 | 9-28 |
| Diameter of the packing-PD (m) | Varied | 16 | 8-20 |
| Number of stages-NS | Varied | 15 | 10-25 |
| Inlet solvent flow rate-MF (tones/ hour) | Varied | 7000 | 6000-16000 |
| Solvent temperature-MT (ºC) | Varied | 40 | 20-48 |
| Solvent pressure (bar) | Fixed | 1 | - |
| Absorber pressure-AP (bar) | Varied | 1 | 0.7-1.1 |
| Solvent lean loading-LL %(mol $CO_2$/ mol MEA) | Varied | 25 | 18-35 |
| Solvent concentration (w/w)% | Fixed | 25 | - |

After the calibration stage, the model must be validated based on independent data. Validation is needed in order to determine the model complexity in terms of number of principal components and also to get an estimate of the prediction performance of the multivariate model [2]. There are several validation techniques available such as cross validation, leverage correction validation and test set validation [2]. However, the test set validation method is used in this study.

## 3. Sensitivity Analysis

The temperature profiles in liquid and gas phase in the absorber column and the $CO_2$ loading profiles are analyzed for the base case model. The temperature bulge was seen at the top of the absorber. The magnitude of the temperature bulge is reached to 353K. Along the absorber, $CO_2$ loading is increasing and the maximum value reached 0.47 [mol $CO_2$/mol MEA] at the bottom. This section is devided into four different sub sections following matrix plot and scaling, PCA, PCR and PLS-R. It describes data pre-processing and explorative data analysis using PCA.

### *4.1 Matrix Plot*

The histogram plot of the simulation data and the matrix plot can be used to check the necessity of scaling. Scaling is the method of weighting when parameters have different units and different variance. In order to ensure that all the data set roundly of same variance, pre-processing of the data before analysis is done. If any data set has higher variance, then the analysis might only explain the variation in the variable with higher magnitude. The important tool to decide whether the data set need scaling or not is called matrix plot (Fig. 2). According to the Fig. 2 the highest variance is given by MF (solvent flow rate). From the matrix plot, Fig. 2, it is clear that the data set has to be scaled and centred because of the variance of solvent flow rate is very high in comparison to the variance of other variables. Thus for making the loading plot to explain the variance of all the variables, the data set has to be scaled else the loading plot will explain mostly the variance in the solvent flow rate only.

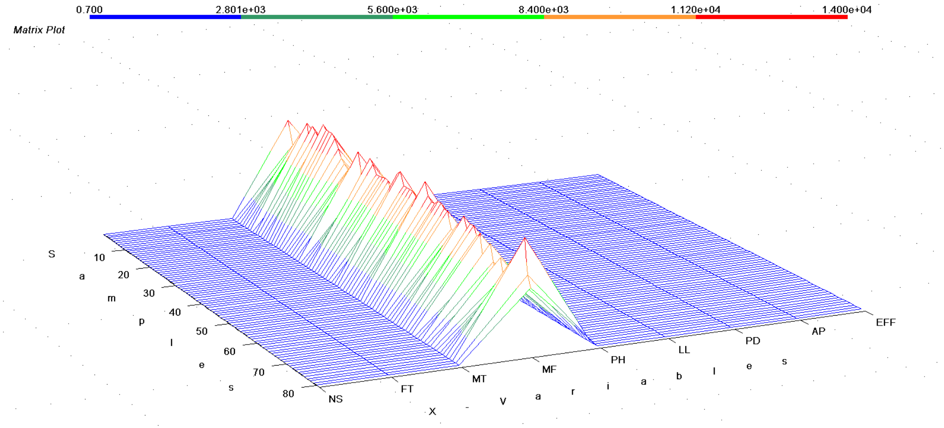

Fig. 2. Matrix plot of all the data samples and variables

### 4.2 Principal Component Analysis (PCA)

PCA is carried out to find the explorative model in order to observe the inter-dependability among the variables. The score plot is simply a relevant pair of score vectors plotted against each other. Score vectors are the coordinates of the objects projected down to the principal components.

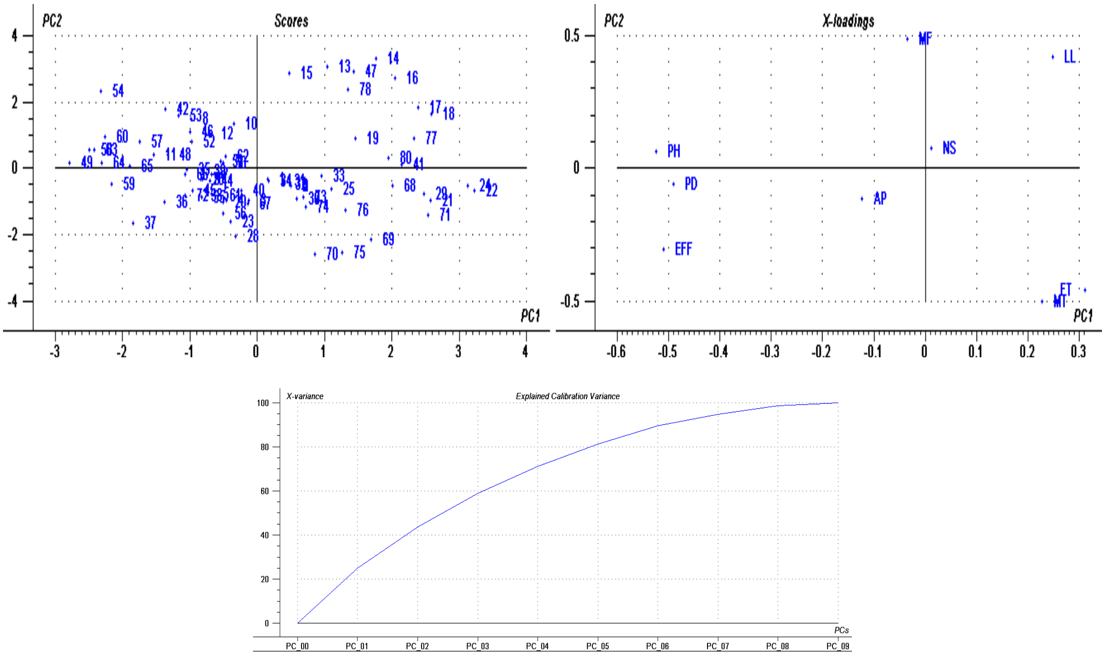

Fig. 3. Scores, Loading and Calibration Variance plot from PCA analysis without outliers: upper left figure shows score plot; upper right figure shows loading plot; bottom figure represents the calibration variance

Fig. 3 shows the scores and loading plot for PCA after deleting the outliers 43, 79 and 27. Outliers are selected which is given unexpected characteristics than rest of the data set. Score plot shows the location of the samples along each model component, and can be used to detect the sample pattern and understand the similarities of data. The samples along the Principal Components (PCs) PC1 and PC2 are considered because the PC1 and PC2 explain most of the structure and information in the raw data. PC1 explains 25% of the total data variance while 19% is explained by PC2. Sample number 22 has highest score along PC1 direction whereas sample 14 scored most in PC2 direction.

Analysing loading plot of Fig. 3, MEA Temperature (MT) and Fluegas Temperature (FT) and Lean loading (LL) are negatively correlated to the $CO_2$ removal efficiency variable. Packing height (PH), packing diameter (PD) and MEA flowrate (MF) are other variables which are positively correlated with the output variable i.e. efficiency (EFF). From explained calibration variance plot, it can be seen that 6 PCs are required to explain almost 90% variance in X variables and 8 PCs are required to explain 100% variance in X.

### *4.3 Principal Component Regression (PCR)*

Multivariate calibration is also called multivariate modeling (X, Y). The Y vector contains the dependent variable whilst the X matrix is a set of independent variables. The multivariate model for (X, Y) is simply a regression relationship between X and Y established through multivariate calibration [2]. The model is used in the next stage for predicting new Y values. The matrix X and the corresponding Y are collectively known as calibration or training set. The training set is thus important to represent the future population. Mostly, two types of the calibration methods are used, namely PCR and PLS-R. After the model calibration, the model should be validated with the next data set of the same experimental setup, simulation data in this case. There are numerous mathematical validation techniques available like cross validation, leverage correction validation, test set validation, and however, the further analysis just focuses on test set validation. Test set validation is the only reliable one for validation.

The residual validation variance and predicted Y values are shown in Fig. 4. Test set validation method is used to validate the predicted model. The test set data (30 samples) are randomly selected. The slope of the predicted line is 0.60, the offset is 1.63 and the RMSEP (Root mean square error of prediction) is 8.64%. It is apparent from Fig. 4 that some included samples are extremed than the normal clustered values. So, the marked samples i.e. sample 27, 66, 72 and 78 have high score value regardless of others indicating that they don't match the whole clustered data, and are deleted considering outlier. After removing the outliers, the PCR is again performed. The score and loading along with the residual validation variance plot and the prediction plot are included in the Fig. 5.

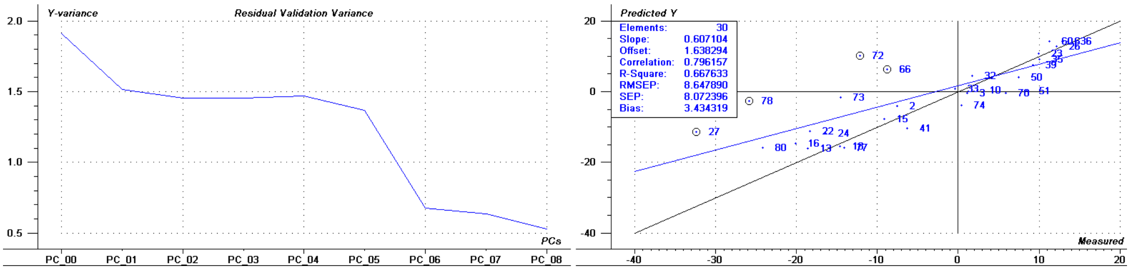

Fig. 4. PCR analysis of complete data set with efficiency as Y variable before removing the outliers; left side figure shows residual validation variance; right figure shows predicted Y.

From the residual validation variance plot, it can be seen that 6 PCs are required to explain the Y variance. Further, the slope of the predicted line is 0.79, the offset is 0.36 and the RMSEP (Root mean square error of prediction) is 4.57. This shows that there is improvement in these parameter analysis than before i.e with outliers. Again the X-Y loading plots can be seen in the Fig. 5 which shows that the MT, FT and LL are negatively correlated with the efficiency where as rest of the X variables are positively correlated to the efficiency. After all the refinements, the RMSEP is improved from 8.64% to 4.57%. Likewise significant improvement has been noticed in the slope of predicted line from 0.60 to 0.79 which can be seen from Fig. 4 and 5.

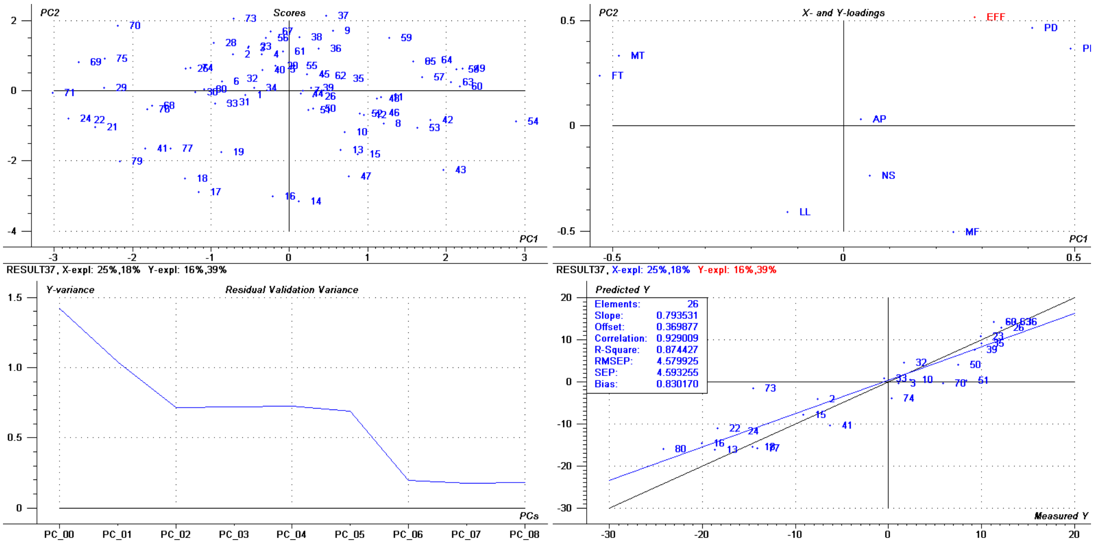

Fig. 5. PCR plots after removing all the outliers; upper left figure shows score plot; upper right figure shows loading plot; lower left figure shows residual validation variance; lower right figure represents predicted Y.

## *4.4 Partial Least Square-regression (PLS-R)*

PLS-R uses the y-data structure, the y-variance, directly as a guiding hand in decomposing the X-matrix so that the outcome constitutes an optimal regression, precisely in the strict prediction validation sense [2]. In PLS, the components are not the principal components but the PLS components, however PC will be used for the simplicity [2]. The random test set taken for this PLS analysis are listed as: 2-3, 10, 13, 15-16, 18, 22-24, 26, 32-33, 35-36, 39,41, 50-51, 60, 63, 70, 73-74, 77, 80. Apart from these samples, other samples are used for calibration of model. Fig. 6 shows the PLS-R analysis for all the data sets before removing any outlier.

The PC1 explains 18% of X-variance whereas 70% of Y-variance. The number of PCs to explain optimal Y-variance seems to be 3. Slope of the predicted Y curve is 0.82 with offset 1.42% giving the RMSEP as 5.83%. The bottom figure shows weights of the regression coefficients which indicate that negative and positive impacts of parameters on $CO_2$ removal efficiency. According to that, LL and NS are negatively correlated with the removal efficiency and the rest of the other variables are positively correlated.

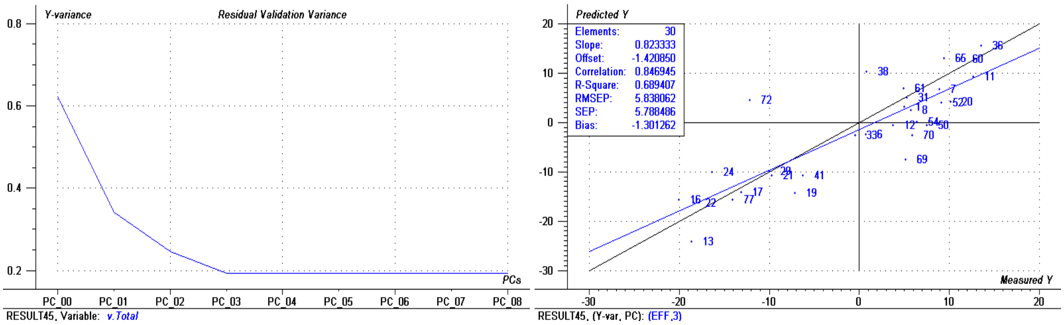

Fig. 6. PLS analysis of data set with 30 random test samples; left figure shows residual validation variance; right figure shows predicted Y.

The PLS-R is again performed without the marked outlier and the response obtained is analysed. Sample numbers 38 and 72 are identified as outlier and removed. Once more PLS-R is carried out and the obtained response is included in the Fig. 7. From the figure, it is seen that the slope has increased than before (Fig. 6) and there is considerable decrease in the RMSEP value which is the positive aspect as slope is expected to be 1 and RMSEP is expected to be 0 for making the perfect model. Further, the number of PCs required to explain sufficient Y variance is decreased to 2. The outliers in case of the PCR and PLS-R are different which is because the test set for the validation of data is taken in random from the total data set.

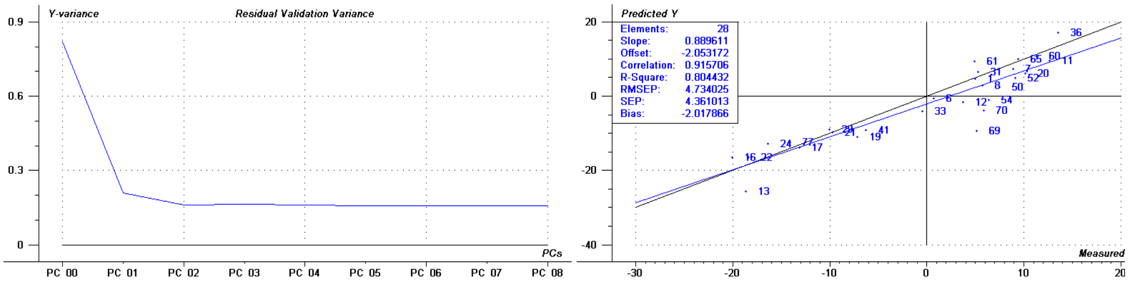

Fig. **7.** PLS model after deleting an outlier; left figure shows residual validation variance; right figure shows predicted Y.

From the regression coefficient chart (Fig. 8), it can be noted that the number of stages (NS) and Lean Loading (LL) have negative regression coefficients. NS and FT has no significant effect on the removal efficiency. LL has high negative correlation meaning, increase in LL with very small magnitude will cause a decrease in efficiency. In contrary to that, MF and PD have high positive correlation which means that the increase in MF and PD will cause an increase in the removal efficiency. From the regression coefficients plot, it can also be verified that LL, MF and PD are the most important X variables. MT, PH and AP have positive correlation with the efficiency and slightly less effect on efficiency than LL, MF and PD.

In PLS-R model, number of principal components (PCs) is less in comparison to PCR and thus it can also be noted that the PLS-R is faster and needs less number of PCs for explaining sufficient Y variance. Moreover, 18% of X variance and 69% of Y variance is explained only by PC1. X-loading weight in

Fig. 8 shows the importance of the variables in PC1 (blue), PC2 (red). For instance, NS, MF, PH and LL are the important variables for PC2. However, as almost 70% of Y variance is explained by PC1, our discussion and conclusion will be focused on the variables effect on PC1. For PC1 analysis, PH, LL and PD are the most important variables.

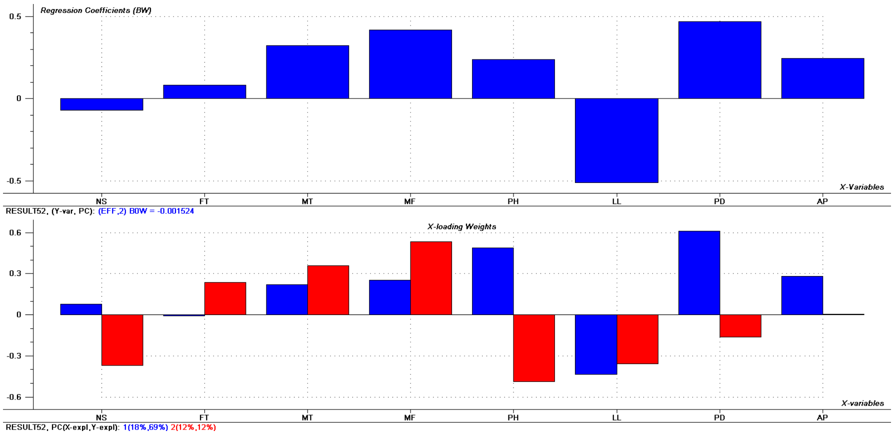

Fig. **8.** Regression Coefficient and X-loading weights plot; upper figure shows regression coefficients and bottom figure shows importance of the variables in PC1 and PC2.

## 5. Conclusion

The post combustion $CO_2$ capture model was developed and implemented in Aspen Plus. Correlations between the variables were studied, which indicate that inlet solvent flow rate (MF), absorber packing height (PH) and diameter (PD), absorber pressure (AP) and temperature of the solvent stream (MT) are positively correlated with the efficiency whereas the lean loading (LL) is negatively correlated with efficiency. From the regression coefficient plot in the PLS-R analysis, it can be noticed that inlet solvent flow rate, lean loading and packing diameter are the most important variables for removal efficiency. Number of stages and flue gas temperature are found to be less significant for the removal efficiency. Multivariate data analysis of the absorber column of the $CO_2$ capture plant is a promising technique for selection of optimal parameters to modify in order to achieve higher $CO_2$ removal efficiency. The single variable effect on efficiency was previously been studied with keeping other variables constant. Both the main effects (the effect of each individual parameter) and the interaction effects have been studied in this paper. Effect of the parameters on $CO_2$ removal efficiency is given the same conclusion in both cases. Single variable effect (by keeping other variables as constant value and change only one at once) is not good enough to understand the effect on that variable on removal efficiency. The regression coefficients can be used to develop the model that can predict the future variations with parameters.

## References

**[1]** Arachchige USPR, Aryal N, Melaaen MC. Case study for flue gas separation of a coal fired power plant and parameters' effect on removal efficiency, Proceedings, APCRE'11 chemical engineering symposium, Beijing, China; 2011.

[2] Esbensen KH. *Multivariate Data Analysis – in practice.* 5.th Ed. (Oct. 2001), CAMO AS Publ. ISBN 82-993330-2-4; 2001.

[3] Martens H, Næs T. *Multivariate Calibration.* John Wiley & Sons Ltd., UK; 1989 (reprint 1994).

[4] Alie CF. $CO_2$ Capture with MEA: Integrating the Absorption Process and Steam Cycle of an Existing Coal-Fired Power Plant. Master Thesis, University of Waterloo, Canada; 2004.

[5] Michael AD. A model of vapour-liquid equilibria for acid gas-alkanolamine-water systems. PhD Thesis, University of Texas, USA; 1989.

[6] Freguia S. Modeling of $CO_2$ removal from Flue Gas with Mono-ethanolamine. Master Thesis, University of Texas, USA; 2002.

[7] Martens H, Karstang T, Næs T. *Improved selectivity in spectroscopy by multivariate calibration.* Journal of Chemometrics 1(4):201-219; 1987.

## Paper J

# Optimized CO2 flue gas separation model for a coal fired power plant

This paper is published in the International Journal of Energy and Environment, 4, No. 1: 39-48, 2013.

INTERNATIONAL JOURNAL OF
ENERGY AND ENVIRONMENT

*Volume 4, Issue 1, 2013 pp.39-48*
*Journal homepage: www.IJEE.IEEFoundation.org*

# Optimized $CO_2$-flue gas separation model for a coal fired power plant

**Udara S. P. R. Arachchige[1], Muhammad Mohsin[1], Morten C. Melaaen[1,2]**

[1] Telemark University College, Porsgrunn, Norway.
[2] Tel-Tek, Porsgrunn, Norway.

**Abstract**
The detailed description of the $CO_2$ removal process using mono-ethylamine (MEA) as a solvent for coal-fired power plant is present in this paper. The rate based Electrolyte NRTL activity coefficient model was used in the Aspen Plus. The complete removal process with re-circulating solvent back to the absorber was implemented with the sequential modular method in Aspen Plus. The most significant cost related to $CO_2$ capture is the energy requirement for re-generating solvent, i.e. re-boiler duty. Parameters' effects on re-boiler duty were studied, resulting decreased re-boiler duty with the packing height and absorber packing diameter, absorber pressure, solvent temperature, stripper packing height and diameter. On the other hand, with the flue gas temperature, re-boiler duty is increased. The temperature profiles and $CO_2$ loading profiles were used to check the model behavior.

**Keywords:** Carbon dioxide capture; Coal fired power plant; Parameters effect; Re-boiler duty.

## 1. Introduction

Due to the large number of fossil fuel based power plants, the bulk amount of $CO_2$ is releasing to the atmosphere. In order to maintain the atmospheric green house gases, mitigation technologies have to be developed. Post combustion capture technologies are the best and widely used method for $CO_2$ recovery process. $CO_2$ capture by absorption and stripping process is currently considered as the most feasible option for $CO_2$ removal from fossil fuel fired power plants. The main drawback of this technology is energy consumption and the capital cost. Post combustion $CO_2$ capture technology with amine solvent is a reactive system. Hence, mass transfer of $CO_2$ from the bulk vapor to the liquid solvent and chemical reactions between amine and flue gas are the main two phenomena to be considered.

In the chemical absorption, flue gas enters the absorber at the bottom whilst the solvent enters at the top. The reactions start between MEA and $CO_2$ while flowing through the column (packing bed). An un-reacted gas leaves the column at the top, while the $CO_2$ rich solvent discharges at the bottom. The rich solvent goes through the heat exchanger to increase the temperature before sending it to the stripper section. The heated rich MEA stream then goes to the stripper at the top. In the stripper, steam is used for the regeneration process. Finally, separated acid gases leave the stripper at the top. The lean MEA then leaves the system at the bottom of the stripper and goes through the heat exchanger. The MEA and water are added to the lean MEA stream to balance the component before recycled back to the absorber unit.

The main problem with installing capture plant to the fossil fuel fired power industry is operating cost. Installation of capture plant increases the electricity unit cost. The main point that requires considering operating cost is the energy requirement to run the carbon capture process. Therefore, it is necessary to perform research on this topic to reduce the operating cost and to improve the existing technologies to capture the $CO_2$. This paper primarily focuses on developing the model for gas treating plant of $CO_2$ from the coal-fired power plant flue gas and simulates the adaptable model to reduce the re-boiler duty.

## 2. Model development

A simulation of a 500MW coal-fired power plant flue gas is considered. The flue gas composition and inlet conditions are extracted from the literatures [1]. The comprehensive flow sheet is developed in Aspen Plus for three different $CO_2$ removal models with 85, 90 and 95% efficiency.

The suitable operating conditions are selected from previous studies, and sensitivity analysis is performed to check the validity of the parameters. A simplified flow sheet of the implemented model which employs $CO_2$ capture by absorption/stripping with an aqueous amine solution is shown in Figure 1.

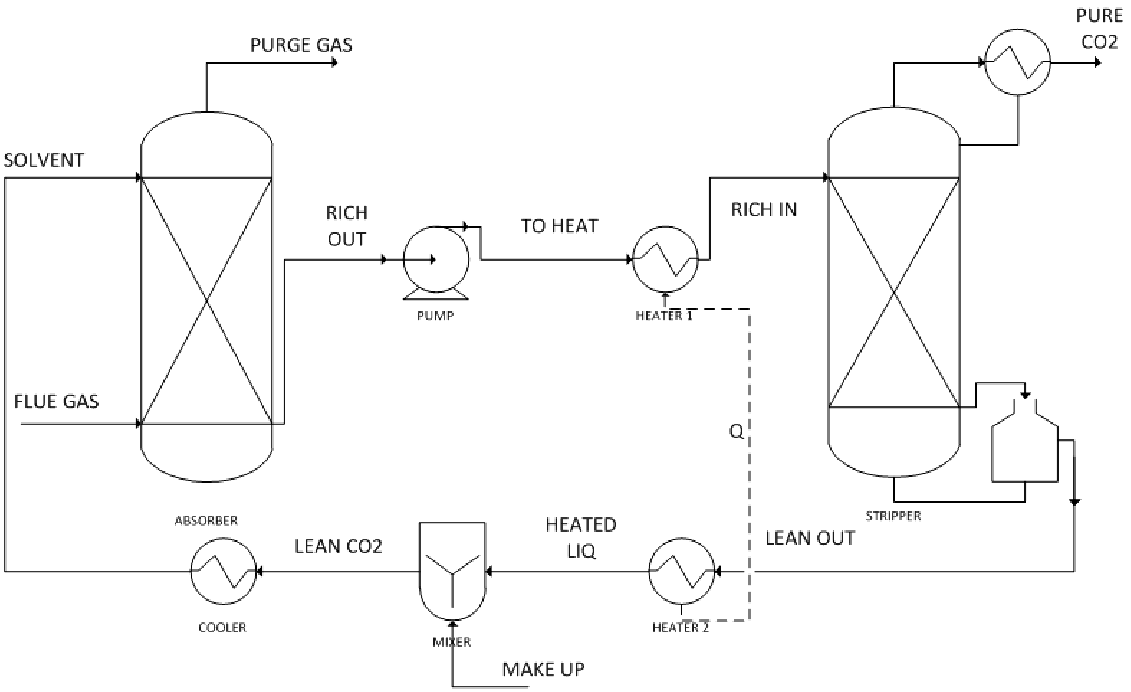

Figure 1. Process flow diagram

### *2.1 Operating conditions*

The process flow diagram is developed to capture 85, 90 and 95% of $CO_2$ from coal-fired power plant flue gas. Absorber and stripper are the main two-unit operation blocks in the capture process. Inlet flue gas and solvent stream are supplied at 313K, and absorber is operating at 1bar absolute pressure. The rich solvent stream is heated up to 382K using a heat exchanger unit before sending it to stripper section for maximum performance. The stripper is operating at 2 bar absolute pressure and reflux ratio (fraction of the condensed is coming back to the stripper section) and distillate rate (flow rate of the PURE CO2 line) are used to implement the stripper unit. The inlet flue gas stream data are selected from Alie, 2004 [1] and tabulated in Table 1 and selected solvent conditions from simulation studies are given in Table 2.

The main component in the pure gas stream of the stripper (PURE CO2 in Figure 1) is $CO_2$, and the rest of that is MEA and water. High temperature (393K) steam (produce in the re-boiler) is used to remove the $CO_2$ from the solvent. Steam is produced in the re-boiler and main energy requirement in the process is related to re-boiler duty. Therefore, the $CO_2$ capture model is implemented to reduce the re-boiler duty so that energy requirement can be minimized. The operating conditions of absorber and stripper section are tabulated in Table 3. Due to several reasons Aspen Plus Rad-Frac model is selected for absorber and stripper:

- It is the active unit operation model for vapour- liquid absorption and stripping section.
- The simulation time is faster for Rad-Frac column in comparison with other available options.
- Fewer convergence problems compared to other available options in Aspen Plus with high accuracy.

Table 1. Flue gas composition and parameters [1]

| Parameter | Coal Fired |
|---|---|
| Flow rate [kg/s] | 673.4 |
| Temperature [K] | 313 |
| Pressure [bar] | 1.1 |
| Major Composition | Mol% |
| $H_2O$ | 8.18 |
| $N_2$ | 72.86 |
| $CO_2$ | 13.58 |
| $O_2$ | 3.54 |
| $H_2S$ | 0.05 |

Table 2. Solvent stream parameters

| Specification | 85% Removal Efficiency | 90% Removal Efficiency | 95% Removal Efficiency |
|---|---|---|---|
| Coal fired power plant $CO_2$ capture | | | |
| MEA concentration [w/w%] | 40 | 40 | 40 |
| $CO_2$ lean loading [mole $CO_2$/mole MEA ] | 0.27 | 0.27 | 0.25 |
| Solvent flow rate [kg/s] | 2212 | 2422 | 2483 |

Table 3. Absorber and stripper column specifications

| Specification | Coal fired flue gas | |
|---|---|---|
| | Absorber | Stripper |
| Number of stages | 15 | 15 |
| Operating pressure | 1 bar | 2 bar |
| Re-boiler | None | Kettle |
| Condenser | None | Partial-vapour |
| Packing type | Mellapak,Sulzer, Standard, 250Y | Flexipac, Koch, metal,1Y |
| Packing height | 20m | 18m |
| Packing diameter | 15m | 12m |
| Mass transfer coefficient method [2] | Bravo et al. (1985) | Bravo et al. (1985) |
| Interfacial area method [2] | Bravo et al. (1985) | Bravo et al. (1985) |
| Interfacial area factor | 1.5 | 2 |
| Heat transfer coefficient method | Chilton and Colburn | Chilton and Colburn |
| Holdup correlation [3] | Billet and Schultes (1993) | Billet and Schultes (1993) |
| Film resistance | Discrxn for liquid film and Film for vapour film | Discrxn for liquid film and Film for vapour film |
| Flow model | Mixed | Mixed |

Packed columns are used for the model development and the type of the packing is selected to get better operating conditions. The packing height, section diameter, packing factor and material are important factors and tabulated (Table 3). The number of stages is selected to obtain high accuracy. The input conditions and model specifications used for model development in the absorber, and stripper are shown in Table 3. The specifications are recommended for rate based model of the $CO_2$ capture process by Aspen Tech [4].

### *2.2 Property method selection*

A property method is defined as a collection of property calculation routes. Each unit operation model requires property method to perform the calculation [5]. Mainly, four different property methods are available for $CO_2$+ MEA system:

ELECNRTL - handle both very low and high concentrations of aqueous and mixed solvent systems.
ENTRL-HF- similar to the ELECNRTL property method except that it uses the HF equation of state for vapor phase calculation model.
ENTRL-HG - similar to the ELECNRTL property method except it uses the Helgeson model for standard property calculations.
AMINES - this property method uses Kent-Eisenberg correlation for K-values and enthalpy calculation.
Out of them, the ELECNRTL model is selected for the simulation of the $CO_2$ capture process and electrolyte wizard is used to develop the simulation kinetics and reactions. The ELECNRTL is the most versatile electrolyte property method as it can handle both very low and high concentrations of aqueous and mixed solvent systems. The solubility of gases can be modeled with Henry's law and required coefficients are available in databanks. For the calculation of vapor phase properties, the Redlich-Kwong equation of state is used.

### *2.3 Thermodynamic behavior*

The acid gases in the flue gas are weak acid electrolytes, and amines are weak organic base electrolytes. Combination of those two forms partially ionizes or partially dissociates aqueous solution in reacting system. The reacting system (1-7) can be expressed as dissociation of components as below [6].

Water: $2H_2O \leftrightarrow OH^- + H_3O^+$ (1)

Hydrogen sulfide: $H_2O + H_2S \leftrightarrow HS^- + H_3O^+$ (2)

Hydrogen bisulfide: $H_2O + HS^- \leftrightarrow S^{2-} + H_3O^+$ (3)

Carbon dioxide: $CO_2 + 2H_2O \leftrightarrow HCO_3^- + H_3O^+$ (4)

Bicarbonate: $HCO_3^- + H_2O \leftrightarrow H_3O^+ + CO_3^{2-}$ (5)

Protonated alkanolamine: $MEAH^+ + H_2O \leftrightarrow MEA + H_3O^+$ (6)

Hydrolysis reaction: $MEACOO^- + H_2O \leftrightarrow MEA + HCO_3^-$ (7)

Equilibrium constants are required for each of the above equations to continue their vapour/liquid mole fraction calculations. It can be calculated by,

$$\ln K_j = A_j + \frac{B_j}{T} + C_j \ln T + D_j T \tag{8}$$

where $K_j$ is representing equilibrium constant for thermodynamic model, $T$ is temperature in (K), and constants are given by $A_j$, $B_j$, $C_j$, and $D_j$. Equilibrium constant values are imported from the literature sources [7] and tabulated in Table 4.

Table 4. Values of equilibrium constant equations [7]

| Reaction number | $A_j$ | $B_j$ | $C_j$ | $D_j$ |
|---|---|---|---|---|
| Reaction 1 | 132.89 | -13445.9 | -22.47 | 0 |
| Reaction 2 | 214.58 | -12995.4 | -33.55 | 0 |
| Reaction 3 | -9.74 | -8585.47 | 0 | 0 |
| Reaction 4 | 231.46 | -12092.1 | -36.78 | 0 |
| Reaction 5 | 216.05 | -12431.7 | -35.48 | 0 |
| Reaction 6 | -3.038 | -7008.3 | 0 | -0.00313 |
| Reaction 7 | -0.52 | -2545.53 | 0 | 0 |

It is important to understand the kinetics of the reactions. The reactions (4) and (7) are replaced by kinetic reactions (9), (10) and reverse reactions (11), (12) for rate model.

$$CO_2 + OH^- \rightarrow HCO_3^- \tag{9}$$

$$MEA + CO_2 + H_2O \rightarrow MEACOO^- + H_3O^+ \tag{10}$$

$$HCO_3^- \rightarrow CO_2 + OH^- \tag{11}$$

$$MEACOO^- + H_3O^+ \rightarrow MEA + CO_2 + H_2O \tag{12}$$

The kinetic expression is defined in Aspen Plus and given below in (13) with constant values. Parameters used in (13) are, *rj* rate of reaction, *kj* rate coefficient, *T* and $T_0$ are operating and absolute temperatures in (K), *R* is universal gas constant and *E* is activation energy.

$$r_j = k_j \left(\frac{T}{T_0}\right)^{n_j} exp\left[-\frac{E_j}{R}\left(\frac{1}{T} - \frac{1}{T_0}\right)\right] \tag{8}$$

Table 5 presents the constant values taken for the simulation in Aspen Plus for kinetic calculation. The given values are extracted from the Aspen Plus available databanks and checked with literatures to confirm the accuracy.

Table 5. Rate constant values

| Parameter | Reaction 9 | Reaction 10 | Reaction 11 | Reaction 12 |
|---|---|---|---|---|
| $k_j$ | 4.32e+13 | 9.77e+10 | 2.38e+17 | 2.7963e+20 |
| $n_j$ | 0 | 0 | 0 | 0 |
| $E_j$ (J/mol) | 55433 | 41236 | 123222 | 72089 |
| $T_0$ (K) | 298 | 298 | 298 | 298 |

### *2.4 Parameter selection*

In the amine-$H_2S$-$CO_2$-$H_2O$ system, where the amine is MEA and eight ionic species ($OH^-, H_3O^+, HS^-, S^{2-}, HCO_3^-, CO_3^{2-}, MEAH^+, MEACOO^-$) and four molecular species ($H_2O, H_2S, CO_2, MEA$) are present in the liquid phase. Therefore, pure component parameters, binary parameters as well as electrolyte parameters have to be introduced in order to implement the process model. If any of the parameters are missing, it can be estimated with molecular structure, or using regression with experimental data. The Aspen Plus physical property system contains built in parameters for the electrolyte NRTL model. The databank contains energy parameters and other electrolyte parameters for molecular-electrolyte and electrolyte-electrolyte systems.

## 3. Results and discussion

Sensitivity analysis is performed to understand the parameters' effect on re-boiler duty. Therefore, initially, open loop model was developed for the simulation, and absorber packing height, diameter of the packing bed, absorber pressure, solvent and flue gas temperatures, stripper packing height, and diameter are varied to check the effect on re-boiler duty. For this sensitivity analysis, only 85% removal efficiency is considered. In order to study the effect of one parameter on energy consumption in the re-boiler, other parameters of the model are kept constant. Figure 2 represents the re-boiler duty variation with listed parameters.

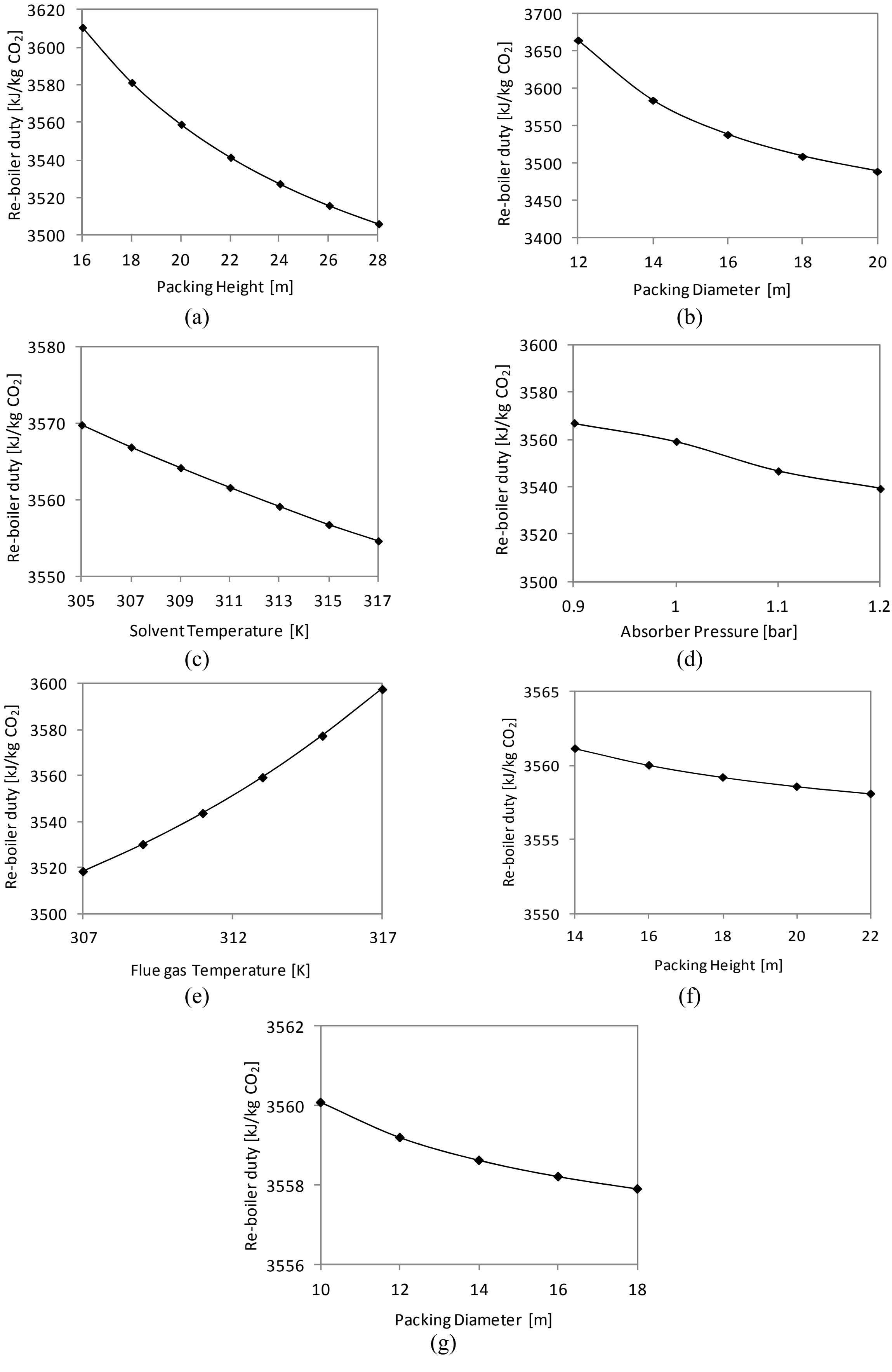

Figure 2. Re-boiler duty variation with model parameters; (a) absorber packing height, (b) absorber packing diameter, (c) solvent temperature, (d) absorber pressure, (e) flue gas temperature, (f) stripper packing height, (g) stripper packing diameter

The re-boiler duty is decreasing with the increase of absorber packing height, packing diameter, absorber pressure, solvent temperature, stripper packing height, and packing diameter. The attained rich loading increased with the increase in the absorber packing height and packing diameter. Hence, required solvent flow rate is decreased and the amount of the liquid solvent process in the stripper is reduced. Therefore, the re-boiler duty to process unit mass of $CO_2$ is reduced and the total energy requirement decreased. Similarly, re-boiler duty decreased with the increase of absorber pressure due to higher $CO_2$ removal efficiency with high absorber operating pressure. Re-boiler duty decreased with the increase of solvent temperature. Reverse is applicable to flue gas temperature effect. The effect of stripper packing parameters on re-boiler duty is negligible.

The efficiency of the $CO_2$ removal (85%, 90%, and 95%) is achieved with distillate rate (vapour stream of the stripper outlet) variation in the stripper. However, before lean MEA stream recycled back to the absorber, rest of the $CO_2$ (15%, 10%, and 5%) remained in the system has to be removed from the system to get material balances. The $CO_2$ removal amount in the purge gas stream is calculated. Exact amount of remaining $CO_2$ can be removed by adjusting the open-loop MEA inlet flow rate to the absorber. Amount of MEA and H2O losses during the process are added to the make-up stream to balance the system and lean MEA stream is recycled back to the absorber (Table 6).

Table 6. Composition of make-up stream

| Process Model | Amount of make-up stream | |
|---|---|---|
| Removal Efficiency (mol %) | Water (kg/s) | MEA (kg/s) |
| 85 | 42.41 | 0.41 |
| 90 | 37.85 | 0.38 |
| 95 | 29.52 | 0.36 |

Finally, the closed-loop $CO_2$ removal process is considered for the re-boiler duty calculation and further analyzing. Re-boiler duty is calculated as 3634.2, 3736.4, 4185.5 kJ/kg $CO_2$ for the 85, 90 and 95% $CO_2$ removal process for coal-fired power plant. Temperature profiles (Figure 3) as well as $CO_2$ loading profiles (Figure 4) are studied to understand the behavior of the absorber process.

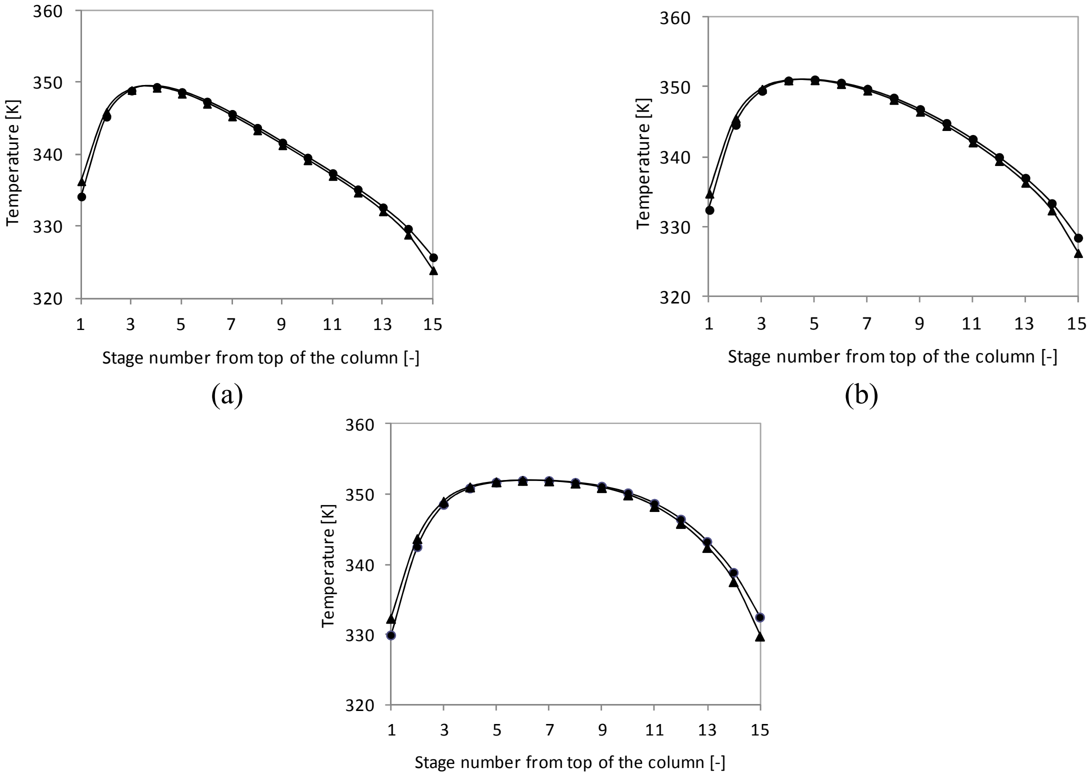

(a)

(b)

(c)

Figure 3. Temperature profiles in absorber for (a) 85%, (b) 90% and (c) 95% removal efficiency; symbols refer to ●, Liquid phase; ▲, Vapour phase

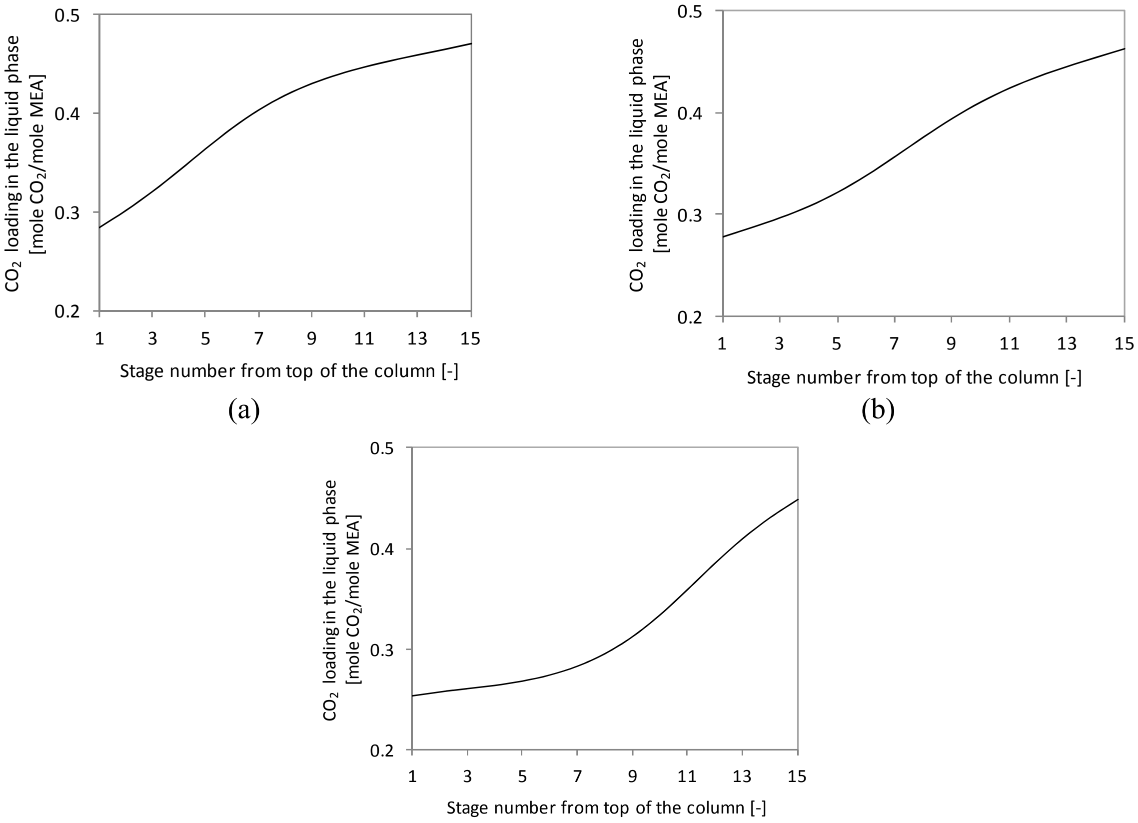

(a) (b)

(c)

Figure 4. $CO_2$ loading profiles in absorber for (a) 85%, (b) 90% and (c) 95% removal efficiency

The absorber tends to exhibit a temperature bulge at the top of the column for both liquid and vapor phase. Temperature bulge is due to highly exothermic reactions at the top of the column. The maximum temperature is reached 350K for all three models. The $CO_2$ loading is increasing alone the absorber and rich loading is reached to 0.4-0.5 [mole $CO_2$/mole MEA] for all three simulation models. The $CO_2$ rich loading is slightly decreasing with the increase of removal efficiency. Highest rich loading is obtained for 85% removal process.

## 4. Conclusion

The implemented model is properly working and converging for coal fired flue gas system. Three different models were developed with 85-95% removal efficiency. The calculated re-boiler duties are 3634.2, 3736.4, 4185.5 kJ/kg $CO_2$ for the 85, 90 and 95% $CO_2$ removal process. Temperature profiles and $CO_2$ loading profiles are having similar patterns for all cases.

## References

[1] Alie C.F. CO2 Capture with MEA: Intergrating the Absorption Process and Steam Cycle of an Existing Coal-Fired Power Plant. Master Thesis, University of Waterloo, Canada, 2004.

[2] Bravo J.L., Rocha J.A. and Fair J.R.. Mass Transfer in Gauze Packings. Hydrocarbon Processing, 1985 (January), 91–95.

[3] Billet R., Schultes M. Predicting Mass Transfer in Packed Columns. Chem. Eng. Technology, 1993,Vol. 16, 1-9.

[4] Aspen Plus. Aspen Physical Property Methods. Aspen Technology Inc, Cambridge, MA, USA, 2006, 61-63.

[5] Aspen Plus. Rate Based model of the CO2 capture process by MEA using Aspen Plus. Aspen Technology Inc, Cambridge, MA, USA, 2008.

[6] Michael A.D. A model of vapour-liquid equilibria for acid gas-alkanolamine-water systems. Ph.D Thesis, University of Texas, USA, 1989.

[7] Freguia S. Modeling of CO2 removal from Flue Gas with Mono-ethanolamine. Master Thesis, University of Texas, USA, 2002.

**Udara S.P.R. Arachchige** received his B.Sc Degree (2007) in Chemical and Process Engineering from University of Moratuwa, Sri Lanka and M.Sc degree (2010) in Energy and Environmental Engineering from Telemark University College, Porsgrunn, Norway. He is presently pursuing his Ph.D in Carbon dioxide capture from power plants, modeling and simulation studies from Telemark University College, Porsgrunn, Norway. He has presented and published five paper in International Conferences. Mr. Udara is a member of American Chemical Society.
E-mail address: udara.s.p.arachchige@hit.no

**Muhammad Mohsin** received his B.Sc Degree (2011) in Electrical Engineering and Automation from Shenyang University of Chemical Technology, Shenyang, China. He is presently pursuing his Master degree in System and Control Engineering in Telemark University College, Porsgrunn, Norway. He also working as a research Assistant in Technology department in same university college. Mr. Mohsin has research interest on carbon capture, modeling and simulation, control systems in process industries.
E-mail address: mohsin.m.ansari@gmail.com

**Morten Chr. Melaaen** is Professor in process technology at Telemark University College, Porsgrunn, Norway. He is also the Dean of Faculty of Technology, Telemark University College and has a part time position at the local research institute Tel-Tek. Earlier, he has worked as a research engineer in Division of Applied Thermodynamics, SINTEF, Norway and as an Associate professor at Norwegian University of Science and Technology (NTNU). He has worked on research projects as a Senior research scientist in Norsk Hydro Research Centre Porsgrunn, Norway. He started to work as a professor at Telemark University College in 1994 and became Head of Department, Department of Process, Energy and Environmental Technology in 2002. He received his MSc in Mechanical Engineer in 1986 and his Ph.D in 1990, both from the NTNU. His research interests are $CO_2$ capture, Modeling and simulation, Fluid mechanics and Heat and Mass Transfer. Professor Morten has more than 90 scientific papers published in the above mentioned related fields in international journals and conferences.
E-mail address: Morten.C.Melaaen@hit.no

Paper K

# Optimized Carbon Dioxide Removal Model for Gas Fired Power Plant

This paper is published in the European Journal of Scientific Research, 86, No. 3: 348-359, 2012.

European Journal of Scientific Research
ISSN 1450-216X Vol. 86 No 3 September, 2012, pp.348-359

http://www.europeanjournalofscientificresearch.com

# Optimized Carbon Dioxide Removal Model for Gas Fired Power Plant

**Udara S. P. R. Arachchige**
*Telemark University College, Porsgrunn, Norway*
E-mail: udara.s.p.arachchige@hit.no
Tel: +47-94284116; Fax: 0047-35575001

**Muhammad Mohsin**
*Telemark University College, Porsgrunn, Norway*
E-mail: mohsin.m.ansari@gmail.com

**Morten C. Melaaen**
*Telemark University College, Porsgrunn, Norway*
*Tel-Tek, Porsgrunn, Norway*
E-mail: Morten.C.Melaaen@hit.no

## Abstract

The carbon capture process model was developed for 500MW gas-fired power plant flue gas treating. Three different efficiencies, 85%, 90%, and 95%, were used to implement the model in Aspen Plus. The electrolyte NRTL rate base model was used to develop the model. The selected solvent properties were used to develop and implemented model is used for further simulations. The implemented open loop base case model of 85% removal efficiency is used to check the parameters' effect on removal efficiency and re-boiler duty. Absorber packing height and diameter, absorber pressure, solvent and flue gas temperatures are positively affected on $CO_2$ removal efficiency. The packing height of absorber and stripper, solvent temperature and absorber pressure are negatively effects on re-boiler duty. The energy requirement in the re-generation process (re-boiler duty) are 3781, 4050, and 4240 kJ/kg $CO_2$ for 85%, 90%, and 95% capture models respectively. Parameter optimization is important to implement the carbon capture process in real industries to get higher removal efficiency and lowest re-boiler duty.

**Keywords:** Gas fired power plant, Carbon capture, Parameters effect, Re-boiler duty, Aspen Plus

## 1. Introduction

The green house gas emissions from the exhaust gases of the fossil fuel fired power plants (coal and natural gas) account for the global warming and climate change. Carbon dioxide ($CO_2$) is the main green house gas causes for most of the environmental problems. Emission reduction technologies with high efficiencies are important in near future to avoid the problems. Carbon capture and sequestration (CCS) is the best available option for the power plant flue gas mitigation. The post combustion chemical absorption process is considered as the most viable option today.

The main advantage of amine scrubbing for post combustion carbon capture process is, it can be installed to the existing power plants without major modifications. Apart from that, it can be used with low partial pressure of $CO_2$ streams as it used to be with flue gases.

This research study will focus on improving existing carbon capture process with solvent improvements. Monoethanolamine (MEA) solvent is considered for model development in the present study. Here, an improvement of solvent concentration and lean loading is used to optimize the model. According to the previous studies [1], solvent concentration and lean loading is selected for gas-fired power plant flue gas treating process. Increasing solvent concentration will lead to reduce the required solution circulation and therefore, the plant operating cost [1].

## 2. Case Studies

### 2.1. Flue Gas and Solvent Properties

The carbon capture model is developed for 500MW gas-fired power plant flue gas stream. The conditions of the flue gas stream are given in Table 1, which is taken from the literature [2]. Aspen Plus rate based model is used to develop the comprehensive process flow sheet (Figure 1). Three different efficiencies, 85%, 90%, and 95%, are used to implement the model.

**Table 1:** Flue gas stream conditions [2]

| Parameter | Value |
|---|---|
| Flow rate [kg/s] | 793.9 |
| Temperature [K] | 313 |
| Pressure [bar] | 1.1 |
| Major Composition | mol% |
| H2O | 8.00 |
| N2 | 76.00 |
| CO2 | 4.00 |
| O2 | 12.00 |

The process flow diagram consists of several unit operation blocks, such as absorber and stripper, pumps, heat exchanger, cooler and make up unit. For absorber and stripper, Rad-frac unit operation block is selected from the Aspen Plus model bank.

**Figure 1:** Process flow diagram

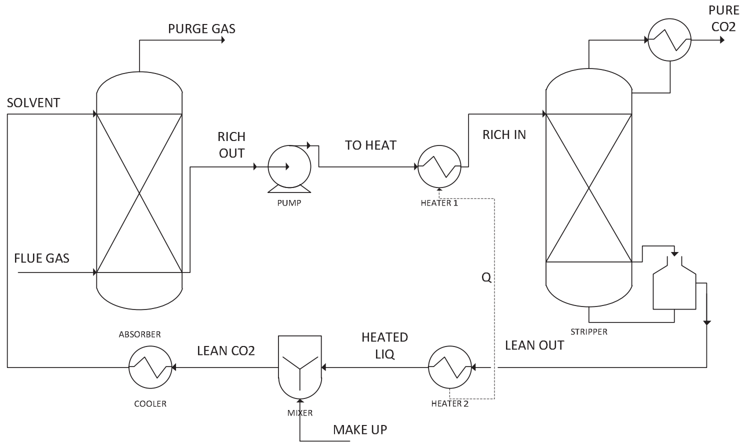

The inlet solvent stream properties which is selected from the previous studies [1], is tabulated below (Table 2). Number of simulation was performed in previous studies to select the best solvent condition for specified efficiencies.

**Table 2:** Solvent stream conditions [1]

| Specification | 85% Removal Efficiency | 90% Removal Efficiency | 95% Removal Efficiency |
|---|---|---|---|
| Gas fired power plant $CO_2$ capture | | | |
| MEA concentration [w/w%] | 40 | 35 | 30 |
| Lean $CO_2$ loading [mole $CO_2$/mole MEA] | 30 | 25 | 25 |
| Solvent flow rate [kg/s] | 1048.6 | 895.6 | 1177.8 |

In the chemical absorption process, flue gas is counter currently passing through the solvent in a packed bed absorber column. Afterwards, rich solvent is transferred to the stripper section to re-generate the solvent by purifying the $CO_2$ using steam. Before sending it to the stripper, rich solvent stream is passing through the heat exchanger to increase the temperature to around 380K. Re-generating solvent step is the main energy-consuming part in the process, is called re-boiler duty. As it is the main drawback of this technology, process optimization is important before install in to the real industry.

## 2.2. Aspen Plus Model Parameters-Reaction Scheme

The MEA-$CO_2$ reacting system consists with several chemical reactions. The main chemical reactions involving in the carbon capture process are considered with thermodynamic and kinetic parameters. When $CO_2$ absorb into the amine solvent, following reversible chemical reactions (Eq. 1-5) are taking place [3].

$$2H_2O \leftrightarrow OH^- + H_3O^+ \tag{1}$$

$$CO_2 + 2H_2O \leftrightarrow HCO_3^- + H_3O^+ \tag{2}$$

$$HCO_3^- + H_2O \leftrightarrow H_3O^+ + CO_3^{2-} \tag{3}$$

$$MEAH^+ + H_2O \leftrightarrow MEA + H_3O^+ \tag{4}$$

$$MEACOO^- + H_2O \leftrightarrow MEA + HCO_3^- \tag{5}$$

The equilibrium constants for above equations can be calculated by Eq. 6 and relevant parameters are taken from the literatures (Table 3).

(6)

where:

$K_j$ is equilibrium constant for thermodynamic model;
$T$ - Temperature in K;
$A_j$, $B_j$, $C_j$, *and* $D_j$ – Constants.

**Table 3:** Constant values of equilibrium constant equation [4]

| Reaction number | $A_j$ | $B_j$ | $C_j$ | $D_j$ |
|---|---|---|---|---|
| Reaction 1 | 132.89 | -13445.9 | -22.47 | 0 |
| Reaction 2 | 231.46 | -12092.1 | -36.78 | 0 |
| Reaction 3 | 216.05 | -12431.7 | -35.48 | 0 |
| Reaction 4 | -3.038 | -7008.3 | 0 | -0.00313 |
| Reaction 5 | -0.52 | -2545.53 | 0 | 0 |

Kinetics of the reacting system is important to understand the model behavior. Equation 2 and 5 is replaces the kinetic reactions 7 and 8 and reverse reactions 9 and 10.

$$CO_2 + OH^- \rightarrow HCO_3^- \tag{7}$$

$$MEA + CO_2 + H_2O \rightarrow MEACOO^- + H_3O^+ \tag{8}$$

$$HCO_3^- \rightarrow CO_2 + OH^- \tag{9}$$

$$MEACOO^- + H_3O^+ \rightarrow MEA + CO_2 + H_2O \tag{10}$$

The kinetic expression is defined in equation (11) and required parameters are tabulated in Table 4.

(11)

where:

$r_j$, *is* rate of reaction;
$k$ - Rate coefficient;
$T$ and $T_0$ - temperatures in K;
$R$ - Universal gas constant;
$E$ - Activation energy.

The constant values used for the simulation in Aspen Plus for kinetic calculation are given in Table 4. The tabulated values are extracted from the Aspen Plus available databanks.

**Table 4:** Constant values for equation (11)

| Parameter | Reaction 7 | Reaction 8 | Reaction 9 | Reaction 10 |
|---|---|---|---|---|
| $k_j$ | 4.32e+13 | 9.77e+10 | 2.38e+17 | 2.7963e+20 |
| $n_j$ | 0 | 0 | 0 | 0 |
| $E_j$ (J/mol) | 55433 | 41236 | 123222 | 72089 |
| $T_0$ (K) | 298 | 298 | 298 | 298 |

## 2.3. Aspen Plus Model Parameters-Absorber and Stripper Column Parameters

The absorber and stripper column parameters used in the implemented model is tabulated in Table 5. Similar conditions are applied in all three efficiency processes (85%, 90%, and 95% removal efficiency). The model specifications used for model development in the absorber, and stripper are shown in Table 5. The selected specifications are recommended for rate based model of the $CO_2$ capture process in literatures [5].

**Table 5:** Absorber and stripper column parameters

| Specification | Value | |
|---|---|---|
| | Absorber | Stripper |
| Number of stages | 15 | 15 |
| Operating pressure | 1 bar | 1.6 bar |
| Pressure drop | 0.1 bar | 0.1 bar |
| Re-boiler | None | Kettle |
| Condenser | None | Partial-vapour |
| Packing Type | MELLAPAK, Sulzer, Standard, 250 Y | FLEXIPAC, KOCH, METAL,1 Y |
| Packing height | 24m | 18m |
| Packing Diameter | 18m | 12m |
| Mass transfer coefficient method [6] | Bravo et al. (1985) | Bravo et al. (1985) |
| Interfacial area method | Bravo et al. (1985) | Bravo et al. (1985) |
| Interfacial area factor | 1.2 | 1.5 |
| Heat transfer coefficient method | Chilton and Colburn | Chilton and Colburn |
| Holdup correlation [7] | Billet and Schultes (1993) | Billet and Schultes (1993) |
| Film resistance | Discrxn for liquid film and Film for vapour film | Discrxn for liquid film and Film for vapour film |

## 2.4. Parameters Effect on Removal Process

At the beginning, open loop process is developed in Aspen Plus to get the exact efficiency which is specified in stripper column. The base case models are developed for 85%, 90% and 95% removal efficiencies. The selected solvent properties are used to develop the model and implemented model is used for further simulations. The implemented open loop 85% removal efficiency base case model is used to check the parameters' effect on removal efficiency and re-boiler duty. Main important parameters, such as absorber packing height and diameter, absorber pressure, flue gas and solvent stream temperature, are used to perform the parameters' effect on $CO_2$ removal efficiency. Similarly, in addition to above parameters, stripper packing height and diameter also varied to check the parameters' effect on re-boiler energy requirement. In order to study the effect of one parameter, other parameters are kept constant. Base case parameter values and range of the parameters are varied for sensitivity analysis is given in Table 6.

**Table 6:** Main input parameters considered for sensitivity analysis

| Input parameter | Base case value | Range of the parameter varied |
|---|---|---|
| Absorber packing height (m) | 24 | 18-30 |
| Absorber packing diameter(m) | 18 | 12-20 |
| Absorber operating pressure (bar) | 1 | 0.8-1.2 |
| Flue gas temperature (K) | 313 | 303-313 |
| Solvent temperature (K) | 313 | 307-319 |
| Stripper packing height (m) | 18 | 14-24 |
| Stripper packing diameter (m) | 12 | 10-18 |

## 2.5. Parameters' Effect on Removal Efficiency

The removal efficiency variation with different parameters such as, absorber packing height and diameter, absorber pressure, flue gas and solvent stream temperature, are analyzed for the implemented base case model. Figure 2 and 3 shows how the $CO_2$ capture efficiency variation with the absorber packing height and diameter. Absorber packing height is varied from 18-30 m, and diameter is varied from 12-20 m to check the removal efficiency variation. Removal efficiency is increasing with packing height and diameter. Reason for that is, solution contact area is increasing with the increase of packing height and diameter. Therefore, residence time for reacting system is increased and removal efficiency increased. The results of the parameters' effect on removal efficiency are compared with the literatures to validate the sensitivity analysis [8].

**Figure 2:** $CO_2$ removal efficiency variation with absorber packing height

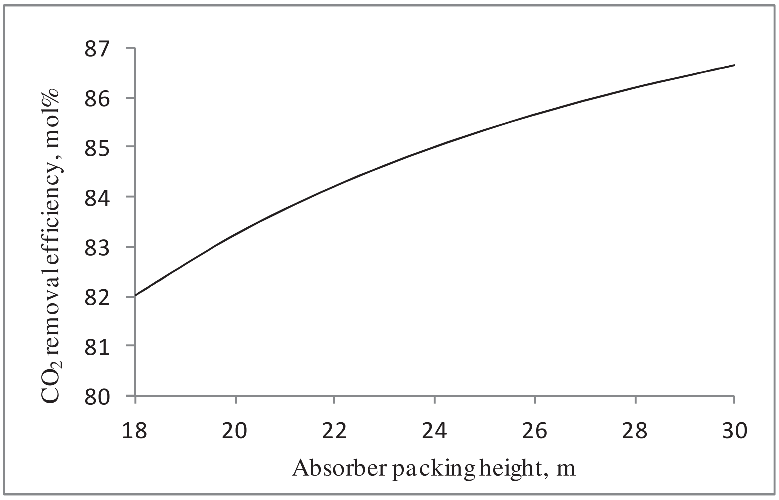

**Figure 3:** $CO_2$ removal efficiency variation with absorber packing diameter

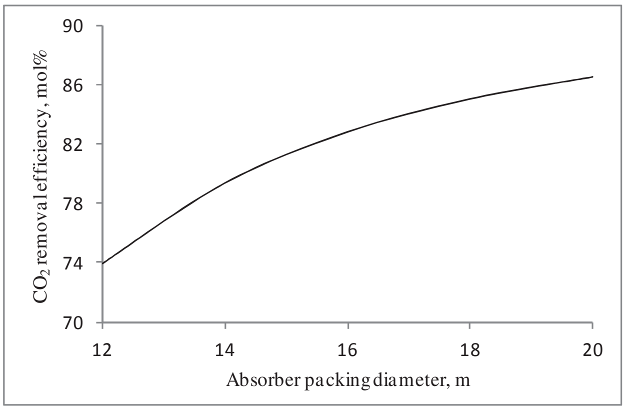

The $CO_2$ removal efficiency variation with absorber column operating pressure is shown in Figure 4. Removal efficiency is increasing with the increase of absorber pressure.

**Figure 4:** $CO_2$ removal efficiency variation with absorber pressure

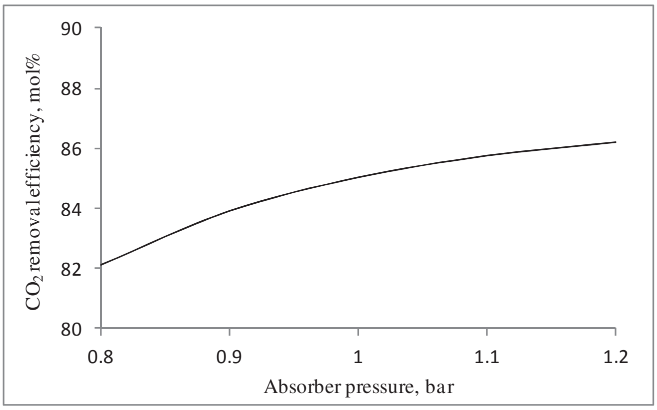

Figure 5 and 6 is presenting removal efficiency variation with flue gas and solvent temperature. The effect of flue gas temperature on removal efficiency is negligible. However, the removal efficiency is slightly increasing with the flue gas temperature. The simulations are carried out in solvent temperature range from 307-319 K. The removal efficiency is increasing with the increase of solvent temperature in the range of studied. As the solvent temperature increases, rate of reaction and diffusivity increase and efficiency of the $CO_2$ removal is increased.

**Figure 5:** $CO_2$ removal efficiency variation with flue gas temperature

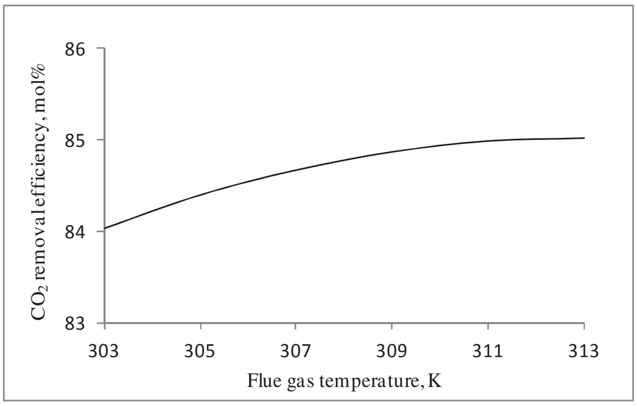

**Figure 6:** $CO_2$ removal efficiency variation with solvent temperature

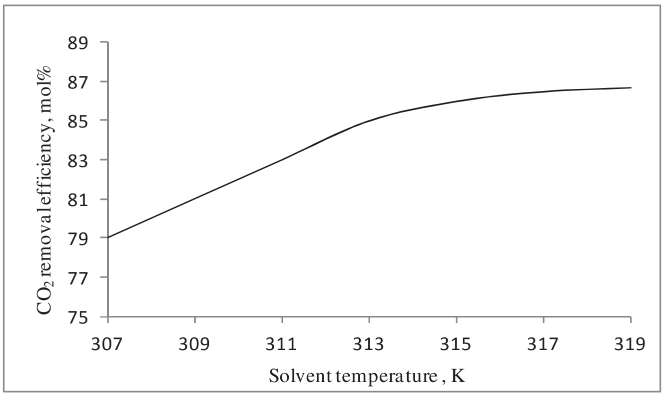

## 2.6. Parameters' Effect on Re-boiler Duty

Parameters' effect on re-boiler duty is analyzed to implement the removal process. Initially, open loop model is used to check the parameters' effect. Similarly, in addition to above parameters, stripper packing height and diameter also varied to check the parameters' effect on re-boiler energy requirement. For this sensitivity analysis, 85% of removal model is used. Figure 7-13 is shown re-boiler duty variation with above mentioned parameters. Regeneration energy requirement mainly can be categorized in to three parts: energy required to release the $CO_2$, energy required to evaporate the water and energy needed for heat up the solvent in the stripper.

**Figure 7:** Re-boiler duty variation with absorber packing height

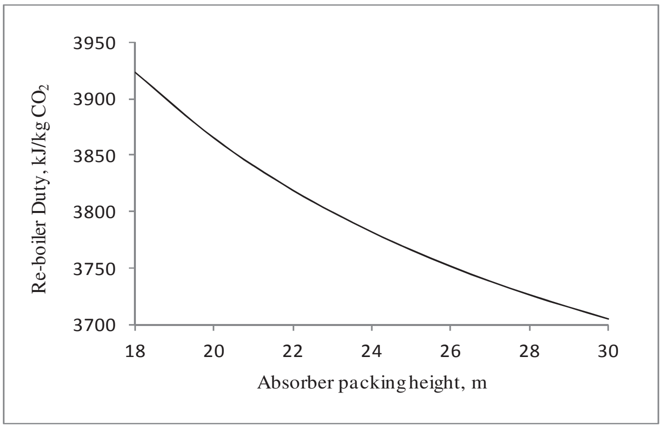

**Figure 8:** Re-boiler duty variation with absorber packing diameter

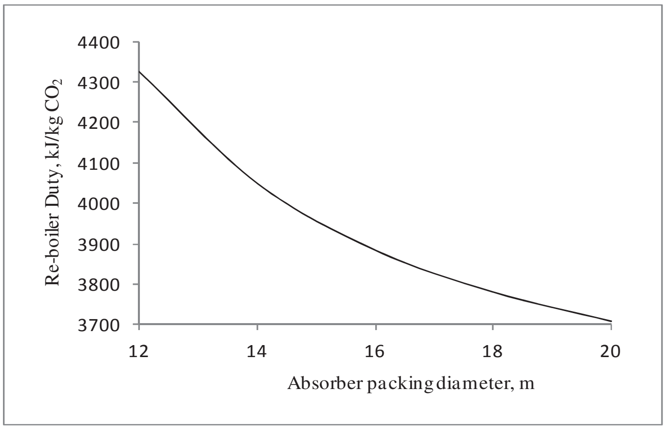

As can be seen from Figure 7 and 8, re-boiler duty is drastically decreasing with the absorber packing height and diameter. When the absorber packing height and diameters increase, contacting surface area for the reaction medium is increase. This means that, amount of solvent required to react with $CO_2$ is reduced. As a result, required energy to heat the solvent in stripper is reduced. Therefore, regeneration energy is decreased in the re-boiler with packing height and diameter. The re-boiler duty variation with absorber pressure is given in Figure 9 and solvent and flue gas temperature effect on re-boiler duty is shown in Figure 10 and 11 respectively.

**Figure 9:** Re-boiler duty variation with absorber pressure

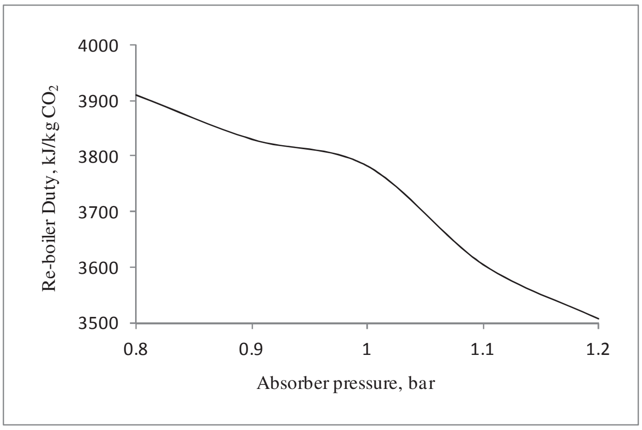

**Figure 10:** Re-boiler duty variation with solvent temperature

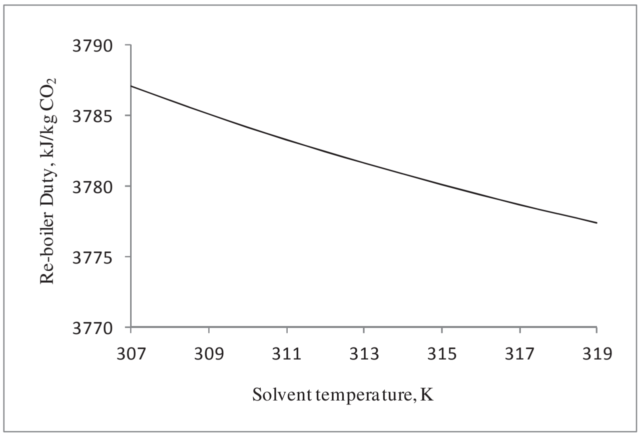

**Figure 11:** Re-boiler duty variation with flue gas temperature

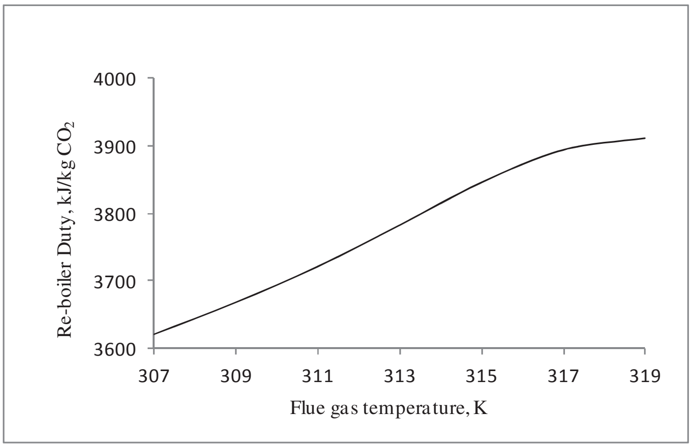

According to the Figure 11, re-boiler duty is increased with the flue gas temperature. The effect of stripper packing height and diameter is given in Figure 12 and 13. However, the effect on re-boiler duty is negligible compared to previous figures. In both cases, re-boiler duty is slightly decreasing with the packing height and diameter of stripper column.

**Figure 12:** Re-boiler duty variation with stripper packing height

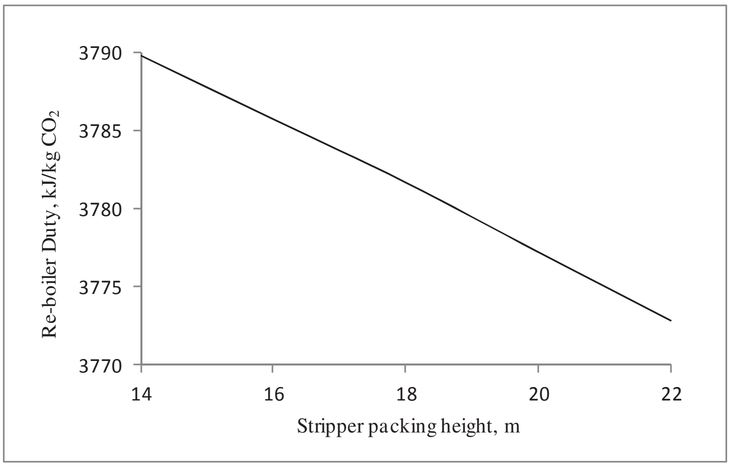

**Figure 13:** Re-boiler duty variation with stripper packing diameter

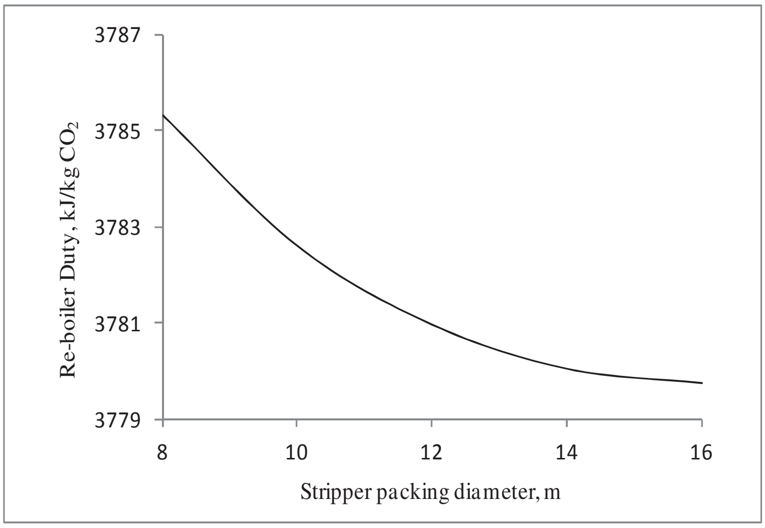

## 3. Complete $CO_2$ Removal Model

The $CO_2$ removal process models for 85%, 90%, and 95% efficiencies are implemented in Aspen Plus to check the exact re-boiler duty requirement. The closed-loop process model is developed with the re-circulating lean amine stream back to the absorber unit. Make-up stream is added with MEA and water to fulfill the losses during the process. The required removal efficiency is specified in the stripper distillate stream. Finally, temperature and $CO_2$ loading profiles in absorber column is analyzed to check the model performance. The required re-boiler duties are 3781, 4050, and 4240 kJ/kg $CO_2$ for 85%, 90%, and 95% removal efficiency models respectively. Figure 14-16 is shown liquid and vapor phase temperature profiles variation in absorber column.

**Figure 14:** Temperature profiles in absorber for 85% removal efficiency; symbols refer to ●, Liquid phase; ▲, Vapour phase

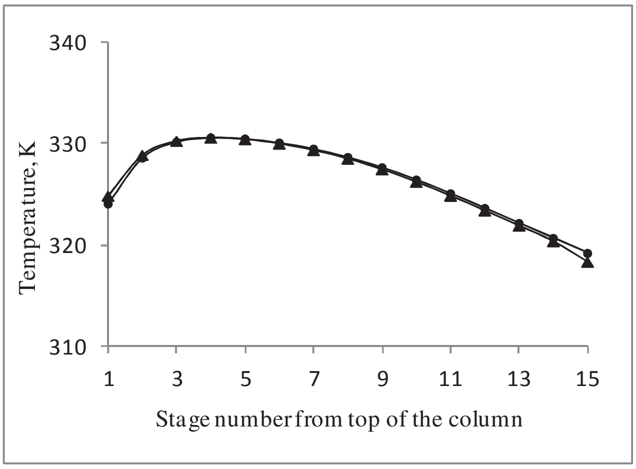

**Figure 15:** Temperature profiles in absorber for 90% removal efficiency; symbols refer to ●, Liquid phase; ▲, Vapour phase

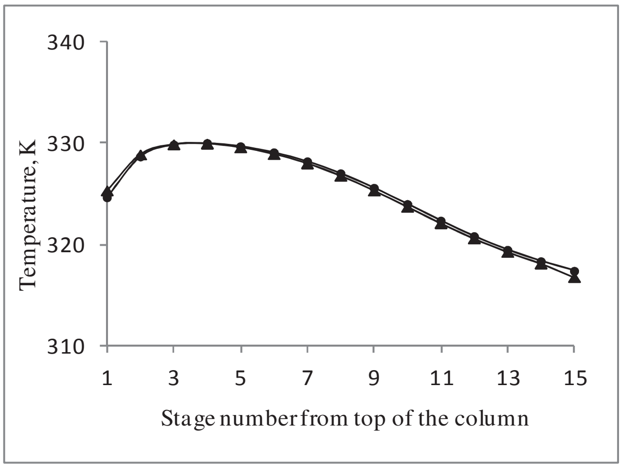

**Figure 16:** Temperature profiles in absorber for 95% removal efficiency; symbols refer to ●, Liquid phase; ▲, Vapour phase

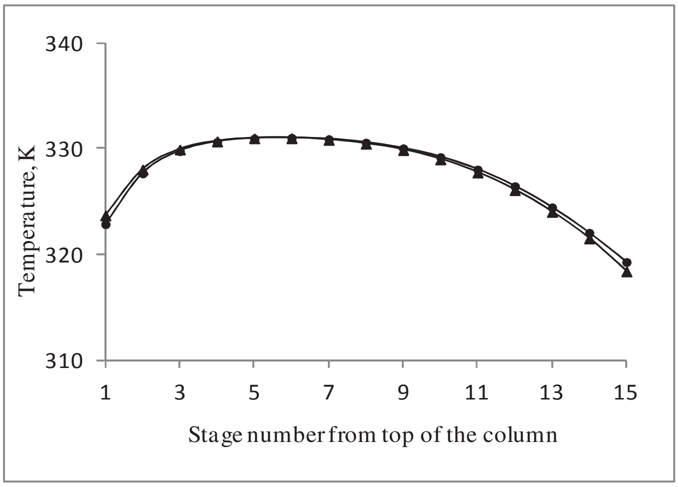

The maximum temperature is reached to 330K for both liquid and vapor phase models, and similar patterns are following in all three cases. Temperature bulge is shown in the top of the absorber column for all three models. Figure 17-19 is indicating that $CO_2$ loading profiles in absorber in liquid phase. The rich $CO_2$ loading is reached to around 0.45 mol $CO_2$/mol MEA.

**Figure 17:** $CO_2$ loading profiles in absorber for 85% removal efficiency

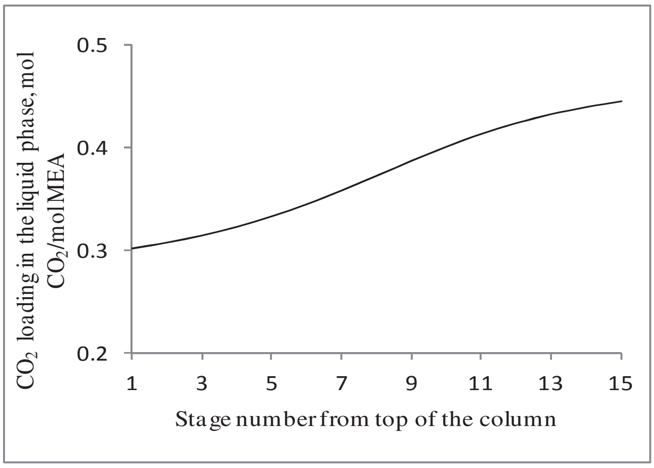

**Figure 18:** $CO_2$ loading profiles in absorber for 90% removal efficiency

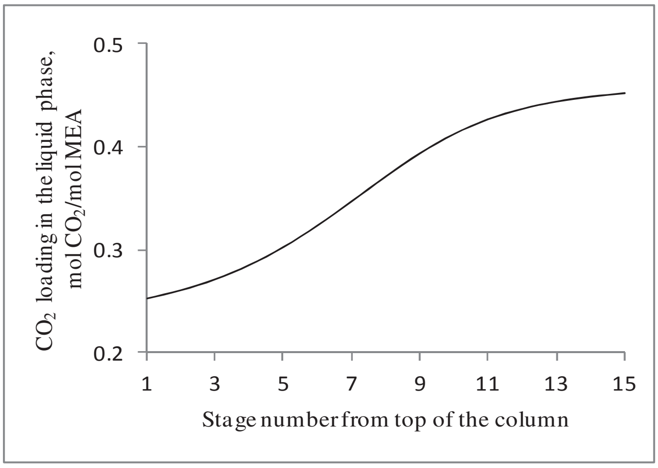

**Figure 19:** $CO_2$ loading profiles in absorber for 95% removal efficiency

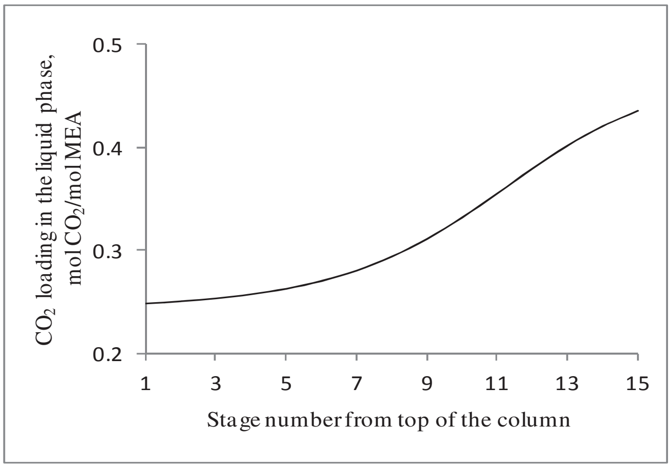

The required make-up stream is calculated and given in Table 7 for all three models. Compare to the inlet solvent stream in an open-loop model, a small amount of make-up flow is required to continue the process with re-circulation. When the removal efficiency is increased, required amount of make-up flow also increased.

**Table 7:** Compositions of make-up stream

| **Process Model** | **Amount of make-up stream** | |
|---|---|---|
| **Removal Efficiency (mol %)** | **Water (kg/s)** | **MEA (kg/s)** |
| 85 | 17.90 | 0.22 |
| 90 | 25.15 | 0.21 |
| 95 | 29.52 | 0.36 |

## 4. Conclusions

The implemented model is properly working for gas-fired power plant flue gas treating. Re-boiler duty values are given as 3781, 4050, and 4240 kJ/kg $CO_2$ for 85%, 90%, and 95% removal efficiency models respectively. Absorber packing height and diameter, absorber pressure, solvent and flue gas temperatures are positively effect on $CO_2$ removal efficiency. The packing height of absorber and stripper, solvent temperature and absorber pressure are negatively effect on re-boiler duty. The flue gas temperature has a slightly positive effect on re-boiler duty. Different types of packing materials effect on carbon capture process and regeneration energy requirement has to be analyzed in future studies.

## References

[1] Arachchige, U.S.P.R., Muhammad, M., Melaaen, M.C, 2012. "Optimization of post combustion carbon capture process-solvent selection", submitted to International Journal of Energy and Environment.

[2] Fluor for IEA GHG Program, 2004. Improvement in Power Generation with Post-Combustion Capture of $CO_2$, Final Report.

[3] Michael, A.D, 1989. "A model of vapor-liquid equilibria for acid gas-alkanolamine-water systems", PhD Thesis, University of Texas, USA.

[4] Freguia, S, 2002. "Modeling of $CO_2$ removal from Flue Gas with Mono-ethanolamine", Master Thesis, University of Texas, USA.

[5] Aspen Plus, 2008. " Rate Based model of the CO2 capture process by MEA using Aspen Plus", Aspen Technology Inc., Cambridge, MA, USA.

[6] Bravo, J.L., Rocha, J.A., Fair, J.R, 1985. "Mass Transfer in Gauze Packing", Hydrocarbon Processing January, pp. 91–95.

[7] Billet, R., Schultes, M, 1993. " Predicting Mass Transfer in Packed Columns", Chem. Eng. Technology, Vol. 16, p. 1.

[8] Arachchige, U. S. P. R., Aryal, N., Melaaen, M.C, 2011. " Case study for flue gas separation of a coal fired power plant and parameters' effect on removal efficiency", Proceedings of the APCRE'11 chemical engineering symposium, Beijing, China.

Paper L

# Model Development for CO2 Capture in the Cement Industry

This paper is published in the International Journal of Modeling and Optimization, 3, No. 6: 535-540, 2013.

International Journal of Modeling and Optimization, Vol. 3, No. 6, December 2013

# Model Development for $CO_2$ Capture in the Cement Industry

Udara S.P.R. Arachchige, Dinesh Kawan, Lars-André Tokheim, and Morten C. Melaaen

*Abstract*—**Climate change has become a prominent global issue due to human activities. One of the major green house gas emitting sources ($CO_2$) to the environment are considered as flue gases, which generated from process industries (coal and gas fired power plants, cement industry, etc.). In this study, a flue gas emission from a cement manufacturing process is considered for development of $CO_2$ capture plant. The cement industry emits approximately 5% of global man-made $CO_2$ emissions. Aspen Plus simulation tool is used for the development of the carbon capture model for three different removal efficiencies, 85%, 90% and 95%. Flue gas data related to the cement industry as well as process development parameters are taken from the literatures. Solvent concentration is varied from 25 to 40 (w/w %) and lean loading is varied from 0.15 to 0.35 (mole $CO_2$/mole MEA) for 85- 95 (mol %) $CO_2$ removal efficiency. Required re-boiler duties are calculated as 3229, 3306, and 3365 kJ/kg $CO_2$ (74, 80 and 86 MW) for 85%, 90% and 95% removal efficiencies, respectively.**

*Index Terms*—**Cement industry, carbon capture, Aspen Plus, post combustion, re-boiler duty**

## I. INTRODUCTION

The cement industry is considered as one of the major contributors of global anthropogenic carbon dioxide emissions [1]. The cement industry emits approximately 900kg of $CO_2$ per ton of cement produced, and the global cement demand is expected to increase by 60-110% by 2020 [2].

Typically 40% of the $CO_2$ comes from fossil fuel combustion in the kiln process, about 50% is due to de-carbonation of limestone ($CaCO_3$) to calcium oxide (CaO), and the remaining 10% is related to transportation and handling [3]. The process flow diagram of a typical cement manufacturing process is shown in Fig. 1.

The first section of the cement manufacturing process is the raw material (raw meal) preparation. The limestone from the quarry is transported to the raw meal processing area, where the limestone is first pre-crushed, whereupon the pre-crushed raw material is transferred to the grinding section to make a fine raw meal by dry or wet grinding. Most of the cement industry is currently using ball mills for this processing step. Raw meal homogenization, typically by air fluidization, is required before the meal is sent to the kiln section.

After homogenization (and intermediate storage), the raw meal is transferred to the second section, which is the kiln process. In the kiln system, the raw meal is first preheated in the pre-heater unit, consisting of several (typically 4-5) cyclones in series, to raise the temperature of the raw meal. The most modern kiln systems will also be equipped with a pre calciner which de-carbonates most of the calcium carbonate in the raw meal before it enters the rotary kiln at a temperature close to 900 °C. The pre-calciner will be located in-between the penultimate and the ultimate cyclone stage, and typically 60% of the supplied fuel will be combusted in the calciner, whereas about 40% will be combusted in the rotary kiln outlet. In a kiln system without a pre-calciner, most of the de-carbonation will take place in the rotary kiln instead. In the rotary kiln, the material temperature rises to about 1400 °C, and clinker minerals are formed. Finally, the hot clinker is cooled in a clinker cooler. Ambient air is used for cooling in the clinker cooler. Hot air from the cooler is then used as preheated combustion air in the rotary kiln, and in the pre-calciner, and the exhaust gas from the rotary kiln and the pre-calciner is further used to counter currently preheat the raw meal in the pre-heater tower. Downstream of the tower the exhaust gas is cooled and cleaned before being released to the stack.

The clinker produced in the kiln system is passed on the third section of the manufacturing process, the cement grinding plant. There, the clinker is mixed with gypsum and other additives and ground to the fine powder which is known as cement. Finally, the cement is packed and stored before being shipped to customers.

The global cement production has increased from 1043 to 2840 million tonnes per year in the last 20 years [5], see Table I [6].

TABLE I: AMOUNT OF CEMENT PRODUCTION PER YEAR [6].

| Country | Amount of cement production per year (million tonnes) |
|---|---|
| Brazil | 51.9 |
| China | 1390 |
| India | 177 |
| Japan | 62.8 |
| South Korea | 53.9 |
| Russia | 53.6 |
| Turkey | 51.4 |
| United states | 87.6 |
| Other countries | 911.8 |
| Total | 2840 |

It can be seen from 1 that it is chemically impossible to create CaO from $CaCO_3$without generating $CO_2$. Hence, primary measures to reduce $CO_2$ emissions from the cement manufacturing process are reduction in specific emissions by

---

Manuscript received June 4, 2013; revised August 23, 2013.

The authors are with the Telemark University College, Porsgrunn, Norway (e-mail: udara.s.p.arachchige@hit.no, kawandinesh@gmail.com).

Lars-André Tokheim is with the Telemark University College, Porsgrunn, Norway (e-mail: Lars.A.Tokheim@hit.no, Morten.C.Melaaen@hit.no).

DOI: 10.7763/IJMO.2013.V3.336

increasing the energy efficiency [7] and replacing fossil fuels with $CO_2$-neutral fuels [8].

$$CaCO_3 \rightarrow CaO + CO_2 \qquad (1)$$

The typical flue gas compositions are given in the following Table II [9].

TABLE II: TYPICAL FLUE GAS COMPOSITION IN CEMENT INDUSTRY FLUE GAS STREAM [9].

| Component | Concentration |
|---|---|
| $CO_2$ | 14-33% (w/w) |
| $NO_2$ | 5-10% of NOx |
| $NO_x$ | <200-3000 mg /Nm3 |
| $SO_2$ | <10-3500mg/Nm3 |
| $O_2$ | 8-14% (v/v) |

Post combustion chemical absorption is the well known technology for $CO_2$ capture in process industries. Post combustion capture studies have been performed for several applications related to the power generation. However, there are relatively few studies carried out for cement manufacturing processes.

Installing a $CO_2$ capture plant will generally not require significant modifications of an existing cement plant. However, the $SO_x$ and $NO_x$ have to be removed from the flue gases before sending it to the $CO_2$ capture plant. Otherwise, these pollutants will react with amines and form heat stable salts, which result in solvent degradation. The maximum $NO_x$ amount is around 20 ppmv, and $SO_x$ is indicated as 10 ppmv for successful $CO_2$ capturing [9]. A simplified process flow diagram of cement production process which includes $CO_2$ capture is shown in Fig. 2. The De-$NO_x$ process is typically carried out by selective non-catalytic reduction (SNCR) in the pre-calciner. The Electrostatic precipitator is indicated by ESP and should be prior to the De-SOx unit.

Since there are two sources for the $CO_2$ in the kiln exhaust gas (the de-carbonation and the combustion), the $CO_2$ concentration in the flue gas is quite high. Depending on where the exhaust gas is extracted or on the false air in leakage in the process, it will be in the range 14-33%. This is high compared to a coal fired power plant (around 12-15%) and indeed a gas fired power plant (around 4%). Therefore, $CO_2$ capture in the cement industry may as well give a correspondingly lower energy requirement. The main objective behind this study is to develop the model for $CO_2$ capturing in cement manufacturing process.

## II. MODEL DEVELOPMENT

In this paper, post combustion amine absorption of $CO_2$ in a cement manufacturing process is modeled with Aspen Plus. Amine concentrations and $CO_2$ lean loadings are varied to simulate the capture process with 85%, 90% and 95% removal efficiencies. After careful evaluation of the simulated results, suitable $CO_2$ concentrations and lean $CO_2$ loadings are selected for different operating efficiencies for the cement flue gas treating process. The amine concentration and $CO_2$ lean loading, which will give the lowest re-boiler duty are then selected. Absorber and stripper packing conditions and operating parameters related to the simulations are selected from the literature [10, 11]. Some of the information related to the absorber and stripper models are given in the Table III.

The flue gas data related to the cement manufacturing process for this study is taken from the literature [12] and given in the Table IV. The data is originated from one of the largest cement plants in Ontario, Canada.

The Aspen Plus simulation tool is used to simulate the $CO_2$ capture. The electrolyte NRTL model is used, and equilibrium and kinetic data, as well as, relevant chemical reactions are selected from the literature [15, 16] and implemented in the model.

TABLE III: INFORMATION RELATED TO THE ABSORBER AND STRIPPER MODELS [10, 11].

| Specification | Parameter values | |
|---|---|---|
| | Absorber | Stripper |
| Number of stages | 15 | 15 |
| Operating pressure | 1 bar | 1.9 bar |
| Re-boiler | None | Kettle |
| Condenser | None | Partial-vapour |
| Packing type | Mellapak, Sulzer, Standard, 350Y | Flexipac, Koch, metal,1Y |
| Packing height | 12m | 8m |
| Packing diameter | 6m | 4m |
| Mass transfer coefficient method [13] | Bravo et al. (1985) | Bravo et al. (1985) |
| Interfacial area method [13] | Bravo et al. (1985) | Bravo et al. (1985) |
| Interfacial area factor | 1.5 | 2 |
| Heat transfer coefficient method | Chilton and Colburn | Chilton and Colburn |
| Holdup correlation [14] | Billet and Schultes (1993) | Billet and Schultes (1993) |
| Film resistance | Discrxn for liquid film and Film for vapour film | Discrxn for liquid film and Film for vapour film |
| Flow model | Mixed | Mixed |

TABLE IV: FLUE GAS STREAM DATA USED FOR SIMULATION STUDIES [12].

| Parameter | |
|---|---|
| Temperature, °C | 160 |
| Pressure, bar | 1.013 |
| Mass flow, kg/hr | 304996 |
| Mole fraction | |
| $H_2O$ | 0.072 |
| $CO_2$ | 0.224 |
| $N_2$ | 0.681 |
| $O_2$ | 0.023 |

## III. OVERVIEW OF CAPTURE PROCESS

The amine based carbon capture process implemented in Aspen Plus is illustrated in Fig. 3. Basically, it consists of two unit operation blocks, an absorber column and a stripper column. The flue gas, which has been de-dusted in a bag filter before entering the $CO_2$ capture unit, is at a temperature of around 160°C. However, the suitable temperature for absorption of $CO_2$ in MEA is around 40°C. Therefore, the flue gas stream is cooled before entering the absorber. The COOLER-1 block is used for reduction of the temperature of flue gas stream to 40°C, and water generated during cooling is separated using a SEP (separator) unit as SEP-OUT.

A primary amine, monoethanolamine (MEA), is used as absorbent (solvent). MEA counter-currently reacts with the flue gas stream in the absorber column to capture the $CO_2$ in the flue gas- Next, the rich solvent is routed to the stripper column, where the $CO_2$ is released, and the solvent is regenerated. The main drawback of the MEA based $CO_2$ capture process is the high energy consumption in regenerating process. Hence, optimization of the regeneration process is required to obtain carbon capture with a lower energy usage.

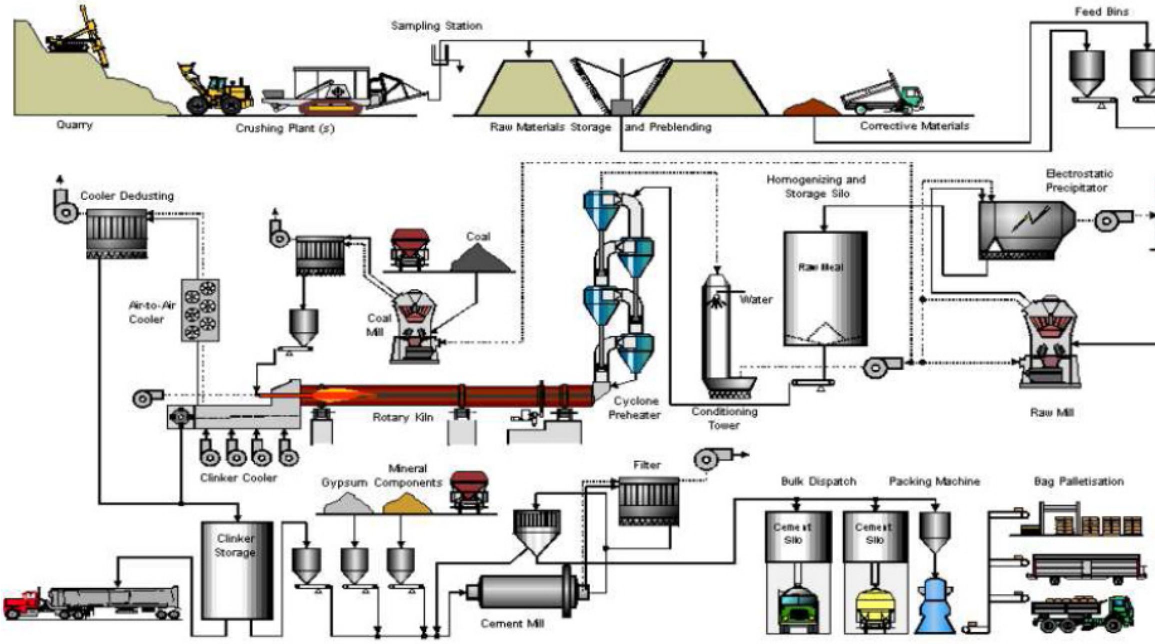

Fig. 1. Typical cement manufacturing process flow diagram [4].

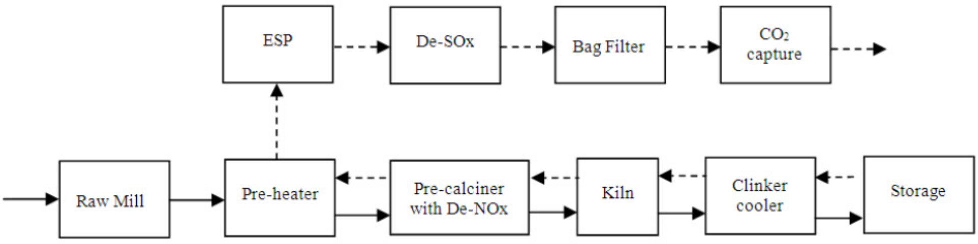

Fig. 2. Cement plant with CO2 capture unit ( material flow, gas flow).

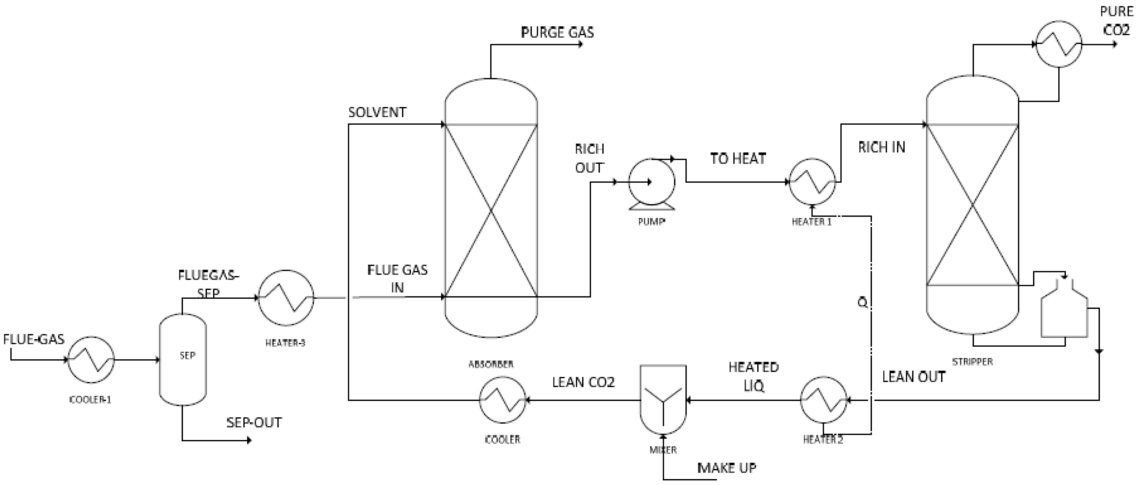

Fig. 3. Process flow diagram.

## IV. SIMULATIONS

Simulations are performed to select the suitable solvent concentration and $CO_2$ lean loading for different efficiencies. The solvent concentration is varied from 25 to 40 (w/w %), and the lean loading is varied from 0.15 to 0.35 mole $CO_2$/mole MEA for 85-95 $CO_2$ removal efficiency. Three different case studies are carried out to determine the best operating conditions. An open loop process flow diagram (without recycling back to the absorber) is used to develop the model with exactly 85, 90 and 95% removal efficiencies, respectively. The solvent flow rate is varied to get the exact amount of removal efficiency in the gas stream from the stripper.

Simulation results are given in the Fig. 4 (a, b, c represent the different removal efficiencies) with the variation of $CO_2$ lean loading.

According to Fig. 4 specific energy requirement in the re-boiler decreases with an increase in $CO_2$ lean loading until the minimum is obtained. The point which gives the lowest re-boiler energy can be defined as the optimum $CO_2$ lean loading. At the same time, the inlet solvent flow rate is varied to achieve the specified $CO_2$ removal efficiency. The efficiency range from 85 to 95% can be considered as good values for the removal process.

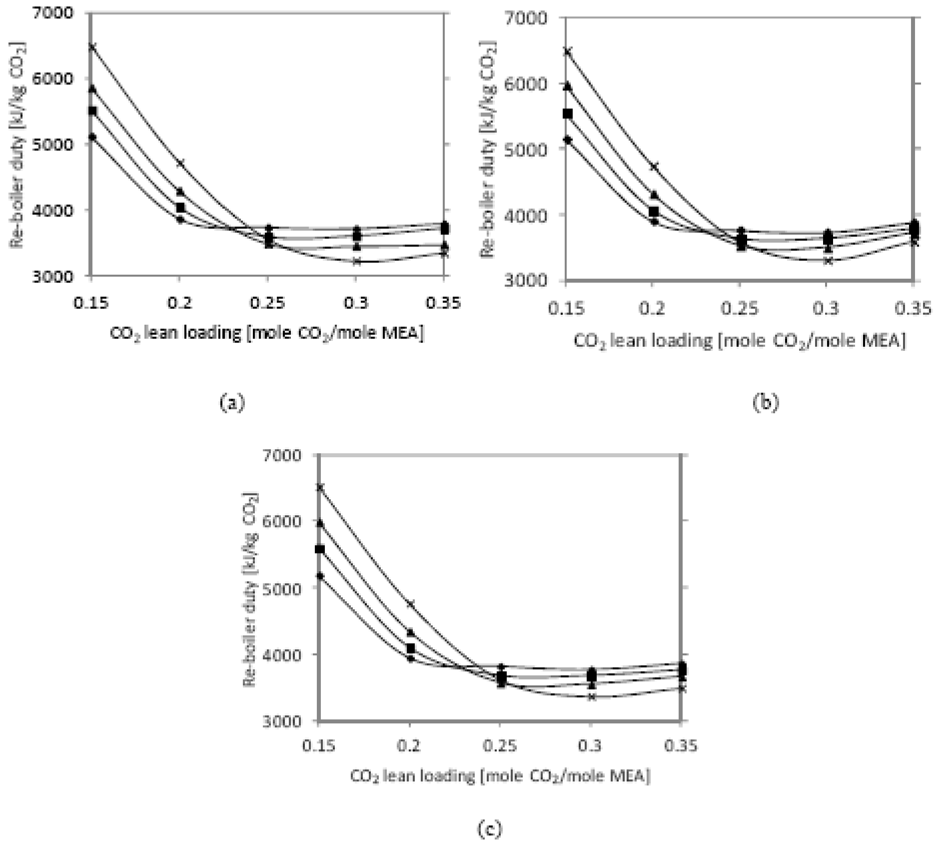

Fig. 4. Re-boiler duty variation with CO2 lean loading (a) 85% (b) 90% (c) 95% removal efficiencies, symbols refer to the MEA concentrations: ♦ , 25; ■, 30; ▲, 35; ×, 40 w/w%.

The overall re-generation energy in the stripper section represents 3 sub sections: the energy required to liberate the bonded $CO_2$, the sensible heat required to heat up the solvent and the energy needed for water evaporation. The contribution of all these three parts is varied with $CO_2$ lean loading [11]. The energy required to release the $CO_2$ is almost constant due to fix removal efficiency in the process. At the low values of $CO_2$ lean loading, amount of steam required is dominant. It means that, re-boiler energy consumption is increasing to produce extra steam. Therefore, with low $CO_2$ lean loading, re-boiler duty reaches higher value. At the high $CO_2$ lean loading, heating up of solvent flow rate is dominant, and re-boiler temperature will be increased for fulfilling that purpose. It will be the reason for reducing re-boiler energy requirement. However, with higher amount of $CO_2$ lean loading, inlet solvent flow rate is increasing. Therefore, heat required to increase the temperature of the solvent stream to stripper temperature is increasing. Therefore, after a certain limit, the total amount of heat requirement (re-boiler energy demand) is increasing.

The simulation results indicate that 40% MEA concentration and 0.30 $CO_2$ lean loading are the most suitable operating conditions for 85%, 90% and 95% $CO_2$ removal efficiencies. Due to the limitations in Aspen Plus data banks for amines, 40% MEA concentration is selected as upper bound for simulation studies. It can be seen that amine solutions with a higher $CO_2$ lean loading easily can be regenerated in the stripper with a lower re-boiler duty than with a lower $CO_2$ lean loading.

The absolute re-boiler duty (in MW) variation with $CO_2$ lean loading is given in Fig. 5, for the three different efficiencies. In those simulations, MEA concentration is maintained at 40 %.

Fig. 5 shows the effect of $CO_2$ lean loading on re-boiler duty for given flue gas data. The re-boiler duty decreases from 150 to 75 MW when the $CO_2$ lean loading is changed from 0.15 to 0.35 (85% removal efficiency). Simulations were performed for 85%, 90% and 95% $CO_2$ recovery with 98% $CO_2$ purity in the stripper exit gas. The specific re-boiler energy requirement is given in Table V for all the simulation studies. When calculating the cement-specific energy consumption, a literature value of 0.9 kg $CO_2$ per kg cement [2] has been applied.

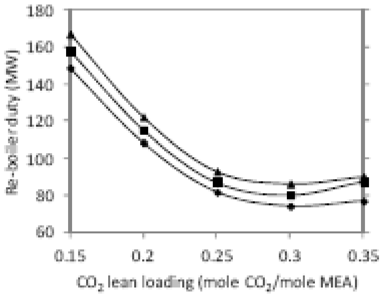

Fig. 5. Re-boiler duty variation with CO2 lean loading, symbols refer to the 3 different efficiencies: ♦ , 85%; ■, 90%; ▲, 95%.

TABLE V: RE-BOILER ENERGY REQUIREMENT.

| | (40% MEA concentration and 0.30 $CO_2$ lean loading) | |
|---|---|---|
| | Removal efficiency | Re-boiler duty |
| kJ/kg CO2 | 85% | 3229 |
| | 90% | 3306 |
| | 95% | 3365 |
| kJ/kg Cement | 85% | 2470 |
| | 90% | 2678 |
| | 95% | 2877 |

\ The re-boiler energy requirement for carbon capture process in the cement industry is 3229, 3306, and 3365 kJ/kg $CO_2$ for 85%, 90% and 95% removal efficiencies, respectively (40% MEA concentration and 0.30 $CO_2$ lean loading). A pinch analysis has to be performed for the cement industry, to find the excess energy availabilities through the process. It may be feasible to use some amount of excess energy to replace part of the re-boiler energy requirement.

The waste heat in the exhaust gas from cement kiln (outlet of the pre-heater tower) may be utilized by installing waste heat boilers downstream of the pre-heater. The temperature in the pre-heater outlet gas stream is around 350-450°C. This high temperature flue gas stream can, in some plants, be used to produce steam using waste heat boilers. The steam can then be used for solvent regeneration in an amine-based carbon capture plant. The waste heat in the cooler exhaust air may be utilized as well. The amount of available waste energy is mainly a function of gas flow rates and temperatures, and whether this heat is utilized for other purposes at the given plant. There are two main options for installing the carbon capture plant; either use the existing waste heat to replace part of the energy requirement in the stripper regeneration section while cleaning the entire exhaust gas stream; or clean only part of the exhaust gas while supplying all the energy required in the stripper. Waste heat utilization will reduce the investment and operational costs of the $CO_2$ capture plant. This scheme will be considered in future work.

It can be seen that the required solvent inlet flow rate is decreasing with an increase in MEA concentration for all cases. The solvent flow rate is increased to achieve higher removal efficiencies. When considering the removal efficiency, the lowest solvent requirement is given for the highest MEA concentration. Increasing the amine concentration may increase the corrosion in different sections of the capture plant. However, this can be counteracted by adding a small amount of corrosion inhibitor to the solvent stream and/or by using corrosion resistant materials instead of carbon steel. The presence of these inhibitors is supposed to have negligible effect on the $CO_2$ removal process.

## V. CONCLUSION

The Aspen Plus process simulation tool has been used with the electrolyte NRTL property method, to simulate $CO_2$ capture applied to a cement kiln flue gas. The $CO_2$ content in the cement flue gas was 22%, and 85%, 90% and 95% removal efficiencies were simulated. The optimum MEA concentration and $CO_2$ lean loading were selected as 40 w/w % and 0.30 (mol $CO_2$/mol MEA), respectively. The required re-boiler duty decreased with an increase in $CO_2$ lean loading. The re-boiler energy requirement for the carbon capture process was calculated to 3229, 3306, and 3365 kJ/kg $CO_2$ for 85%, 90% and 95% removal efficiencies, respectively. A De-NOx unit and a De-SOx unit must be installed upstream of the capture plant in order to reduce the concentrations of $NO_x$ and $SO_x$, respectively. Because of the relatively high $CO_2$ concentration in the in the cement kiln flue gas, $CO_2$ capture in the cement industry may be one of the most favorable solutions for reduction of $CO_2$ emissions and reduced global warming.

## REFERENCES

[1] IPPC, *Climate change 2001: the scientific basis*, Intergovernmental Panel on Climate Change, Cambridge University Press, Cambridge, UK, 2001.

[2] N. Mahasenan, S. Smith, and K. K. Humphreyys, "The cement industry and global climate change: current and potential future cement industry CO2 emissions," in *Proc. of the 6th International Conference on Greenhouse Gas Control Technologies*, Kyoto, Japan, October 2002.

[3] N. Mahasenan, R. T. Dahowski, and C. L. Davidson, "The role of carbon dioxide capture and storage in reducing emissions from cement plants in North America," Pacific Northwest national laboratory, 902 battelle blvd, Richland, USA, 2005.

[4] J. I. Bhatty, F. Miller, and S. Kosmatka, "Innovations in Portland Cement Manufacturing," Portland Cement Association, Illinois, USA, 2004.

[5] W. Shuangzhen and H. Xiaochun, "Sustainable Cement Production with improved energy efficiency and emerging $CO_2$ mitigation," *Advances in chemical engineering and science*, vol. 2, 123-128, 2012.

[6] H. G. V. Oss, "US and world CEMENT production 2008 and 2009," USGS online survey, 2010.

[7] L. A. Tokheim and P. Brevik, "Carbon dioxide emission reduction by increased utilization of waste-derived fuels in the cement industry," in *Proc. International Conference on Sustainability in the Cement and Concrete Industry*, Lillehammer, Norway, September 2007.

[8] L. A. Tokheim, "Kiln system modification for increased utilization of alternative fuels at Norcem Brevik," Cement International, No. 4, 2006.

[9] B. Adina, M. Ondrej, and E. O. John, "$CO_2$ capture technologies for cement industry," *Energy procedia*, pp. 133-140, 2009.

[10] A. Plus, *Rate Based model of the $CO_2$ capture process by MEA using Aspen Plus*, Aspen Technology Inc, Cambridge, MA, USA, 2008.

[11] A. Mohammad, "Carbon dioxide capture from flue gas," Ph.D Thesis, University of Delft, Netherland, 2009.
[12] H. S. M. Nazmul, "Techno-Economic study of CO2 capture process for cement plants," Master thesis, University of waterloo, Ontario, Canada, 2005.
[13] J. L. Bravo, J. A. Rocha, and J. R. Fair, "Mass Transfer in Gauze Packings,"*XCCCCC*, pp. 91-95, 1985.
[14] R. Billet and M. Schultes, "Predicting Mass Transfer in Packed Columns," *Chem. Eng. Technology*, vol. 16, pp. 16, 1-9, 1993.
[15] A. D. Michael, "A model of vapour-liquid equilibria for acid gas-alkanolamine-water systems," PhD Thesis, University of Texas, USA, 1989.
[16] S. Freguia, "Modeling of $CO_2$ removal from Flue Gas with Mono-ethanolamine," Master Thesis, University of Texas, Austin, USA, 2002.

**Udara S. P. R. Arachchige** received his B.Sc degree (2007) in chemical and process engineering from University of Moratuwa, Sri Lanka and M.Sc degree (2010) in energy and environmental engineering from Telemark University College, Porsgrunn, Norway. He is presently pursuing his Ph.D in carbon dioxide capture from power plants- modeling and simulation studies at Telemark University College. He has presented and published 14 papers in International Conferences and journals.

**Dinesh Kawan** received his B.E degree (2010) in electronics and communication engineering from Khwopa Engineering College, Purbanchal University, Nepal. He is presently pursuing his master degree in system and control engineering in Telemark University College, Porsgrunn, Norway.

He also working as a research assistant at faculty of Technology in same university college. Mr. Kawan has research interest on carbon capture, modeling and simulation, and control systems in process industries.

**Lars-André Tokheim** has a PhD degree in combustion (Telemark University College (TUC), Porsgrunn, Norway, 1999), a MSc degree in industrial environmental technology (TUC, 1994) and a BSc degree in chemistry (TUC, 1992). He is associate professor at TUC since 2006, where he teaches gas purification and heat & mass transfer, supervises MSc and PhD students, and coordinatesmaster study programmes in Process Technology and Energy & Environmental Technology as well as a PhD study programme in Process, Energy & Automation Engineering. He has industrial experience from Norcem/HeidelbergCement since 1994: as a research scholar (1994-1998), as a process engineer in the production department (1998-2001), and as head of department for process development and environmental matters (2001-2006). Prof. Tokheim's main research interests include use of alternative fuels in cement clinker production, calciner technology and gas pollution reduction, in particular $CO_2$ captureand $NO_x$ reduction.

**Morten Chr. Melaaen** is professor in process technology at Telemark University College, Porsgrunn, Norway. He is also the Dean of Faculty of Technology, Telemark University College and has a part time position at the local research institute Tel-Tek. Earlier, he has worked as a research engineer in Division of Applied Thermodynamics, SINTEF, Norway and as an Associate professor at Norwegian University of Science and Technology (NTNU).

He has worked on research projects as a Senior research scientist in Norsk Hydro Research Centre Porsgrunn, Norway. He started to work as a professor at Telemark University College in 1994 and became Head of Department, Department of Process, Energy and Environmental Technology in 2002. He received his MSc in Mechanical Engineering in 1986 and his Ph.D in 1990, both from NTNU. His research interests are $CO_2$ capture, modeling and simulation, fluid mechanics and heat and mass transfer. Professor Melaaen has more than 100 scientific papers published in the above mentioned related fields in international journals and conferences.

Paper M

# Impact of kiln thermal energy demand and false air on cement kiln flue gas CO2 capture

This paper is published in the International Journal of Energy and Environment, 5, No. 1: 45-52, 2013.

INTERNATIONAL JOURNAL OF
ENERGY AND ENVIRONMENT

*Volume 5, Issue 1, 2014 pp.45-52*
*Journal homepage: www.IJEE.IEEFoundation.org*

# Impact of kiln thermal energy demand and false air on cement kiln flue gas $CO_2$ capture

**Udara S. P. R. Arachchige[1], Dinesh Kawan[1], Lars-André Tokheim[1], Morten C. Melaaen[1,2]**

[1] Telemark University College, Porsgrunn, Norway.
[2] Tel-Tek, Porsgrunn, Norway.

## Abstract

The present study is focused on the effect of the specific thermal energy demand and the false air factor on carbon capture applied to cement kiln exhaust gases. The carbon capture process model was developed and implemented in Aspen Plus. The model was developed for flue gases from a typical cement clinker manufacturing plant. The specific thermal energy demand as well as the false air factor of the kiln system were varied in order to determine the effect on $CO_2$ capture plant performance, such as the solvent regeneration energy demand. In general, an increase in the mentioned kiln system factors increases the regeneration energy demand. The reboiler energy demand is calculated as 3270, 3428 and 3589 kJ/kg clinker for a specific thermal energy of 3000, 3400 and 3800 kJ/kg clinker, respectively. Setting the false air factor to 25, 50 or 70% gives a reboiler energy demand of 3428, 3476, 3568 kJ/kg clinker, respectively.

**Keywords:** Carbon dioxide capture; Cement; Flue gas; MEA; Reboiler duty.

## 1. Introduction

The emissions of carbon dioxide ($CO_2$) and other greenhouse gases (GHGs) need to be reduced in order to reduce global warming. The main sources of $CO_2$ emissions are power plants (coal and gas), the transport sector (burning fuel) and chemical industries (cement and aluminium). The most well established $CO_2$ capture technology is chemical absorption, in which $CO_2$ is absorbed in a solvent, such as an amine solution. The weak base amines are reacting chemically with $CO_2$ to form new chemical compounds. However the bonds are relatively weak, and therefore quite easily broken in a heating process [1]. Hence, the solvent can be regenerated in a desorber and then re-used in the absorber.

$CO_2$ capture related to the power plants has been in focus for some years. However, capture of $CO_2$ in the cement kiln process has not been widely considered. A model was previously developed for cement kiln flue gas $CO_2$ capture by the current authors [2]. A simple flowsheet illustrating a cement kiln system with $CO_2$ capture is shown in Figure 1.

The present study will focus on the impact of variable flue gas composition, due to variable kiln process energy demand and variable false air ingress, on the energy demand of the $CO_2$ capture process, more specifically on the required regeneration energy in the desorber.

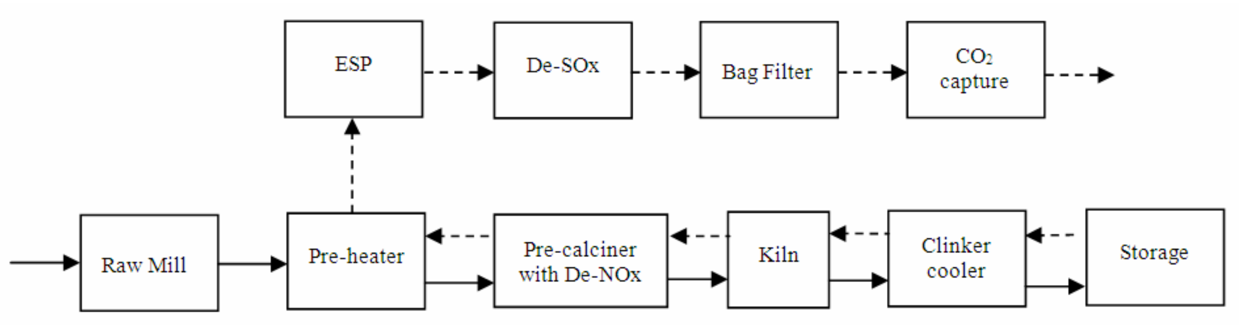

Figure 1. Cement plant with $CO_2$ capture unit

## 2. Model development

The schematic of a typical flue gas capture plant is shown in Figure 2. A detailed description of this process is given in a previous publication [3]. The flue gas leaving the upstream process is around 80°C and has to be reduced to 40°C before entering the capture process in order to improve the performance of the chemical absorption.

The flue gas composition is calculated for a generic cement manufacturing plant producing 1 Mt clinker per year and using coal as the thermal energy source (Table 1). The base case represents a typical modern precalciner cement kiln system, with a typical specific thermal energy demand of 3400 MJ/kg$_{\text{clinker}}$ and 25 % false air ingress, giving a typical exhaust gas composition and flow rate.

However, the exhaust gas composition (and flow rate) will be different if the specific thermal energy consumption of the kiln system is different. For example, the energy consumption may increase if the raw mix reactivity is low, meaning that more fuel will have to be combusted in order to give the same product quality [4]. Hence, to investigate the impact of the kiln energy demand on the $CO_2$ capture process, the specific thermal energy demand of the kiln system is varied from a very low value (3000 MJ/kg$_{\text{clinker}}$) to a value which is quite high (3800 MJ/t_$_{\text{clinker}}$) but still within a range that can be experienced in the cement industry.

The exhaust gas entering the capture plant will also be different if the the false air ingress in the preheater tower (and possibly also in downstream process equipment) is different. The false air ingress is due to the combination of under pressure operation (practically all modern kiln systems are operated with a suction) and unwanted leakage points in the preheater construction or in other process equipment units.Hence, in this study, the false air inleakage factor is varied from the base value via an intermediate value (50 %) to a very high value (70 %).

Collected and calculated data related to the cement manufacturing process are given in Table 1.

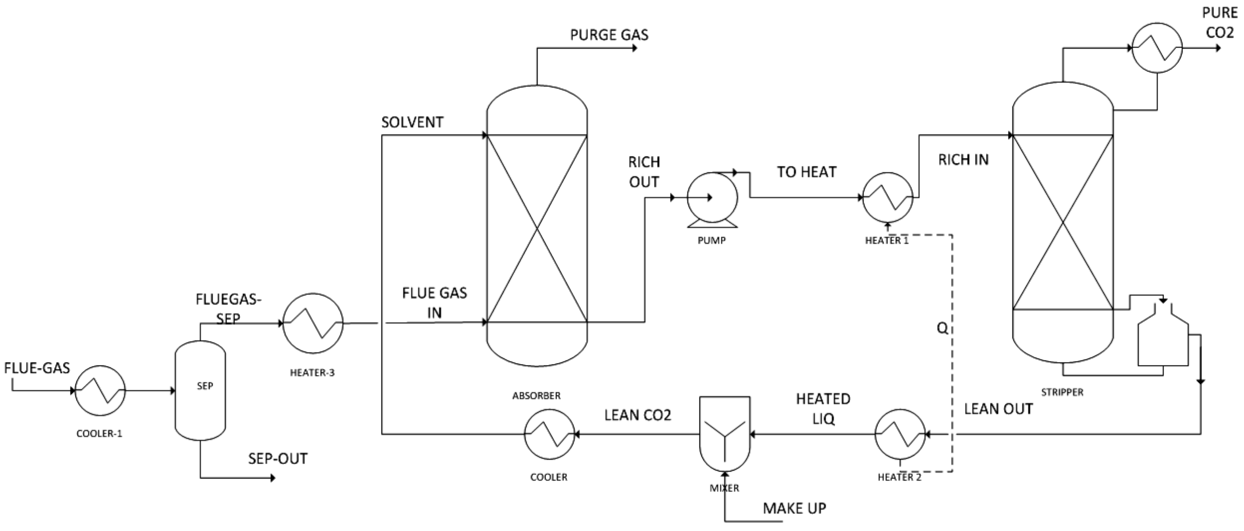

Figure 2. Process flow diagram

Table 1. Parameter values for the cement manufacturing process

| | | | **Specific thermal energy demand** | | | **False air factor** | | |
|---|---|---|---|---|---|---|---|---|
| **Description** | **Unit** | **Base case** | **3000 MJ/t_cli** | **3400 MJ/t_cli** | **3800 MJ/t_cli** | **25 %** | **50 %** | **70 %** |
| Clinker production rate | t/y | 1,000,000 | 1,000,000 | 1,000,000 | 1,000,000 | 1,000,000 | 1,000,000 | 1,000,000 |
| Fuel heating value | MJ/kg_fuel | 27.7 | 27.7 | 27.7 | 27.7 | 27.7 | 27.7 | 27.7 |
| Run factor | - | 85% | 85% | 85% | 85% | 85% | 85% | 85% |
| C in fuel | wt% | 71.8 % | 71.8 % | 71.8 % | 71.8 % | 71.8 % | 71.8 % | 71.8 % |
| H in fuel | wt% | 3.9 % | 3.9 % | 3.9 % | 3.9 % | 3.9 % | 3.9 % | 3.9 % |
| O in fuel | wt% | 5.9 % | 5.9 % | 5.9 % | 5.9 % | 5.9 % | 5.9 % | 5.9 % |
| S in fuel | wt% | 1.2 % | 1.2 % | 1.2 % | 1.2 % | 1.2 % | 1.2 % | 1.2 % |
| N in fuel | wt% | 1.7 % | 1.7 % | 1.7 % | 1.7 % | 1.7 % | 1.7 % | 1.7 % |
| Ash in fuel | wt% | 14.4 % | 14.4 % | 14.4 % | 14.4 % | 14.4 % | 14.4 % | 14.4 % |
| Moisture in fuel | wt% | 1.2 % | 1.2 % | 1.2 % | 1.2 % | 1.2 % | 1.2 % | 1.2 % |
| O2 demand | kg/kg_fuel | 2.18 | 2.18 | 2.18 | 2.18 | 2.18 | 2.18 | 2.18 |
| Specific air demand (stoich.) | kg/kg_fuel | 9.3 | 9.3 | 9.3 | 9.3 | 9.3 | 9.3 | 9.3 |
| Specific air supply | kg/kg_fuel | 10.3 | 10.3 | 10.3 | 10.3 | 10.3 | 10.3 | 10.3 |
| Run time | h/y | 7,446 | 7,446 | 7,446 | 7,446 | 7,446 | 7,446 | 7,446 |
| Fuel consumption | t/h | 16 | 15 | 16 | 18 | 16 | 16 | 16 |
| Air supply | t/h | 170 | 150 | 170 | 189 | 170 | 170 | 170 |
| N2 | Nm³/h | 122,552 | 109,300 | 122,552 | 135,805 | 122,552 | 159,115 | 232,240 |
| CO2 | Nm³/h | 59,708 | 57,109 | 59,708 | 62,306 | 59,708 | 59,708 | 59,708 |
| H2O | Nm³/h | 7,200 | 6,353 | 7,200 | 8,047 | 7,200 | 7,200 | 7,200 |
| O2 | Nm³/h | 7,374 | 6,816 | 7,374 | 7,932 | 7,374 | 17,093 | 36,531 |

The specific thermal energy of the kiln system, E [MJ/t_$_{\text{clinker}}$], is the product of fuel flow rate ($m_{fuelmix}$ [kg/s]) and fuel heating value ($H_{fuelmix}$ [MJ/kg]) divided by the clinker production rate ($m_{clinker}$ [kg$_{\text{clinker}}$/s]):

$$E = \frac{m_{fuelmix} H_{fuelmix}}{m_{clinker}} \tag{1}$$

The false air factor, $r_{\text{false}}$, is the ratio of the false air flow rate, $V^{n}_{false}$ [Nm³/h], and the flow of false air and kiln flue gas upstream of the kiln, $V^{n}_{kiln}$ [Nm³/h]:

$$r_{false} = \frac{V^{n}_{false}}{V^{n}_{false} + V^{n}_{kiln}} \tag{2}$$

Post combustion chemical absorption means using a solvent that has the capacity to absorb acidic gases ($CO_2$). The monoethanolamine (MEA) is the most prominent solvent that has been tested on pilot plants and is often used for experiments. MEA is a primary alkanolamine, R-$NH_2$, where R represents the alkyl group. The rate of reaction as well as the required heat for regeneration are crucial factors for selecting the solvent. The heat of absorption of $CO_2$ by MEA is considerably high. At the same time, MEA is characterized by a relatively high degradation rate, and it has a limited lean $CO_2$ loading. Even though MEA shows those drawbacks, it is considered as the reference solvent for $CO_2$ capture process. The reason for that is that a low partial pressure of $CO_2$ in the flue gas (typical of power plants as well as many industrial processes) can be handled due to the high reactivity of MEA towards $CO_2$ [5, 6].

The solvent concentration and lean $CO_2$ loading in the inlet solvent stream are selected as 30 wt% and 0.3 mol $CO_2$/mol MEA, respectively. In the $CO_2$ capturing process, typically primary and secondary amines form carbamate species ($RNH^{+}COO^{-}$) while reacting with $CO_2$. The basic reactions related to the absorption and stripping process follow the common style given in equation 3-4 [7]. Here, R indicates an alkyl group in primary amines.

$$CO_2 + RNH_2 \leftrightarrow RNH_2^+COO^- \tag{3}$$

$$RNH_2^+COO^- + RNH_2 \leftrightarrow RNH_2COO^- + RNH_2^+ \tag{4}$$

The type of packing and dimensions of packing material are important. Packed columns are used for the model development according to the previous studies. The Mellapak-Sulzer 350 Y is selected for the absorber, and Flexipak-1Y for the stripper, according to previous studies [8]. The most suitable column specification for model development is given in the Aspen Plus documentation [9] and in a quite recent PhD thesis [10].

## 3. Simulations

The Aspen Plus process simulation tool is used for the simulation studies. A base case model was first developed in Aspen Plus using data given in the base case column of Table 1. Then, four more cases were calculated, using data from the other columns of Table 1.

The absorber column configurations are selected according to the superficial gas velocity. By maintaining a superficial gas velocity in the absorber column of 2-3.5 m/s, flooding inside the column is avoided. The flue gas conditions that are used for the simulation studies are given in Table 2 (the percentages are based on the flow rate values given in Table 1).

Table 2. Flue gas stream parameters used for the simulations

| | | | **Specific thermal energy demand** | | | **False air factor** | | |
|---|---|---|---|---|---|---|---|---|
| **Description** | **Unit** | **Base Case** | **3000 MJ/t_cli** | **3400 MJ/t_cli** | **3800 MJ/t_cli** | **25 %** | **50 %** | **70%** |
| Preheater exhaust gas | Nm³/h | 196,834 | 179,578 | 196,834 | 214,090 | 196,834 | 243,116 | 335,679 |
| $N_2$ | vol% | 62.3 % | 60.9 % | 62.3 % | 63.4 % | 62.3 % | 65.4 % | 69.2 % |
| $CO_2$ | vol% | 30.3 % | 31.8 % | 30.3 % | 29.1 % | 30.3 % | 24.6 % | 17.8 % |
| $H_2O$ | vol% | 3.7 % | 3.5 % | 3.7 % | 3.8 % | 3.7 % | 3.0 % | 2.1 % |
| $O_2$ | vol% | 3.7 % | 3.8 % | 3.7 % | 3.7 % | 3.7 % | 7.0 % | 10.9 % |
| Temperature | °C | 80 | | | | | | |
| Pressure | bar | 1 | | | | | | |

The model is developed for 90% $CO_2$ removal efficiency. The solvent flow rate is varied to achieve exactly this removal efficiency for every case. The relevant flue gas composition and total flue gas flow rate are inserted for each simulation according to Tables 1 and 2.

Table 3 shows the parameter values for calculating superficial gas velocity inside the absorption column. For every simulation case, the diameter of the absorber column is maintained at 6m. Keeping the absorber column diameter constant and changing the superficial gas velocity is equivalent to allowing for a variation in the flue gas flow rate from the cement kiln while using the same (existing) capture equipment. Anyway, the simulations showed that the energy consumption of the fan downstream of the absorption column is almost negligible (< 1MW) compared to reboiler energy demand, even if the superficial gas velocity is incresed ,so the effect of flow rate on the fan power is actually not necessary to consider.

The regeneration energy demand and the solvent recirculation rate are given in Table 4. The required reboiler energy demand per kg $CO_2$ and per kg clinker is calculated.

Another set of simulations is performed for using a constant superficial gas velocity and instead adjusting the column diameter (Table 5). The simulated results are given in Table 6. The main idea of maintaining a constant superficial gas velocity is to obtain the same pressure drop over the absorber column in every case. This approach is more relevant in a design phase, when the equipment is still not in place. The column diameter is selected according to a superficial gas velocity of 2.52 m/s, which is within a velocity range 2-3.5 m/s, which can be considered as a typical operational range of packed absorption towers.

Table 3. Inlet gas conditions

| | | | Specific thermal energy demand | | | False air factor | | |
|---|---|---|---|---|---|---|---|---|
| **Description** | **Unit** | **Base Case** | **3000 MJ/t_cli** | **3400 MJ/t_cli** | **3800 MJ/t_cli** | **25 %** | **50 %** | **70%** |
| Preheater exhaust gas at 80°C | Nm$^3$/h | 196,834 | 179,578 | 196,834 | 214,090 | 196,834 | 243,116 | 335,679 |
| | m$^3$/h | 254483 | 232172 | 254482 | 276792 | 254482 | 314319 | 433992 |
| Preheater exhaust gas at 40°C | m$^3$/h | 207671 | 189462 | 207671 | 225880 | 207671 | 256524 | 354226 |
| Absorber diameter | m | 6 | 6 | 6 | 6 | 6 | 6 | 6 |
| Superficial velocity | m/s | 2.04 | 1.86 | 2.04 | 2.22 | 2.04 | 2.52 | 3.48 |

Table 4. Regeneration energy demand with constant absorber packing diameter

| | | | Specific thermal energy demand | | | False air factor | | |
|---|---|---|---|---|---|---|---|---|
| **Description** | **Unit** | **Base Case** | **3000 MJ/t_cli** | **3400 MJ/t_cli** | **3800 MJ/t_cli** | **25 %** | **50 %** | **70%** |
| Reboiler duty | MW | 107.7 | 102.5 | 107.7 | 113.2 | 107.7 | 110.2 | 113.1 |
| Amount of CO$_2$ captured | kg/s | 29.2 | 28.0 | 29.2 | 30.6 | 29.2 | 29.3 | 29.3 |
| Specific Reboiler duty | kJ/kg CO$_2$ | 3679 | 3655 | 3679 | 3700 | 3679 | 3753 | 3853 |
| | kJ/kg clinker | 3399 | 3233 | 3399 | 3571 | 3399 | 3476 | 3566 |
| Solvent flow rate | tonne/hr | 2770 | 2633 | 2770 | 2912 | 2770 | 2840 | 2927 |

Table 5. Inlet gas conditions and superficial gas velocity

| | | | Specific thermal energy demand | | | False air factor | | |
|---|---|---|---|---|---|---|---|---|
| **Description** | **Unit** | **Base Case** | **3000 MJ/t_cli** | **3400 MJ/t_cli** | **3800 MJ/t_cli** | **25 %** | **50 %** | **70%** |
| Preheater exhaust gas at 40°C | m$^3$/h | 207671 | 189462 | 207671 | 225880 | 207671 | 256524 | 354226 |
| Absorber diameter | m | 5.4 | 5.15 | 5.4 | 5.63 | 5.4 | 6 | 7.05 |
| Superficial velocity | m/s | 2.52 | 2.52 | 2.52 | 2.52 | 2.52 | 2.52 | 2.52 |

Table 6. Regeneration energy demand with equal superficial gas velocity

| | | | Specific thermal energy demand | | | False air factor | | |
|---|---|---|---|---|---|---|---|---|
| **Description** | **Unit** | **Base Case** | **3000 MJ/t_cli** | **3400 MJ/t_cli** | **3800 MJ/t_cli** | **25 %** | **50 %** | **70%** |
| Reboiler duty | MW | 108.7 | 103.7 | 108.7 | 113.8 | 108.7 | 110.2 | 113.2 |
| Amount of CO$_2$ captured | kg/s | 29.2 | 28.0 | 29.2 | 30.6 | 29.2 | 29.3 | 29.3 |
| Specific Reboiler duty | kJ/kg CO$_2$ | 3710.3 | 3697 | 3710 | 3719 | 3710 | 3753 | 3855 |
| | kJ/kg clinker | 3428 | 3270 | 3428 | 3589 | 3428 | 3476 | 3568 |
| Solvent flow rate | tonne/hr | 2795 | 2665 | 2795 | 2928 | 2795 | 2840 | 2925 |

The reboiler energy demand variation with those factors is shown in Figure 3. As can be seen from the figures, the regeneration energy is increasing with in increase in both factors (specific thermal energy and false air factor). However, the value of the regeneration energy demand increment with specific thermal energy demand is more or less negligible; the reboiler duty increases with only 0.4 % when increasing the thermal energy demand from 3000 to 3800 MJ/t$_{\_clinker}$. The reason why the impact is so small is that the CO$_2$ concentration in the flue gas inlet stream is almost the same in all cases. However, the thermal energy demand of the kiln system will affect the size of the absorption column, and hence have an impact on the investment costs.

The false air factor has more impact on the regeneration energy. An increase in false air from 25 to 70 % gives a reboiler duty increase of about 4 %, which is not negligible. The reason for this more severe impact is that the total gas flow rate drastically increases with an increase in the false air factor. Accordingly, the amount of gas that has to be purified in the capture plant increases.

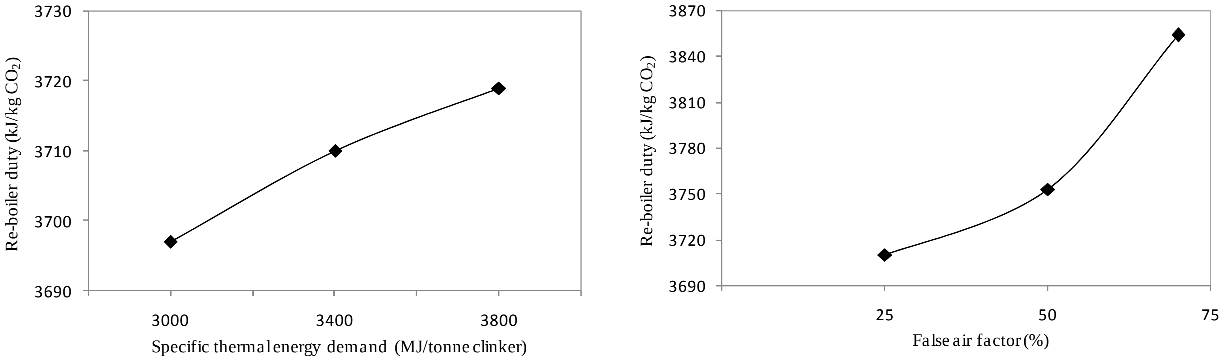

Figure 3. Reboiler duty variation with parameters; Left hand side figure is Re-boiler duty variation with specific thermal energy demand and right hand side is Re-boiler duty variation with false air factor

## 4. Conclusion

The simulations showed that a variation in specific thermal energy demand of the kiln process within a relatively wide range, applicable to real cement kiln systems, does not give a substantial impact on the operation of the $CO_2$ capture plant. However, increasing the false air ingress in the kiln system preheater from 25 to 70 % results in a 4 % increase in the reboiler duty. This indicates that false air ingress, which is a well-known phenomenon in the cement industry, should be kept low in order to reduced the energy consumption of the $CO_2$ capture plant. If, alternatively, the dimension of the absorber column in the capture plant is increased to allow for the higher gas flow rate resulting from an increase in thermal energy demand or false air, then that will lead to increased capital costs when constructing the capture plant. Hence, also for this reason, the false air ingress in the kiln system should be minimized.

## Nomenclature

| | |
|---|---|
| $m$ | mass flow rate [kg/s] |
| $V^n$ | normal volumentric flow rate [Nm$^3$/h] |
| H | lower heating value [MJ/kg] |

## References

[1] IPPC. Intergovernmental Panel on Climate Change (IPPC) special report on carbon dioxide capture and storage, Cambridge University Press, Cambridge, UK, 2005.

[2] Arachchige U.S.P.R., Kawan D., Tokheim L.A., Melaaen M.C. Model Development for CO2 capture in the cement industry, 2013, submitted to the International journal of engineering and technology.

[3] Arachchige U.S.P.R., Aryal N., Melaaen M.C. Case study for flue gas separation of a coal fired power plant and parameters' effect on removal efficiency, Proc. APCRE'11 chemical engineering symposium, Beijing, China, 2011.

[4] Ariyaratne, W.K.H., Melaaen, M.C. and Tokheim, L.-A. The effect of alternative fuel combustion in the cement kiln main burner on production capacity and improvement with oxygen enrichment, Proceedings, 3rd International Conference on Environmental Pollution and Remediation (ICEPR 2012), Johannesburg, South Africa, April 29-30, 2013

[5] Gabrielsen J., Svendsen H.F., Michelsen M.L., Stenby E.H., Kontogeorgis G.M. Experimental validation of a rate-based model for CO2 capture using an AMP solution. Chemical Engineering Science, 2007, Vol. 62, 2397-2413.

[6] Bae H.K., Kim S.Y., Lee B. Simulation of CO2 removal in a split-flow gas sweetening process. Korean J.Chem.Eng, 2011, Vol. 28 (3), 643-648.

[7] Freguia S. Modeling of CO2 removal from Flue Gas with Mono-ethanolamine. Master Thesis, University of Texas, USA, 2002.

[8] Arachchige U.S.P.R., Melaaen M.C. Selection of Packing Material for Gas Absorption. European Journal of Scientific Research, 2012, Vol. 87, No. 1, 117-126.

[9] Aspen Plus. Rate Based model of the CO2 capture process by MEA using Aspen Plus. Aspen Technology Inc, Cambridge, MA, USA, 2008.
[10] Mohammad A. PhD Thesis, University of Delft, Netherland, 2009.

**Udara S.P.R. Arachchige** received his B.Sc Degree (2007) in Chemical and Process Engineering from University of Moratuwa, Sri Lanka and M.Sc degree (2010) in Energy and Environmental Engineering from Telemark University College, Porsgrunn, Norway. He is presently pursuing his Ph.D in Carbon dioxide capture from power plants- modeling and simulation studies at Telemark University College. He has presented and published 14 papers in International Conferences and journals. His research interests are $CO_2$ capture, modeling and simulation, air pollution control and energy optimization.
E-mail address: udara.s.p.arachchige@hit.no

**Dinesh Kawan** received his B.E Degree (2010) in Electronics and Communication Engineering from Khwopa Engineering College, Purbanchal University, Nepal. He is presently pursuing his Master degree in System and Control Engineering in Telemark University College, Porsgrunn, Norway. He also working as a research assistant at faculty of Technology in same university college. Mr. Kawan has research interest on carbon capture, modeling and simulation, and control systems in process industries.
E-mail address: kawandinesh@gmail.com

**Lars-André Tokheim** has a PhD degree in combustion (Telemark University College (TUC), Porsgrunn, Norway, 1999), a MSc degree in industrial environmental technology (TUC, 1994) and a BSc degree in chemistry (TUC, 1992). He is associate professor at TUC since 2006, where he teaches gas purification and heat & mass transfer, supervises MSc and PhD students, and coordinatesmaster study programmes in Process Technology and Energy & Environmental Technology as well as a PhD study programme in Process, Energy & Automation Engineering. He has industrial experience from Norcem/HeidelbergCement since 1994: as a research scholar (1994-1998), as a process engineer in the production department (1998-2001), and as head of department for process development and environmental matters (2001-2006). Prof. Tokheim's main research interests include use of alternative fuels in cement clinker production, calciner technology and gas pollution reduction, in particular $CO_2$ captureand $NO_x$ reduction.
E-mail address: Lars.A.Tokheim@hit.no

**Morten Chr. Melaaen** is Professor in process technology at Telemark University College, Porsgrunn, Norway. He is also the Dean of Faculty of Technology, Telemark University College and has a part time position at the local research institute Tel-Tek. Earlier, he has worked as a research engineer in Division of Applied Thermodynamics, SINTEF, Norway and as an Associate professor at Norwegian University of Science and Technology (NTNU). He has worked on research projects as a Senior research scientist in Norsk Hydro Research Centre Porsgrunn, Norway. He started to work as a professor at Telemark University College in 1994 and became Head of Department, Department of Process, Energy and Environmental Technology in 2002. He received his MSc in Mechanical Engineering in 1986 and his Ph.D in 1990, both from NTNU. His research interests are CO2 capture, modeling and simulation, fluid mechanics and heat and mass transfer. Professor Melaaen has more than 100 scientific papers published in the above mentioned related fields in international journals and conferences.
E-mail address: Morten.C.Melaaen@hit.no

Paper N

# Waste heat utilization for CO2 capture in the cement industry

This paper is published in the International Journal of Modeling and Optimization, 4, No. 6: 438-442, 2014.

International Journal of Modeling and Optimization, Vol. 4, No. 6, December 2014

# Waste Heat Utilization for $CO_2$ Capture in the Cement Industry

Udara S. P. R. Arachchige, Dinesh Kawan, Lars-André Tokheim, and Morten C. Melaaen

*Abstract*—**The focus of this work is utilization of waste heat in a cement kiln flue gas in an amine-based $CO_2$ absorption process. The high temperature flue gas from the cement kiln is used to generate steam in a waste heat boiler. The steam is then used to replace some of the steam required in the stripping section of the $CO_2$ capture plant. The required surface area for heat exchange, the cost of installing this area and the payback time of the installation is calculated. The flue gas capture model was developed using the Aspen Plus simulation software. The available excess heat in the cement manufacturing process is calculated to 18 MW for the base case considered. The heat transfer area is calculated as 3115m$^2$. The total cost of the heat exchanger was $ 3.9 million, and the payback time is about 1 year, demonstrating the economic feasibility of applying heat integration when implementing an amine-based $CO_2$ capture process in a cement kiln system.**

*Index Terms*—**Carbon dioxide capture, waste heat boiler, flue gas, MEA, cement industry.**

## I. INTRODUCTION

The concentration of the atmospheric carbon dioxide ($CO_2$) has risen with the impact of the industrial revolution. The atmospheric $CO_2$ concentration is calculated as 380 ppmv approximately [1].

One of the main reasons for global warming is the huge impact of fossil fuel combustion in power plants, continuously contributing to the increase in atmospheric $CO_2$ concentration. However, also industry processes, such as aluminium, steel and cement production, contribute to $CO_2$ emissions.

Different technologies have been proposed for the purpose of carbon capture [2]. and post combustion chemical absorption is the more mature approach. Amine-based absorption of $CO_2$ from a cement kiln exhaust gas is considered in this study.

A sketch of a typical kiln system is shown in Fig. 1. The $CO_2$ is formed in two different processes.

The first Udara S. P. R. Arachchige, Dinesh Kawan, Lars-André Tokheim, and Morten C. Melaaen process is the calcination of calcium carbonate ($CaCO_3$) to produce calcium oxide (CaO). This process is called the process related $CO_2$ generation. The second source of $CO_2$ is the combustion of fossil fuels required to heat the kiln system to a sufficiently high temperature to facilitate the chemical reactions. The average carbon dioxide production of cement flue gas varies from 14 to 33% according to the raw material type and other factors [3].

The high energy penalty in the regeneration process is a main disadvantage of the $CO_2$ capture plant, and minimizing the amount of energy required in the stripper column is important. Therefore, heat integration plays a vital role in carbon capture processes. Such heat integration is possible when a capture plant is coupled with a cement kiln system.

The technical and economic feasibility of installing a waste heat boiler in the cement kiln system, for the purpose of supplying thermal energy to the capture plant, is the topic of this article.

## II. MODEL DEVELOPMENT

The flue gas data and other necessary information for model development are taken from the literature. The flue gas capture model is developed in the Aspen Plus simulation software. The $CO_2$ capture model was previously developed by the authors [4] and the flue gas characteristics from that study is used here as well. A detailed description of the model development and the parameters used in the model development is given in other articles [4], [5]. The flue gas data used to implement the carbon capture model is given in Table I [4], and the basic process flow diagram of the gas absorption process is given in Fig. 2.

TABLE 1: FLUE GAS STREAM DATA [4]

| Description | Unit | Base Case |
|---|---|---|
| Preheater exhaust gas | Nm³/h | 196,834 |
| $N_2$ | vol% | 62.3 % |
| $CO_2$ | vol% | 30.3 % |
| $H_2O$ | vol% | 3.7 % |
| $O_2$ | vol% | 3.7 % |

TABLE II: EXCESS HEAT AVAILABILITY IN THE WASTE HEAT BOILER [4]

| Description | Unit | Reference Case |
|---|---|---|
| Re-boiler duty | MW | 107.7 |
| Heat availability | MW | 18.0 |
| Percentage of available heat | % | 17 |

The temperature of the flue gas leaving the cement pre heater section is typically 350-400 °C, and downstream of the conditioning tower, the temperature is still around 150 °C. The required temperature in the absorption process, on the other hand, is only around 40°C, so the flue gas has to be cooled before it is sent to the capture section. The available

Manuscript received June 12, 2014; revised August 31, 2014.

The authors are with the Telemark University College, Porsgrunn, Norway (e-mail: udara.s.p.arachchige@hit.no, kawandinesh@gmail.com, Morten.C.Melaaen@hit.no, Lars.A.Tokheim@hit.no).

DOI: 10.7763/IJMO.2014.V4.414

excess heat in the kiln gas can be utilized by replacing the conditioning tower with a waste heat boiler downstream of the pre heater section.

The amount of waste heat available in the process is around 18MW for a calculated base case based on 350 and 150 °C inlet and outlet temperatures. The heat recovery unit should be installed as shown in the Fig. 3.

The steam produced in the waste heat boiler is transferred to the re-boiler unit of the stripper section in the $CO_2$ capture plant. The waste heat is not sufficient to cover the entire regeneration energy demand, but part of the energy can be replaced with energy generated in the waste heat boiler. The energy requirement in the stripper column as well as excess heat availability in the waste heat boiler is shown in Table II.

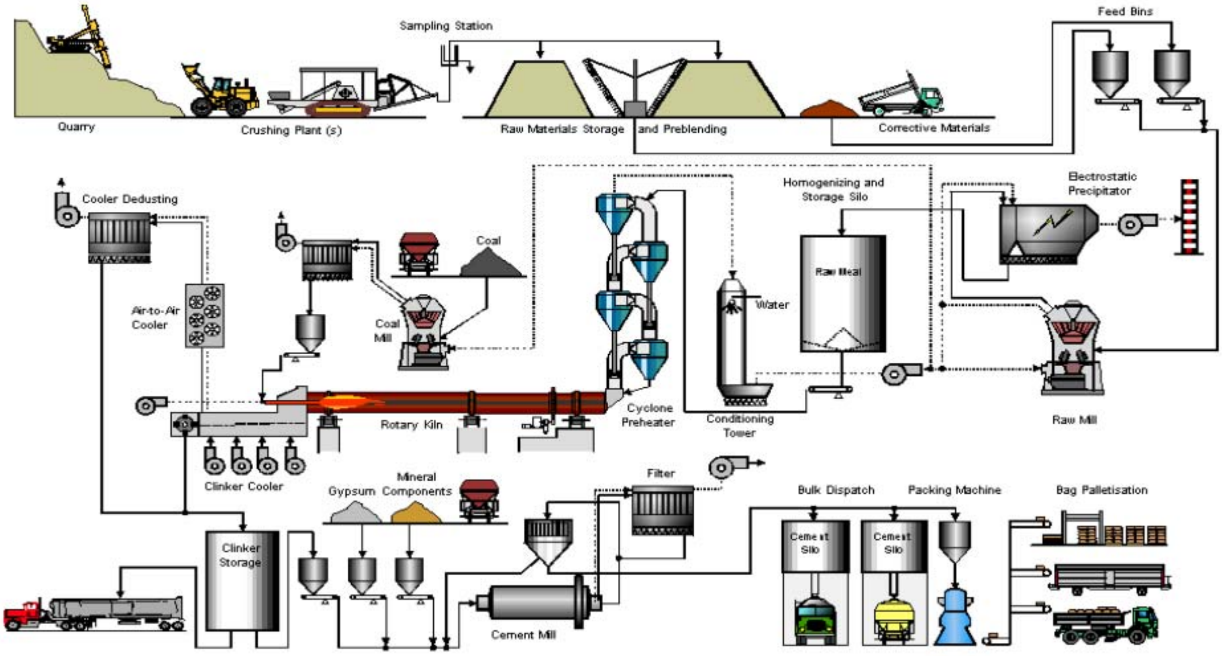

Fig. 1. Typical cement kiln system [6].

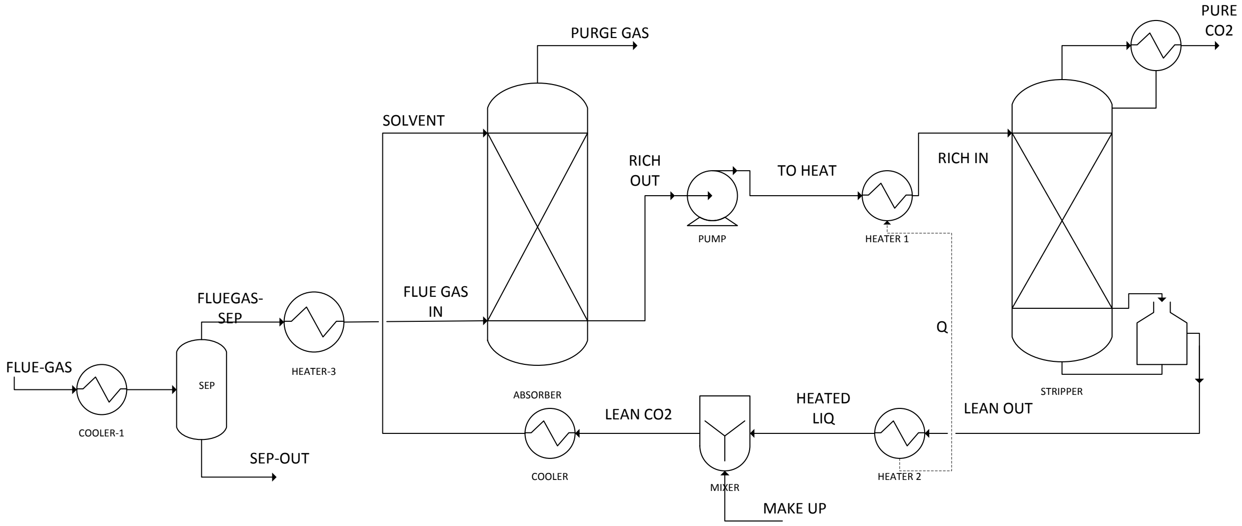

Fig. 2. Process flow diagram [4].

As described above, a significant amount of the required re-boiler energy can be provided by heat integration with the cement kiln process. However, the physical size as well as the installation costs and operational costs should be determined in order to evaluate the feasibility of such a waste heat boiler system. A brief description of the calculation procedure is given in the following section. The purpose of the calculation is to evaluate the required surface area of the cooling tubes to exchange the available heat in the flue gas and to use the heat exchange area as a basis for calculating the investment costs. Next, the payback time for the installation can be determined by calculating the savings in energy costs.

## III. HEAT TRANSFER AREA CALCULATION

The main steps in the calculation procedure are briefly discussed here. The calculation can be subdivided into four main parts:

- Evaluate the excess energy availability in the process.
- Calculate the required water flow rate for the heat exchange in the waste heat boiler.

- Calculate the overall heat transfer coefficient of the waste heat boiler.
- Calculate the required surface area for heat transfer.

The heat availability was calculated as 18MW in the simulation studies [4], [5], or simply carrying out a heat balance by hand calculations.

The required water flow rate can be calculated by a simple energy balance and is found to be 28862 kg/hr. The system has to operate at 120-130 °C and 2.5 bars to comply with the temperature requirements of the re-boiler.

The slightly superheated steam coming from the waste heat boiler has a temperature of 130°C and a pressure of 2.5 bar The steam is sent to the re-boiler, where it can replace 18% of the regeneration energy demand of the stripper. The steam condenses to water in the re-boiler, and water at about 120 °C is returned to the waste heat boiler where it is heated, converted to steam and slightly superheated, before being sent to the re-boiler for another cycle.

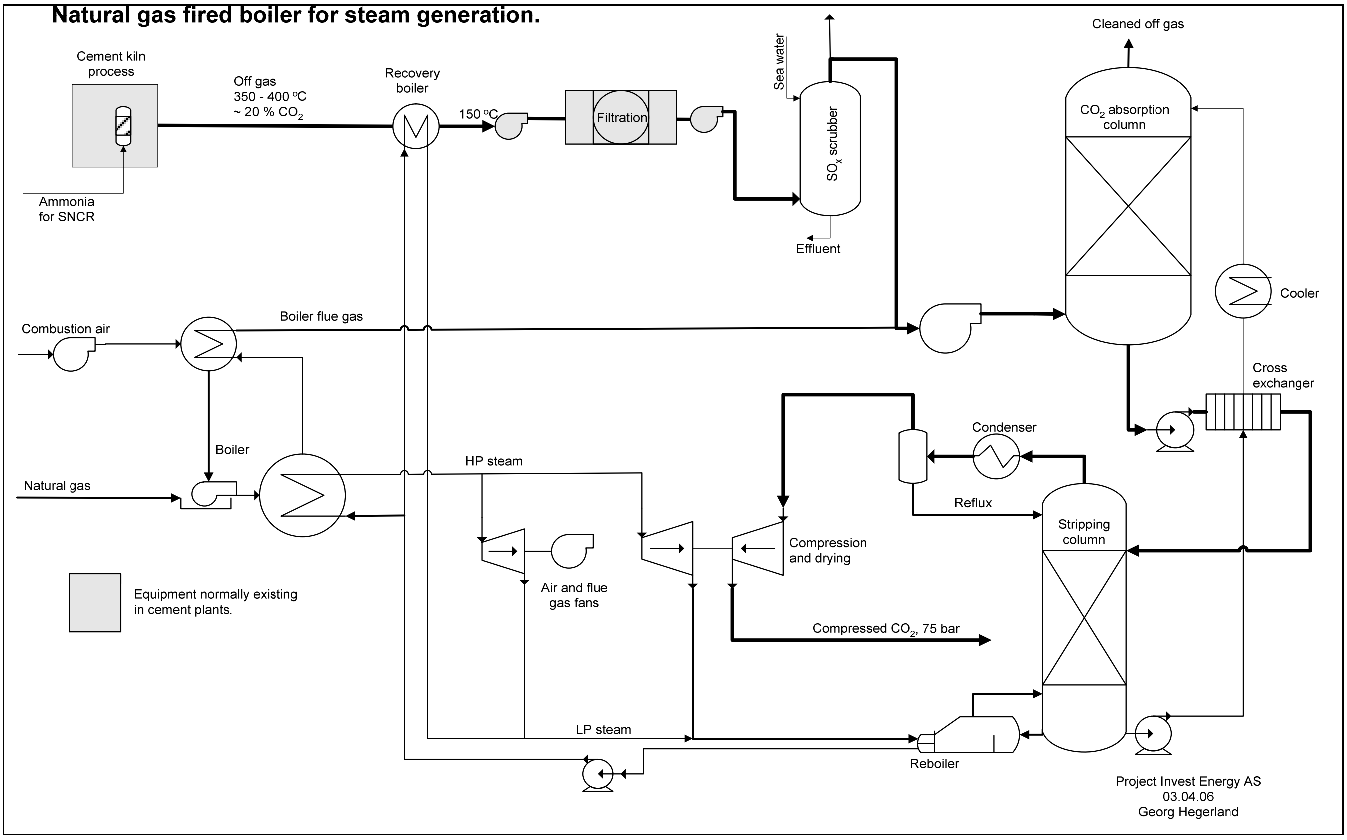

Fig. 3. Block diagram for NOx, **SOx** and CO$_2$ removal from cement plant off gases [7].

The overall heat transfer coefficient can be calculated by equation 1 [8].

$$U = \frac{1}{\frac{1}{h_1} + \frac{r_1}{k_A}\ln\frac{r_2}{r_1} + \frac{r_1}{k_B}\ln\frac{r_3}{r_2} + \frac{r_1}{r_4}\frac{1}{h_4}} \tag{1}$$

Here,

$h_1$= convection heat transfer coefficient for the water side [W/(m$^2$·K)]

$h_4$= convection heat transfer coefficient for the air side [W/(m$^2$·K)]

$r_1$=inner radius of the water tube [m]

$r_2$= outer radius of the water tube without dust layer [m]

$r_3$= outer radius of the water tube with dust layer [m]

$k_A$= thermal conductivity of the tube material [W/(m·K)]

$k_B$= thermal conductivity of the dust layer [W/(m·K)]

The convection heat transfer coefficient on the water side (inside the tubes) can be calculated by Nusselt number correlation.

The convection heat transfer coefficient on the gas side (outside the tubes) can be calculated by Nusselt number correlation.

Nusselt number correlation is given by: $Nu = \frac{h \times L}{k}$,

where, $Nu$=Nusselt number; $h$=convective heat transfer coefficient; $L$=Characteristic length; $k$ = thermal conductivity.

Input values used for the calculation are given in Table II, and the resulting overall heat transfer coefficient is 85 W/(m²·K).

TABLE III: INPUT VALUES FOR CALCULATION OF OVERALL HEAT TRANSFER COEFFICIENT

| Parameter | Unit | Value |
|---|---|---|
| Thickness of the water tube | mm | 2 |
| Thickness of the dust layer | mm | 2 |
| Diameter of the tube | mm | 10 |
| Flue gas inlet temperature | °C | 360 |
| Flue gas outlet temperature | °C | 140 |
| Water inlet temperature | °C | 120 |
| Water outlet temperature | °C | 134 |

The required area can be calculated from equation 2: $Q = UA(\Delta T)_{lm}$

The required surface area for heat transfer is calculated as 3115 $m^2$.

## IV. HEAT EXCHANGER COST CALCULATION

The area-specific capital cost of heat transfer water tubes, $C_P^0$, is taken as 140 $/$m^2$ [8]. The bare module cost of the heat exchanger, $C_{BM}$, is given by equation 2 [9].

$$C_{BM} = C_P^0 \left[ B_1 + B_2 F_M F_P \right] \tag{2}$$

Here,

$B_1$ and $B_2$ are constants taken as 1.63 and 1.66, respectively, for U - tube heat exchangers [9].

$FM$ = material factor, taken as 2.7 [9].

$FP$ = Pressure factor which is calculated from the equation 3 [9] given below.

$$\log_{10} F_P = C_1 + C_2 \log_{10} P + C_3 (\log_{10} P)^2 \tag{3}$$

Here,

$C_1$, $C_2$, $C_3$ are constants.

FP is calculated as 1 due to the low system pressure. The bare module cost is calculated as 856 $/$m^2$.

Total cost of heat exchanger is calculated as the product of the area and the area-specific cost, and is found to be $ 2,665,506. This value is calculated according to 2001 cost values and must be converted to 2014 data using relevant inflation factors. The total cost of heat exchanger for 2014 is then calculated as $ 3.9 million.

All direct and indirect costs related to the construction and installation of the heat exchanger unit is included in the bare module cost. Examples of direct costs are equipment cost, material cost and labor cost, and examples of direct cost are freight, overhead and engineering costs. The input values for calculation is given in the Table IV.

TABLE IV: INPUT VALUES FOR CALCULATION OF HEAT EXCHANGER COST

| Parameter | Value |
|---|---|
| B1 | 1.63 |
| B2 | 1.66 |
| FM | 2.7 |
| $C_P^0$ | 140 $/$m^2$ |

TABLE V: INPUT VALUES FOR CALCULATION OF STEAM COST

| Parameter | Value |
|---|---|
| Heating value of Methane [10] | 50 MJ/kg |
| Latent heat of steam | 2.26 MJ/kg |
| Energy loss | 15% |

## V. STEAM COST CALCULATION

The cost of the gas purchased for generating steam in regenerating process is around 1.1 NOK/$Sm^3$ according to the price at 2001[7]. The amount of energy can be replaced by installing waste heat boiler is calculated as 18 MW. The equivalent amount of steam recovered by installing waste heat boiler is calculated as 28862 kg/hr. The payback time period is calculated.

The input values used for calculation procedure is given in the Table V. Assume 15% of the energy losses during the heat transferring to steam generating.

Amount of steam generated by methane gas = 42.5 / 2.26 = 18.8 kg steam/ kg of gas.

Required amount of gas to generate steam recovery by waste heat boiler = 28862 / 18.8 = 1535 kg/hr (2326 $m^3$/hr).

Total amount of gas to generate amount of steam recovery per year (considering 7000 operating hours per year) = 16.28 million $m^3$.

Cost of the savings by steam recovery is around 26.4 million NOK / yr according to the current price. The equivalent amount of dollar is 4.4 million $.

The payback time period is approximately 10.5 months.

## VI. CONCLUSION

The amount of energy available in the cement kiln exhaust gas is around 18MW for case considered in this study. This will cover 18% of the total energy requirement in the stripper regeneration process. The equivalent amount of steam generated by installing a waste heat boiler in the cement kiln system is 28862 kg/hr. The required heat exchange area is calculated as 3115$m^2$. The total cost of the waste heat boiler installation is calculated as 3.9 million dollars. The installation cost for the waste heat boiler is paid back through a reduction in consumption in externally generated steam. The payback time is calculated approximately as 1 year. Therefore, heat integration with the cement kiln system by installing a waste heat boiler may be economically very attractive when implementing an amine-based carbon capture process in the cement industry.

## ACKNOWLEDGEMENT

The support of Nils Henrik Eldrup, clarifying possible improvements to obtain more accurate results and instructions to the calculation of equipment cost, is gratefully acknowledged.

## REFERENCES

[1] *Intergovernmental Panel on Climate Change (IPPC), Summary for policymakers, Climate Change 2007, The Physical Science Basis*, Cambridge University Press, 2007.

[2] L. Faramarzi, "Post- combustion capture of $CO_2$ from fossil fueled power plants," Ph.D thesis, Technical University Of Denmark, Denmark, 2010.

[3] K. Thambimuthu, J. Davison, and M. M. Gupta, "$CO_2$ capture and reuse," in *Proc. IPCC Workshop on Carbon Capture*, Regina, Canada, pp. 26-44, 2002.

[4] U. S. P. R. Arachchige, D. Kawan, L. A. Tokheim, M. C. Melaaen, "Impact of kiln thermal energy demand and false air on cement kiln flue gas $CO_2$ capture," *International Journal of Energy and Environment*, vol. 1, no. 5, pp. 45-52, 2014.

[5] U. S. P. R. Arachchige, D. Kawan, L. A. Tokheim, and M. C. Melaaen, "Model development for $CO_2$ capture in cement industry," *International Journal of Modeling and Optimization*, vol. 3, no. 6, pp. 535-540, 2013.

[6] J. I. Bhatty, F. Miller, and S. Kosmatka, "Innovations in Portland Cement Manufacturing," Portland Cements Association, Illinois, USA, 2004.

[7] G. Hegerland, J. O. Pande, H. A. Haugen, N. Eldrup, L. A. Tokheim, and L. M. Hatlevik, "Capture of $CO_2$ from a cement plant – technical possibilities and economical estimates," in *Proc. the 8th International*

*Conference on Greenhouse Gas Control Technologies: GHGT -8*, Trondheim, Norway, 2006.

[8] F. P. Incropera, D. P. Dewitt, T. L. Bergman, and A. S. Lavine, *Fundamentals of Heat and Mass Transfer*, John Wiley & Sons. Sixth edition. 2007.

[9] R. Turton, R. C. Bailie, W. B. Whiting, J. A. Shaeiwitz, and D. Bhattacharyya, "Analysis Synthesis and design of chemical processes," Pearson Education Inc. Fourth edition, 2013.

[10] International Energy Agency. Key World Energy Statistics. (2010). [Online]. Available: http://www.iea.org/textbase/nppdf/free/2010/key_stats_2010.pdf.

**Udara S. P. R. Arachchige** received his B.Sc degree (2007) in chemical and process engineering from University of Moratuwa, Sri Lanka and M.Sc degree (2010) in energy and environmental engineering from Telemark University College, Porsgrunn, Norway. He is presently pursuing his Ph.D in carbon dioxide capture from power plants-modeling and simulation studies at Telemark University College. He has presented and published 14 papers in international conferences and journals.

**Dinesh Kawan** received his B.E degree (2010) in electronics and communication engineering from Khwopa Engineering College, Purbanchal University, Nepal. He is presently pursuing his master degree in system and control engineering in Telemark University College, Porsgrunn, Norway.

He is also working as a research assistant at Faculty of Technology in same university college. Mr. Kawan has research interest in carbon capture, modeling and simulation, and control systems in process industries.

**Lars-André Tokheim** has a PhD degree in combustion (Telemark University College (TUC), Porsgrunn, Norway, 1999), a MSc degree in industrial environmental technology (TUC, 1994) and a BSc degree in chemistry (TUC, 1992). He is an associate professor at TUC since 2006, where he teaches gas purification and heat & mass transfer, supervises MSc and PhD students, and coordinatesmaster study programmes in Process Technology and Energy & Environmental Technology as well as a PhD study programme in Process, Energy & Automation Engineering. He has industrial experience from Norcem/HeidelbergCement since 1994: as a research scholar (1994-1998), as a process engineer in the Production Department (1998-2001), and as the head of Department of Process Development and Environmental Matters (2001-2006). Prof. Tokheim's main research interests include use of alternative fuels in cement clinker production, calciner technology and gas pollution reduction, in particular $CO_2$ captureand $NO_x$ reduction.

**Morten Chr. Melaaen** is a professor in process technology at Telemark University College, Porsgrunn, Norway. He is also the dean of Faculty of Technology, Telemark University College and has a part time position at the local research institute Tel-Tek. Earlier, he has worked as a research engineer in Division of Applied Thermodynamics, SINTEF, Norway and as an associate professor at Norwegian University of Science and Technology (NTNU).

He has worked on research projects as a senior research scientist in Norsk Hydro Research Centre Porsgrunn, Norway. He started to work as a professor at Telemark University College in 1994 and became Head of Department, Department of Process, Energy and Environmental Technology in 2002. He received his MSc in Mechanical Engineering in 1986 and his Ph.D in 1990, both from NTNU. His research interests are $CO_2$ capture, modeling and simulation, fluid mechanics and heat and mass transfer. Professor Melaaen has more than 100 scientific papers published in the above mentioned related fields in international journals and conferences.

Paper O

# Simulation of carbon dioxide capture for aluminium production process

This paper is published in the International Journal of Modeling and Optimization, 4, No. 1: 43-50, 2014.

# Simulation of Carbon Dioxide Capture for Aluminium Production Process

Udara S. P. R. Arachchige, Dinesh Kawan, and Morten C. Melaaen

*Abstract*—**A carbon capture process model was developed for the flue gas from aluminium production process. There are four different cases, which were considered for the simulation studies in Aspen Plus process simulation tool. Several $CO_2$ concentrations, 3, 4, 7 and 10 vol%, in the flue gas from the aluminium production is investigated. The required re-generation energy in the stripper section is in the range of 3.0 - 3.5 MJ/kg $CO_2$ for 85% removal efficiency and 3.2 - 3.5MJ/kg $CO_2$ for 90% removal efficiency and 3.4 - 3.6MJ/kg $CO_2$ for 95% removal efficiency. It can be clearly seen that, (58-65)%, (67-75)%, (61-67)% and (52-60)% of energy requirement of case I, II, III and IV (3%, 4%, 7% and 10% of $CO_2$ in the flue gas) can be replaced by available heat for replacing the re-generation process. According to the present study, it can be stated that, 4% $CO_2$ content in the flue gas is given the optimum available heat to replace the maximum amount of energy requirement in re-generation process.**

*Index Terms*—**Aluminium, carbon capture, flue gas, post combustion, re-boiler duty.**

## I. INTRODUCTION

The level of green house gases in the atmosphere has rapidly risen after the industrial revolution. The principle gases associated with climate change are considered as carbon dioxide ($CO_2$), methane ($CH_4$), and nitrous oxide ($N_2O$), which accounts for 99% of global green house gas (GHG) emissions in the atmosphere [1]. Carbon dioxide is considered as the main green house gas due to the huge amount of emission to the atmosphere. The global concentration of $CO_2$ in the atmosphere has been approximately increased from 280 parts per million by volume (ppmv) in 1830 to 316 ppmv in 1958, and then rapidly increased to 369 ppmv in 2005 and predicted to be increased to 750 ppmv in 2100 if there will not be any action taken in to consideration [2].

Stabilizing the concentration of atmospheric acid gases, mainly carbon dioxide ($CO_2$) will require massive reduction in $CO_2$ emissions from flue gases. Alternative fuels that produce less carbon or no carbon will take several decades to reach to fulfill the demand of energy requirement. Carbon capture and sequestration (CCS) are the only means of reducing $CO_2$ emissions in the near term future. The leading carbon emitting sources can be defined as large scale electrical power generating plants (coal and gas fired power plants) and process industries (cement, steel, aluminum, etc.) [1].

However, $CO_2$ capturing technologies require a substantial amount of energy to isolate the captured $CO_2$. The energy required for separation of flue gases lowers the overall efficiency of the power generating process or production process. Therefore, reduction of energy penalty for $CO_2$ capture process is prime importance to implement the technology in industrial applications.

The basic idea behind this study is to develop and implement the $CO_2$ capture model for flue gas from aluminium production plant. Aluminium is the second most commonly used metal in the world [3]. The most notable use of aluminium is in transportation and construction sections, and it will cover more than half of the total consumption.

The task is to find the optimal solvent concentration and lean $CO_2$ loading to capture the $CO_2$ from flue gas stream with lowest re-boiler energy requirement. At the same time, the most crucial parameter values regarding to carbon capture will be calculated. Flue gas properties were taken from Hydro aluminium manufacturing plant located in Norway. The $CO_2$ capture process is going to be simulated in Aspen Plus with Monoethanolamine (MEA) as the absorption medium in the capture plant. Several $CO_2$ concentrations, 3, 4, 7 and 10 vol%, in the flue gas from the aluminium production will be investigated. Finally, according to the simulated results, percentage of optimum $CO_2$ concentration in the flue gas will be concluded.

## II. ALUMINIUM PRODUCTION PROCESS

Aluminium compounds can be found in all types of clay, but the most useful ore that can be used to produce aluminium is bauxite. Aluminium is manufactured in two phases: the Bayer process (chemical process) and Hall-Heroult process (electrolytic process). The Bayer process is used to refine the bauxite ore to obtain aluminium oxide while the Hall-Heroult process of smelting the aluminium oxide to release pure aluminium. It takes about 4 kg of bauxite to produce 1 kg of aluminium. Flow diagram of the aluminium production is given in Fig. 1. In the first step of the process, sodium aluminate solution is produced by dissolving the already washed bauxite in caustic soda (sodium hydroxide) solution at high temperature and pressure. The sodium aluminate solution containing undissolved bauxite residues of iron, silicon and titanium. The impurities are removed by settling process and resulting clear sodium aluminate solution is transfer to a precipitator to extract particles of pure alumina. Further processing is taken to remove the chemically combined water and finally end with pure alumina. The produced alumina is dissolved in an electrolytic cryolite bath

Manuscript received September 20, 2013; revised November 28, 2013.

The authors are with the the Telemark University College, Porsgrunn, Norway (e-mail: udara.s.p.arachchige@hit.no, kawandinesh@gmail.com, Morten.C.Melaaen@hit.no).

DOI: 10.7763/IJMO.2014.V4.345

within a large carbon or graphite lined steel pot. An electric current is passed through the electrolyte at low voltage and high current to produce molten aluminium [4].

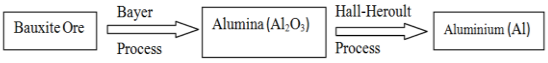

Fig. 1. Aluminium process flow diagram.

The overall chemical reaction of aluminium production is given in 1.

$$2Al_2O_3 + 3C \leftrightarrow 4Al + 3CO_2 \tag{1}$$

Due to the melting point of the cryolitic solution, the operating temperature of the process is close to 1000 ℃. To maintain the temperature rising in the cell, the process is cooled by an air flow above the cryolitic solution. Because of cooling air mixed with waste gases like $CO_2$, $SO_2$ and other impurities released from the cell, process gas is generated and transported from the cell. The waste gas components ($CO_2$, $SO_2$, HF, PM, etc.) are removed by flue gas treatment unit before released to the atmosphere. To introduce the $CO_2$ capture unit for aluminium production process, aluminium cell technology has to be modified. In the Hall-Heroult process illustrated in the Fig. 2, $CO_2$ formed at the carbon anode is mixed with the cooling air supply to the system. The large volumetric air flow drop down the $CO_2$ concentration to 1 vol% approximately [5].

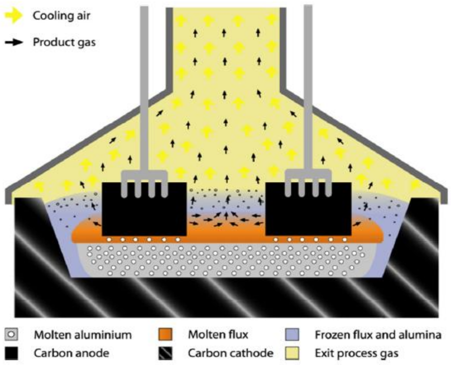

Fig. 2. Cross sectional view of the current generation of cells using the Hall-Heroult process for aluminium production [5].

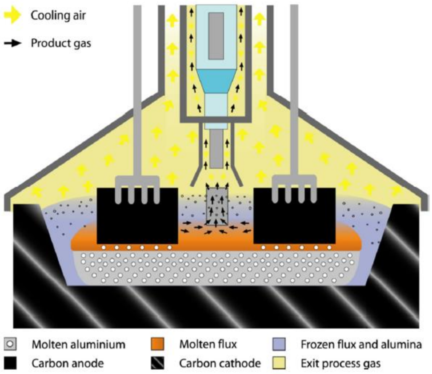

Fig. 3. Cross sectional view of the HAL Ultra cell with separate collector for product gas [5].

Due to the low $CO_2$ concentration in the high flue gas flow rate, size of the capture plant will obviously be large, and that will be an impact on aluminium production cost. Therefore, to reduced impact on production cost, volumetric concentration of $CO_2$ has been increased by modifying the cell in Hydro aluminium plant. The modified cell is shown in Fig. 3. As shown in the figure, new process gas collector is introduced by reducing the gas flow rate. That will reduce the total amount of process gas release to the flue gas treatment unit. This will help to increase $CO_2$ concentration.

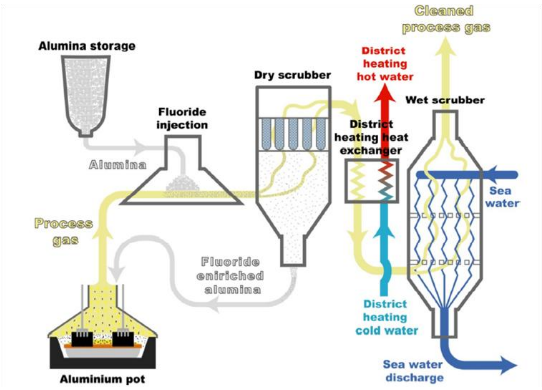

Fig. 4. The flow sheet of the process gas treatment [5].

The process gas treatment unit is in the aluminium production plant are given in the Fig. 4. It consists of several unit operation blocks to remove, $SO_2$, HF, PM and for de-dusting, as well. The cleaned gas leaving the wet scrubber can be used as an inlet of the $CO_2$ capture unit. However, there may be some additional unit operations needed prior to the $CO_2$ capture unit. As an example, cyclone unit to remove additional dust and additional scrubbers to remove unwanted sulphur compounds.

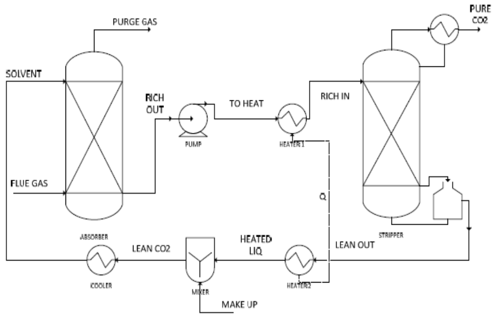

Fig. 5. Process flow diagram.

## III. MODEL DEVELOPMENT

The main fields of environmental implications from aluminium production relates to the smelting, electrolysis and production process. The principal inputs to the aluminum smelting process can be stated as alumina, aluminum fluoride, carbon (as anodes) and electricity and the principal outputs are aluminum metal, $CO_2$, and some solid wastes. A greenhouse gas (GHG) like $CO_2$ is believed to contribute to climate change by increasing the ability of the atmosphere to trap heat.

According to the main chemical reaction of aluminium process, the emissions of $CO_2$ have to be considered to maintain the environmentally friendly operation. The flue gas emission from aluminium production plant is considered for the simulation studies. There are four different compositions are considered to check the best $CO_2$ content in the flue gas to be optimized for the capture process (Table I).

The basic process of $CO_2$ capture consists of absorber and stripper units. The flue gas, which contains $CO_2$, is flowing upward the absorber column while solvent is counter currently flowing downward. The loaded solvent is pumped to a stripping section where $CO_2$ is generated with high temperature steam. The bottom flow of the stripper is recycling back to the absorber unit through a heat exchanger which cools the hot solvent stream and preheats the rich solvent flowing to the stripper unit. The majority of the energy demand in carbon capture process is consumed for heating the rich solvent in the stripper column. Fig. 5 shows the basic process flow diagram for post combustion carbon capture.

TABLE I: FLUE GAS DATA OF ALUMINIUM PRODUCTION PROCESS

| Flue gas composition (vol %) | | | | Flow rate (tonnes/hr) | Temperature (℃) | Pressure (bar) |
|---|---|---|---|---|---|---|
| $CO_2$ | $O_2$ | $H_2O$ | $N_2$ | | | |
| 3 | 20.7 | 1.0 | 75.3 | 403.6 | 225 | 1.1 |
| 4 | 20.0 | 0.9 | 75.1 | 304.2 | 265 | 1.1 |
| 7 | 19.4 | 0.6 | 73.0 | 176.7 | 329 | 1.1 |
| 10 | 18.8 | 0.3 | 70.9 | 125.7 | 365 | 1.1 |

TABLE II: ABSORBER PACKING DETAILS

| | Packing height in the Absorber (m) | | | | | | Packing diameter in the Absorber (m) | | | | | |
|---|---|---|---|---|---|---|---|---|---|---|---|---|
| $CO_2$ vol% | MEA 30% | | | MEA 40% | | | MEA 30% | | | MEA 40% | | |
| | 85% | 90% | 95% | 85% | 90% | 95% | 85% | 90% | 95% | 85% | 90% | 95% |
| 3 | 24 | 24 | 24 | 24 | 24 | 24 | 7 | 7 | 7 | 7 | 7 | 7 |
| 4 | 24 | 24 | 24 | 24 | 24 | 24 | 6 | 6 | 6 | 6 | 6 | 6 |
| 7 | 24 | 24 | 24 | 24 | 24 | 24 | 4.6 | 4.6 | 4.6 | 4.6 | 4.6 | 4.6 |
| 10 | 24 | 24 | 24 | 24 | 24 | 24 | 3.8 | 3.8 | 3.8 | 3.8 | 3.8 | 3.8 |

TABLE III: SUPERFICIAL GAS VELOCITY OF ABSORBER COLUMN

| | 9.5 ℃ flue gas | | 40 ℃ flue gas | |
|---|---|---|---|---|
| | Flow rate ($m^3$/hr) | Superficial gas velocity (m/s) | Flow rate ($m^3$/hr) | Superficial gas velocity (m/s) |
| 3% (Case I) | 294884.7 | 2.13 | 326820.4 | 2.36 |
| 4% (Case II) | 221135.7 | 2.17 | 245086.2 | 2.41 |
| 7% (Case III) | 128402.8 | 2.15 | 140202.9 | 2.35 |
| 10% (Case IV) | 88438.13 | 2.17 | 98020.9 | 2.40 |

The post combustion process is the well established carbon capture technology. The MEA is considered as the solvent for the capturing process. Three different solvent conditions are used to develop the process model to check most suitable operating conditions. The flow diagram of the base case process is developed with MEA concentration 30% and 40% and 0.30 (mol $CO_2$/mol MEA) $CO_2$ lean loading for simulation studies with 85%, 90%, and 95% removal efficiencies. The main input parameters for development of the model is extracted from the previous studies [6], [7]. The main chemical reactions between MEA and $CO_2$ are taken into consideration [8] with available thermodynamic and kinetic data [9].

The packing material and parameters related to packing section are considered for optimization. The packing height and diameter are varied to find the optimum packing conditions which give lowest re-boiler energy demand. The Mellapak-Sulzer 350 Y for absorber and Flexipak-1Y for stripper are selected according to the previous studies [10]. The optimum packing conditions for the absorber column for the base case simulations is selected according to the simulation results which gives lowest re-boiler duty (in Table II). However, superficial gas velocity also considered while selecting the optimum packing dimensions to avoid flooding.

While selecting absorber diameter, superficial gas velocity is taken into consideration. The superficial gas velocity is managed to keep around 2-3 m/s. The calculated superficial gas velocity according to the selected diameter is given in the Table III.

## IV. SIMULATIONS

Simulations are performed to determine the $CO_2$ loading effect on re-boiler duty for all four cases. The $CO_2$ loading is varied from 0.15 - 0.35 (mol $CO_2$/mol MEA) with MEA concentration 30% and 40%. Carbon capture models are simulated for 3 different efficiencies, 85%, 90% and 95%. The temperature of the flue gas is considered as 9.5 ℃ (the temperature of flue gas in the aluminium industry) for initial case and 40 ℃ (most suitable temperature for gas absorption) after that.

### *A. Flue Gas Temperature 9.5 ℃*

Re-boiler duty variation with $CO_2$ lean loading is analyzed. Fig. 6 shows re-boiler duty variation with $CO_2$ lean loading for Case I with 85% removal efficiency. Two lines are representing the different MEA concentrations, 30% and 40%. The temperature of the flue gas stream is around 9.5 ℃.

According to the Fig. 6, specific energy demand in re-boiler is decreasing until a minimum is obtained. All other cases are followed a similar trend and the optimum $CO_2$ lean loading is selected according to the minimum re-boiler energy. The MEA concentration 40% and $CO_2$ lean loading 0.3 give the optimum solvent condition for 85% removal efficiency in Case I (3% $CO_2$ in flue gas).

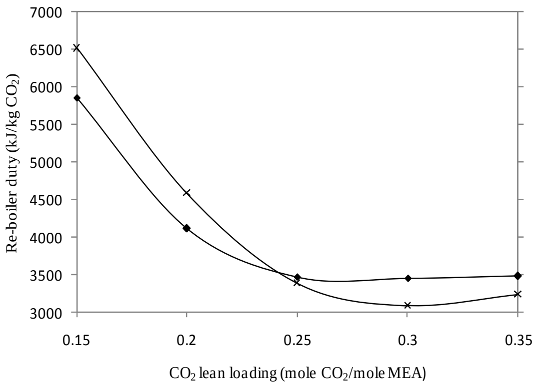

Fig. 6. Re-boiler duty variation with $CO_2$ lean loading, symbols refer to the MEA concentrations: ♦, 30; ×, 40 w/w%.

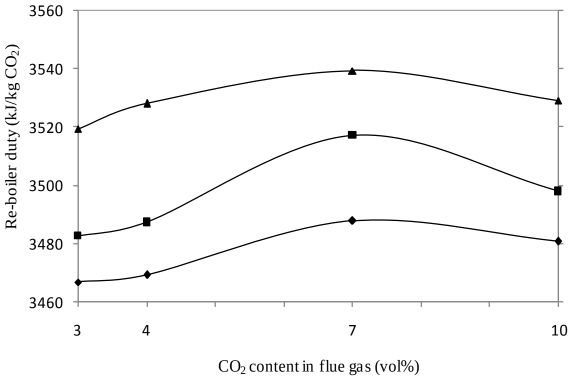

Fig. 7. Re-boiler duty variation according to the $CO_2$ content in the flue gas for 30w/w% MEA concentration and 0.25 (mol $CO_2$/mol MEA) $CO_2$ lean loading, symbols refer to the removal efficiency: ♦, 85%; ■, 90%; ▲, 95%.

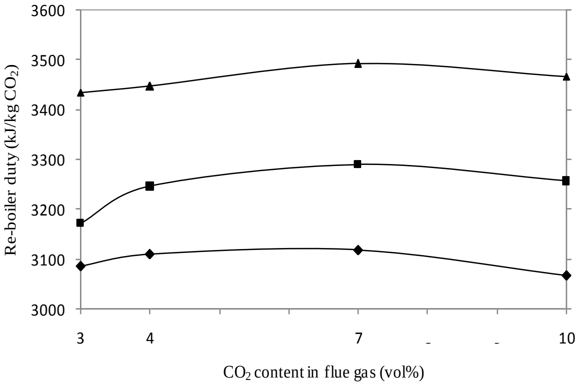

Fig. 8. Re-boiler duty variation according to the $CO_2$ content in the flue gas for 40w/w% MEA concentration and 0.30 (mol $CO_2$/mol MEA) $CO_2$ lean loading, symbols refer to the removal efficiency: ♦, 85%; ■, 90%; ▲, 95%.

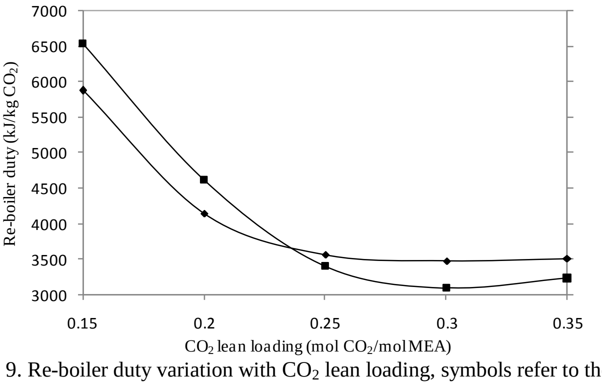

Fig. 9. Re-boiler duty variation with $CO_2$ lean loading, symbols refer to the MEA concentrations: ♦, 30; ■, 40 w/w%.

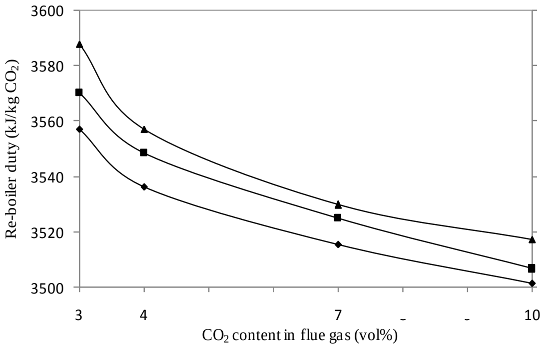

Fig. 10. Re-boiler duty variation according to the $CO_2$ content in the flue gas for 30w/w% MEA concentration and 0.25 (mol $CO_2$/mol MEA) $CO_2$ lean loading, symbols refer to the removal efficiency: ♦, 85%; ■, 90%; ▲, 95%.

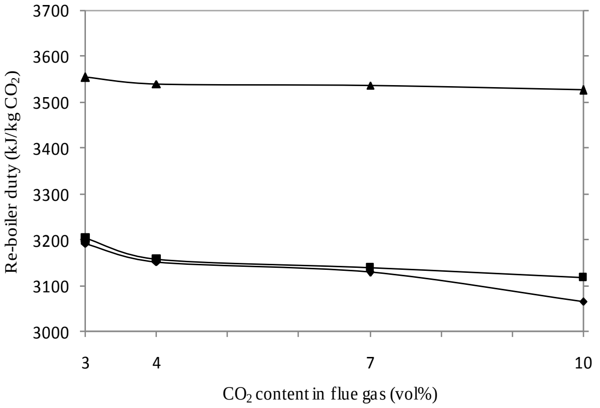

Fig. 11. Re-boiler duty variation according to the $CO_2$ content in the flue gas for 40w/w% MEA concentration and 0.30 (mol $CO_2$/mol MEA) $CO_2$ lean loading, symbols refer to the removal efficiency: ♦, 85%; ■, 90%; ▲, 95%.

### A. *Flue Gas Temperature 40 ℃*

Fig. 7 and Fig. 8 represent the re-boiler duty variation according to the $CO_2$ content in the flue gas. Figures doesn't show considerable variation according to the flue gas $CO_2$ composition. However, 3% $CO_2$ content in the flue gas gives the minimum re-boiler duty compared to other cases. With the removal efficiency, re-boiler duty is increasing, and the minimum is given by 85% removal efficiency.

Similar to the previous section, simulations are performed to determine the re-boiler duty variation with lean $CO_2$ loading. Fig. 9 shows the re-boiler duty variation with lean $CO_2$ loading for case I (3% $CO_2$ in flue gas) with 85% $CO_2$ removal efficiency.

Fig. 10 and Fig. 11 represent the re-boiler duty variation according to the $CO_2$ content in the flue gas.

Moreover, Fig. 12 illustrates the variation of the re-boiler duty with the flue gas inlet temperatures of 9.5 ℃ and 40 ℃ for 85% removal efficiency. It can be concluded that, specific re-boiler duty for $CO_2$ capture process is increasing with the flue gas temperature. As can be seen from Fig.12, re-boiler energy is reducing with the $CO_2$ content in flue gas for 40 ℃ temperature case. The absorber column dimensions have a strong dependence on the specific re-boiler heat duty of the system. The optimum absorber and stripper dimensions were different for each case which has been studied due to superficial gas velocity. The absorber column dimensions can be varied slightly within the required superficial velocity range. That will again change the optimum re-boiler energy requirement for all cases.

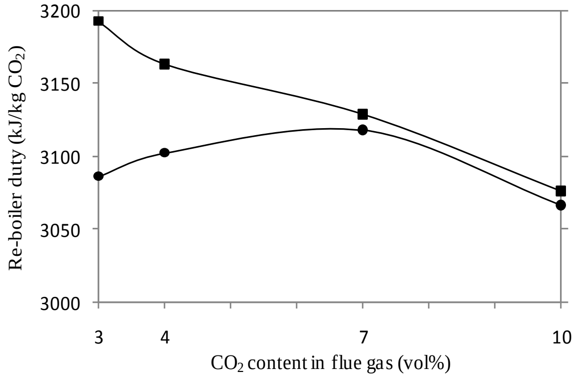

Fig. 12. Variation of the re-boiler duty with the flue gas inlet temperature, symbols refer to the flue gas temperature: ●, 9.5°C; ■, 40°C. (MEA concentration is 40w/w% and $CO_2$ lean loading 0.30 (mol $CO_2$/mol MEA for 85% removal efficiency).

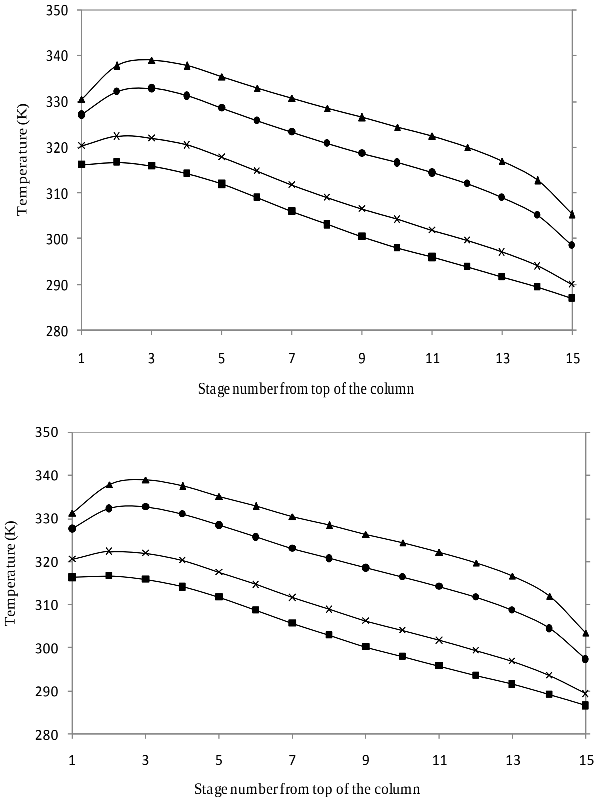

Fig. 13. Temperature profiles alone the absorption column, left hand side figure indicating liquid phase temperature and right hand side indicates vapor phase temperature for 30w/w% MEA concentration and 0.25 (mol $CO_2$/mol MEA) $CO_2$ lean loading with 85% removal efficiency, symbols refer to the $CO_2$ content in the flue gas: ■, 3%; ×, 4%; ●, 7%; ▲, 10%.

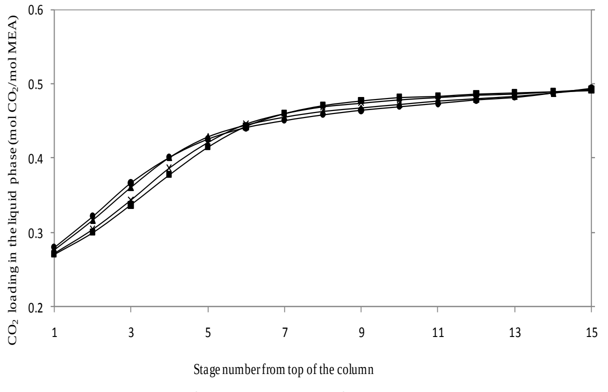

Fig. 14. $CO_2$ loading profiles in absorber for 30w/w% MEA concentration and 0.25 (mol $CO_2$/mol MEA) $CO_2$ lean loading with 85% removal efficiency, symbols refer to the $CO_2$ content in the flue gas: ■, 3%; ×, 4%; ▲, 7%; ●, 10%.

The optimum re-boiler duties for all simulation models are given in the Table IV. It can be seen from the Table IV; the re-boiler duty is increased with the removal efficiency. The reason for that is the total amount of $CO_2$ re-generate in the stripper is high with higher removal efficiency. Therefore, the amount of solvent required to capture the $CO_2$ in the absorption column is higher for higher efficiency. The amount of solvent will directly have an effect on re-boiler energy requirement. At the same time, the amount of $CO_2$ content in the flue gas weakly effect on re-boiler energy. However, total amount of flue gas process in the absorption column is less with high amount of $CO_2$ concentration in the flue gas (Case I > Case II > Case III> Case IV). Because of that the absorption column size is also reduced and it will directly effect on capital cost of the capture plant. Even though, high $CO_2$ content (Case IV) has small impact on energy duty, it will be considerable benefit while considering the cost of capturing. Flue gas temperature has a slight impact on re-boiler energy requirement. However, higher flue gas temperature require a higher amount of energy in stripper re-generation process compare to lower flue gas temperature value. A summary of the optimum results obtained from the simulations is presented in the Table IV. Purity of the captures $CO_2$ stream in stripper is maintained around 95 mol% for every case of studies.

The $CO_2$ capture process model is completed as a closed loop process after completing the process optimization for parameter values and solvent conditions. It can be used to calculate the required make-up stream for re-circulating back the lean solvent stream out from the stripper. The make-up stream is adjusted to fulfill water and MEA losses during the $CO_2$ capturing process. After completing the closed loop model, temperature and the $CO_2$ loading profiles are analyzed to study the performance of the model. Temperature profiles for Case I - IV are given in the Fig.13 for liquid and vapor phase, respectively. For profile generation, 30 w/w% MEA concentration and 0.25 $CO_2$ lean loading is considered with 85% $CO_2$ removal efficiency with the flue gas temperature 9.5 ℃.

From the above figure, it can be observed that the maximum liquid and vapor phase temperature inside the absorption column is around 340K (67 ℃). Both liquid and vapor phases are following same trends. It can be conclude that 10% $CO_2$ gives highest temperature as 67 ℃ and, 3% $CO_2$ gives lowest temperature value as 42 ℃. All four cases illustrate the temperature bulge at the top of the column for both liquid and vapor phase. Temperature bulge is due to highly exothermic reactions at the top of the column. When the ratio between liquid (L) and gas (G) is relatively small, the reactions are mostly occur at the top of the column. Therefore, temperature profiles show optimum value closer to the top of the absorption column.

Furthermore, $CO_2$ loading in the liquid phase is reached at around 0.5 (mol $CO_2$/mol MEA) at the rich solvent stream leaving the absorption column. Fig. 14 represent the $CO_2$ loading variation along the absorption column. All four cases follow the same trend along the column from top to bottom

## V. HEAT INTEGRATION

The main drawback of the $CO_2$ capture process is high energy demand in the re-generation process. Therefore, heat integration plays a vital role in process optimization with carbon capture. The available excess heat is calculated using standard cooler block placing between the outlet of aluminium electrolyte cells and dry scrubber unit. The inlet temperature to the dry scrubber maintains around 150 ℃. The heat recovery unit should be installed as shown in the Fig. 15 as proposed by previous studies [11]. The recovered heat can be used to replace part of the energy requirement in re-generation section in $CO_2$ capture process. Additional heat has to be supplied trough separate energy plant. The flue gases generated from that energy plant will also be sent through the proposed $CO_2$ capture section. Additional unit operations necessary prior to the $CO_2$ capture section in order to purify the flue gas to remove dust and additional compounds.

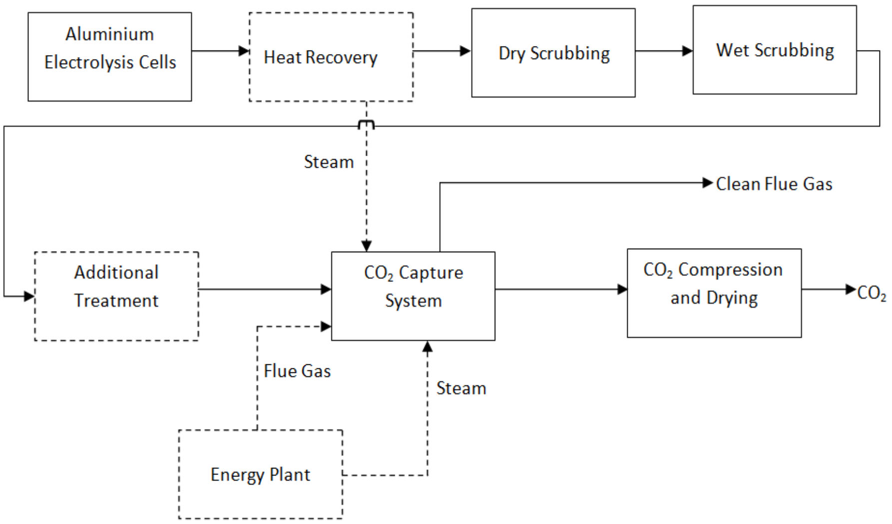

Fig. 15. Process flow diagram with heat integration section [11].

TABLE IV: SUMMARY OF THE SIMULATION STUDIES WHEN FLUE GAS TEMPERATURE IS 9.5C °(RE-BOILER HEAT DUTIES ARE GIVEN BY MW AND SPECIFIC ENERGY BY KJ/KG $CO_2$).

| $CO_2$ content in the flue gas | 3 vol% | | | 4 vol% | | | 7 vol% | | | 10 vol% | | |
|---|---|---|---|---|---|---|---|---|---|---|---|---|
| Capture efficiency | 85% | 90% | 95% | 85% | 90% | 95% | 85% | 90% | 95% | 85% | 90% | 95% |
| Re-boiler heat duty (MW) | | | | | | | | | | | | |
| 30% MEA and 0.25 $CO_2$ lean loading | 14.93 | 15.88 | 16.94 | 14.94 | 15.90 | 16.98 | 15.02 | 16.22 | 16.94 | 14.99 | 15.95 | 16.89 |
| 40% MEA and 0.3 $CO_2$ lean loading | 13.29 | 14.46 | 15.64 | 13.39 | 14.80 | 16.07 | 13.60 | 15.01 | 16.79 | 12.99 | 14.85 | 16.45 |
| Specific Re-boiler heat duty (kJ/kg $CO_2$) | | | | | | | | | | | | |
| 30% MEA and 0.25 $CO_2$ lean loading | 3466 | 3482 | 3519 | 3469 | 3487 | 3528 | 3487 | 3517 | 3539 | 3480 | 3497 | 3529 |
| 40% MEA and 0.3 $CO_2$ lean loading | 3085 | 3171 | 3433 | 3109 | 3245 | 3446 | 3117 | 3289 | 3492 | 3066 | 3256 | 3467 |

The calculated available excess heat in aluminium production process is tabulated with required re-generation energy. The energy requirement of $CO_2$ capture process for the four different cases are considered. The required re-boiler duties are in the range of 3.0 - 3.5 MJ/kg $CO_2$ for 85% removal efficiency and 3.2 - 3.5MJ/kg $CO_2$ for 90% removal efficiency and 3.4 - 3.6MJ/kg $CO_2$ for 95% removal efficiency. If it is possible to replace part of the energy requirement using excess heat in the aluminium industry, it will be a feasible option to perform $CO_2$ capture for aluminium flue gas processing. Depending on the $CO_2$ content in the flue gas, the temperature of the flue gas exit the aluminium cells is different. The calculated available heat for all four cases is given in Table V along with the flue gas conditions.

The available heat and required heat for re-generation section is taken in to consideration. Fig. 16 and Fig. 17 present the required and available energy in aluminium production process for $CO_2$ capturing. Fig. 16 indicates the MEA concentration 30w/w% and 0.25 (mol $CO_2$/mol MEA) $CO_2$ lean loading and Fig. 17 for MEA concentration 40w/w% and $CO_2$ lean loading 0.30 (mol $CO_2$/mol MEA).

TABLE V: AVAILABLE HEAT AND FLUE GAS CONDITIONS AT DIFFERENT $CO_2$ CONCENTRATIONS

| $CO_2$ concentration (vol%) | Inlet temperature of the energy recovery section (℃) | Outlet temperature of the energy recovery section (℃) | Mass flow rate (kg/s) | Available heat duty (MW) |
|---|---|---|---|---|
| 3 | 225 | 150 | 112.12 | 8.69 |
| 4 | 265 | 150 | 84.49 | 10.08 |
| 7 | 329 | 150 | 49.09 | 9.19 |
| 10 | 365 | 150 | 34.92 | 7.84 |

TABLE VI: REQUIRED HEAT DUTY VS. AVAILABLE HEAT FOR 85% REMOVAL EFFICIENCY (30% MEA AND 0.25 $CO_2$ LOADING)

| $CO_2$ concentration (vol%) | Required re-boiler Energy (MW) | Available heat duty (MW) | Percentage of available heat (%) |
|---|---|---|---|
| 3 | 14.93 | 8.69 | 58 |
| 4 | 14.94 | 10.08 | 67 |
| 7 | 15.02 | 9.19 | 61 |
| 10 | 14.99 | 7.84 | 52 |

TABLE VII: REQUIRED HEAT DUTY VS. AVAILABLE HEAT FOR 85% REMOVAL EFFICIENCY (40% MEA AND 0.30 $CO_2$ LOADING).

| $CO_2$ concentration (vol%) | Required re-boiler Energy (MW) | Available heat duty (MW) | Percentage of available heat (%) |
|---|---|---|---|
| 3 | 13.29 | 8.69 | 65 |
| 4 | 13.39 | 10.08 | 75 |
| 7 | 13.6 | 9.19 | 67 |
| 10 | 12.99 | 7.84 | 60 |

Table VI and VII are representing the available heat as a percentage of required re-boiler duty. It can be clearly seen that, 75% of energy penalty of case II (4% $CO_2$) gives the maximum available heat for replacing re-generation process.

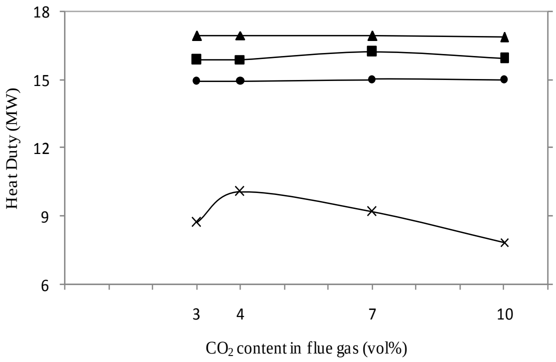

Fig. 16. Available heat duty vs. required re-generation energy for 30w/w% MEA concentration and 0.25 (mol $CO_2$/mol MEA) $CO_2$ lean loading, symbols refer to : ▲, 95% Eff; ■, 90% Eff; ●, 85%Eff; ×, Available heat.

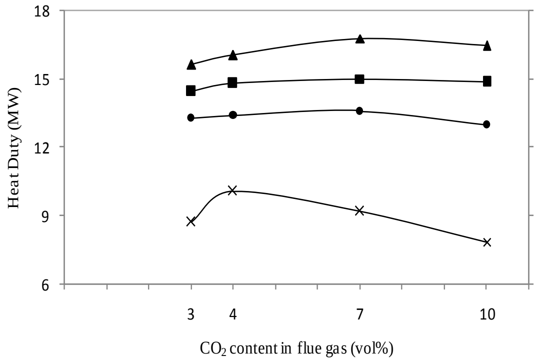

Fig. 17. Available heat duty vs. required re-generation energy for 40w/w% MEA concentration and 0.30 (mol $CO_2$/mol MEA) $CO_2$ lean loading, symbols refer to: ▲, 95% Eff; ■, 90% Eff; ●, 85%Eff; ×, Available heat.

## VI. CONCLUSION

The basic idea behind this study is to develop and implement the $CO_2$ capture model for flue gas from aluminium production plant. Several $CO_2$ concentrations, 3, 4, 7 and 10 vol%, in the flue gas from the aluminium production are investigated to find the optimum $CO_2$ content in the flue gas. Finally, according to the simulated results, percentage of optimum $CO_2$ concentration in the flue gas was concluded. The $CO_2$ loading is varied from 0.15 - 0.35 (mol $CO_2$/mol MEA) with MEA concentration 30% and 40%. Carbon capture models are developed for 3 different efficiencies, 85%, 90% and 95%. The temperature of the flue gas is considered as 9.5 ℃ for initial condition and 40 ℃ after that.

The MEA concentration 40% and lean $CO_2$ loading 0.3 give the optimum solvent condition for $CO_2$ capture process. With the removal efficiency, re-boiler duty is increasing and the minimum is given by 85% removal efficiency. It can be concluded that, specific re-boiler duty for $CO_2$ capture process is increasing with the flue gas temperature. The required re-boiler duties are in the range of 3.0 - 3.5 MJ/kg $CO_2$ for 85% removal efficiency and 3.2 - 3.5MJ/kg $CO_2$ for 90% removal efficiency and 3.4 - 3.6MJ/kg $CO_2$ for 95% removal efficiency. It can be concluded that 10% $CO_2$ gives highest temperature as 67 ℃, and 3% $CO_2$ gives temperature value as 42 ℃. All four cases show the temperature bulge at the top of the column for both liquid and vapor phase. It can be clearly seen that, 75% of energy requirement of case II (4% $CO_2$) gives the maximum available heat for replacing re-generation process. According to the present study, it can be clearly stated that, 4% $CO_2$ content in the flue gas is given the optimum available heat to replace the re-generation energy. That will save the energy cost for $CO_2$ capture process of the aluminium production process. However, optimum results will vary with the trade-off between capital cost and energy cost.

## REFERENCES

[1] B. Metz, O. R. Davidson, P. R. Bosch, R. Dave, and L. A. Meyer, "Climate change 2007:Mitigation of climate change," in *Proc. Contribution of Working Group III to the Fourth Assessment Report of the Intergovernmental Panel on Climate Change*, Cambridge University, Cambridge, pp. 2-23, 2007.

[2] M. Wang, A. Lawal, P. Stephenson, J. Sidders, and C. Ramshaw, "Post-combustion $CO_2$ capture with chemical absorption: A state of the art review," *Chemical Engineering Research and Design*, vol. 89, pp. 1609-1624, 2011.

[3] D. A. Roling and M. Lynch, *An Analyst's Outlook for Aluminium Funda-Mentals, Metal Price, and the Value of Equities*, Technical report, Platts Aluminium Symposium: Targeting Transparency, 2004.

[4] International Aluminium Institute, "Selection of articles from IAI-Web," Technical report, International Aluminium Institute, Haymarket, London, vol. 32, no. 2, 2004.

[5] H. Björk and J. Aronsson, "Process Integration and Performance of Chilled Ammonia $CO_2$ Capture Technology," M.Sc Thesis, Department of Energy and Environment, Chalmers University of Technology, 2011.

[6] A. Plus, "Rate Based model of the $CO_2$ capture process by MEA using Aspen Plus," Aspen Technology Inc, Cambridge, MA, USA, 2008.

[7] A. Mohammad, "Carbon dioxide capture from flue gas," Ph.D Thesis, University of Delft, Netherland, 2009.

[8] A. D. Michael, "A model of vapour-liquid equilibria for acid gas-alkanolamine-water systems," PhD Thesis, University of Texas, USA, 1989.

[9] S. Freguia, "Modeling of $CO_2$ removal from Flue Gas with Mono-ethanolamine," Master Thesis, University of Texas, Austin, USA, 2002.

[10] U. S. P. R. Arachchige and M. C. Melaaen, "Selection of Packing Material for Gas Absorption," *European Journal of Scientific Research*, vol. 87, no. 1, pp. 117-126, 2012.

[11] V. D. Sørhaug, "$CO_2$ capture from aluminium production," M.Sc. Thesis, Telemark University College, 2012.

**Udara S. P. R. Arachchige** received his B.Sc degree in 2007 in chemical and process engineering from University of Moratuwa, Sri Lanka and M.Sc degree in 2010 in energy and environmental engineering from Telemark University College, porsgrunn, Norway.

He is presently pursuing his Ph.D in Carbon dioxide capture from power plants- modeling and simulation studies at Telemark University College. He has presented and published 14 papers in International Conferences and journals.

**Dinesh Kawan** received his B.E degree in 2010 in electronics and communication engineering from Khwopa Engineering College, Purbanchal University, Nepal. He is presently pursuing his master degree in system and control engineering in Telemark University College, Porsgrunn, Norway.

He also working as a research assistant at faculty of Technology in same university college. Mr. Kawan has research interest on carbon capture, modeling and simulation, and control systems in process industries.

**Morten C. Melaaen** is a professor in process technology at Telemark University College, Porsgrunn, Norway. He is also the dean of Faculty of Technology, Telemark University College and has a part time position at the local research institute Tel-Tek. Earlier, he has worked as a research engineer in Division of Applied Thermodynamics, SINTEF, Norway and as an associate professor at Norwegian University of Science and Technology (NTNU).

He has worked on research projects as a senior research scientist in Norsk Hydro Research Centre Porsgrunn, Norway. He started to work as a professor at Telemark University College in 1994 and became the head of Department, Department of Process, Energy and Environmental Technology in 2002. He received his MSc in mechanical engineering in 1986 and his Ph.D in 1990, both from NTNU. His research interests are $CO_2$ capture, modeling and simulation, fluid mechanics and heat and mass transfer. Professor Melaaen has more than 100 scientific papers published in the above mentioned related fields in international journals and conferences.

## Paper P

# Viscosities of pure and aqueous solutions of Monoethanolamine (MEA), Diethanolamine (DEA) and N-Methyldiethanolamine (MDEA)

This paper is published in the Annual Transactions - The Nordic Rheology Society 2012, 21, 2012.

ANNUAL TRANSACTIONS OF THE NORDIC RHEOLOGY SOCIETY, VOL. 21, 2013

# Viscosities of Pure and Aqueous Solutions of Monoethanolamine (MEA), Diethanolamine (DEA) and N-Methyldiethanolamine (MDEA)

Udara S. P. R. Arachchige[1,a]; Neelakantha Aryal[1]; Dag A. Eimer[1]; Morten C. Melaaen[1]

[1] Telemark University College, Porsgrunn, 3901, Norway.

## ABSTRACT

Viscosities of monoethanolamine, diethanolamine and methyldiethanolamine solutions were examined at a temperature range from (293.15 to 423.15) K for pure amines and (293.15 to 353.15) K for aqueous amines at different compositions. The experimental viscosities measured in this work are in good agreement with those reported in the literature.

## INTRODUCTION

Alkanolamines have been used for the acid gas absorption process for a long period. The physical properties of those alkanolamines are important for process design. The main objective of this paper is to provide values for viscosities of different aqueous amines at different temperatures which are needed for the acid gas absorption process. Acid gas absorption process take place at 313 K temperature. However, different operating temperatures are interested for high performance. Therefore, physical properties like viscosity of amines are important to calculate for different temperature range to perform mathematical calculations. The physical properties such as density, viscosity and solubility data of solvents are important for the acid gas absorption and regeneration process. Different types of amines are available, such as primary amines (MEA, DGA), secondary amines (DEA), tertiary amines (MDEA, TEA), hindered amines (AMP) and cyclic amines (Piperazine). Important alkanolamines for industrial application are monoethanolamine (MEA), diethanolamine (DEA), di-2-propanolamine (DIPA) and N-methyldiethanolamine (MDEA) [1]. Aqueous MEA solutions are widely used for gas treating processes due to high reactivity, low operating cost and ease of reclamation [2]. However, the possibilities of using other solvents like DEA and MDEA have to be analyzed in order to lower the cost of CO2 capturing. This work has been carried out to determine the effect of temperature on the viscosity of different types of amines at different concentration levels at atmospheric pressure. The experiments were performed to check the viscosities of monoethanolamine (MEA), diethanolamine (DEA) and methyldiethanolamine (MDEA). The pure alkanolamine viscosity measurements were carried out for the temperature range (293.15 to 423.15) K and alkanolamine solution viscosity were measured in the range of (293.15 to 353.15) K. This represents an extension of previously reported data.

The measured data for the different kind of amines are compared with those available from the literature. The pure viscosity data for MEA, DEA and MDEA solutions are compared with data from Li and Lie1, DiGuilio et al. [3] and Mandal et al. [4] The data given by Amundsen et al. [5], Rinker et al. [6] and Li and Lie [1] are used to compare the aqueous viscosity data for MEA, DEA and MDEA solutions. Agreement between the measurement data and literature values were found to be satisfactory.

The obtained results were used to produce correlations for amine viscosity at different temperatures. A number of correlations for computation of viscosity of liquids are presented in the literature. Vogel [7] has reported the simple three constant correlation for pure liquid viscosity and Viswanath and Natarajan [8] utilized a similar form for both dynamic and kinematic viscosities.

The equation presented by Vogel was modified by Goletz and Tassios [9] to include the boiling point of the substance. Dutt [10] described a similar idea to Goletz and has derived a correlation using density and boiling point of the component. Pure liquid viscosity can be represented by polynomial type equation mentioned by Girifalco [11] which was extended by Thorpe and Rodger [12].

Digullio et al. [3] have reported a three constant equation which is closer to Vogel's equation for pure amines' viscosity. Among those, Digullio's equation is selected for calculation of pure amines' viscosity due to less deviation when fitting experimental values.

The aqueous amine viscosities measured in this work are used to regress the polynomial for representation of amine viscosities. Teng et al. [13] and Chowdhury et al. [14] have reported the correlations for aqueous amine viscosity variation with molar concentration for specific temperature values. The correlation from Teng et al. [13] is selected for this study because of less deviation when fitted to experimental values.

## EXPERIMENTAL SECTION

Dynamic viscosity was measured using MCR 101 Anton Paar double-gap rheometer. The viscometer was calibrated against the petroleum distillate and mineral oil calibration fluid from Paragon Scientific ltd. The calibration factor was decided according to the given temperature for the calibration liquid and experimental viscosity achieved during the calibration. The low-temperature measurements were achieved by applying cooling water supply to the rheometer setup at (293.15, 298.15 and 303.15) K. The MEA was purchased from Merck KGaA, DEA and the MDEA from Merck Schuchardt OHG. The purity of the chemicals in mass basis are 99.5%, 99% and 98% respectively for MEA, DEA and MDEA. The information about chemicals are given in Table 1. Without further purification, all these amines were used for experimental studies. De-gassed distilled water was used for preparation of aqueous amine solutions. All the experiments are performed at 1.01 bar operating pressure.

**Table 1.** Purity of the amines used in experiments.

| Amine type | Mass Purity % | Supplier |
|---|---|---|
| MEA | 99.5 | Merck KGaA |
| DEA | 99 | Merck Schuchardt OHG |
| MDEA | 98 | Merck Schuchardt OHG |

## RESULTS AND DISCUSSION

The results from the experimental work have been sub-divided into two sections: viscosities of pure amines and viscosities of aqueous amines.

## Pure Amine Viscosities

Viscosities of pure MEA, DEA and MDEA from temperature range (293.15 to 423.15) K are tabulated in Tables 2, 3 and 4, respectively. The experimental viscosity results for pure amines, tabulated in Tables 2 to 4, are plotted in Fig. 1 as viscosity vs. temperature. As shown in the Fig. 1, viscosities of pure amines are decreasing with the increase of temperature. The viscosities of pure MEA, DEA and MDEA measured in this work agree well with the literature values taken from Li and Lie1, DiGuilio et al. [3] and Mandal et al. [4], respectively. The average absolute deviations between the literature values and our data are (0.019, 1.21, 0.39) mPa·s for pure MEA, DEA and MDEA respectively. The deviations are in the range of experimental uncertainties which is given under the each table.

**Table 2.** Comparison of the Viscosities η of Pure MEA Measured in This Work with Literature Values from Temperature T = (293.15 to 423.15) K

| ***T*/K** | **This work** | **Li and Lie[1]** | **DiGuilio et al.[3]** | **Mandal et al.[4]** |
|---|---|---|---|---|
| | | *η*/mPa·s | | |
| 293.15 | 24.085 | | | 24.1 |
| 298.15 | 18.924 | | | 18.98 |
| 303.15 | 15.151 | 15.1088 | 14.86 | 15.11 |
| 313.15 | 10.006 | 10.0209 | 9.89 | 10.02 |
| 323.15 | 6.962 | 6.9715 | | 6.972 |
| 333.15 | 5.037 | 5.0473 | 4.99 | 5.047 |
| 343.15 | 3.775 | 3.7793 | | 3.779 |
| 353.15 | 2.919 | 2.912 | 2.90 | 2.912 |
| 363.15 | 2.334 | | | |
| 373.15 | 1.914 | | 1.85 | |
| 383.15 | 1.586 | | | |
| 393.15 | 1.324 | | 1.268 | |
| 403.15 | 1.105 | | | |
| 413.15 | 0.934 | | 0.918 | |
| 423.15 | 0.806 | | 0.796 | |

Standard uncertainties u are u(T) = ± 0.3 K and the combined expanded uncertainties Uc are Uc(η) = ± 0.015 mPa·s

**Table 3.** Comparison of the Viscosities η of Pure DEA Measured in This Work with Literature Values from Temperature T = (293.15 to 423.15) K

| T/K | This work | DiGuilio et al.3 | Mandal et al.4 |
|---|---|---|---|
| | η/mPa·s | | |
| 293.15 | 889.655 | 890.5 | 890.5 |
| 298.15 | 562.315 | | 566.3 |
| 303.15 | 380.18 | 356 | 383.9 |
| 313.15 | 192.85 | 200.9 | 188.2 |
| 323.15 | 106.936 | | 119.5 |
| 333.15 | 57.304 | 61.22 | 57.69 |
| 343.15 | 36.177 | | 35.09 |
| 353.15 | 22.974 | 23.4 | 22.43 |
| 363.15 | 15.655 | | |
| 373.15 | 10.938 | 10.53 | |
| 383.15 | 7.702 | | |
| 393.15 | 5.708 | 5.67 | |
| 403.15 | 4.345 | | |
| 413.15 | 3.346 | 3.38 | |
| 423.15 | 2.687 | 2.7 | |

Standard uncertainties u are u(T) = ± 0.3 K and the combined expanded uncertainties Uc are Uc(η) = ± 0.843 mPa·s

**Table 4.** Comparison of the Viscosities η of Pure MDEA Measured in This Work with Literature Values from Temperature T = (293.15 to 423.15) K

| T/K | This work | Li and Lie [1] | DiGuilio et al. [3] | Mandal et al. [4] |
|---|---|---|---|---|
| | | η/mPa·s | | |
| 293.15 | 103.67 | | 102.7 | 104.5 |
| 298.15 | 77.32 | | | 77.19 |
| 303.15 | 57.50 | 57.859 | 57.95 | 57.86 |
| 313.15 | 34.622 | 34.3085 | 34.02 | 34.31 |
| 323.15 | 22.402 | 21.6716 | 21.5 | 21.67 |
| 333.15 | 15.276 | 14.3856 | | 14.39 |
| 343.15 | 9.965 | 9.9789 | | 9.987 |
| 353.15 | 7.146 | 7.0875 | 7.151 | 7.088 |
| 363.15 | 5.818 | | | |
| 373.15 | 4.385 | | 3.987 | |
| 383.15 | 3.362 | | | |
| 393.15 | 2.656 | | 2.504 | |
| 403.15 | 2.122 | | | |
| 413.15 | 1.696 | | 1.679 | |
| 423.15 | 1.375 | | 1.406 | |

Standard uncertainties u are u(T) = ± 0.3 K and the combined expanded uncertainties Uc are Uc(η) = ± 0.122 mPa·s

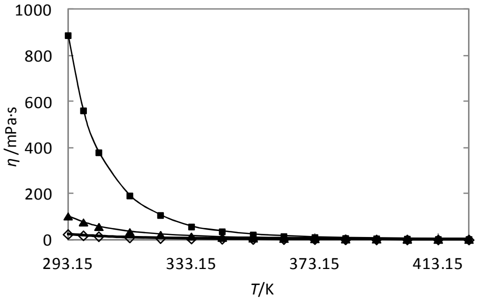

**Figure 1.** Pure amines' viscosity variation with temperature at (293.15 to 423.15) K: ◊, MEA; ▲, MDEA; ■, DEA.

Aqueous Amine Viscosities

The viscosity data for aqueous MEA, DEA and MDEA solutions are presented in Tables 5, 6 and 7, respectively. The experiments were performed to measure viscosities of amines with concentrations in the range from mass fraction (0.1 to 0.9) for the temperature range (293.15 to 353.15) K. The aqueous MEA, DEA and MDEA viscosity data of Amundsen et al. [5], Rinker et al. [6] and Li and Lie [1] are compared with our experimental data (Figures 2, 3 and 4). The average absolute deviations are (0.08, 0.02, 0.02) mPa·s for aqueous MEA, DEA and MDEA, respectively and the maximum deviation is 0.25 mPa·s when compared against the literature sources. Hence, aqueous amine viscosities measured in this work are in good agreement with those reported by Amundsen et al. [6], Edward et al.5, Li and Lie [1].

The dynamic viscosities of aqueous MEA, DEA and MDEA are plotted versus temperature in Figures 2, 3 and 4.

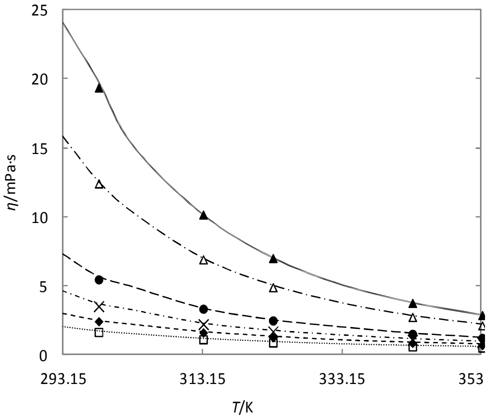

**Figure 2.** Comparison of aqueous MEA viscosity as a function of temperature. Lines are experimental data: …, 20%; ---, 30%; −·−, 40%;— —, 50%;— · —, 70%; ——, 90%. Symbols refer to literature data [5]: □, 20%; ♦, 30%; x, 40%; ●, 50%; Δ, 70%; ▲, 90%.

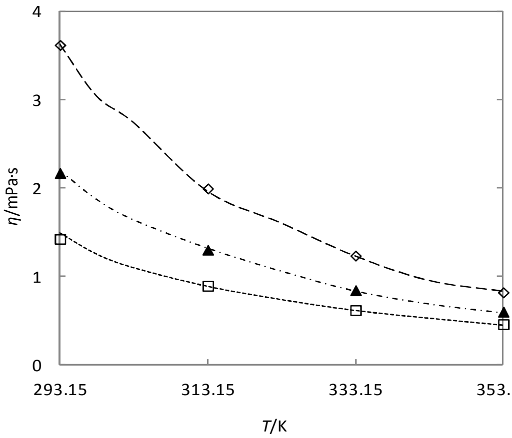

**Figure 3**. Comparison of aqueous DEA viscosity variation with temperature. Lines are experimental data: … , 10%; −·−, 20%; — —, 30%. Symbols refer to literature data6: □, 10%; ▲, 20%; ◊, 30%.

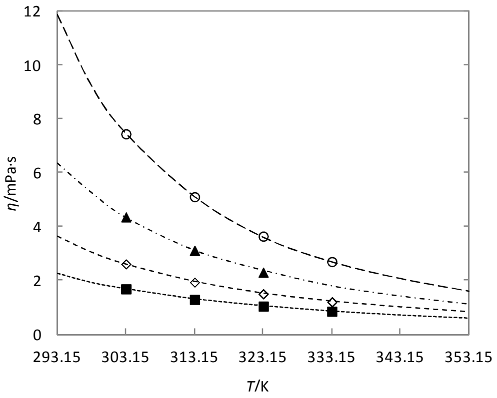

**Figure 4**. Comparison of aqueous MDEA viscosity variation with temperature: Lines are experimental data: … , 20%; ---, 30%; −·−, 40%; — —, 50%. Symbols refer to literature data1: ■, 20%; ◊, 30%; ▲, 40%; o, 50%.

**Table 5**. Viscosities of Aqueous MEA Solutions Measured in This Work from Temperature T = (293.15 to 353.15) K as a function of mass fraction.

| Temp | 10 % | 20 % | 30 % | 40 % | 50 % | 60 % | 70 % | 80 % | 90 % |
|---|---|---|---|---|---|---|---|---|---|
| T/K | η/mPa·s | | | | | | | | |
| 293.15 | 1.442 | 2.005 | 2.990 | 4.667 | 7.345 | 11.295 | 15.774 | 21.003 | 24.023 |
| 298.15 | 1.299 | 1.702 | 2.489 | 3.765 | 5.547 | 9.062 | 12.602 | 16.290 | 19.904 |
| 303.15 | 1.121 | 1.501 | 2.195 | 3.279 | 4.960 | 7.417 | 10.313 | 13.148 | 15.200 |
| 313.15 | 0.909 | 1.169 | 1.671 | 2.311 | 3.423 | 5.291 | 7.024 | 8.950 | 10.220 |
| 323.15 | 0.715 | 0.945 | 1.338 | 1.782 | 2.566 | 3.771 | 5.055 | 6.273 | 7.090 |
| 333.15 | 0.626 | 0.775 | 1.065 | 1.434 | 2.041 | 2.973 | 3.757 | 4.585 | 5.110 |
| 343.15 | 0.520 | 0.671 | 0.903 | 1.168 | 1.594 | 2.243 | 2.854 | 3.449 | 3.830 |
| 353.15 | 0.449 | 0.589 | 0.779 | 0.977 | 1.291 | 1.774 | 2.226 | 2.676 | 2.936 |

Standard uncertainties u are u(T) = ± 0.3 K and the combined expanded uncertainties Uc are Uc(η) = ± 0.015 mPa·s

**Table 6.** Viscosities of aqueous DEA solutions measured in this work from T = (293.15 to 353.15) K as a function of mass fraction.

| Temp | 10 % | 20 % | 30 % | 40 % | 50 % | 60 % | 70 % | 80 % | 90 % |
|---|---|---|---|---|---|---|---|---|---|
| T/K | η/mPa·s | | | | | | | | |
| 293.15 | 1.499 | 2.204 | 3.630 | 6.515 | 12.367 | 25.810 | 53.677 | 143.30 | 353.71 |
| 298.15 | 1.259 | 1.875 | 3.040 | 5.221 | 9.782 | 19.237 | 39.150 | 97.87 | 245.43 |
| 303.15 | 1.106 | 1.644 | 2.740 | 4.420 | 8.008 | 15.322 | 31.187 | 73.47 | 162.68 |
| 313.15 | 0.896 | 1.323 | 1.965 | 3.145 | 5.492 | 10.020 | 17.889 | 41.02 | 88.541 |
| 323.15 | 0.747 | 1.063 | 1.604 | 2.310 | 3.884 | 6.501 | 12.206 | 24.08 | 52.487 |
| 333.15 | 0.624 | 0.838 | 1.231 | 1.720 | 2.869 | 4.807 | 7.732 | 14.67 | 29.894 |
| 343.15 | 0.537 | 0.691 | 0.954 | 1.341 | 2.150 | 3.552 | 5.595 | 10.11 | 19.317 |
| 353.15 | 0.459 | 0.590 | 0.833 | 1.099 | 1.685 | 2.659 | 4.216 | 07.11 | 13.035 |

Standard uncertainties u are u(T) = ± 0.3 K and the combined expanded uncertainties Uc are Uc(η) = ± 0.843 mPa·s

**Table 7.** Viscosities of aqueous MDEA solutions measured in this work from T = (293.15 to 353.15) K as a function of mass fraction.

| Temp | 10 % | 20 % | 30 % | 40 % | 50 % | 60 % | 70 % | 80 % | 90 % |
|---|---|---|---|---|---|---|---|---|---|
| T/K | η/mPa·s | | | | | | | | |
| 293.1 | 1.541 | 2.268 | 3.637 | 6.345 | 11.838 | 22.644 | 37.144 | 71.950 | 101.89 |
| 298.1 | 1.316 | 1.924 | 3.036 | 5.245 | 9.196 | 17.250 | 29.030 | 58.287 | 81.670 |

| | | | | | | | | | |
|---|---|---|---|---|---|---|---|---|---|
| 303.1 | 1.161 | 1.697 | 2.594 | 4.325 | 7.437 | 13.374 | 22.690 | 42.409 | 54.659 |
| 313.1 | 0.931 | 1.325 | 1.952 | 3.107 | 5.101 | 8.843 | 14.907 | 24.450 | 34.229 |
| 323.1 | 0.773 | 1.068 | 1.514 | 2.367 | 3.599 | 6.015 | 9.618 | 14.362 | 19.222 |
| 333.1 | 0.638 | 0.868 | 1.218 | 1.786 | 2.686 | 4.084 | 6.356 | 10.280 | 13.716 |
| 343.1 | 0.543 | 0.719 | 0.998 | 1.406 | 2.070 | 3.081 | 4.889 | 6.875 | 9.616 |
| 353.1 | 0.468 | 0.605 | 0.816 | 1.109 | 1.601 | 2.181 | 3.664 | 4.916 | 6.674 |

Standard uncertainties u are u(T) = ± 0.3 K and the combined expanded uncertainties Uc are Uc(η) = ±0.121 mPa·s

## CORRELATIONS

### Correlation for Pure Amine Viscosities

The eq 1 can be used to correlate the pure amines' viscosities as a function of temperature [3]. Table 8 lists the coefficients of Eq 1 obtained by regression and also include the average absolute deviation between the experimental data and regression value.

$$\ln[\eta/(mPa\cdot s)] = b_1 + \frac{b_2}{T/(K) - b_3} \qquad (1)$$

The b1, b2 and b3 are constants. Average absolute deviation (AAD), $(\eta\text{-}\eta_{reg})$, is 0.05, 2.85 and 0.35 mPa·s respectively for pure MEA, DEA and MDEA.

**Table 8**. Constants for viscosity correlation (eq. 1).

| Substance | b1 | b2 | b3 | AAD |
|---|---|---|---|---|
| MEA | -3.9303 | 1021.8 | 149.1969 | 0.05 |
| DEA | -5.0559 | 1601.4 | 157.6487 | 2.85 |
| MDEA | -4.7986 | 1476.9 | 136.3343 | 0.35 |

### Correlation for Aqueous Amine Viscosities

Aqueous amine viscosities measured in this work are used to generate the polynomial for representation of amine viscosities using regression. The following polynomial (Eq 2) which is taken from the Teng et al. [13] is used for the regression.

$$\ln[\eta/(\mathrm{mPa.s})] = \ln\eta_0 + \sum_0^m a_k \mathrm{x}^k \qquad (2)$$

where η represents the viscosity of the binary solution while $\eta_o$ is the viscosity of pure water, and x the mole fraction of the amines. Pure water viscosity is taken from Li and Lie [1].

Calculated polynomial coefficients indicated by $a_k$ are tabulated in Table 9. Deviation of calculated versus measured aqueous amines' viscosities are calculated as AAD and tabulated for different temperature values in the same table. For MEA, AAD values vary from 0.01 to 0.07 and similarly for DEA and MDEA the values vary from 0.01 to 0.08 and 0.002 to 0.05 mPa·s, respectively.

## EVALUATION OF EXPERIMENTAL UNCERTAINTIES

Viscosity measurement uncertainties are arising as a combination of the temperature uncertainties, sample preparation uncertainties and instrument uncertainties. The MCR rheometer has itself specified temperature accuracy of ± 0.3K. The samples were measured using an analytical balance which has accuracy of ± 0.0001g (0.1mg). The estimated uncertainty in mass fraction of MEA, DEA and MDEA are 0.5%, 0.4% and 0.4% respectively.

Rheometer accuracy is mentioned as ± 0.002 mPa·s for viscosity measurements up to 453K temperature level. Total value of uncertainties for experimental viscosities calculated using combination of all mentioned uncertainties with root sum of square method. The combined expanded uncertainties for pure amines calculated as ± 0.015 mPa·s, ± 0.843 mPa·s and ± 0.122 mPa·s for MEA, DEA and MDEA respectively. The combined expanded uncertainties for aqueous amines calculated as ± 0.015 mPa·s, ± 0.843 mPa·s and ± 0.121 mPa·s for MEA, DEA and MDEA respectively.

## CONCLUSION

The viscosity of MEA, DEA and MDEA were measured at a temperature range from (293.15 to 423.15) K for pure amines and (293.15 to 353.15) K for aqueous amines. Aqueous amine viscosities were measured for a mass fraction range 0.10 to 0.90. As the temperature increased, viscosity of pure and aqueous amine solutions decreased. Moreover, the viscosity of aqueous amine solutions increased as the mass fraction of amine increased for a given temperature.

The measured viscosity data are in good agreement with literature data to the extent available. Two different available correlations were used to fit the experimental values for pure and aqueous amines. Finally, calculated the deviation for all fitted correlations and correlation which gives lowest deviation is selected for this work. The deviation of regression values and measured values are varied as 0.05, 2.85 and 0.35 mPa·s respectively for pure MEA, DEA and MDEA amines and 0.002 to 0.08 mPa·s for aqueous amines. Deviations are in the range of expanded experimental uncertainties except pure DEA and MDEA deviation. Deviation of the pure DEA and MDEA is slightly higher than the calculated experimental uncertainties.

## ACKNOWLEDGMENT

The support of Statoil's research center in Porsgrunn, especially Morten Tande, clarifying possible improvements to obtain more accurate viscosity results and instructions to the equipment used, is gratefully acknowledged.

**Table 9.** Coefficients of the Polynomial for the binary solutions between MEA, DEA and MDEA and water at different temperatures.

| *T/ K* | *amine* | $a_0$ | $a_1$ | $a_2$ | $a_3$ | $a_4$ | $a_5$ | $a_6$ | *AAD* |
|---|---|---|---|---|---|---|---|---|---|
| 293.15 | MEA | 0.0508 | 7.9019 | 18.0593 | -98.1123 | 126.1164 | -19.3461 | -39.3815 | 0.01 |
| | DEA | 0.0316 | 9.8306 | 10.0557 | 0.5268 | -213.0635 | 493.5456 | -322.356 | 0.08 |
| | MDEA | 0.0112 | 12.5526 | -36.2613 | 302.8214 | -1152.5 | 1807 | -994.287 | 0.05 |
| 298.15 | MEA | 0.1174 | 7.4531 | 7.8148 | -30.2603 | -26.0201 | 116.833 | -77.2204 | 0.07 |
| | DEA | -0.0174 | 11.2239 | -5.4608 | 53.4597 | -289.7572 | 529.0203 | -316.2074 | 0.01 |
| | MDEA | 0.102 | 7.6836 | 41.9129 | -253.5218 | 647.1595 | -803.8854 | 383.0985 | 0.03 |
| 303.15 | MEA | 0.0931 | 6.2491 | 31.2894 | -185.3907 | 411.4389 | -440.4103 | 186.2332 | 0.01 |
| | DEA | -0.0853 | 12.5851 | -14.6494 | 44.9598 | -143.5531 | 227.0852 | -130.8371 | 0.04 |
| | MDEA | 0.0064 | 11.5024 | -21.017 | 145.1402 | -561.1386 | 896.9202 | -502.7806 | 0.02 |
| 313.15 | MEA | 0.0137 | 10.0756 | -38.9883 | 242.2987 | -777.1085 | 1094.3 | -557.2303 | 0.03 |
| | DEA | -0.1249 | 15.2392 | -76.9155 | 466.7223 | -1433.3 | 2022.5 | -1050.6 | 0.01 |
| | MDEA | 0.0147 | 10.366 | -12.7884 | 67.2199 | -248.1521 | 372.3297 | -196.2842 | 0.01 |
| 323.15 | MEA | -0.0887 | 11.8014 | -51.7879 | 253.5452 | -691.4558 | 883.0652 | -421.2013 | 0.02 |
| | DEA | -0.0719 | 12.2527 | -31.7779 | 117.2989 | -256.8023 | 276.6759 | -115.2711 | 0.03 |
| | MDEA | 0.0477 | 8.7035 | 1.3063 | -26.4952 | 44.9838 | -46.1525 | 23.4403 | 0.02 |
| 333.15 | MEA | 0.0468 | 7.3836 | -16.7796 | 129.9925 | -495.2924 | 757.0601 | -403.1124 | 0.01 |
| | DEA | -0.0943 | 13.2504 | -74.2482 | 458.2775 | -1390.3 | 1924.8 | -980.5914 | 0.02 |
| | MDEA | 0.029 | 8.2709 | 2.7312 | -43.5071 | 80.7989 | -47.998 | -1.5757 | 0.002 |
| 343.15 | MEA | -0.0835 | 11.4691 | -59.8806 | 305.1176 | -838.2553 | 1081 | -521.4676 | 0.01 |
| | DEA | -0.0176 | 10.0958 | -51.1028 | 358.8246 | -1155.2 | 1642.2 | -847.6918 | 0.01 |
| | MDEA | 0.0542 | 6.3832 | 24.7464 | -200.711 | 615.4432 | -868.3154 | 453.2909 | 0.005 |
| 353.15 | MEA | -0.1557 | 13.9979 | -90.1129 | 442.9951 | -1150.4 | 1429.6 | -673.9559 | 0.01 |
| | DEA | -0.067 | 10.638 | -47.4738 | 263.1139 | -742.4101 | 969.9961 | -472.0667 | 0.01 |
| | MDEA | 0.1378 | 1.6411 | 86.4756 | -594.4721 | 1794.4 | -2487.2 | 1274.5 | 0.02 |

REFERENCES

1. Li, M. H. and Lie, Y. C. (1994), "Densities and Viscosities of Solutions of Monoethanolamine + N-methyldiethanolamine + Water and Monoethanolamine + 2-Amino-2-methyl-1-propanol + Water", *J. Chem. Eng. Data.*, , **39**, 444-447.

2. Isaacs, E. E., Otto, F. D., and Mather, A. E. (1980), "Solubility of mixtures of hydrogen sulfide and carbon dioxide in a monoethanolamine solution at low partial pressures", *J. Chem. Eng. Data.*, **25**, 118-120.

3. DiGuilio, R. M., Lee, R.-J., Schaeffer, S. T., Brasher, L. L., and Teja, A. S. (1992), "Densities and viscosities of the ethanolamines", *J. Chem. Eng. Data.*, **37**, 239-242.

4. Mandal, B. P., Kundu, M., and Bandyopadhyay, S. S. (2003), "Density and Viscosity of Aqueous Solutions of (N-Methyldiethanolamine + Monoethanolamine), (N-Methyldiethanolamine + Diethanolamine), (2-Amino-2-methyl-1-propanol + Monoethanolamine), and (2-Amino-2-methyl-1-propanol + Diethanolamine)", *J. Chem. Eng. Data.,* **48**, 703-707.

5. Amundsen, T. G., Øi, L. E., and Eimer, D. A. (2009). "Density and Viscosity of Monoethanolamine + Water + Carbon Dioxide from (25 to 80) °C", *J. Chem. Eng. Data.,* **54,** 3096-3100.

6.Rinker, E. B., Oelschlager, D. W., Colussi, A. T., Henry, K. R., and Sandall, O. C. (1994), "Viscosity, Density, and Surface Tension of Binary Mixtures of Water and N-Methyldiethanolamine and Water and Diethanolamine and Tertiary Mixtures of These Amines with Water over the Temperature Range 20-100.degree.C", *J. Chem. Eng. Data.*, **39,** 392-395.

7.Vogel, H. Das. (1921), "Temperaturabhängigkeitsgesetz der Viskosität von Flüssigkeiten", *Physikz.*, **22,** 645-646.

8.Viswanath, D. S. and Natarajan, G. (1989), "*Databook on Viscosity of Liquids"*, Hemisphere, New York.

9. Goletz, Jr. E., and Tassios, D. (1977), "An Antoine type equation for liquid viscosity dependency to temperature", *Ind. Eng. Chem. Proc.*, **16(1)**, 75-79.

10.Dutt, N. V. K. (1990), "A simple method of estimating the viscosity of petroleum crude oil and fractions", *Chem. Eng. J.*, **45**, 83-86.

11.Girifalco, L. A. (1955), "Temperature dependence of viscosity and its relation to vapor pressure for associated liquids", *J. Chem. Phys.*, **23(12)**, 2446-2447.

12.Thorpe, T. E. & Rodger, J. W. (1895), "Bakerian Lecture: On the relations between the viscosity (internal friction) of liquids and their chemical nature", *Phil. Trans.*, **185,** 397-710.

13. Teng, T. T., Maham, Y., Helper, L. G., and Mather, A. E. (1994), "Viscosity of Aqueous Solutions of N-Methyldiethanolamine and of Diethanolamine", *J. Chem. Eng. Data.*, **39**, 290-293.

14. Chowdhury, F. I., Akhtar, S., and Saleh, M. A. ( 2010), "Viscosities and excess viscosities of aqueous solutions of some diethanolamines", *Journal of Molecular Liquids.,* **155**: 1-7.

Paper Q

# Viscosities of Aqueous Solutions of Monoethanolamine (MEA), Diethanolamine (DEA) and N-Methyldiethanolamine (MDEA) at T = (90-150) °C.

This paper is published in the Annual Transactions - The Nordic Rheology Society 2014, 22, 2014.

ANNUAL TRANSACTIONS OF THE NORDIC RHEOLOGY SOCIETY, VOL. 22, 2014

# Viscosities of Aqueous Solutions of Monoethanolamine (MEA), Diethanolamine (DEA) and N-Methyldiethanolamine (MDEA) at T = (90-150) °C

Udara S. P. R. Arachchige[1,a]; Bhupendra Singh[1]; Kishan Prajapati[1]; Morten C. Melaaen[1]

[1] Telemark University College, Porsgrunn, 3901, Norway.

## ABSTRACT

Aqueous amine viscosities of monoethanolamine (MEA), diethanolamine (DEA) and methyldiethanolamine (MDEA) solutions were examined at a high temperature range from (90 to 150) °C for different concentrations. The measured experimental viscosity data were used to correlate the equation suggested by literatures for aqueous amines. The deviation between experimental viscosities measured in this work and viscosities calculated by regression equation is negligible.

## INTRODUCTION

Removal of acid gas impurities such as $CO_2$, $H_2S$ is of prime importance due to environmental regulations. The most common acid gas absorption methods are running with amine solvents. However, lack of available physical property data gives difficulties in developing calculation models for gas absorption and stripping. A wide variety of alkanolamines such as monoethanolamine (MEA), diethanolamines (DEA), N-Methyldiethanolamine (MDEA) can be used for acid gas absorption. The dynamic viscosity of the amine is one of the most important physical properties related to the amine solvent gas absorption. Therefore, the main interest of this study is focused around dynamic viscosity of the amines. The pure amine viscosities over the temperature range 20 - 150 °C have been reported by DiGuilio et al. [1]. The aqueous amine viscosities up to certain temperature range are already given in the literatures. Aqueous MEA viscosities of high concentration (mass ratio of MEA, $r = M_{amine}/M_{amine+water} = 0.2 - 0.9$) in the range of temperature T = (25 to 80) °C have been reported by Amundsen et. at [2]. Moreover, aqueous DEA viscosity of low concentration (r = 0.1 to 0.3) in the range of temperature T = (20 to 80) °C has been measured by Rinker et. al [3]. Aqueous MDEA solution viscosity of concentration of r = (0.2 to 0.5) in the range of temperature T = (30 to 60) °C has been reported by Li and Lie [4]. This work presents a set of measurements covering completed concentration range (r = 0.1 to 0.9) in the range of temperature T = (90 to 150) °C. The measured viscosity data are used to generate the polynomial for representation of amine viscosities using regression. The polynomial equation given by Teng et al. [5] is used to model the dynamic viscosities of aqueous MEA, DEA and MDEA samples over a temperature range.

## EXPERIMENTAL SECTION

This section provides a brief description of sample preparation, sample concentration limits and measurement of performance. Dynamic viscosity was measured using Anton Paar MCR 101 rheometer. Operating pressure is maintained at 5 bars to analyze high temperatures. First, the viscometer is calibrated with petroleum distillate and mineral oil calibration fluid from Paragon Scientific Company. According to the calibration factor, measuring setup was changed to get a high accuracy for measurements. The amine concentration and the supplier are mentioned in the Table 1.

**Table 1.** Purity of the amines used in experiments.

| Amine type | Mass Purity % | Supplier |
|---|---|---|
| MEA | 99.5 | Merck KGaA |
| DEA | 99 | Merck Schuchardt OHG |
| MDEA | 98 | Merck Schuchardt OHG |

The purity of the amines is given in the table in mass basis 99.5, 99 and 98% respectively for MEA, DEA and MDEA. De-gassed distilled water was used to prepare the aqueous amine solution for experimental studies. All the experiments are performed under 5 bar pressure continuously over the temperature range.

## RESULTS AND DISCUSSION

Viscosity measurements of this study are categorized into three parts:

- Aqueous MEA viscosity where r = (0.1 to 0.9) in the temperature range T = (90 to 150) °C
- Aqueous DEA viscosity where r = (0.1 to 0.9) in the temperature range T = (90 to 150) °C
- Aqueous MDEA viscosity where r = (0.1 to 0.9) in the temperature range T = (90 to 150) °C

The viscosity measurements of MEA, DEA and MDEA samples are tabulated in the Table 2, 3 and 4, respectively.

**Table 2**. Viscosities of aqueous MEA solutions (r = 0.1 to 0.9) measured in this work for temperature T = (90 to 150) °C.

| Temp | Concentration (r) | | | | | | | | |
|---|---|---|---|---|---|---|---|---|---|
| | 0.1 | 0.2 | 0.3 | 0.4 | 0.5 | 0.6 | 0.7 | 0.8 | 0.9 |
| T/°C | η/mPa·s | | | | | | | | |
| 90 | 0.441 | 0.554 | 0.669 | 0.824 | 1.091 | 1.344 | 1.673 | 2.010 | 2.462 |
| 100 | 0.372 | 0.500 | 0.574 | 0.706 | 0.898 | 1.085 | 1.293 | 1.651 | 1.897 |
| 110 | 0.327 | 0.471 | 0.540 | 0.584 | 0.758 | 0.898 | 1.048 | 1.325 | 1.522 |
| 120 | 0.305 | 0.441 | 0.489 | 0.518 | 0.656 | 0.743 | 0.881 | 1.093 | 1.257 |
| 130 | 0.268 | 0.389 | 0.449 | 0.486 | 0.564 | 0.629 | 0.741 | 0.913 | 1.030 |
| 140 | 0.245 | 0.360 | 0.423 | 0.444 | 0.512 | 0.559 | 0.637 | 0.775 | 0.862 |
| 150 | 0.210 | 0.325 | 0.405 | 0.413 | 0.484 | 0.512 | 0.568 | 0.638 | 0.684 |

**Table 3**. Viscosities of aqueous DEA solutions (r = 0.1 to 0.9) measured in this work for temperature T = (90 to 150) °C.

| Temp | Concentration (r) | | | | | | | | |
|---|---|---|---|---|---|---|---|---|---|
| | 0.1 | 0.2 | 0.3 | 0.4 | 0.5 | 0.6 | 0.7 | 0.8 | 0.9 |
| T/°C | η/mPa·s | | | | | | | | |
| 90 | 0.447 | 0.568 | 0.724 | 0.971 | 1.565 | 2.328 | 3.692 | 6.159 | 10.059 |
| 100 | 0.413 | 0.491 | 0.602 | 0.882 | 1.353 | 1.829 | 2.840 | 4.449 | 6.994 |
| 110 | 0.366 | 0.449 | 0.533 | 0.769 | 1.157 | 1.511 | 2.269 | 3.409 | 5.164 |
| 120 | 0.327 | 0.411 | 0.487 | 0.663 | 0.999 | 1.270 | 1.856 | 2.689 | 3.921 |
| 130 | 0.297 | 0.371 | 0.449 | 0.577 | 0.874 | 1.088 | 1.538 | 2.154 | 3.074 |
| 140 | 0.255 | 0.349 | 0.412 | 0.520 | 0.754 | 0.934 | 1.320 | 1.757 | 2.439 |
| 150 | 0.216 | 0.306 | 0.368 | 0.465 | 0.648 | 0.826 | 1.120 | 1.428 | 1.869 |

**Table 4**. Viscosities of aqueous MDEA solutions (r = 0.1 to 0.9) measured in this work for temperature T = (90 to 150) °C.

| Temp | Concentration (r) | | | | | | | | |
|---|---|---|---|---|---|---|---|---|---|
| | 0.1 | 0.2 | 0.3 | 0.4 | 0.5 | 0.6 | 0.7 | 0.8 | 0.9 |
| T/°C | η/mPa·s | | | | | | | | |
| 90 | 0.463 | 0.543 | 0.739 | 0.985 | 1.398 | 1.953 | 2.802 | 3.803 | 5.082 |
| 100 | 0.431 | 0.488 | 0.594 | 0.805 | 1.127 | 1.535 | 2.145 | 2.797 | 3.685 |
| 110 | 0.400 | 0.448 | 0.518 | 0.680 | 0.948 | 1.263 | 1.719 | 2.172 | 2.825 |
| 120 | 0.362 | 0.417 | 0.469 | 0.599 | 0.816 | 1.058 | 1.403 | 1.726 | 2.226 |
| 130 | 0.323 | 0.377 | 0.427 | 0.532 | 0.702 | 0.941 | 1.170 | 1.403 | 1.776 |
| 140 | 0.294 | 0.335 | 0.408 | 0.487 | 0.600 | 0.755 | 0.987 | 1.158 | 1.457 |
| 150 | 0.246 | 0.302 | 0.364 | 0.442 | 0.512 | 0.621 | 0.831 | 0.938 | 1.213 |

Viscosities of MEA, DEA and MDEA decrease with the increasing of operating temperature, and increase with the increasing of amine concentration. Some of the viscosity data variations with temperature are given in the Figure 1, 2 and 3 for MEA, DEA and MDEA respectively. Figures are drawn for temperature range from (90 to 150) °C for every case.

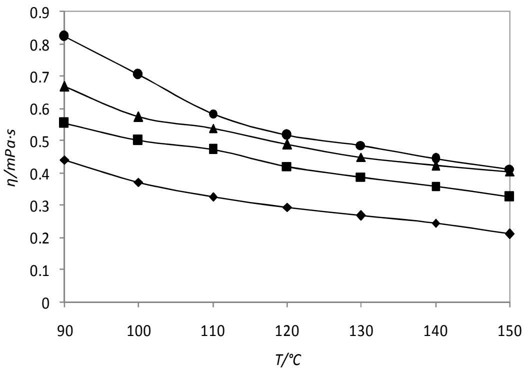

Figure 1: Aqueous MEA viscosity as a function of temperature. Symbols refer to concentration of amine (mass basis) ,♦, 10%; ■, 20%; ▲, 30%; ●, 40%.

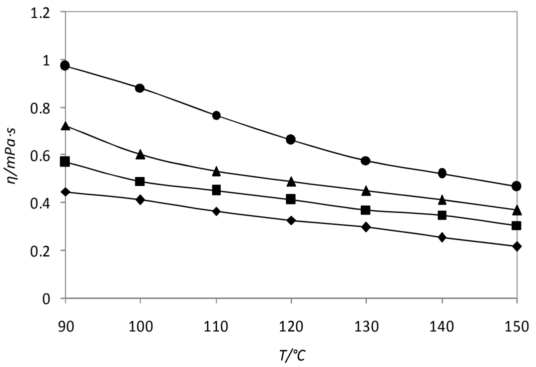

Figure 2: Aqueous DEA viscosity as a function of temperature. Symbols refer to concentration of amine (mass basis) ,♦, 10%; ■, 20%; ▲, 30%; ●, 40%.

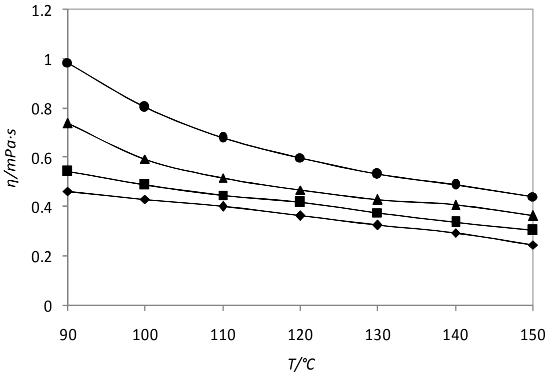

Figure 3: Aqueous MDEA viscosity as a function of temperature. Symbols refer to concentration of amine (mass basis) ,♦, 10%; ■, 20%; ▲, 30%; ●, 40%.

As can be seen from Figure 1, 2 and 3, viscosity of the amine are decreasing with the increase of temperature.

Viscosity measurements of the MEA, DEA and MDEA solutions with r = 0.1 to 0.9 are used to model the equation that is representing aqueous amine viscosity. The equation 1 is suggested by Teng et al. for estimation of aqueous amine viscosities.

$$\ln[\eta/(\text{mPa.s})] = \ln\eta_0 + \sum_{0}^{m} a_k \mathrm{x}^{\mathrm{k}} \qquad (1)$$

In this equation, η represents the viscosity of the binary solution while $\eta_o$ is the viscosity of pure water, and x the mole fraction of the amines. Pure water viscosity is measured for the complete temperature range. Measured viscosity data for different temperatures are separately used to develop the constant values that are required for this equation. Calculated polynomial coefficients which are given by the regression of equation 1 is indicated by $a_k$ in Table 5. Deviation of calculated versus measured aqueous amines' viscosities are calculated as average absolute deviation (AAD) and tabulated in the same table.

**Table 5.** Coefficients of the polynomial of the binary solutions between MEA, DEA and MDEA and water at different temperatures.

| T/°C | ***amine*** | $a_0$ | $a_1$ | $a_2$ | $a_3$ | $a_4$ | $a_5$ | $a_6$ | ***AAD*** |
|---|---|---|---|---|---|---|---|---|---|
| 90 | MEA | 0.3453 | 3.4619 | -14.4202 | 119.735 | -371.1737 | 491.5896 | -236.6139 | 0.01 |
| | DEA | 0.3329 | 4.7260 | -42.4504 | 386.9422 | -1167.1 | 1636.8 | -855.6841 | 0.08 |
| | MDEA | 0.4736 | -2.0905 | 62.9991 | -294.7465 | 824.7204 | -1134.7 | 583.5687 | 0.05 |
| 100 | MEA | 0.2133 | 6.6914 | -60.1462 | 373.9031 | -1103 | 1511.5 | -771.5124 | 0.07 |
| | DEA | 0.5515 | -7.1398 | 114.4023 | -527.9142 | 1313.4 | -155.8 | 703.7359 | 0.01 |
| | MDEA | 0.4736 | -2.7278 | 53.5302 | -224.9534 | 580.7206 | -776.2963 | 398.1262 | 0.03 |
| 110 | MEA | 0.0593 | 11.8655 | -126.6862 | 711.4526 | -1944.9 | 2520.9 | -1234.4 | 0.01 |
| | DEA | 0.4640 | -5.1285 | 87.4062 | -400.6163 | 984.6645 | -1163.5 | 524.2393 | 0.04 |
| | MDEA | 0.4218 | -1.3781 | 28.1658 | -84.6120 | 184.8714 | -254.0793 | 139.4344 | 0.02 |
| 120 | MEA | 0.076 | 10.0953 | -103.0506 | 550.3446 | -1451.0 | 1834.4 | -882.9911 | 0.03 |
| | DEA | 0.3682 | -2.4144 | 51.1804 | -219.4658 | 519.5077 | -597.8328 | 263.3452 | 0.01 |
| | MDEA | 0.3525 | 0.1449 | 8.8563 | 3.3596 | -38.5952 | 30.3710 | 2.8030 | 0.01 |
| 130 | MEA | 0.0838 | 7.6582 | -65.7286 | 310.5228 | -755.703 | 910.0895 | -426.188 | 0.02 |
| | DEA | 0.2493 | 2.0840 | -16.9533 | 174.7263 | -570.5933 | 804.8258 | -412.6446 | 0.03 |
| | MDEA | 0.2419 | 3.5695 | -39.5729 | 282.2498 | -823.4096 | 1066.2 | -508.7170 | 0.02 |
| 140 | MEA | 0.0557 | 7.8983 | -69.9447 | 333.3806 | -822.4012 | 1002.1 | -473.0645 | 0.01 |
| | DEA | 0.2139 | 1.3075 | 7.3841 | -33.8689 | 120.9994 | -198.3091 | 114.2200 | 0.02 |
| | MDEA | 0.2840 | -0.3376 | 24.4690 | -151.0273 | 477.3292 | -703.2198 | 379.2793 | 0.002 |
| 150 | MEA | 0.0195 | 7.7825 | -64.9183 | 293.5027 | -696.1422 | 819.678 | -375.6467 | 0.01 |
| | DEA | 0.1375 | 3.0216 | -16.0308 | 92.3158 | -217.8615 | 229.5957 | -89.6132 | 0.01 |
| | MDEA | 0.2395 | -0.6921 | 36.9316 | -263.3742 | 853.1105 | -1245.5 | 662.3318 | 0.005 |

Predicted viscosity values of the fitted correlation and the experimental data are in good agreement with negligible deviation.

## EVALUATION OF EXPERIMENTAL UNCERTAINTIES

The uncertainty of the viscosity measurements of MEA, DEA and MDEA aqueous amines arises as a combination of the uncertainty of the temperature measurements, sample preparation and measuring instrument uncertainties.

The temperature accuracy, U(T), which is related to rheometer temperature controller, is given as ±0.3K. The maximum viscosity gradient against the temperature, $\Delta\eta/\Delta T$, is calculated as 0.040 $\text{mPa}\cdot\text{s}\cdot\text{K}^{-1}$. The corresponding uncertainty in η, $(\Delta\eta/\Delta T)\cdot\Delta T$, is then estimated as ±0.0120 mPa·s. The uncertainties of the sample preparation were found by calculating the error values (difference between the expected value and measured value r) of the prepared sample. The mass ratio uncertainty ±0.004, U(r), and the viscosity gradient $(\Delta\eta/\Delta r)$ with 0.05 mPa·s are used for calculating the uncertainty of sample preparation. The resulting uncertainty in the sample preparation is calculated as, $(\Delta\eta/\Delta r).\Delta r$, ±0.00020. The rheometer accuracy is given as ± 0.002 mPa·s. The overall uncertainty of η, U(η), is calculated by combining the partial uncertainties reported in this section with root sum of square method. The value is calculated as ±0.0122 mPa·s. The combined expanded uncertainty of the viscosity, Uc(η), is calculated as ±0.024 mPa·s (level of confidence 0.95). The combined expanded uncertainty, suggested by symbol Uc, is obtained by multiplying overall uncertainty, U(η), by a coverage factor, suggested symbol k. Typically, k is assumed to be 2 with the level of confidence 0.95.

## CONCLUSION

The viscosity of MEA, DEA, and MDEA were measured at a temperature range from (90 to 150) °C for aqueous amines. Aqueous amine viscosities were measured for a mass fraction range 0.10 to 0.90. As the temperature increase, viscosity of aqueous amine solutions decreases. Moreover, the viscosity of aqueous amine solutions increases as the mass fraction of amine increase for a given temperature. The equation suggested by Teng et al. is used for estimation of aqueous amine viscosities. The required coefficient for the suggested equation is generated by regression. The deviation of regression values and measured values are calculated for all three aqueous amines.

## REFERENCES

1. DiGuilio, R. M., Lee, R.-J., Schaeffer, S. T., Brasher, L. L., and Teja, A. S. (1992), "Densities and viscosities of the ethanolamines", *J. Chem. Eng. Data.*, **37**, 239-242.

2. Amundsen, T. G., Øi, L. E., and Eimer, D. A. (2009). "Density and Viscosity of Monoethanolamine + Water + Carbon Dioxide from (25 to 80) °C", *J. Chem. Eng. Data.,* **54,** 3096-3100.

3.Rinker, E. B., Oelschlager, D. W., Colussi, A. T., Henry, K. R., and Sandall, O. C. (1994), "Viscosity, Density, and Surface Tension of Binary Mixtures of Water and N-Methyldiethanolamine and Water and Diethanolamine and Tertiary Mixtures of These Amines with Water over the Temperature Range 20-100.degree.C", *J. Chem. Eng. Data.*, **39,** 392-395.

4. Li, M. H. and Lie, Y. C. (1994), "Densities and Viscosities of Solutions of Monoethanolamine + N-methyldiethanolamine + Water and Monoethanolamine + 2-Amino-2-methyl-1-propanol + Water", *J. Chem. Eng. Data.*, , **39**, 444-447.

5. Teng, T. T., Maham, Y., Helper, L. G., and Mather, A. E. (1994), "Viscosity of Aqueous Solutions of N-Methyldiethanolamine and of Diethanolamine", *J. Chem. Eng. Data.*, **39**, 290-293.

Paper R

# Viscosity of Aqueous Solutions of N-Methyldiethanolamine + Monoethanolamine (MDEA+MEA).

This paper is submitted to the International Journal of Thermo Physics.

# Viscosity of Aqueous Solutions of N-Methyldiethanolamine + Monoethanolamine (MDEA+MEA)

U. S. P. R. Arachchige,[1, a)] B. Singh,[1] K. Prajapati,[1] M. C. Melaaen[1]

[1]*Telemark University College, Porsgrunn, 3901, Norway.*

The blended amine viscosities of N-methyldiethanolamine and monoethanolamine (MDEA+MEA) are measured for temperature range from 293.15 to 413.15 K. The total amine strength in the solution is maintained at 0.2, 0.3 and 0.4 mass basis. Temperature range 293.15 to 303.15 K is performed with cooling system to achieve the lower stable temperatures during the experiment. Operating pressure is maintained at 1 bar for temperature range 293.15 to 353.15 K and 4.5 bar for higher temperatures. Measured viscosity data is compared with available literature data as well as with modeled data by Grunberg and Nissan model. The viscosity values are available up to 353.15 K for some blended amine concentrations. The viscosity of blended MDEA and MEA mixtures with different mixing ratios are experimentally measured for temperature range 293.15 to 413.15 K. Therefore, this study is given highly importance for gas absorption process while developing regression models for reacting systems in the gas separation. The average absolute deviation between measured viscosity values and viscosity calculated by regression model is around 2.1%. Therefore, measured blended amine viscosities are in good agreement with the predicted viscosity by regression model which is given by Grunberg and Nissan equation.

## I. INTRODUCTION

The various types of amines such as Monoethanolamine (MEA), diethanolamine (DEA), N-Methyldiethanolamine (MDEA) have been used for gas treating systems in a wide variety of applications [1]. However, single amine for gas treating is economically unfavorable due to high energy demand. Therefore, searching of alternative solvents is an important factor to continue the process. In that case, blended amines (mixture of primary and tertiary or secondary and tertiary) will play a vital role in gas absorption and desorption process. The tertiary amine, which has higher equilibrium capacity, together with primary or secondary amines which has higher reaction rate will bring the considerable effect. The physical properties of those amines and blended amines are important to understand the complete process. However, lack of physical property data such as viscosity of blended amines forced us to continue this research. The viscosity data of blended amines has been reported in several literatures such as (MEA+MDEA+H2O) [2, 3, 4], DEA+MDEA+H2O [5, 6, 7, 8].

All most reported data in above literatures are available for the viscosities of blended amines over the temperature range (303 to 353) K. Bishnu et.al 2003 [9] has been performed the density and viscosity measurements for temperature range (293 to

---

a) Author to whom correspondence should be addressed. Electronic mail: udara.s.p.aracchige@hit.no.

323) K to complete the gap with previous works. Hence, in this work the viscosity measurements of blended amines have done in the temperature range, T= (293 to 413) K to complete the range with high temperature. Viscosities of pure and aqueous solutions of MDEA, MEA and DEA has been already completed and reported in the previous paper [10]. In this paper, we are reporting the viscosity of blended amine systems. The viscosity of (MDEA+MEA+H2O) are measured over the temperature range (293- 413) K. The total amine concentration (mass basis) is maintained at 20%, 30% and 40% separately. The mass ratio, *r*, is defined as $r = M_{\text{amine}}/M_{\text{amine+water}}$ = 0.2, 0.3 and 0.4 for this study.

## II. EXPERIMENTAL SECTION

The MEA was purchased from Merck KGaA and the MDEA from Merck Schuchardt OHG. The purity of the amines is 99.5% and 98% (mass basis) respectively for MEA and MDEA. The Amine solutions were prepared with degassed distilled water. Amine solutions are prepared to get total concentration of amine mixture as 20%, 30% and 40% mass basis. There are several mass fraction variations followed to develop the measuring samples. The mixture after adding amines and distilled water, is well stirred to get uniformity of the solution. Dynamic viscosity was measured using MCR 101 Anton Paar double-gap rheometer. The viscometer was calibrated against the petroleum distillate and mineral oil calibration fluid which is purchased from Paragon Scientific Ltd. The calibration factor was decided according to the experimental value and given literature value. The low-temperature measurements (293.15 – 303.15) K were achieved by applying cooling system Physica VT2 connected together with the rheometer setup. Without further purification, all these amines were used for experimental studies. The temperature range from 313.15 – 413.15 K is measured without cooling system. Two different pressure values are used for the measuring process in order to avoid the water vaporization at high temperatures. First part of the process (293.15 – 353.15) K was completed with pressure 1.01 bar and the second part of the process (363.15 – 413.15) K is completed with the 4.5 bar pressure.

## III. RESULTS AND DISCUSSION

Viscosities of MDEA+MEA+H2O tertiary mixture are experimentally calculated for mass ratio 0.2, 0.3 and 0.4 of total amine weight base concentrations. The experimental viscosity values are tabulated in Table I, II and III for r = 0.2, 0.3 and 0.4 concentration respectively.

TABLE I. Viscosity of MDEA+MEA amine mixture when $r = 0.2$.

| T/K | Composition of the sample (MDEA/MEA)% | | | |
|---|---|---|---|---|
| | 20/0 | 15/5 | 5/15 | 0/20 |
| | η/mPa·s | | | |
| 293.15 | 2.264 | 2.180 | 2.064 | 2.002 |
| 298.15 | 1.921 | 1.868 | 1.784 | 1.700 |
| 303.15 | 1.695 | 1.631 | 1.534 | 1.496 |
| 313.15 | 1.320 | 1.263 | 1.206 | 1.163 |
| 323.15 | 1.062 | 1.016 | 0.976 | 0.942 |
| 333.15 | 0.862 | 0.830 | 0.808 | 0.772 |
| 343.15 | 0.716 | 0.705 | 0.678 | 0.665 |
| 353.15 | 0.602 | 0.595 | 0.588 | 0.583 |
| 363.15 | 0.532 | 0.523 | 0.480 | 0.398 |
| 373.15 | 0.476 | 0.464 | 0.432 | 0.362 |
| 383.15 | 0.426 | 0.406 | 0.386 | 0.329 |
| 393.15 | 0.396 | 0.368 | 0.320 | 0.286 |
| 403.15 | 0.362 | 0.324 | 0.294 | 0.246 |
| 413.15 | 0.34 | 0.294 | 0.264 | 0.201 |

TABLE II. Viscosity of MDEA+MEA amine mixture when $r = 0.3$.

| | Composition of the sample (MDEA/MEA)% | | | | | | | |
|---|---|---|---|---|---|---|---|---|
| T/K | 30/0 | 28.5/1.5 | 25/5 | 20/10 | 15/15 | 10/20 | 5/25 | 0/30 |
| | η/mPa·s | | | | | | | |
| 293.15 | 3.53 | 3.52 | 3.50 | 3.44 | 3.25 | 3.06 | 3.07 | 2.97 |
| 298.15 | 2.99 | 2.95 | 2.92 | 2.90 | 2.74 | 2.59 | 2.53 | 2.46 |
| 303.15 | 2.54 | 2.52 | 2.50 | 2.47 | 2.36 | 2.22 | 2.18 | 2.13 |
| 313.15 | 1.89 | 1.86 | 1.83 | 1.80 | 1.79 | 1.68 | 1.67 | 1.64 |
| 323.15 | 1.45 | 1.42 | 1.40 | 1.37 | 1.32 | 1.29 | 1.26 | 1.23 |
| 333.15 | 1.14 | 1.12 | 1.08 | 1.04 | 1.02 | 1.00 | 0.97 | 0.95 |
| 343.15 | 0.93 | 0.90 | 0.87 | 0.84 | 0.81 | 0.80 | 0.79 | 0.77 |
| 353.15 | 0.77 | 0.75 | 0.74 | 0.73 | 0.71 | 0.69 | 0.66 | 0.64 |
| 363.15 | 0.64 | 0.62 | 0.59 | 0.55 | 0.54 | 0.48 | 0.46 | 0.41 |
| 373.15 | 0.58 | 0.56 | 0.52 | 0.50 | 0.47 | 0.44 | 0.41 | 0.39 |
| 383.15 | 0.53 | 0.50 | 0.48 | 0.46 | 0.42 | 0.40 | 0.38 | 0.36 |
| 393.15 | 0.47 | 0.44 | 0.42 | 0.40 | 0.38 | 0.36 | 0.32 | 0.30 |
| 403.15 | 0.42 | 0.40 | 0.36 | 0.35 | 0.32 | 0.31 | 0.29 | 0.28 |
| 413.15 | 0.38 | 0.37 | 0.32 | 0.31 | 0.30 | 0.28 | 0.26 | 0.24 |

TABLE III. Viscosity of MDEA+MEA amine mixture when $r = 0.4$.

| T/K | Composition of the sample (MDEA/MEA)% | | | | | | | | |
|---|---|---|---|---|---|---|---|---|---|
| | 40/0 | 35/5 | 30/10 | 25/15 | 20/20 | 15/25 | 10/30 | 5/35 | 0/40 |
| | η/mPa·s | | | | | | | | |
| 293.15 | 6.35 | 6.01 | 5.85 | 5.34 | 5.21 | 5.03 | 4.84 | 4.73 | 4.64 |
| 298.15 | 5.25 | 5.02 | 4.89 | 4.47 | 4.31 | 4.27 | 3.92 | 3.86 | 3.76 |
| 303.15 | 4.34 | 4.19 | 4.09 | 3.77 | 3.69 | 3.63 | 3.37 | 3.32 | 3.27 |
| 313.15 | 3.14 | 3.04 | 3.00 | 2.71 | 2.57 | 2.49 | 2.44 | 2.35 | 2.30 |
| 323.15 | 2.36 | 2.29 | 2.25 | 2.05 | 2.01 | 1.96 | 1.86 | 1.82 | 1.78 |
| 333.15 | 1.82 | 1.79 | 1.74 | 1.61 | 1.53 | 1.45 | 1.43 | 1.41 | 1.39 |
| 343.15 | 1.48 | 1.42 | 1.39 | 1.27 | 1.23 | 1.19 | 1.18 | 1.16 | 1.15 |

| | | | | | | | | | |
|---|---|---|---|---|---|---|---|---|---|
| 353.15 | 1.19 | 1.15 | 1.16 | 1.03 | 1.01 | 0.98 | 0.96 | 0.95 | 0.94 |
| 363.15 | 0.97 | 0.95 | 0.93 | 0.90 | 0.88 | 0.86 | 0.85 | 0.85 | 0.84 |
| 373.15 | 0.92 | 0.90 | 0.88 | 0.86 | 0.85 | 0.82 | 0.80 | 0.80 | 0.78 |
| 383.15 | 0.81 | 0.76 | 0.73 | 0.72 | 0.70 | 0.68 | 0.64 | 0.62 | 0.60 |
| 393.15 | 0.72 | 0.69 | 0.66 | 0.64 | 0.63 | 0.60 | 0.58 | 0.58 | 0.57 |
| 403.15 | 0.58 | 0.66 | 0.62 | 0.60 | 0.58 | 0.54 | 0.52 | 0.50 | 0.50 |
| 413.15 | 0.46 | 0.45 | 0.43 | 0.42 | 0.40 | 0.38 | 0.34 | 0.32 | 0.30 |

The pure amine viscosities of MDEA, MEA, and Water are given in Table IV [10].

TABLE IV. Pure amine and water viscosity variation with temperature [10].

| T/K | MEA | MDEA | H2O |
|---|---|---|---|
| | | η/mPa·s | |
| 293.15 | 24.085 | 103.67 | 1.051 |
| 298.15 | 18.924 | 77.32 | 0.900 |
| 303.15 | 15.151 | 57.50 | 0.843 |
| 313.15 | 10.006 | 34.622 | 0.665 |
| 323.15 | 6.962 | 22.402 | 0.557 |
| 333.15 | 5.037 | 15.276 | 0.478 |
| 343.15 | 3.775 | 9.965 | 0.414 |
| 353.15 | 2.919 | 7.146 | 0.360 |
| 363.15 | 2.334 | 5.818 | 0.315 |
| 373.15 | 1.914 | 4.385 | 0.281 |
| 383.15 | 1.586 | 3.362 | 0.254 |
| 393.15 | 1.324 | 2.656 | 0.232 |
| 403.15 | 1.105 | 2.122 | 0.210 |
| 413.15 | 0.934 | 1.696 | 0.190 |

The viscosity variation of blended amines is analyzed with following figures. As an example, r = 0.2 of blended amine viscosities also compared with available literatures. Literature values are taken from the Li and Lie [3]. However, they have performed experiments for temperature range 303.15-353.15 K only. Figure1 represents the comparison of viscosities for mass ratio 0.2. According to the figures, it can be seen that viscosity of blended amine is decreasing with the increase of the temperature. The measurement values are in good agreement with available literature data.

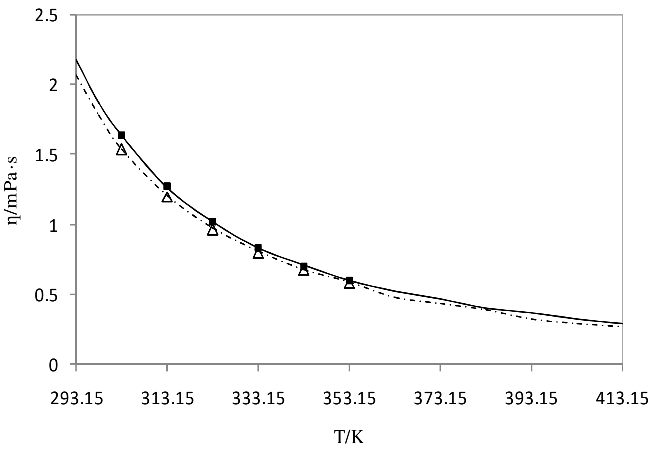

FIG. 1.Viscosity of MDEA/MEA blends for 15/5% and 5/15%. Lines are experimental data; Symbols refer to the literature data [3]: ■, 15/5%; Δ, 5/15%.

Similarly, MDEA+MEA blend of 28.5+1.5% and 25+5% for complete temperature is considered. At the same time, literature data is plotted in the same figure (Figure2 and 3) for available temperature range. Literature values of 28.5/1.5% are taken from the Bishnu et. al [9]. However, they have performed experiments for temperature from 293.15 to 323.15 K only.

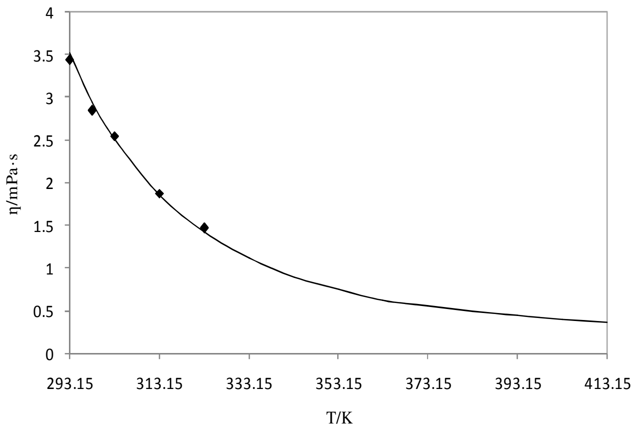

FIG. 2.Viscosity of MDEA/MEA blends for 28.5/1.5%. Lines are experimental data and symbols refer to the literature data [9].

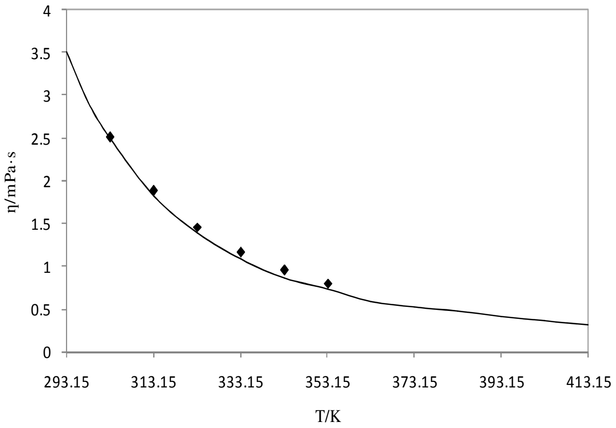

FIG. 3.Viscosity of MDEA/MEA blends for 25/5%. Lines are experimental data (25/5%) and symbols refer to the literature data (24/6%) [3].

As can be seen from both figures, viscosity of the blended amine is decreasing with the increase of temperature. According to the Figure3, literature data is given for 24/6% of MDEA/MEA mixture. However, experimental data is plotted for 25/5% of MDEA/MEA mixture. When the MEA composition in the blended amine is decreasing, viscosity of the blend is also decreasing. This is because of the viscosity of MEA is less compared to the MDEA viscosity. All the literature values are fallen above the experimental viscosity line in Figure3. There for experimental results are in good agreement with the literature data. However, there is a slight deviation between experimental data and regression data. The reason may be due to the practical errors or different amine conditions.

## IV. RESULTS VALIDATION

The experimental viscosity values in this study are compared with the Grunberg and Nissan model [9]. The Grunberg and Nissan model is suggested for calculating viscosity of the liquid mixtures. The Grunberg and Nissan equation has the following form (equation 1):

$$\ln \eta_m / mPa \cdot s = \sum x_i \ln \eta_i + \sum \sum x_i x_j G_{ij} \tag{1}$$

Where $\eta_m$ is the viscosity of the liquid mixture, $\eta_i$ is the viscosity of the $i^{th}$ pure fluid and mole fraction of the $i^{th}$ component is given by the $x_i$. Pure liquid viscosities are given in the Table 4. The component $G_{ij}$ is given by temperature dependent equation which is assumed to follow the equation 2 which is given below.

$$G_{ij} = a + b(T/K) + c(T/K)^2 \tag{2}$$

The parameter values for a, b and c is taken from the literatures and given in the Table V [9].

TABLE IV. Constant values for equation 2, MEA (1) + MDEA (2) +H2O (3) [10].

| Parameter - Gij | Constant values from equation (2) | MDEA+MEA+H2O |
|---|---|---|
| $10^3$ $G_{12}$ | a | 2061147.2 |
| | b | -12381.298 |
| | c | 18.523985 |
| $10^3$ $G_{13}$ | a | -23598.380 |
| | b | 196.27770 |
| | c | -0.3298253 |
| $10^3$ $G_{23}$ | a | 126845.80 |
| | b | -625.32640 |
| | c | 0.8442153 |

The calculated viscosity values using equation (1) and experimental viscosity values measured in this study are in good agreement. The average absolute deviation of the viscosity data is 2.1% for MDEA+MEA+H2O system. The parameter values used for the equation 1 was taken from the regression results developed by Bishnu et.al [9]. However, they have performed experiments for temperature range 293.15-323.15 K only. That may be the reason for deviation of the current study. The experimental viscosity values and the viscosity values calculated by the equation 1 are representing by Figure4-6 for 20%, 30% and 40% total amine concentration respectively.

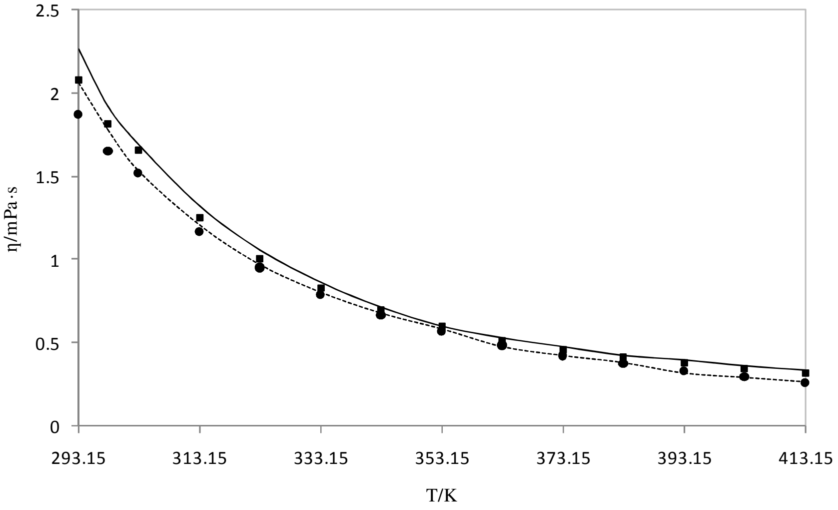

FIG. 4.Experimental results vs. equation modeled results for MDEA+MEA+H2O mixture: Symbols refer to equation values: ■, 20/0%; ●, 5/15%. Lines are experimental data.

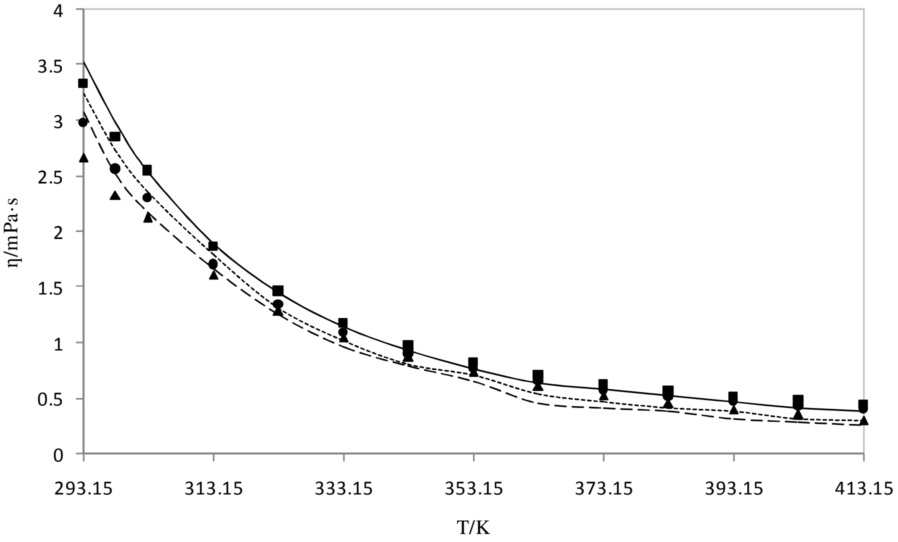

FIG. 5. Experimental results vs. equation modeled results for MDEA+MEA+H2O mixture: Symbols refer to equation values: ■, 30/0%; ●, 15/15%; ▲, 5/25%. Lines are experimental data.

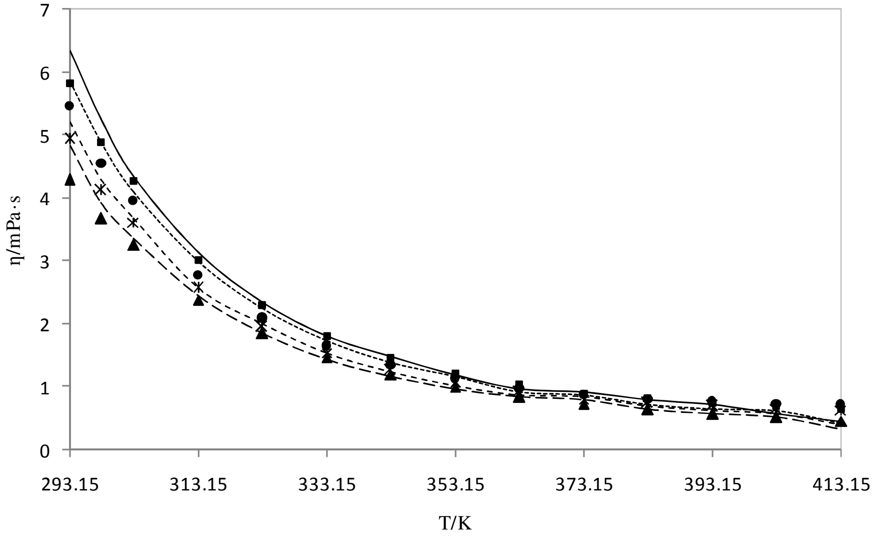

FIG. 6. Experimental results vs. equation modeled results for MDEA+MEA+H2O mixture: Symbols refer to equation values: ■, 40/0%; ●, 30/10%; ∗, 20/20%; ▲, 10/30%. Lines are experimental data.

There are slight changes of experimental data trend after 353.15K temperature for every case. Reason for that may be use of high pressure after that temperature value. However, the fluctuation of the trend is negligible.

## V. EXPERIMENTAL UNCERTAINTIES

The experimental uncertainties have to be discussed for better understandings. The uncertainty of the viscosity measurements of MEA+MDEA amine mixtures arises as a combination of the uncertainty of the temperature measurements and sample preparation uncertainties due to measuring instrument uncertainties.

The temperature accuracy, U(T), which is related to rheometer temperature controller, is given as ±0.3K. The maximum viscosity gradient against the temperature, $\Delta\eta/\Delta T$, is calculated as 0.044 $mPa\cdot s\cdot K^{-1}$. The corresponding uncertainty in η, $(\Delta\eta/\Delta T).\Delta T$, is then estimated as ±0.0132 mPa·s. The uncertainties of the sample preparation were found by calculating the error values (difference between the expected value and measured value r) of the prepared sample. The ±0.004 of mass ratio uncertainty, U(r), is calculated with 0.06 mPa·s viscosity gradient ($\Delta\eta/\Delta r$). The resulting uncertainty in the sample preparation is calculated as, $(\Delta\eta/\Delta r).\Delta r$, ±0.00024. The rheometer accuracy is given as ± 0.002 mPa·s. The overall uncertainty of η, U(η), is calculated by combining the partial uncertainties reported in this section with root sum of square method. The value is calculated as ±0.0134 mPa·s. The combined expanded uncertainty of the viscosity, Uc(η), is calculated as ±0.0268 mPa·s (level of confidence 0.95). The combined expanded uncertainty, suggested by symbol Uc, is obtained by multiplying overall uncertainty, U(η), by a coverage factor, suggested symbol k. Typically, k is assumed to be 2 with the level of confidence 0.95.

## VIII. CONCLUSION

The viscosities of MDEA+MEA+H2O mixtures for different concentrations have been analyzed for temperature range from 293.15 to 413.15 K. High temperature data was measured by keeping high pressure of the measuring system. An decrease in the viscosity with increasing temperature were observed. Measured viscosities were compared with the available literature values as well as with viscosities calculated by Grunberg and Nissan equation. The experimental data is in good agreement with literature data as well as with the calculated data. The average absolute deviation between the experimental values and values predicted by equation is around 2.1%. The parameter values used in the equation is developed by using experimental data from 293.15 to 323.15K. Same parameters used for comparison with the present study even though this study was performed at temperature range 293.15 to 413.15K. That may be the main reason behind the deviation between viscosities of this study and the calculated values by equation.

## REFERENCES

[1] A. L. Kohl, R. B. Nielsen, *Gas Purification*, 5th edition; Gulf Publishing Company: Houston, 1997.

[2]M. H. Li andK. P. Shen,J. Chem. Eng. Data.37 (3), 288 (1992).

[3] M. H. Li and Y. C. Lie, J.Chem. Eng. Data.39, 444 (1994).

[4] D. P. Hagewiesche, S. S. Ashour and O. C. Sandall, J. Chem. Eng. Data.40, 627 (1995).

[5] E. B. Rinker, D. W. Oelschlager, A. T. Colussi, K. R. Henry and O. C. Sandall, J. Chem. Eng. Data.39, 392 (1994).

[6] T. T. Teng, Y. J. Maham, L. G. Hepler and A. E. Mather, J. Chem. Eng. Data.39, 290 (1994).

[7] C. H. Hsu and M. H. Li, J. Chem. Eng. Data. 42, 502 (1997)

[8] C.H. Hsu and M. H. Li, J.Chem. Eng. Data. 42, 714 (1997).

[9] B. P. Mandal, M. Kundu and S. S. Bandyopadhyay, J. Chem. Eng. Data. 48, 703 (2003).

[10] U. S. P. R. Arachchige, A. Neelakantha, D. A. Eimer, M. C. Melaaen.Annual Transactions - The Nordic Rheology Society.21, 299 (2013).

Paper S

# Dynamic Viscosity of Partially Carbonated Aqueous Monoethanolamine (MEA) from (20 to 150) °C.

This paper is published in Applied Chemical Engineering (2018) Volume 1: 1-9

Applied Chemical Engineering (2018) Volume 1
doi:10.24294/ace.v1i2.660

# Dynamic Viscosity of Partially Carbonated Aqueous Monoethanolamine (MEA) from (20 to 150) ℃

**Udara S. P. R. Arachchige, Bhupendra Singh, Kishan Prajapati, Morten C. Melaaen**

Telemark University College, Porsgrunn, 3901, Norway.

## ABSTRACT

Viscosities of liquid solutions of monoethanolamine (MEA), water ($H_20$), and carbon dioxide ($CO_2$) have been measured. The mass fraction of MEA was (10, 20, 30, 40, and 50)%, and $CO_2$ loading values was between (0.1 to 0.5) mol $CO_2$/mol MEA. The operating temperature was varied between (20 to 150) ℃. The available literature data for temperature range (25 to 80) ℃ for mass fraction of (20, 30 and 40)% were used to compare the measurement data. The dynamic viscosity increase with the increase of $CO_2$ loading and decrease with an increase of temperature. The measured data were compared with the data predicted from available regression equation for certain temperature range. Agreement between measured data and the correlation data was satisfactory.

***Keywords:*** Monoethanolamine, Viscosity, $CO_2$ loading, Rheometer, Temperature effect

## 1. Introduction

The various types of amines such as Monoethanolamine (MEA), diethanolamine (DEA), N-Methyldiethanolomine (MDEA) have been used for gas treating systems in a wide variety of applications[1]. The information available in literatures related to the physical properties of amines is limited. The uses of physical properties are typically for calculating of column dimensions and mass transfer correlations in gas absorption process[2,3].

Moreover, dynamic viscosities of partially carbonated aqueous amines are rare to find in the literatures. However, some of the data are available with limited concentration values and limited temperature range. Weiland *et al.*[4] has performed the experiments for $CO_2$ loaded aqueous MEA for temperature for 25 ℃ with 10, 20, 30 and 40% mass concentration. However, they have performed the experiments only for temperature 25 ℃.

Scarcity of physical properties availability was motivated to perform the experiments. Solution viscosity is one of the main parameters when considering the gas absorption process. Most of the literatures are reported the data only to temperature 80 ℃ and for limited concentration values only. Amundsen *et al.*[5] has reported the viscosity data for temperature range from (25 to 80) ℃ for concentration of MEA 20, 30 and 40 % mass basis. However, they have considered the $CO_2$ loading values $\alpha \in [0.1, 0.5]$ for their experiments. Therefore, more viscosity values are missing in the range while considering the available data for aqueous MEA with $CO_2$ loaded. This reason motivated us to perform the experiments for this study.

Modeling and simulation of gas absorption process require number of parameter values that related to the mass transfer rate[4]. This work was taken to determine the dynamic viscosity of Monoethanolamine (MEA) which is mainly considered for gas absorption. The $CO_2$ loaded amine viscosities are analyzed for the solutions with the mass ration, $r \in [0.1, 0.5]$ and $CO_2$ loading, $\alpha \in [0.1, 0.5]$ at temperatures, $T \in [20, 150]$ ℃. The measured data were compared with the available literature data[5]. At the same time, data were compared with the correlation presented in Weiland *et al.*[4].

## 2. Experimental section

The pure MEA was purchased from Merck KGaA supplier. The purity of the amine is 99.5% (mass basis). Amine solutions are prepared to get total concentration of amine mixture as 10%, 20%, 30%, 40% and 50% mass basis. The mixture after adding amines and distilled water is well stirred to get uniformity of the solution.

Aqueous solutions of amines were prepared using degassed, purified water and amines. Sample concentration maintained by adding required portion of amine and water with the help of analytical balance that has an accuracy of $\pm 1 \cdot 10^{-7}$.The high $CO_2$ loaded samples, $\alpha = (>0.5)$, prepared by bubbling $CO_2$ gas through an unloaded solution at required mass flow rate of $CO_2$ for an appropriate period. The required $CO_2$ loaded samples were prepared by diluting

---

doi: 10.24294/ace.v1i2.660

of high $CO_2$ loading with an unloaded solution in an appropriate ratio to get required loading values, $\alpha$ = (0.1 to 0.5).

The high loaded amine solutions were analyzed using titration method to check the exact $CO_2$ loading value and the amine concentration. The 1 mol $L^{-1}$ HCl solution is used to perform the titration to check the mass concentration of the amine solution. The sample is prepared by adding 2 g of each prepared amine solution with de-ionized water until each sample became 100 $cm^3$ in total. The amount of amine present in the sample is calculated by using the amount of HCl used for the titration. The sample preparation for the loading analysis was carried out by mixing about (0.5 to 1.0) g of the loaded amine solution with 50 $cm^3$ each from 0.3 mol $L^{-1}$ $BaCl_2$ and 0.1 mol $L^{-1}$NaOH. Those samples were heated around 5 min to let $CO_2$ in the samples to react with $BaCl_2$ and make precipitate as $BaCO_3$, then cooled down in a water bath. Moreover, the precipitate is collected and added to the 100 $cm^3$ of de-ionized water and then titrated with 0.1 mol $L^{-1}$HCl solution until the mixture reached the equilibrium point. The mixture was heated to remove the all of the dissolved $CO_2$. Then, same mixture was used for back titration with 0.1 mol $L^{-1}$NaOH solution to check the amount of excess HCl. At last, the moles of HCl reacted with $BaCO_3$ precipitate was used to find the amount of $CO_2$ in the corresponding partially carbonated aqueous amine sample and subsequently the $CO_2$ loading value of the sample.

Dynamic viscosity was measured using MCR 101 Anton Paar double-gap rheometer. The viscometer was calibrated against the petroleum distillate and mineral oil calibration fluid which is purchased from Paragon Scientific Ltd. The calibration factor was decided according to the experimental value and given literature value. The low-temperature measurements (20 – 30) ℃ were achieved by applying cooling system Physica VT2 connected together with the rheometer setup. Without further purification, all these amines were used for experimental studies. The temperature range from (40 – 150) ℃ is measured without cooling system. Two different pressure values are used for the measuring process in order to avoid the water vaporization at high temperatures. First part of the process (20 – 80) ℃ was completed with pressure 1.01 bar and the second part of the process (90 – 150) ℃ is completed with a 4.5 bar pressure.

The measured data for the different amines are compared with those available from the literature. The results that are obtained from the experiments were compared with the regression viscosity values which are predicted by correlations for viscosity at different temperatures.

## 3. Results and discussion

The viscosity data for partially carbonated MEA solutions, mass ratio $r \in [0.1, 0.5]$, are presented in the **Table 1-Table 5** respectively. Five different concentration levels considered with five different $CO_2$ loading values for complete temperature range.

| **Temperature (℃)** | **$CO_2$ loading (mol $CO_2$/mol MEA)** | | | | |
|---|---|---|---|---|---|
| | $\alpha$ = 0.1 | $\alpha$ = 0.2 | $\alpha$ = 0.3 | $\alpha$ = 0.4 | $\alpha$ = 0.5 |
| 20 | 1.46 | 1.49 | 1.51 | 1.54 | 1.58 |
| 25 | 1.31 | 1.34 | 1.37 | 1.43 | 1.48 |
| 30 | 1.16 | 1.19 | 1.21 | 1.22 | 1.25 |
| 40 | 0.93 | 0.96 | 0.98 | 0.99 | 1.04 |
| 50 | 0.74 | 0.77 | 0.79 | 0.83 | 0.87 |
| 60 | 0.65 | 0.67 | 0.69 | 0.72 | 0.75 |
| 70 | 0.56 | 0.59 | 0.63 | 0.66 | 0.69 |
| 80 | 0.47 | 0.49 | 0.52 | 0.55 | 0.58 |
| 90 | 0.41 | 0.43 | 0.46 | 0.53 | 0.55 |
| 100 | 0.37 | 0.38 | 0.42 | 0.46 | 0.48 |
| 110 | 0.34 | 0.36 | 0.39 | 0.42 | 0.44 |
| 120 | 0.31 | 0.33 | 0.36 | 0.39 | 0.4 |
| 130 | 0.27 | 0.29 | 0.32 | 0.34 | 0.36 |
| 140 | 0.25 | 0.26 | 0.28 | 0.3 | 0.31 |

| | | | | | |
|---|---|---|---|---|---|
| 150 | 0.22 | 0.23 | 0.25 | 0.28 | 0.29 |

**Table 1.** Viscosity of MEA with different $CO_2$ loading, r = 0.1

| **Temperature ( ℃)** | **$CO_2$ loading (mol $CO_2$/mol MEA)** | | | | |
|---|---|---|---|---|---|
| | α = 0.1 | α = 0.2 | α = 0.3 | α = 0.4 | α = 0.5 |
| 20 | 2.09 | 2.15 | 2.34 | 2.46 | 2.68 |
| 25 | 1.81 | 1.86 | 1.94 | 2.16 | 2.27 |
| 30 | 1.58 | 1.62 | 1.68 | 1.88 | 1.98 |
| 40 | 1.27 | 1.34 | 1.42 | 1.48 | 1.63 |
| 50 | 1.02 | 1.08 | 1.17 | 1.21 | 1.28 |
| 60 | 0.85 | 0.89 | 0.99 | 1.02 | 1.08 |
| 70 | 0.72 | 0.75 | 0.82 | 0.85 | 0.90 |
| 80 | 0.61 | 0.65 | 0.70 | 0.72 | 0.75 |
| 90 | 0.52 | 0.6 | 0.68 | 0.7 | 0.72 |
| 100 | 0.47 | 0.57 | 0.64 | 0.66 | 0.69 |
| 110 | 0.41 | 0.51 | 0.56 | 0.61 | 0.64 |
| 120 | 0.37 | 0.48 | 0.5 | 0.54 | 0.58 |
| 130 | 0.33 | 0.44 | 0.48 | 0.52 | 0.54 |
| 140 | 0.3 | 0.37 | 0.42 | 0.46 | 0.48 |
| 150 | 0.27 | 0.33 | 0.37 | 0.39 | 0.42 |

**Table 2.** Viscosity of MEA with different $CO_2$ loading, r = 0.2

| **Temperature ( ℃)** | **$CO_2$ loading (mol $CO_2$/mol MEA)** | | | | |
|---|---|---|---|---|---|
| | α = 0.1 | α = 0.2 | α = 0.3 | α = 0.4 | α = 0.5 |
| 20 | 3.33 | 3.49 | 3.82 | 3.97 | 4.21 |
| 25 | 2.87 | 2.94 | 3.14 | 3.47 | 3.76 |
| 30 | 2.47 | 2.56 | 2.72 | 2.94 | 3.27 |
| 40 | 1.92 | 2.04 | 2.09 | 2.39 | 2.67 |
| 50 | 1.55 | 1.61 | 1.66 | 1.87 | 2.22 |
| 60 | 1.25 | 1.31 | 1.38 | 1.52 | 1.81 |
| 70 | 1.02 | 1.08 | 1.16 | 1.24 | 1.51 |

| | | | | | |
|---|---|---|---|---|---|
| 80 | 0.84 | 0.89 | 0.99 | 1.05 | 1.26 |
| 90 | 0.76 | 0.82 | 0.95 | 1.01 | 1.16 |
| 100 | 0.64 | 0.72 | 0.82 | 0.93 | 1.07 |
| 110 | 0.57 | 0.66 | 0.75 | 0.86 | 0.96 |
| 120 | 0.5 | 0.58 | 0.64 | 0.72 | 0.84 |
| 130 | 0.44 | 0.52 | 0.6 | 0.68 | 0.75 |
| 140 | 0.38 | 0.46 | 0.53 | 0.59 | 0.64 |
| 150 | 0.34 | 0.4 | 0.46 | 0.52 | 0.58 |

**Table 3.** Viscosity of MEA with different $CO_2$ loading, r = 0.3

| **Temperature (℃)** | **$CO_2$ loading (mol $CO_2$/mol MEA)** | | | | |
|---|---|---|---|---|---|
| | α = 0.1 | α = 0.2 | α = 0.3 | α = 0.4 | α = 0.5 |
| 20 | 5.01 | 5.56 | 6.70 | 7.49 | 7.89 |
| 25 | 4.25 | 4.82 | 5.39 | 6.16 | 6.98 |
| 30 | 3.56 | 4.10 | 4.61 | 5.22 | 5.84 |
| 40 | 2.74 | 3.02 | 3.28 | 3.63 | 4.05 |
| 50 | 2.13 | 2.37 | 2.65 | 2.97 | 3.22 |
| 60 | 1.64 | 1.82 | 2.15 | 2.52 | 2.72 |
| 70 | 1.30 | 1.52 | 1.77 | 2.05 | 2.37 |
| 80 | 1.07 | 1.24 | 1.39 | 1.71 | 1.94 |
| 90 | 1.01 | 1.16 | 1.24 | 1.66 | 1.84 |
| 100 | 0.93 | 1.05 | 1.11 | 1.42 | 1.65 |
| 110 | 0.84 | 0.96 | 0.99 | 1.21 | 1.43 |
| 120 | 0.73 | 0.84 | 0.86 | 0.96 | 1.1 |
| 130 | 0.67 | 0.74 | 0.79 | 0.85 | 0.98 |
| 140 | 0.56 | 0.61 | 0.68 | 0.76 | 0.84 |
| 150 | 0.45 | 0.53 | 0.58 | 0.6 | 0.66 |

**Table 4.** Viscosity of MEA with different $CO_2$ loading, r = 0.4

| **Temperature (℃)** | **$CO_2$ loading (mol $CO_2$/mol MEA)** | | | | |
|---|---|---|---|---|---|
| | α = 0.1 | α = 0.2 | α = 0.3 | α = 0.4 | α = 0.5 |
| 20 | 7.49 | 9.66 | 11.60 | 14.30 | 16.66 |
| 25 | 6.14 | 7.91 | 9.48 | 11.30 | 13.50 |
| 30 | 5.14 | 6.56 | 7.83 | 9.37 | 11.35 |
| 40 | 3.72 | 4.60 | 5.92 | 6.78 | 8.05 |
| 50 | 2.79 | 3.52 | 4.30 | 5.20 | 5.96 |
| 60 | 2.15 | 2.78 | 3.09 | 4.09 | 4.55 |
| 70 | 1.72 | 2.27 | 2.49 | 3.37 | 3.62 |
| 80 | 1.40 | 1.89 | 2.06 | 2.91 | 3.27 |
| 90 | 1.24 | 1.57 | 1.89 | 2.65 | 2.89 |
| 100 | 1.10 | 1.30 | 1.64 | 1.96 | 2.61 |
| 110 | 0.96 | 1.16 | 1.32 | 1.74 | 2.28 |
| 120 | 0.86 | 1.01 | 1.18 | 1.46 | 1.96 |
| 130 | 0.74 | 0.96 | 1.04 | 1.30 | 1.64 |
| 140 | 0.65 | 0.82 | 0.95 | 1.13 | 1.42 |
| 150 | 0.56 | 0.63 | 0.73 | 0.84 | 1.12 |

**Table 5.** Viscosity of MEA with different $CO_2$ loading, r = 0.5

The viscosity data measured for loaded mixtures at temperature from 25 to 80 ℃ are compared with data from Amundsen *et al.*[5] in **Figure 1** to **Figure 3** for three different amine concentration. The literature data only available for temperature up to 80 ℃ and concentration, r = (0.2, 0.3, 0.4).

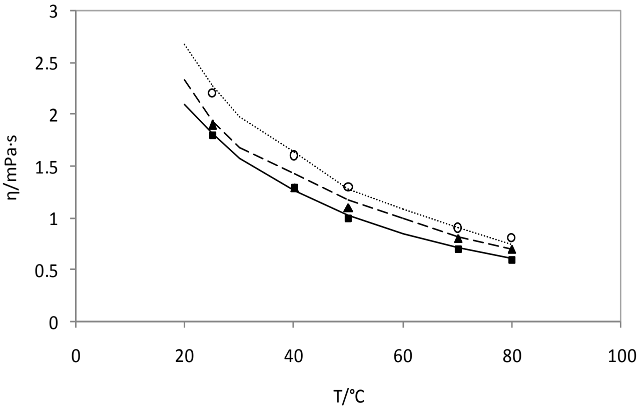

**Figure 1.** Viscosity variation with temperature, r = 0.2, Lines are experimental data: −, α = 0.1; - -, α = 0.3; ..., α = 0.5. Symbols refer to literature data: ■, α = 0.1; ▲, α = 0.3; ○, α = 0.5.

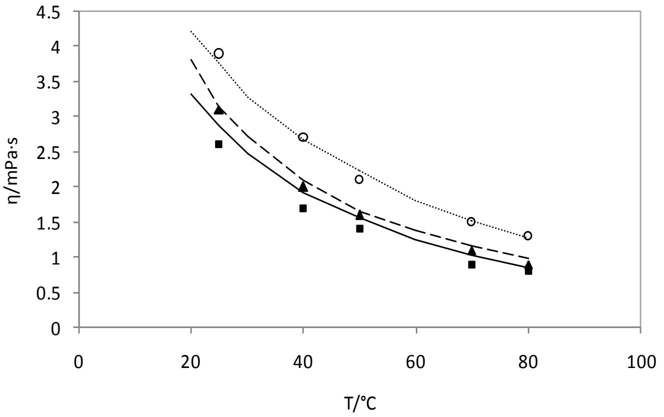

**Figure 2.** Viscosity variation with temperature, r = 0.3, Lines are experimental data: ─, α = 0.1; - -, α = 0.3; ..., α = 0.5. Symbols refer to literature data: ■, α = 0.1; ▲, α = 0.3; ○, α = 0.5.

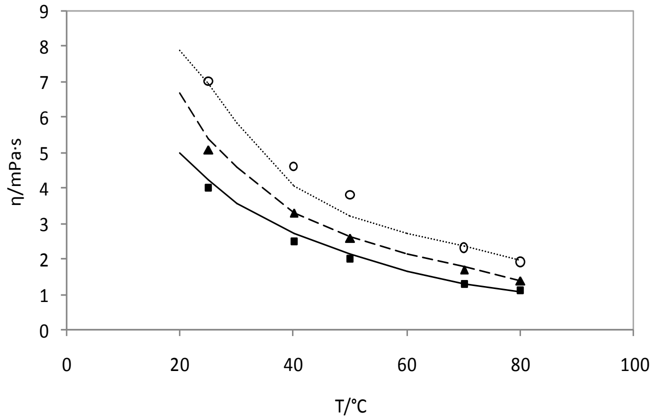

**Figure 3.** Viscosity variation with temperature, r = 0.4, Lines are experimental data: ─, α = 0.1; - -, α = 0.3; ..., α = 0.5. Symbols refer to literature data: ■, α = 0.1; ▲, α = 0.3; ○, α = 0.5.

The literature data and experimental work in this study are in good agreement. The average absolute deviation (AAD) is 0.03 mPa s at r = 0.2, 0.04 mPa s at r = 0.3 and 0.003 mPa s at r = 0.4. The correlation suggested by Weiland *et al*. [4] is used to calculate the estimation values of viscosity for different temperatures (Equation 1).

$$\frac{\eta}{\eta_{H_2O}} = \exp\frac{[(aw+b)T+(cw+d)][\alpha(ew+fT+g)+1]w}{T^2} \qquad (1)$$

Where η and $\eta_{H2O}$are the viscosities of the amine mixture and water viscosity at that temperature respectively in mPa s. w is the mass percent of the solution, T is the operating temperature in K, and α is the $CO_2$ loading in amine mixture (mol $CO_2$/mol MEA). The required coefficients are given in the **Table 6**.

| Parameter | Value for MEA |
|---|---|
| a | 0 |
| b | 0 |
| c | 21.186 |
| d | 2373 |
| e | 0.01015 |
| f | 0.0093 |
| g | -2.2589 |

**Table 6.** Parameters for solvent viscosity[4]

The equation can be used to calculate MEA solution viscosity up to amine concentration 40% mass basis with $CO_2$ loading up to 0.5 (mol $CO_2$/mol MEA) and to a maximum temperature 398 K[4]. Due to the limitations of applicability of the equation 1, experimental data are compared up to temperature 120 ℃ and r = (0.1, 0.2, 0.3, 0.4) solution concentration. The required water viscosity for an above equation is taken from the previous studies[6]. **Figure 4, Figure 5**, **Figure 6** and **Figure 7** show the measurements from this work compared to the correlation viscosity values at T ∈ [20, 120] ℃ for amine solution mass ration, r ∈ [0.1, 0.4]. Figures show the viscosity (Y axis) variation with temperature (X axis) for different $CO_2$ loading values. The part of the experiential values is only compared with available regression viscosity values as it has limitations in equation.

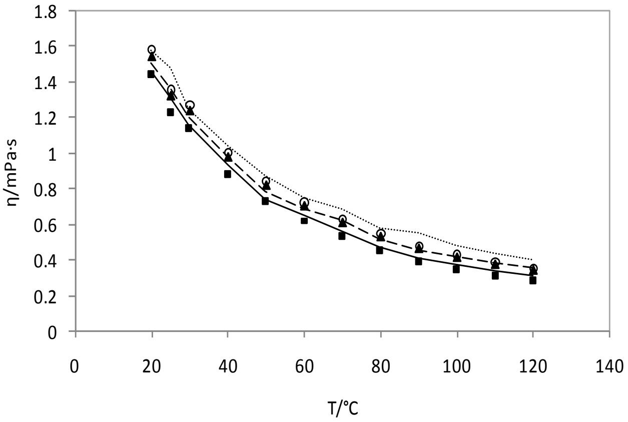

**Figure 4.** Viscosity variation with temperature, r = 0.1, Lines are experimental data: –, α = 0.1; - -, α = 0.3; ..., α = 0.5. Symbols refer to regression data: ■, α = 0.1; ▲, α = 0.3; ○, α = 0.5.

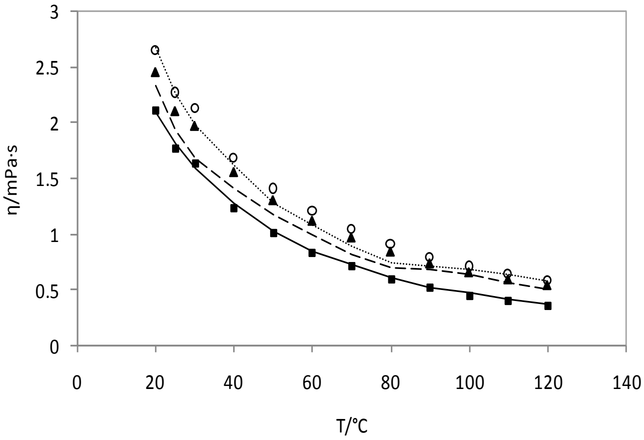

**Figure 5.** Viscosity variation with temperature, r = 0.2, Lines are experimental data: –, α = 0.1; - -, α = 0.3; ..., α = 0.5. Symbols refer to regression data: ■, α = 0.1; ▲, α = 0.3; ○, α = 0.5.

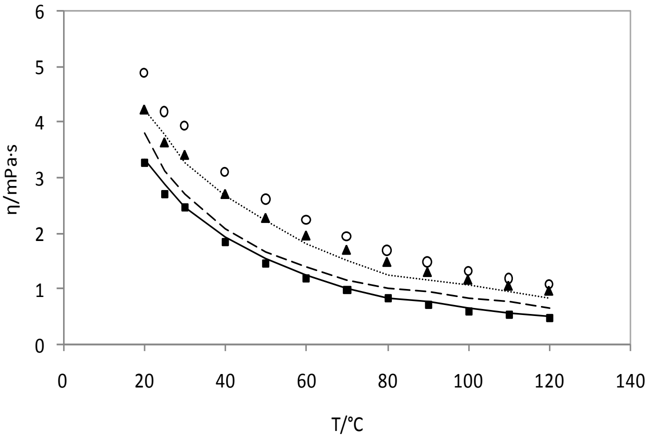

**Figure 6.** Viscosity variation with temperature, r = 0.3, Lines are experimental data: –, α = 0.1; - -, α = 0.3; ..., α = 0.5. Symbols refer to regression data: ■, α = 0.1; ▲, α = 0.3; ○, α = 0.5.

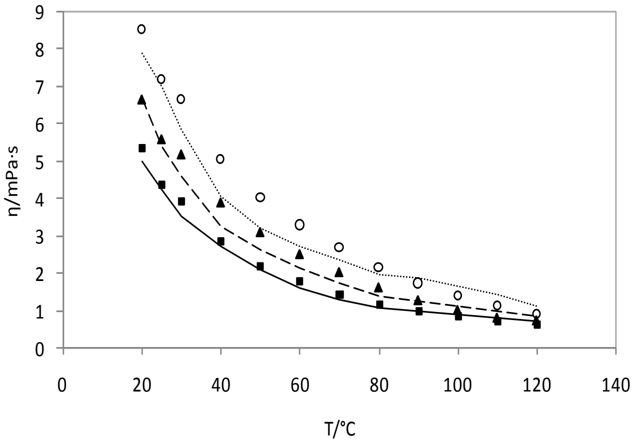

**Figure 7.** Viscosity variation with temperature, r = 0.4, Lines are experimental data: –, α = 0.1; - -, α = 0.3; ..., α = 0.5. Symbols refer to regression data: ■, α = 0.1; ▲, α = 0.3; ○, α = 0.5.

The agreement between correlation results and this work in satisfactory. However, correlation shows over predicts for most of the viscosity values for every concentration. The average absolute deviation (AAD) between this work and equation regression data are 0.02, 0.09, 0.36, 0.19 mPa s respectively for mass fraction of amine, r = (0.1, 0.2, 0.3, 0.4).

## 4. Experimental uncertainties

The uncertainty of the viscosity measurements of $CO_2$ loaded aqueous amines arises as a combination of the uncertainty of the temperature measurements, sample preparation, $CO_2$ loading and measuring instrument uncertainties. The temperature accuracy, U(T), which is related to rheometer temperature controller, is given as ±0.3K. The maximum viscosity gradient against the temperature, $\Delta\eta/\Delta T$, is calculated as 0.040 mPa·s·$K^{-1}$. The corresponding uncertainty in η, $(\Delta\eta/\Delta T)\cdot\Delta T$, is then estimated as ±0.0120 mPa·s. The uncertainties of the sample preparation were found by calculating the error values (difference between the expected value and measured value r) of the prepared sample. The mass ratio uncertainty ±0.004, U(r), and the viscosity gradient $(\Delta\eta/\Delta r)$ with 0.05 mPa·s are used for calculating the uncertainty of sample preparation. The resulting uncertainty in the sample preparation is calculated as, $(\Delta\eta/\Delta r).\Delta r$, ±0.00020. The uncertainty of loading, U(α), was found to be ±0.005 (mol $CO_2$/mol MEA) for MEA. The viscosity gradient, $\Delta\eta/\Delta\alpha$ was found as 2.1 mPa s (mol $CO_2$/ mol MEA)$^{-1}$ . The corresponding uncertainty was calculated as $(\Delta\eta/\Delta\alpha)\cdot\Delta\alpha$, ±0.0105 mPa s. The rheometer accuracy is given as ± 0.002 mPa s. The overall uncertainty of η, U(η), is calculated by combining the partial uncertainties reported in this section with root sum of square method. The value is calculated as ±0.0161 mPa·s. The combined expanded uncertainty of the viscosity, Uc(η), is calculated as ±0.032 mPa s (level of confidence 0.95). The combined expanded uncertainty, suggested by symbol Uc, is obtained by multiplying overall uncertainty, U(η), by a coverage factor, suggested symbol k. Typically, k is assumed to be 2 with the level of confidence 0.95.

## 5. Conclusions

The dynamic viscosity of partially carbonated MEA solution was measured for the temperature range (20 to 150) ℃ for mass fraction (10 to 50)% and $CO_2$ loading (0.1 to 0.5) mol $CO_2$/mol MEA. The agreement with the literature data for temperature range (25 to 80) ℃ is satisfactory for mass fraction (20 to 40)%. The comparison between Weiland's proposed model and measurement data are in good agreement. However, regression model is valid only for mass fraction of MEA up to 40% and temperature up to 125 ℃. Therefore, measurement data were compared only for valid operating conditions. The AAD between this work and equation regression data are 0.02, 0.09, 0.36, 0.19 mPa s respectively for mass fraction of amine, r = (0.1, 0.2, 0.3, 0.4). However, Weiland's regression model can be used for estimation of viscosity inside the limitations. Further measurements have to perform for other amines as well.

## References

1. Kohl, A. L., Nielsen, R. B.Gas Purification, 5th edition; Gulf Publishing Company: Houston, 1997.
2. Wang, G. Q., Yuan, X. G., Yu, K. T. Review of mass transfer correlations for packed columns. Ind. Eng. Chem 2005, 44, 8715-8729.

3. Eckert, J.S. Selecting the proper distillation column packing. Chem. Eng. Prog 1970, 66 (3), 39-44.
4. Weiland, R.H., Dingman, J.C., Cronin, D.B., Browning, G.J. Density and viscosity of some partially carbonated aqueous alkanolamine solutions and their blends. J. Chem. Eng. Data1998, 43, 378-382.
5. Amundsen, T. G., Øi, L. E., Eimer, D. A. Density and Viscosity of Monoethanolamine + Water + Carbon Dioxide from (25 to 80) ℃.J. Chem. Eng. Data 2009, 54, 3096-3100.
6. Arachchige, U. S. P. R., Aryal, N., Eimer, D. A., Melaaen, M. C.Annual Transactions - The Nordic Rheology Society 2013, 21, 299-308.

Doctoral dissertation no. 26
**2019**

—

# Carbon Dioxide Capture by Chemical Absorption: Energy Optimization and Analysis of Dynamic Viscosity of Solvents

Dissertation for the degree of Ph.D

—

Udara S. P. R. Arachchige

—

ISBN: 978-82-7206-515-6 (print)
ISBN: 978-82-7206-516-3 (online)

usn.no